Distribution of Zooplankton and Nekton above Hydrothermal Vents on the Juan de Fuca and Explorer Ridges.

By

Kristina Michelle Skebo
B.Sc., University of Victoria, 1994

A Thesis Submitted in Partial Fulfillment of the Requirements for the Degree of

MASTER OF SCIENCE

in the Department of Biology

Supervisor: Dr. Verena Tunnicliffe

ABSTRACT

Buoyant hydrothermal vent fluids vertically advect near-bottom production and contain compounds that support bacterial growth. Previous studies have shown that zooplankton aggregating above the neutrally buoyant plume feed on benthic particulates and chemosynthetic microbes associated with the effluent. In this study, I explore how vent effluent affects pelagic organisms near the seafloor.

The remotely operated vehicle JASON flew a 3.4 x 0.5 km grid at 20 m above bottom over vent and non-vent areas on the Endeavour Segment, Juan de Fuca Ridge. My primary source of information for organism dispersion was visual: I distinguished organisms by form and motion in high resolution video. Environmental and navigational data collected every three seconds in conjunction with video data allowed organism dispersion to be linked with physical water characteristics. In addition, net tows taken over vent and non-vent areas on the Endeavour Segment, Axial Seamount and Explorer Ridge were used to characterize zooplankton assemblages above non-vent, diffuse vent and smoker vent sites within the axial valley.

Multiple sampling methods are useful to identify benthopelagic assemblages accurately. Video is better at capturing large pelagic organisms. Mounted 63 μm net consistently captures larger and more diverse assemblages than the 180 μm net although net position on the submersible may affect capture efficiency. Cyclopoids, typically under-sampled in zooplankton studies, are well represented.

Vent effluent influences the spatial pattern of near-bottom pelagic organisms. Zooplankton (e.g. copepods) and gelatinous zooplankton in particular appear to avoid areas of intense venting. Zooplankton are relatively low in abundance over vent fields and gelatinous zooplankton occur in relatively low abundance along the central length of the sample area.

Zooplankton aggregate above diffuse vents (14.6 individuals/m^3) and above non-vent areas (9.6-17.3 individuals/m^3) within a few hundreds metres of vent fields. Because physico-chemical anomalies are not detectable, I speculate the zooplankton aggregate in these non-vent areas in response to enhanced microbe concentrations associated with vent

effluent. Similar increases in zooplankton abundance occur downstream of upwelling sources. Aggregations of gelatinous zooplankton and zoarcids in non-vent areas likely occur in response to increased zooplankton abundance. Shrimp appear to aggregate in response to increased zooplankton and vent benthos. Macrourids aggregate at the edges of smoker and diffuse vent fields likely feeding on vent biomass. Effluent may play a role in cuing macrourids to vents.

Zooplankton assemblages are primarily composed of copepods. Of the 72 copepod species found in 20 m above bottom samples, 24 are common to non-vent, diffuse vent and smoker vent assemblages. Smoker vent assemblages are most diverse; 15 of the 57 species found over smoker vents are not found in any other samples. Diffuse vent assemblages are least diverse; only 5 of 34 species found in diffuse vent samples are unique. *Oithona similis, Oncaea sp.* and calanoid copepodites dominate most assemblages.

Similar to previous benthopelagic studies, most copepod species are female dominated. *Oithona similis* is the exception - males are consistently more abundant. Calanoid copepodites are consistently more abundant than adults whereas cyclopoid, harpacticoid and dirivultid copepodites are consistently less abundant than adults. Unlike most benthopelagic studies, percent of copepod exoskeletons (8-14%) is significantly less than percent of live copepods.

Vent productivity may represent a significant resource for near-bottom zooplankton and nekton within the axial valley. Localized increases in zooplankton abundance occur over diffuse vent sites and are patchily dispersed throughout non-vent areas. I speculate that zooplankton, copepods in particular, are able to feed on free-living chemosynthetic bacteria associated with vent effluent in areas where effluent signature is weak. Zooplankton near the seafloor may thus play a role in the transfer of vent productivity to the deep sea.

This study is unique: it relates dispersion of pelagic organisms to measured vent effluent characteristics and compares composition of zooplankton assemblages from vent and non-vent sites to previous benthic-pelagic studies. This work contributes to our understanding of the role hydrothermal vents play in the deep sea ecosystem.

TABLE OF CONTENTS **Page**

List of Tables **Page**

List of Tables (continued) **Page**

List of Figures **Page**

List of Figures (continued) **Page**

Acknowledgements

First and foremost, I would like to thank my supervisor, Dr. Verena Tunnicliffe, who encouraged me in my work, thesis and otherwise. She is one of the bravest and strongest people I know. I am proud to have had her as a supervisor for two degrees! Thank you also to my lab mates Dr. Jean Marcus and Amanda Bates for their ideas and discussion. Jean and Amanda made life as a graduate student much easier.

Dr. Paul Johnson, Irene Garcia Berdeal and Tor Bjorklund provided me with the video tapes and the processed environmental data. Thank you for answering all of my questions about the physical and geological setting of my study area. Dr. Maia Tsurumi was also instrumental in collecting and organizing the videos.

I would also like to thank my committee members, Dr. Pat Gregory and Dr. John Dower, for their advice and willingness to tackle difficult statistical concepts.

A number of people helped point me in the right direction when it came to analyzing my video data. Without their guidance, I would have been completely lost. In particular, I would like to thank Dr. Dave Mackas (IOS), Dr. Rolf Lueck (SEOS) and Dr. Richard Dewey (SEOS) for helping me to clarify some of the more confusing aspects of autocorrelation analysis.

I am indebted to Moira Galbraith (IOS) who taught me how to identify copepods and even sorted through some of my "large" samples.

A huge thank you to Dr. Rob Campbell and Tom Bird, who helped my negotiate the frightening task of trying to write programs in Matlab. I would still be organizing my data without your help!

Thank you to the ROPOS crew and the captain of the Tully (who sewed my plankton nets back together) for their work in developing the net tow system and for collecting the plankton samples.

Without the support, patience and encouragement of my parents, I would not be where I am today.

Last, but definitely not least, I would like to thank Ted Allison who supported me through all of the ups and downs, listened to me talk about my data and analysis *ad nauseum* and who has always been there when I needed him. Thank you.

Chapter 1

General Introduction

Benthic-pelagic coupling refers to the two-way exchange of matter between the benthos and the overlying water body (Raffaelli et al. 2003). Typically, benthic-pelagic coupling processes are studied in terms of food supply to the deep sea from photosynthetically-derived surface material: large seaweeds; sinking of phytoplankton patches, sometimes repackaged as copepod fecal pellets; terrestrial material; and fish and marine mammal carcasses are all sources of organic carbon on seafloor (Graf 1992, Marcus and Boero 1998). Conversely, the contribution of living benthic particles to pelagic systems, e.g. larvae, can also profoundly influence the dynamics of water column populations and communities (Raffaelli et al. 2003).

At hydrothermal vents, heated seawater is expelled from the ocean crust. The rising effluent 1) alters deep sea circulation (Helfrich and Speer 1995), 2) expels particulates, including metal sulphides, that provide energy for free-living bacteria (Jannasch and Mottl 1985, Winn and Karl 1986, Jannasch 1995) and 3) provides food resources for abundant benthic vent fauna (Van Dover and Fry 1994). Pelagic organisms may be attracted to the abundant benthic biomass associated with the vents, but in exchange, must contend with toxic conditions (reduced metals released with hydrothermal fluids), changes in flow speed and direction, changes in temperature and salinity and changes in particle flux (Kaartvedt et al. 1994). Alternatively, environmental conditions may be too variable and pelagic organisms may avoid the vents. The response of deep sea pelagic animals to vent effluent remains unclear.

Most studies of plume-associated zooplankton lack environmental data. One of the main benefits of using the Juan de Fuca Ridge, particularly the Endeavour Segment, to study zooplankton-plume interaction is that there are many studies of plume dynamics along this ridge. Detailed surveys are 'easily' conducted along the Juan de Fuca Ridge; it is medium-rate spreading ridge, has abundant plume emission and the narrowness of the ridge crest permits 2-D mapping effort (Baker et al. 1995). Thomson et al (1992), Burd et al (1992) and Burd and Thomson (1994, 1995, 2000) took the first steps in linking

benthic and pelagic realms at vents on the Juan de Fuca Ridge by studying zooplankton associated with the neutrally buoyant plume, 200 m above the seabed.

The main goal of this thesis is to explore how vents affect pelagic organisms near the seafloor. This work: 1) provides analyses of simultaneous organism distribution and environmental data and 2) provides a link between what is happening near the seafloor and what occurs at neutrally buoyant plume depths.

1.1 Hydrothermal vents

Hydrothermal vents are water jets on the seafloor, emitting heated, chemical- and metal-rich fluid that often supports thriving benthic communities. Vents are found at a range of depths, from 800 m (Azores) to >3700 m (TAG, Mid-Atlantic Ridge), at seafloor spreading centres in all oceans (Von Damm 1995). Mid-ocean ridges are mountain ranges in the ocean where new seafloor is created. Active spreading ridges are marked by an axial valley or trough usually only a few kilometres wide (Van Dover 2000). In the temperate northeast Pacific Ocean, venting is primarily confined to the Explorer-Juan de Fuca-Gorda Ridge complex, an isolated set of spreading ridges that extends almost 1000km along the west coasts of Canada and the US (Figure 1.1) (Baker et al. 1995).

1.1.1 Explorer Ridge

The Explorer Ridge spreading locus is a 1 km wide, 4 km long, 100 m deep axial valley at the centre of an upraised ridge, roughly 1800 m below the ocean surface (Tunnicliffe et al. 1986, Tunnicliffe 1991). While the vents along this ridge have remained relatively unexplored since the 1980s, the New Millenium Observatory (NeMO) cruise (July-August 2002) found 30 active vents, emitting fluid of 20-311°C at four different sites (Embley 2002). As in the 1980s, much of the venting is confined to Magic Mountain, at 49°46'N and 139°16'W, an area comprised of four vent fields (Figure 1.2) (Embley 2002). Magic Mountain is a topographic high located outside the primary rift valley (Tunnicliffe et al. 1986). Individual vents are situated near the wall of the axial valley. Despite active venting, many of the vents are devoid of benthic fauna as the vent fluid emissions lack the sulphides found at sites on the Juan de Fuca (Embley 2002).

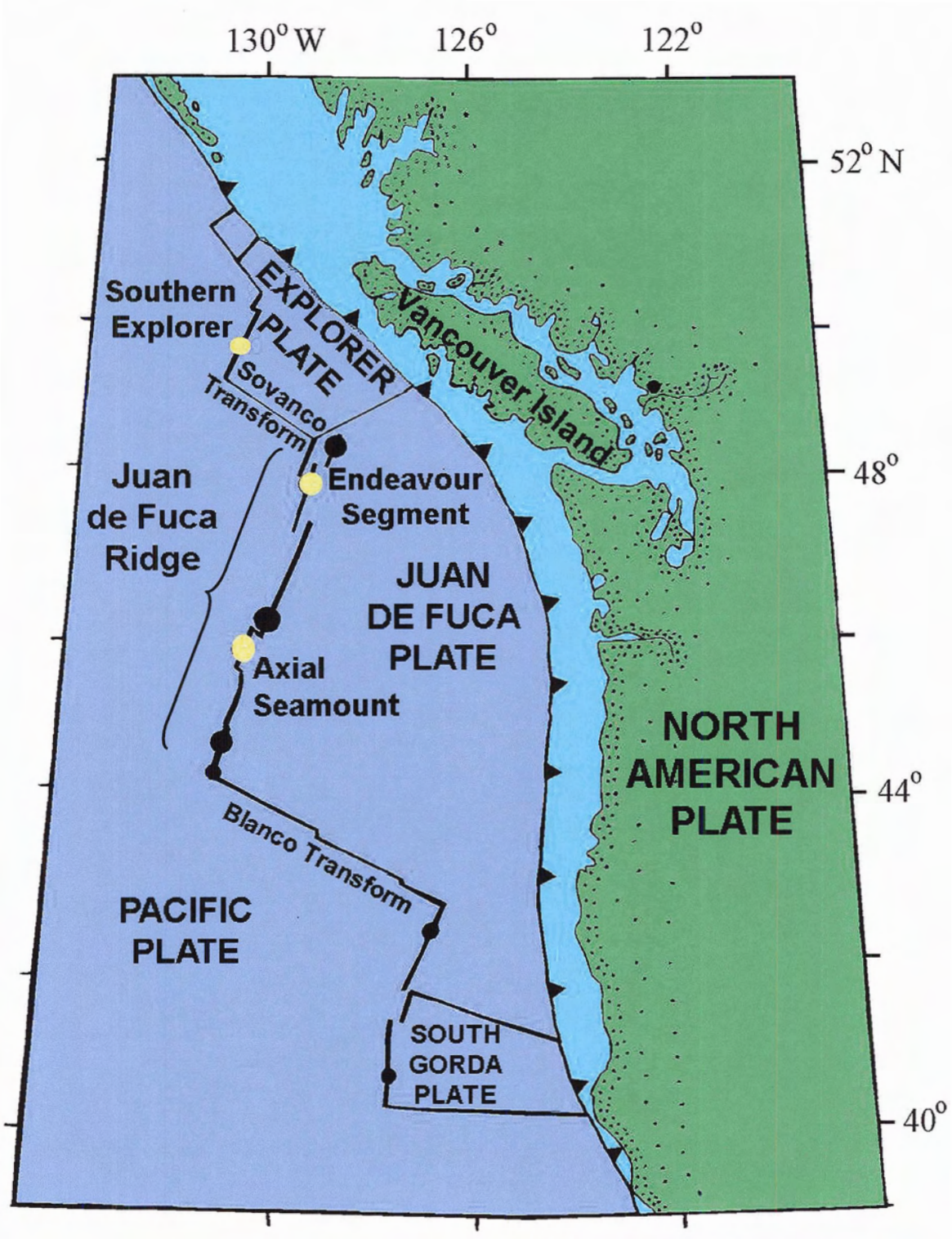

Figure 1.1 Explorer-Juan de Fuca-Gorda spreading ridge, off the west coast of North America. Dots on the ridge represent segments with active vent sites. Yellow dots indicate vent sites relevant to this thesis. Adapted from Juniper and Tunnicliffe (1997).

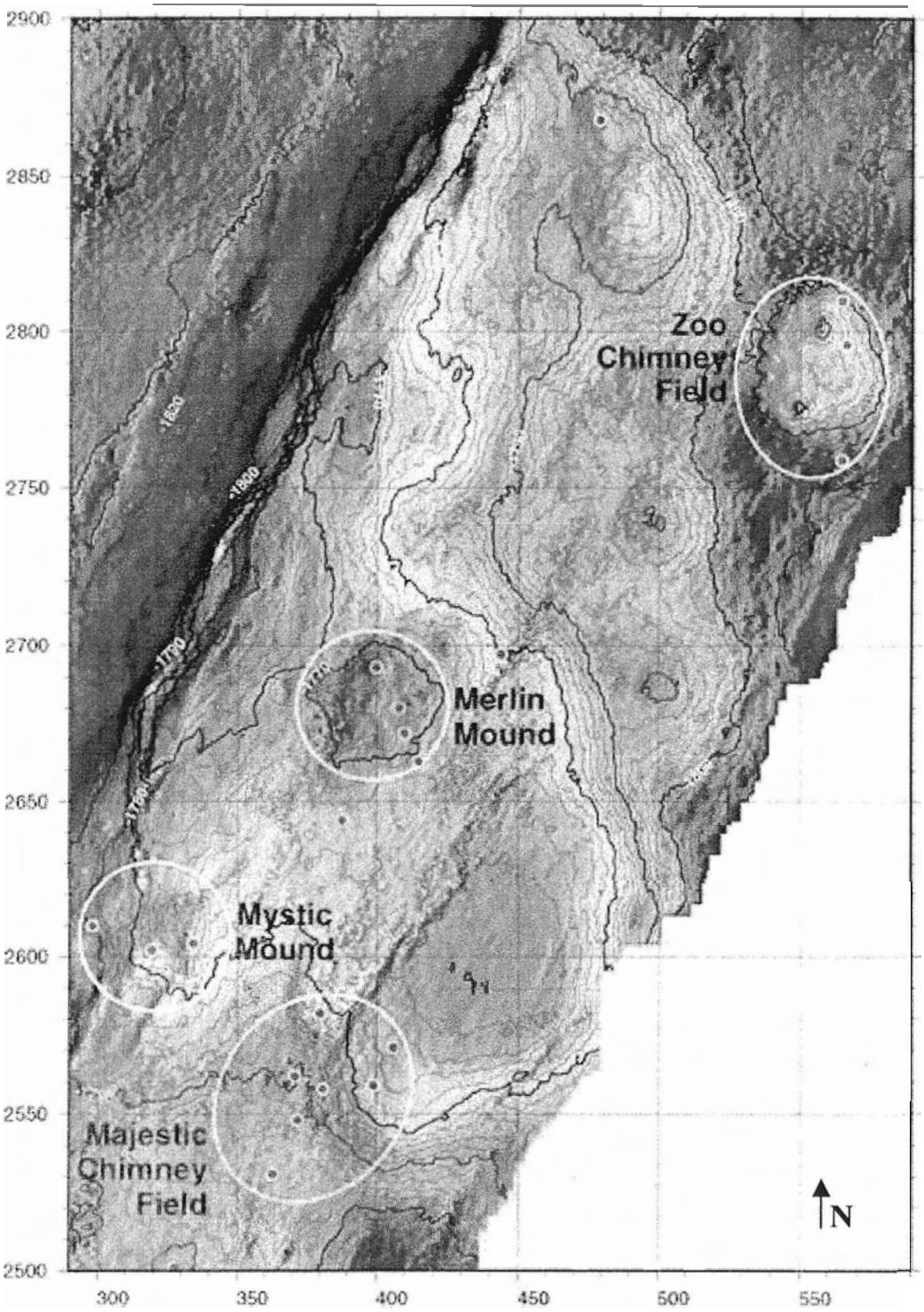

Figure 1.2 Distribution of vent fields on Magic Mountain on the Southern Explorer Ridge, modified from Embley (2002). Magic Mountain vent site is located at 49°46'N, 130°16'W.

1.1.2 Juan de Fuca Ridge

The Juan de Fuca Ridge is bounded on the south by the Blanco Fracture Zone and on the north by a triple junction formed by the ridge, the left-lateral Nootka fault and the Sovanco Fracture Zone (see Figure 1.1) (Johnson and Embley 1990). It is a medium-rate spreading zone (6 cm/yr) (Tunnicliffe 1991). The Juan de Fuca can be divided into six 50-100 km long segments: Middle Valley, Endeavour, Co-Axial, Axial, North Cleft and South Cleft (Johnson and Embley 1990). Of these, my study focuses on Endeavour Segment and Axial Seamount.

Endeavour Segment

Located at 47°56-58'N and 129°08'W, the Endeavour Segment axial valley is bounded by 100-150 m high walls and is about 0.5-1 km wide (Delaney et al. 1997). The north end of the segment is about 2050 m deep and deepens southward to depths >2700 m (Delaney et al. 1997). Most of the venting is on well-fractured, unsedimented, older basalt near the west wall of axial valley (Delaney et al. 1992). The majority of the venting occurs at four high temperature vent fields, each separated by roughly 2 km of primarily non-venting area (Figure 1.3) (Delaney et al. 1992). Vent fields at Endeavour lie on deep faults away from the main spreading centre (Delaney et al. 1992). Hydrothermal activity is linked to active tectonic movement (Delaney et al. 1992, Robigou et al. 1993). The eastern wall of the valley is unfissured and the seafloor on this side of the segment is indented rather than elevated (Delaney et al. 1992).

Axial Seamount

Both volcanically and hydrothermally active, Axial Seamount lies at the intersection of the Cobb-Eickelberg Seamount Chain and the Juan de Fuca Ridge (see Figure 1.1) (Johnson and Embley 1990). Located at 45°57'N, 130°01'W, the seamount rises to about 1000 m above the surrounding basin to a depth of about 1410 m (Hammond 1990). A 100 m caldera depression characterizes the summit (Figure 1.4) (Hammond 1990). ASHES, CASM and the South Rift Zone are the three major vent fields on the seamount (Tsurumi and Tunnicliffe 2001).

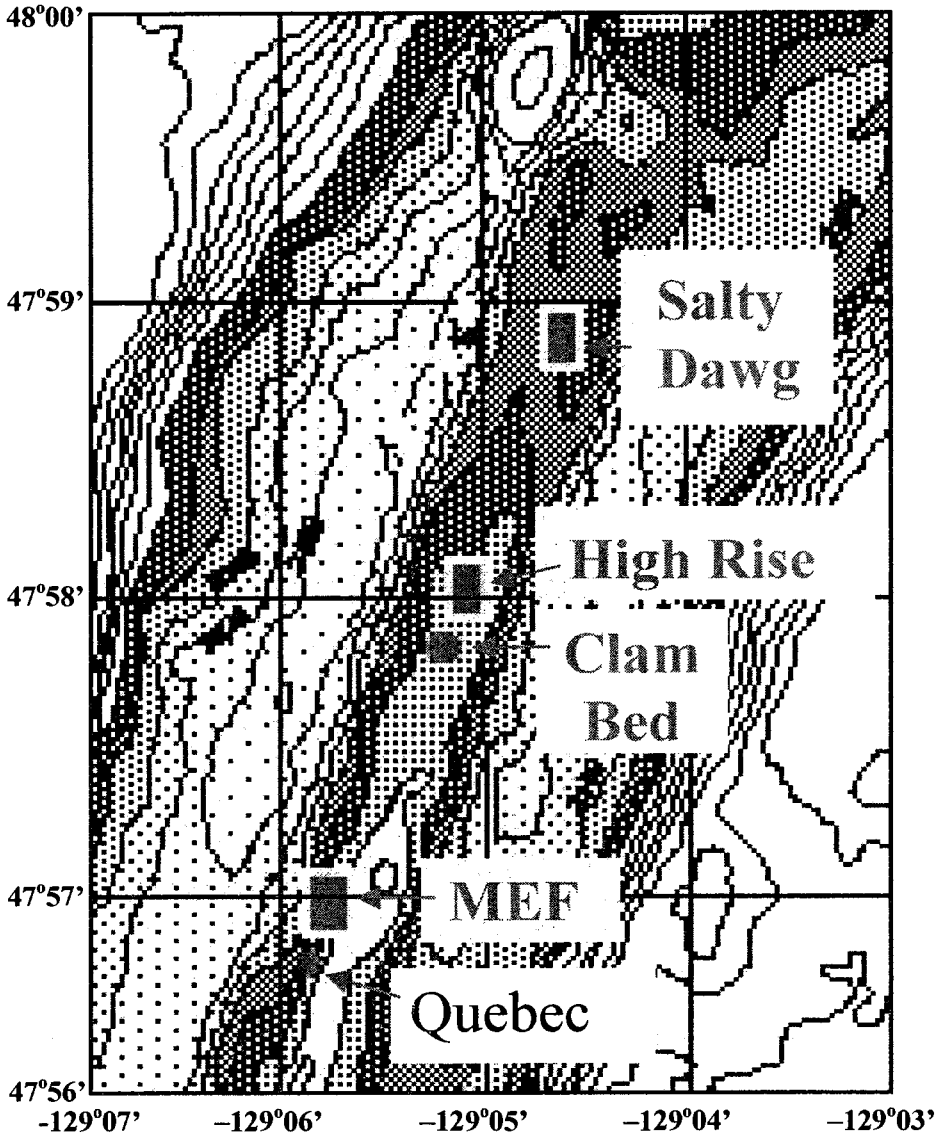

Figure 1.3 Distribution three of the five major vent fields on Endeavour Segment, modified from Delaney et al (1997). Mothra, to the south, and Sasquatch, to the north, are beyond map boundaries.

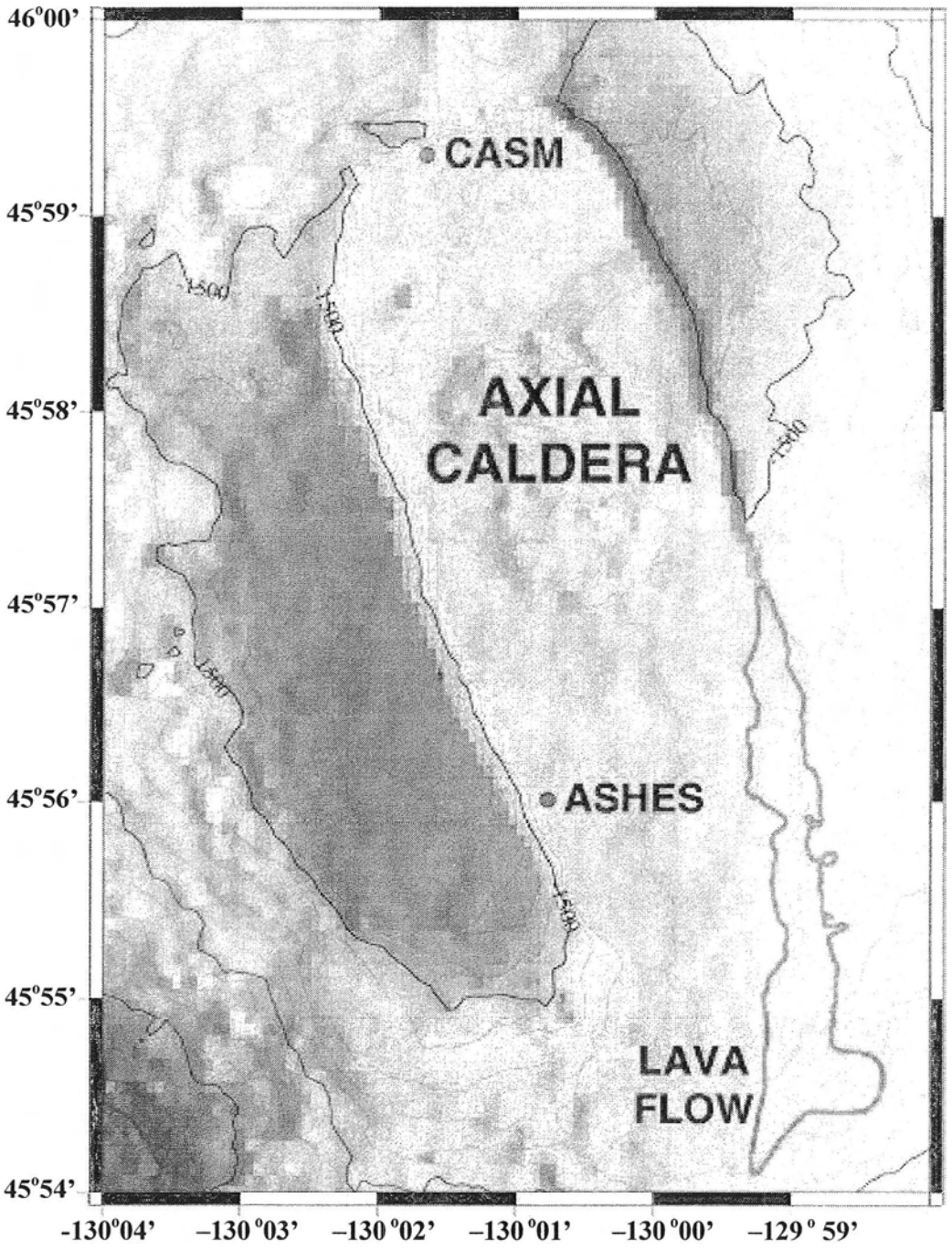

Figure 1.4 Axial Seamount caldera, modified from NeMO website (2001). CASM and ASHES are the two major vent fields on the summit. A relatively recent eruption (1998) covered the southeast side of the summit in new lava flows (South Rift Zone).

1.1.3 Vent field characteristics

An **individual vent**, e.g. a single smoker chimney, is a localized expression of emergent vent water on the ocean floor (Tunnicliffe 1991). Chimneys form as metal and sulphide-rich, high temperature, acidic fluids mix with ambient seawater causing metal sulphides to precipitate (Van Dover 2000). These structures can extend tens of metres into the water column and may have multiple narrow orifices at the top from which fluid is emitted. Clusters of tubeworms or bivalves are also indicative of emerging effluent when distinct geological structures are lacking (Figure 1.5). In general, vent biota tend to cluster around diffuse sources of flow (<60°C). A **vent field** is a cluster of vents which appear to be linked via subsurface water conduits. A field can range from tens to hundreds of metres in diameter (Tunnicliffe 1991). A **vent site**, e.g. Endeavour Segment, is a general area of hydrothermal activity on a ridge segment, which may include one or more vent fields (Tunnicliffe 1991). Within a vent site, vent fields are often separated by non-venting seafloor which is 1) outside the boundaries of the geographically defined vent fields and 2) non-fissured and thus does not release any fluid.

As in Figure 1.5, most vent fields are characterized by **discrete** and **diffuse** venting sources. Black smokers are typical sources of discrete flow. Black smokers release metal- and sulphide-rich, high temperature fluid (~300-400°C) that, when entrained with ambient seawater, causes metal sulphides to precipitate, forming particle rich "black smoker" plumes (Van Dover 2000). White smokers release intermediate temperature fluid (100-300°C) and lack the metal and sulphide concentration to produce black smoke upon mixing with ambient water. Instead, fluid from white smokers precipitates white particles of silica, anhydrite and barite (Van Dover 2000).

Diffuse flow issues from porous surfaces of active chimneys or directly from fissures and cracks in basalt lavas (Trivett 1994). Diffuse fluids are high temperature fluids that have undergone dilution with cold seawater either below surface or within the matrix of a sulphide structure like a chimney (Trivett 1994). Diffuse fluids have lost most of their metal sulphide load and are primarily responsible for sustaining thermophilic bacteria and benthic invertebrate populations (Von Damm 1995).

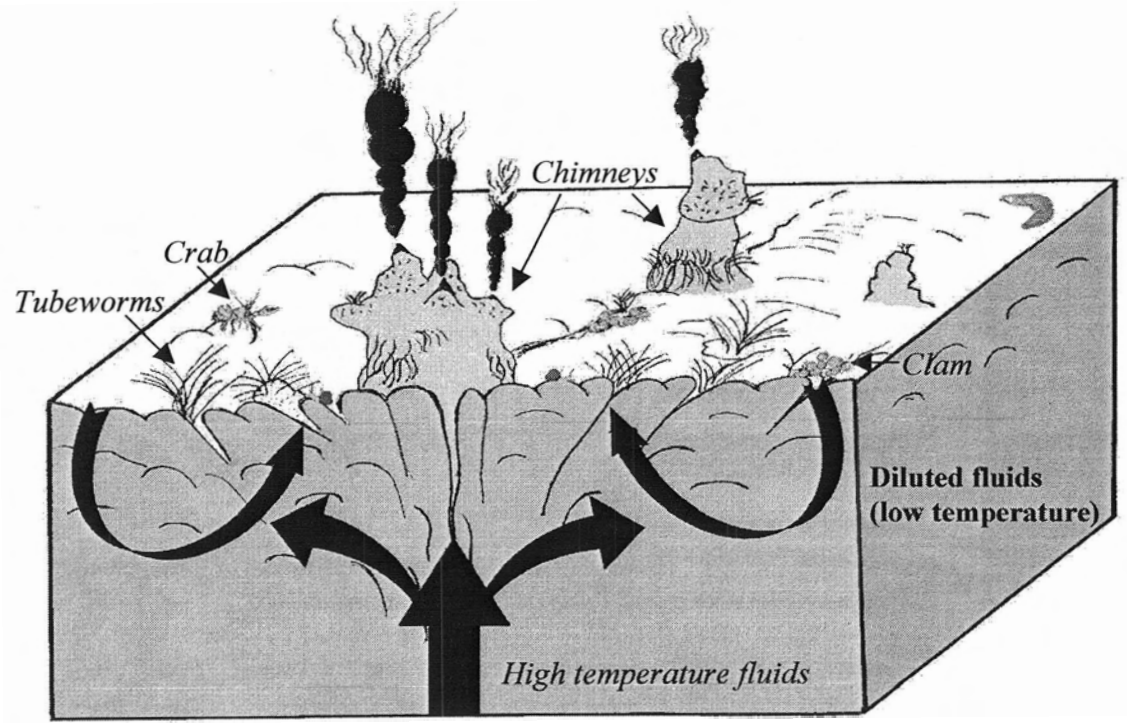

Figure 1.5 Illustration of a "typical" vent field, modified from Tunniclife et al (2003). Smokers or chimneys can have one or multiple orifices through which high temperature vent fluid is released. Vent organisms (tubeworms, clams) are clustered around low temperature fluid emissions seeping through cracks in the seafloor or at the base of the chimneys.

1.2 Hydrothermal Plumes

1.2.1 Dynamics and properties

Seafloor hydrothermal circulation is the principal agent of energy and mass exchange between the ocean and the earth's crust (Baker et al. 1995). Fluids emerging from hydrothermal sources can alter deep-sea mixing and circulation patterns, and profoundly influence ocean chemistry and biology (Baker et al. 1995).

As seawater percolates through porous seafloor, it is heated and entrains various metal and mineral species through contact with subsurface rock. Vent fluids are reducing in nature; they contain no oxygen and have high concentrations of sulphides, primarily in the form of H_2S (Von Damm 1995). In the absence of sulphide measures, temperature is often used as a proxy for the toxicity of fluid chemistry in low temperature settings. It is assumed that the higher the temperature of the emitted fluid, the less that fluid has been diluted through mixing with ambient seawater thus high concentrations of sulphide, methane, metals etc. are retained (Van Dover 2000).

Vent effluent is emitted in the form of a plume, a feature produced by continuous release of buoyant fluid (Figure 1.6) (Lupton 1995). Within a vent site, individual vent fields can exhibit different chemical signatures based on the type of rock contacted during sub-surface flow (Von Damm 1995). Because hydrothermal fluid is hot, it is buoyant in ambient deep-sea water. As the buoyant plume ascends, shear flow at the boundary between the plume and ambient water produces turbulent eddies, which act to engulf ambient fluid and mix it into the ascending fluids (Lupton et al. 1985, Lupton 1990, Rona et al. 1991) resulting in continuous dilution of the buoyant plume. With increasing height above the seafloor, the vertical velocity and the buoyancy of the plume decrease while the radius of the plumes increases (Rona et al. 1991, Lupton 1995).

Because the ocean is stratified, i.e. density increases with depth, the buoyant plume rises to a height at which the density of the plume is equal to the density of the surrounding water (Lupton 1995). Within the axial valley of the southern Juan de Fuca Ridge, buoyant hydrothermal emissions rise 150-200 m above the seafloor before reaching neutral buoyancy (Baker and Massoth 1987). At neutral buoyancy, the plume spreads laterally (Lupton et al. 1985, Klinkhammer and Hudson 1986, Cannon et al. 1991).

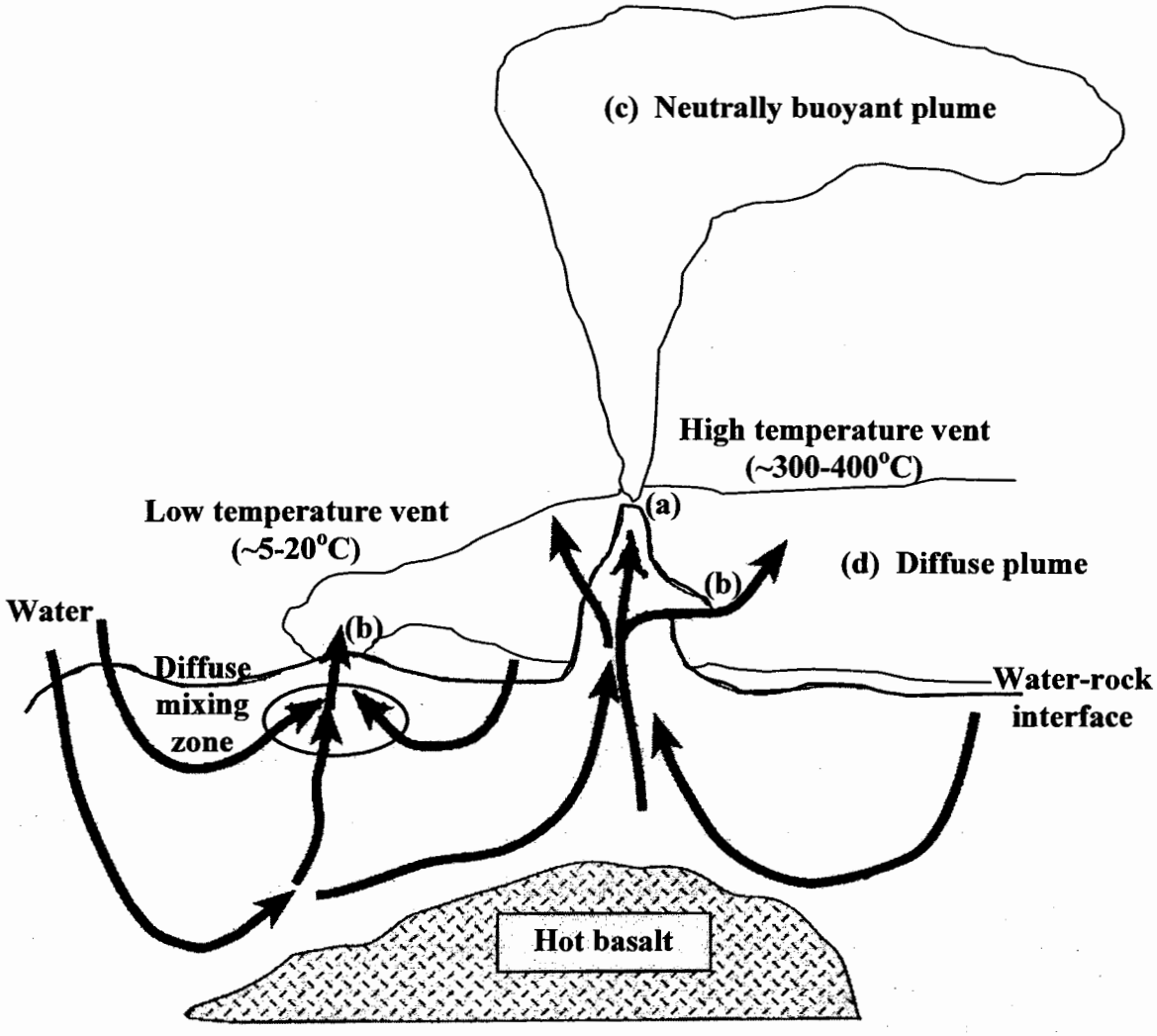

Figure 1.6 Illustration of hydrothermal circulation and plume formation at a vent field, modified from McCollom (2000). Water percolates through the crust, entrains metals and minerals, is heated and is released through (a) discrete and (b) diffuse venting sources. The diffuse mixing zone is where heated seawater mixes with ambient seawater below the seafloor, diluting fluid that will be emitted from vents. Water released from the discrete source rises (buoyant plume), eventually forming (c) hundreds of metres above bottom. The majority of diffuse outflow or plume (d) remains trapped near the seafloor, heating the bottom water layer.

The effluent layer or neutrally buoyant plume is a mix of:

1. highly diluted vent fluid, usually from several individual vent sources;
2. ambient water from the same depth as the effluent layer; and
3. an "entrained component" - water entrained into the buoyant plume during ascent, but which is not derived from a single depth (Lupton et al. 1985, Lupton 1995).

In the Pacific, buoyant vent effluent is characterized by higher temperature, higher salinity (from entrained deep water), lower density and higher particulate count than ambient water (Lupton 1995).

1.2.2 Discrete flow

Discrete flow is characterized by the release of a jet of heated, sulphide rich seawater through a single, small (on the scale of a few centimeters) opening in a mineralized chimney, often at speeds of 1 m/s (Rona and Speer 1989, Rona and Trivett 1992, McDuff 1995). As hot, buoyant seawater is released from the vent, it rises and entrains ambient seawater at a rate proportional to that with which it is rising (Helfrich and Speer 1995; McDuff 1995). Buoyant plumes are diluted by a factor of 10^3 in the first 5-10 m above the source and by another order of magnitude before neutral buoyancy is reached (Speer and Rona, 1989; Lupton, 1995). Thus within the buoyant plume, locally steep concentration gradients can exist (McDuff 1995).

Much of the discrete flow rises to form the neutrally buoyant plume hundreds of metres above the seafloor. Directly above Main Endeavour vent field (Endeavour Segment), the neutrally buoyant plume is composed of 0.01% vent effluent, 30% ambient water normally found at that depth and ~70% entrained water that has been transported from deeper layers (Lupton et al. 1985). The physical effects of entrainment are complicated since buoyant plumes are not rising through ambient water, but rather through bottom water affected by 1) shearing action at the plume boundary and 2) ubiquitous low temperature diffuse venting (Trivett 1994, Lupton 1995, McDuff 1995, Murton et al. 1999).

1.2.3 Diffuse flow

The majority of heat advected from hydrothermal sites to the deep ocean is carried by diffuse rather than discrete flow (Trivett and Williams 1994). Less is known about the dynamics and heat flux of diffuse flow as flow velocity and fluid temperatures from diffuse sources are low and discharge is unevenly distributed over large areas (Rona and Trivett 1992, Von Damm 1995).

Diffuse venting is typically characterized by fluid flow or seepage from cracks and fissures in the seafloor (Rona and Trivett 1992; Von Damm 1995). Diffuse flow is slightly warmer than ambient seawater (5-20°C) and has lost much of its metal sulphide load and hence, does not "smoke" (Von Damm 1995). Diffuse flow appears to 'shimmer' due to density differences with the surrounding ambient water (Von Damm 1995). 'Shimmering' microplumes are generated and behave similarly to buoyant smoker plumes, rapidly mixing with ambient water to create a near-bottom warm layer (Trivett 1994; Helfrich and Speer 1995; Lupton 1995).

Patchiness in temperature and velocity of the rising microplume is due to mixing and inconsistent source discharge (Schultz et al. 1992). The height to which the microplumes rise is determined primarily by the buoyancy of the water (Trivett 1994). Because the microplumes lack the momentum and density contrast of the smoker plumes, microplumes are essentially trapped near the seafloor, usually within 50m of the bottom (Trivett 1994) (Figure 1.6).

1.2.4 Plume dispersal

How plumes disperse is important to understanding heat budgets, transport of chemical species, and establishment and maintenance of vent field communities (Helfrich and Speer 1995). Overall, little mixing of diffuse and discrete flow occurs as diffuse flow is laterally advected by prevailing currents below discrete discharge (Rona and Trivett 1992) therefore, diffuse and neutrally buoyant plumes are considered separately.

Diffuse plume

At hydrothermal vents, the benthic boundary layer is complex. Typically, a well-mixed layer of near-bottom water is generated (benthic boundary layer) as shearing

between bottom water and seafloor causes turbulent mixing (Armi and Millard 1976). At vents, toxic, heated water expelled from the seafloor causes chaotic mixing (I. Garcia Berdeal, pers. comm.) such that turbulence increases with distance from the seafloor (Trivett and Williams 1994) rather than decreases as in typical deep sea benthic boundary environments.

Diffuse flow rapidly mixes with ambient seawater and is trapped near the bottom (Helfrich and Speer 1995). It quickly merges into ambient circulation through either ground-hugging horizontal advection or a combination of vertical and horizontal advection caused by entrainment into high-temperature plumes (Helfrich and Speer 1995). Trivett (1994) found that, near the seafloor, diffuse flow can be carried hundreds of metres from the source during a single tidal cycle.

Horizontal currents play a significant role in the dispersion of diffuse flow often advecting the microplume further downstream than it rises in height (Rona and Trivett 1992; Trivett 1994). Cross flow is not often incorporated into many models of plume physics as there is great variability in intensity and direction of cross currents (McDuff 1995). Instantaneous cross current velocities of up to 10 cm/s have been measured on the Endeavour Segment (Thomson et al. 1992). As this is comparable to vertical velocity in the core of the buoyant smoker plume, significant deflection of the plume in the direction of the current can occur (McDuff 1995).

Neutrally buoyant plume

Lateral spreading of the neutrally buoyant plume (Figure 1.6) is caused by unbalanced pressure gradients and influence of bottom currents (Helfrich and Speer 1995). The rotation of earth slows lateral spreading and causes the plume to rotate (Helfrich and Speer 1995). This forms a horizontal vortical flow of vent fluid at neutral buoyancy; this flow is unsteady and leads to vortex shedding in the plume effluent (Helfrich and Speer 1995). Vortices can be carried downstream by currents or by their own momentum (Cannon et al. 1991, Helfrich and Speer 1995).

The neutrally buoyant plume at Endeavour follows a meandering path from the vent fields to the west, driven primarily by prevailing southwest currents (Thomson et al. 1990). The complicated interaction of northerly advection superimposed over mean

southwest flow plus tidal and inertial currents helps to disperse the Endeavour plumes (Thomson et al. 2003).

High-temperature hydrothermal venting at ridge crests is capable of forcing circulation on scales many orders of magnitude larger than the vent field size or the plume rise height (Helfrich and Speer 1995). Heat input, from plume water, affects mid-depth thermohaline circulation by entraining saltier deep water (Von Damm 1995). Thermohaline circulation is driven by variations in temperature and salinity that primarily control the rising and sinking of deep water masses (Brown et al. 1991).

Characteristics of the neutrally buoyant plume are maintained for large distances. Cannon et al (1995) observed temperature and salinity anomalies hundreds of kilometres west of the Juan de Fuca Ridge that were consistent with hydrothermally derived fluids. Dissipation of heat and salinity anomalies as well as chemical (CH_4) and mineral (Mn) species scavenging are often used as tracers for plume path (Baker et al. 1995). In the Cascadia Basin, regional conductive heating and local hydrothermal venting, despite being confined to small 1 km^2 outcrops, significantly alter bottom water composition over distances of up to 10 km (Thomson et al. 1995).

Because plumes can alter physical characteristics of the deep sea, it is reasonable to assume that biological characteristics may also be affected.

1.2.5 Microbial activity

In the rising plume, microbial biomass and particulate DNA concentration substantially increase relative to background water (Corliss et al. 1979, Cowen et al. 1986, Winn and Karl 1986, Straube et al. 1990, Lilley et al. 1995). Karl et al (1980) found microbial ATP biomass within Galápagos vent water to be 334 times greater than that in 'control' deep water samples collected at the same depth and 3.9 times greater than that found in productive surface waters.

Chemical reactions caused by rapid mixing between vent fluid and ambient water can provide significant metabolic energy for chemolithoautotrophic microbes within hydrothermal plumes (Lilley et al. 1995, Lupton 1995). Microbes are able to oxidize sulphide (H_2S), methane (CH_4), hydrogen (H_2) or metals (Fe and Mn) found in buoyant effluent and use the energy gained in the fixation of CO_2 (Jannasch and Mottl 1985).

Elemental sulphur and iron sulphides can be carried considerable distances with the plume and represent a substantial source of energy for autotrophic metabolism regardless of whether particles remain suspended in the plume or settle to the ocean floor (Feely et al. 1987, Feely et al. 1994). As elemental sulphur (S) and hydrogen (H_2) are depleted through biological or chemical processes, the activity of S and H_2 oxidizers will diminish within the early stages of plume development thus the majority of primary productivity in the plume may actually occur in close proximity to the vent (McCollom 2000).

1.2.6 Particle flux

Chemical scavenging and sedimentation of coarse-grained particles play important roles in the composition of buoyant and neutrally buoyant plumes (Feely et al. 1990). Rapid particle growth of sediment grains occurs in the first few centimetres above a vent orifice; large sulphide particles rapidly precipitate out in close proximity to the vent source while finer sulphide particles may be carried along with the plume over larger distances (Walker and Baker 1988, Feely et al. 1990, Feely et al. 1994). Particle-size distributions of hydrothermal origin can be readily distinguished from those of benthic nephloid layers, often being less than 2 μm, and are necessary in estimating bacterial activity within the plume (Walker and Baker 1988).

Bacterial chemosynthesis is fueled by anomalously high concentrations of dissolved gases (Jannasch and Mottl 1985) and reduced metals (Klinkhammer and Hudson 1986) generating organic matter in the advecting plume (Roth and Dymond 1989, Cowen et al. 1990, McCollom 2000). Chemical and metal species are broken down through biologically mediated reactions, are precipitated and sink to the seafloor (Lilley et al. 1995).

Roth and Dymond (1989) found that more than 95% of the organic carbon collected 21 m above the Main vent field on the Endeavour Segment (Juan de Fuca) has a near-bottom chemosynthetic source. At the neutrally buoyant plume, 100-200 m above bottom (mab), organic carbon/carbonate carbon ratios increase sharply as the result of an increase in input of chemosynthetically derived carbon, primarily obtained from microbial processes within the plume (about 62%). At 400-500 mab, a minimum in flux of organic particles was observed, suggesting that zooplankton feeding (removing

particles from laterally spreading plume), biologically mediated particle breakdown and effect of currents on particle collection were consuming particles. These patterns of particle flux suggest nutrient cycling is occurring and support the hypothesis that laterally dispersing plumes are three-dimensional, biologically active zones in the deep sea.

The chemically and organically enriched plume has well-defined physical 'boundaries'; it presents a volume of 'confined' water that zooplankton can easily locate (Roth and Dymond 1989). Cowen et al. (2001) showed that plume and epiplume (above the neutrally buoyant plume) zooplankton at Endeavour feed on a mix of hydrothermal and chemosynthetic sources of nutrition. Sources of hydrothermal particulate organic carbon (POC) include: organic compounds derived from subsurface microbial and thermochemical processes (Comita et al. 1984, Deming and Baross 1993); exudation, sloughing, feeding and release of eggs and larvae contributed by vent biota (Comita et al. 1984); and *in situ* production within buoyant and neutrally buoyant plumes (Cowen et al. 1990, McCollom 2000). The ascending flux of vent particulate organic matter at Endeavour is six times greater over vent fields than in non-vent areas and is roughly equivalent to the downward particulate fluxes at similar oceanic depths (Wakeham et al. 2001). These ascending particles are enriched up to 200 fold in lipid-rich particles compared to descending particles (Wakeham et al. 2001). Cowen et al (2001) speculate that ascending particles might provide the mechanism for delivering food from the zooplankton-scarce zone within plumes to zooplankton-rich regions above plumes.

1.3 Pelagic organisms at vents

Zooplankton and nekton found within tens of metres of the bottom near vents have to contend with rapidly changing chemical and physical conditions, changing flow speed and direction and variable particle flux (Kaartvedt et al. 1994). Little research focuses specifically on zooplankton, endemic or otherwise, particularly in the NE Pacific. Studies of zooplankton at hydrothermal vents are summarized in Table 1.1.

Table 1.1 Summary of zooplankton studies at hydrothermal vents. MAB=metres above bottom. EPR=East Pacific Rise, JdFR=Juan de Fuca Ridge, MAR=Mid-Atlantic Ridge.

Source	Location	Depth (m)	MAB	Study Complexity	Major Results
Near-bottom studies					
Smith (1985)	EPR 21°N Clam Acres	2600	1	-*in situ* rates of O_2 consumption	-vent and non-vent dominated by calanoid *Isaacsicalanus paucisetus* (Spinocalanidae)
Berg and Van Dover (1987)	EPR	2600	1-23	-compare abundance, biomass and composition at vent and non-vent sites	-amphipods, copepods dominate -abundance: 3.4-19 individuals/m^3 -amphipod endemic to vent; mostly juveniles
	Guaymas Basin	2000	1-23		-biomass dominants: copepods (1-3 mab) -abundance: 1.5-9.1 individuals/m^3
	Non-vent	2000	1-5 186-207		-biomass dominants: copepods (200 mab) -abundance: 1.8-4.4 individuals/m^3 **Overall findings:** -one to two order magnitude difference between (a) vent and non-vent and (b) surface and vent zooplankton biomass -vent copepods primarily siphonostome and poecilostome copepods (rarely found in "typical" deep-sea)
Wiebe et al. (1988)	EPR Guaymas Basin	2000	100	-distribution and composition of total standing stock	-little or no evidence for enrichment of biomass -total numbers ind. 2600-4800/1000m^3 -most abundant (in order): calanoids, cyclopoids, ostracods, chaetognaths, amphipods

Table 1. continued

Source	Location	Depth (m)	MAB	Study Complexity	Major Results
Near-bottom studies					
Kaartvedt et al. (1994)	EPR Venture Fields 9°31-46'N	2500	0.5	-characteristics of amphipod swarm	-monospecific assemblage of pardaliscid amphipods -density exceed 1000 ind/L -swim to maintain position in current
Kim and Mullineaux (1998)	EPR 9°50'N	2500	<15 >15 within and away from valley	-distribution of larvae and holoplankton with respect to current meter records -determine if vent-associated plankton community exists in addition to benthic community	–no detailed vertical patterns discerned -all taxa more abundant in <15mab samples -copepods and amphipods most abundant, but not quantified -larvaceans and siphonophores taken in pump sample from diffuse flow (in swarm of amphipods) appear highly tolerant of elevated temperature, reduced chemicals and heavy metals
Tunnicliffe (2000)	JdFR High Rise field, Endeavour Segment	2000	20-30	-visual study of fauna in water column above vent field	-zooplankton less abundant along fault axis than along edges of vent field; possibly in response to effluent characteristics -jellyfish appear to be less abundant where particulate load is higher -nekton concentrate along venting axis; fish species is known predator at vent fields
Khripounoff et al. (2001)	MAR Rainbow vent field	2200	1.5, 150, 300	-particle flux and transport -production and dispersion of particles	-high variation in zooplankton density with distance from vent site -common holoplankton more abundant in trap closer to vents (500m) than those far away (1-2 km) -copepods found closer to vents than euphausiids; maybe less sensitive to plume toxicity

Table 1. continued

Source	Location	Depth (m)	MAB	Study Complexity	Major Results
Neutrally buoyant plume studies					
Thomson et al. (1992)	JdFR Endeavour Segment	1800-2000	100-200m	-acoustic profile and net tows to describe deep scattering layer associated with neutrally buoyant plume	-83 taxa; wet weight biomass 21mg/m^3 -few large zooplankton found in zone of maximum chemical enrichment (plume core)
Burd et al. (1992)	JdFR Endeavour Segment	1700-2000	200-300	-concurrent T, S, light attenuation and backscatter profiles -describe composition, size distribution and biomass of zooplankton	-region of enhanced zooplankton concentration within 100m of plume top; may be associated with plume-related nutrient enrichment vertical zonation caused by animal migration -carnivorous and filter-feeding species -few organisms present in plume core -copepods dominant
Burd and Thomson (1994)	JdFR Endeavour Segment	1700-2000	200-300	-better define extent and composition of deep zooplankton scattering layers -compare standing stock over vent site versus standing stock 10-50km off axis	-two distinct copepod assemblages within 3km of vent site (1. epipelagic/mid-depth species, 2. deep species) -shallow infiltrate deep assemblage in vent area through vertical migration -standing zooplankton stock 15km and 50km off axis composed entirely of deep-sea fauna -link enhanced biomass over vents with vertical migration between lower and upper ocean layers
Burd and Thomson (1995)	JdFR Endeavour Segment	1700-2000	200-300	-better define extent and composition of deep zooplankton scattering layers	-abundance and biomass at all depths higher and more variable over main vent field than 10-50km off axis -species most enriched in abundance are normally found between 400-900 m depth

Table 1. continued

Source	Location	Depth (m)	MAB	Study Complexity	Major Results
Neutrally buoyant plume studies					
Burd and Thomson (2000)	JdFR Endeavour Segment	To 3000	>100	-better define extent and composition of deep zooplankton scattering layers	-medusae enhanced (biomass) near vent field, especially Trachymedusae -predaceous medusae respond opportunistically to enhance zooplankton biomass -salps and ctenophores were rare (fragile)
Burd et al. (2002)	JdFR Endeavour Segment	1700-2000	200-300	-compare stable carbon and nitrogen isotope ratios in zooplankton	-epiplume zooplankton groups show $\delta^{15}N$ and $\delta^{13}C$ ratios similar to those found within vent bacteria and consumers -may consume upwelled organic matter and newly synthesized organic matter from plume
Water column studies					
Vereshchaka and Vinogradov (1999)*	MAR Broken Spur	3050-3150	Surface to 2000m and 2000m to bottom	-composition, abundance and biomass profiles throughout water column	-two aggregations – one in pycnocline and one near plume -biomass depleted within plume core -gelatinous animals and radiolarians dominate both aggregations by biomass -abundant: copepods, euphausiids
Vinogradov et al. (2003)*	MAR 6 vent fields	Range from 800-3670	Seafloor to 50m, 50m to surface	-zooplankton distributions above southern abyssal and northern abyssal vent fields	-zooplankton more abundant over northern fields where surface productivity higher -only gelatinous zooplankton increase in abundance near plume depth and seafloor (especially ctenophores) -overall, zooplankton are not more abundant in water column over vent fields than over Porcupine abyssal plains (N. Atlantic)

**In situ* observation from manned submersible in addition to plankton tows.

Near-bottom

One of the earliest studies of near bottom zooplankton composition and distribution is that of Berg and Van Dover (1987). At altitudes between 1 and 20 mab, they found zooplankton biomass at vents to be one to two orders of magnitude greater than at non-vent deep sea sites. Zooplankton groups (siphonostome and poecilostome copepods, amphipods) enriched at vent sites were virtually absent from non-vent areas. The chemically enriched vent fluids that support free-living populations of chemoautotrophic bacteria may present a highly valuable resource to only a few species of copepods and amphipods (Van Dover and Fry 1994, Khripounoff et al. 2001). Conversely, Wiebe et al (1988) found little evidence of zooplankton enrichment 100m above vent fields sampled by Berg and Van Dover.

Monospecific assemblages of calanoid copepods and pardaliscid amphipods are common over vent fields on the East Pacific Rise (Smith 1985, Kaartvedt et al. 1994) while *Rimicaris* shrimp are the dominant fauna at Mid-Atlantic Ridge sites (Herring and Dixon 1998, Polz et al. 1998). No swarms of pelagic fauna have been found at NE Pacific vent sites.

More recent work near the benthic-pelagic interface at vents has focused on larval transport of benthic species (Kim et al. 1994, Mullineaux et al. 1995, Kim and Mullineaux 1998, Metaxas 2001). Only Kim and Mullineaux (1998) made any attempt to quantify zooplankton. They found copepods and amphipods to be numerically dominant, as well as juvenile siphonophores and adult larvaceans. Most notable is that gelatinous zooplankton are found in pump samples taken from diffuse flow. This suggests that they may be tolerant of elevated temperatures, reduced chemicals and heavy metals that are associated with hydrothermal fluid flow.

Tunnicliffe (2000) used video to assess the spatial pattern of zooplankton and nekton above a hydrothermal vent field on Endeavour Segment. A preliminary study that led to the development of this thesis documented decreased zooplankton abundance directly over the main area of venting. Nekton, such as shrimp and macrourid fish, appeared to concentrate along the major fault scarp where venting occurs. Macrourids are known predators at vents (Tunnicliffe et al. 1990). Because zooplankton abundance showed little relation to particulate load, Tunnicliffe suggested that their dispersion was

likely related to other plume characteristics, e.g. chemical concentration and microbial activity.

Neutrally buoyant plume

Some of the most comprehensive work on benthic-pelagic interaction in the vicinity of hydrothermal vents is by Burd et al (1992), Burd and Thomson (1994, 1995, 2000) and Burd et al (2002) (see Table 1.1). Their work on zooplankton sampled from a deep scattering layer in the water above and below the neutrally buoyant plume suggests that surface and mid-depth zooplankton and nekton are attracted to and feed on particles vertically advected by the buoyant plume to altitudes 200 mab. The composition of these populations varies with distance from the vent source and with season however, the majority of species are found in typical mid or deep ocean environments (e.g. *Neocalanus* sp., *Spinocalanus* sp.). Zooplankton feeding in or near the neutrally buoyant plume within 3 km of the source vent fields are primarily mid-depth species found roughly 1000 m below their 'typical' depth range. As distance from the source increases, plume signature decreases and with it, particulate and bacteria food resources. At 50 km from the source vent field, the deep scattering layer has disappeared and typical deep sea copepods dominate the sparse communities. No mid-depth or surface species are found in these distant deep scattering layers.

Also notable are studies by Vereshchaka and Vinogradov (1999) and Vinogradov et al (2003). They have documented zooplankton composition and abundance in the water column over hydrothermal vent fields in the Mid-Atlantic using net tows as well as *in situ* observation from manned submersibles. Zooplankton are identified and counted using a 2 x 2 m frame mounted on the outside of the submersible. They found two distinct assemblages: one in the pycnocline and one near the neutrally buoyant plume. Unlike other studies, Vinogradov et al (2003) found that zooplankton abundance did not significantly increase in association with the hydrothermal vent fields. They observed that gelatinous zooplankton, particularly ctenophores, increased in abundance at plume depth and near the seafloor at vent sites. However, in a study of vertical zooplankton distribution over the Porcupine abyssal plains in the NE Atlantic, Vinogradov et al (2003) found that similar increases in gelatinous zooplankton abundance occur over non-vent

areas suggesting that increased gelatinous zooplankton abundance over vents was not necessarily associated with venting activity.

While the majority of studies have found increased abundance of zooplankton near vent fields, no studies have looked at the effect of vent effluent on zooplankton and nekton near the seafloor at multiple scales. Are certain characteristics of vent effluent more influential in organism distribution than others?

1.4 Objectives

In this study, I look at how hydrothermal outflow influences the dispersion of zooplankton and nekton near the seafloor. I assess:

1. horizontal spatial patterns over a 3 km distance;
2. relationships between organism distribution and environmental characteristics; and
3. composition of zooplankton assemblages among vent environments.

In **Chapter 2**, I use video of the water layer 20 mab to assess spatial patterns of organisms and to relate these to environmental processes. Specifically, I:

1. identify patterns in abundance over the whole area (vent and non-vent) and over the individual vent fields at different scales; and
2. highlight relationships between organism abundances and environmental conditions unique to the vent system.

This study is unique: video assessment of pelagic organism dispersion is rare. Only one other video study of pelagic organisms has been made at hydrothermal vents (Tunnicliffe 2000). No other vent studies have collected navigation and environmental data at such high resolution.

In **Chapter 3**, using samples collected from Juan de Fuca and Explorer Ridges, I assess zooplankton assemblage characteristics (e.g. species composition, sex ratio, life stage) among vent and non-vent areas. I compare my results to those found in other studies of zooplankton at vents and in the typical deep sea. This work is more representative of traditional approaches in sampling pelagic organisms in the deep sea.

In the **Summary**, I attempt to 1) address the issue of the role of vent productivity in the deep sea and 2) synthesize a comprehensive picture of how vent effluent influences the dispersion of zooplankton and nekton near the seafloor.

1.5 References

Armi, L. and Millard, R. C. J. 1976. The bottom boundary layer of the deep ocean. Journal of Geophysical Research **81**: 4983-4990.

Baker, E. T., German, C. R. and Elderfield, H. 1995. Hydrothermal plumes over spreading-centre axes: Global distributions and geological inferences. In: Humphris, S. E., Zierenberg, R. A., Mullineaux, L. S. and Thomson, R. E. (eds.), Seafloor hydrothermal systems: Physical, chemical, biological and geological interactions. American Geophysical Union, pp. 47-71.

Baker, E. T. and Massoth, G. J. 1987. Characteristics of hydrothermal plumes from two vent fields on the Juan de Fuca Ridge, northeast Pacific Ocean. Earth and Planetary Science Letters **85**: 59-73.

Berg, C. J. J. and Van Dover, C. L. 1987. Benthopelagic macrozooplankton communities at and near deep-sea hydrothermal vents in the eastern Pacific Ocean and the Gulf of California. Deep-Sea Research **34**: 379-401.

Brown, J., Colling, A., Park, D., Phillips, J., Rothery, D. and Wright, J. 1991. Seawater: Its composition, properties and behaviour. Pergammon Press.

Burd, B. J. and Thomson, R. E. 1994. Hydrothermal venting at Endeavour Ridge: Effect on zooplankton biomass throughout the water column. Deep-Sea Research I **41**: 1407-1423.

Burd, B. J. and Thomson, R. E. 1995. Distribution of zooplankton associated with the Endeavour Ridge hydrothermal plume. Journal of Plankton Research **17**: 965-997.

Burd, B. J. and Thomson, R. E. 2000. Distribution and relative importance of jellyfish in a region of hydrothermal venting. Deep-Sea Research I **47**: 1703-1721.

Burd, B. J., Thomson, R. E. and Calvert, S. E. 2002. Isotopic composition of hydrothermal epiplume zooplankton: evidence of enhanced carbon recycling in the water column. Deep-Sea Research I **49**: 1877-1900.

Burd, B. J., Thomson, R. E. and Jamieson, G. S. 1992. Composition of a deep scattering layer overlying a mid-ocean ridge hydrothermal plume. Marine Biology **113**: 517-526.

Cannon, G. A., Pashinski, D. J. and Lemon, M. R. 1991. Middepth flow near hydrothermal venting sites on the southern Juan de Fuca Ridge. Journal of Geophysical Research **96**: 12,815-12,831.

Cannon, G. A., Pashinski, D. J. and Stanley, T. J. 1995. Fate of event hydrothermal plumes on the Juan de Fuca Ridge. Geophysical Research Letters **22**: 163-166.

Comita, P. B., Gagosian, R. B. and Williams, P. M. 1984. Suspended particulate organic material from hydrothermal vent waters at 21°N. Nature **307**: 450-453.

Corliss, J. B., Dymond, J., Gordon, L. I., Edmond, J. H., von Herzen, R. P., Ballard, R. D., Williams, K. D., Bainbridge, A., Crane, R. and van Andel, T. H. 1979. Submarine thermal springs on the Galapagos Ridge. Science **203**: 1073-1083.

Cowen, J. P., Bertram, M. A., Wakeham, S. G., Thomson, R. E., Lavelle, J. W., Baker, E. T. and Feely, R. A. 2001. Ascending and descending particle flux from hydrothermal plumes at Endeavour Segment, Juan de Fuca Ridge. Deep-Sea Research I **48**: 1093-1120.

Cowen, J. P., Massoth, G. J. and Baker, E. T. 1986. Bacterial scavenging of Mn and Fe in a mid- to far-field hydrothermal vent plum. Nature **322**: 169-171.

Cowen, J. P., Massoth, G. J. and Feely, R. A. 1990. Scavenging rates of dissolved manganese in a hydrothermal vent plume. Deep-Sea Research **37**: 1619-1637.

Delaney, J. R., Kelley, D. S., Lilley, M. D., Butterfield, D. A., McDuff, R. E., Baross, J. A., Deming, J. W., Johnson, H. P. and Robigou, V. 1997. The Endeavour hydrothermal system I: Cellular circulation above an active cracking front yiedls large sulfide structures, "fresh" vent water and hyperthermophilic Archaea. RIDGE Events **July**: 11-20.

Delaney, J. R., Robigou, V. and McDuff, R. E. 1992. Geology of a vigorous hydrothermal system on the Endeavour Segment, Juan de Fuca Ridge. Journal of Geophysical Research **97**: 19,663-19,682.

Deming, J. W. and Baross, J. A. 1993. Deep-sea smokers: Windows to a subsurface biosphere? Geochimica et Cosmochimica Acta **57**: 3219-3230.

Embley, R. W. 2002. Ring of Fire. http://oceanexplorer.noaa.gov/explorations/02fire/logs/yr_sum/yr_sum.html

Feely, R. A., Geiselmand, T. L., Baker, E. T. and Massoth, G. J. 1990. Distribution and composition of hydrothermal plumes particles from the ASHES vent field at Axial Volcano, Juan de Fuca Ridge. Journal of Geophysical Research **95**: 12,855-12,873.

Feely, R. A., Lewison, M., Massoth, G. J., Robert-Baldo, G., Lavelle, J. W., Byrne, R. H., Von Damm, K. L. and Curl, H. C. J. 1987. Composition and dissolution of black

smoker particulates from active vents on the Juan de Fuca Ridge. Journal of Geophysical Research **92**: 11,347-11,363.

Feely, R. A., Massoth, G. J., Trefry, J. H., Baker, E. T., Paulson, A. J. and Lebon, G. T. 1994. Composition and sedimentation of hydrothermal plume particles from North Cleft segment, Juan de Fuca Ridge. Journal of Geophysical Research **99**: 4985-5006.

Graf, G. 1992. Benthic-pelagic coupling: a benthic view. Oceanography and Marine Biology: An Annual Review **30**: 149-190.

Hammond, S. R. 1990. Relationships between lava types, seafloor morphology and the occurence of hydrothermal venting in the ASHES vent field of Axial Volcano. Journal of Geophysical Research **95**: 12875-12893.

Helfrich, K. R. and Speer, K. G. 1995. Oceanic hydrothermal circulation: Mesoscale and basin-scale flow. In: Humphris, S. E., Zierenberg, R. A., Mullineaux, L. S. and Thomson, R. E. (eds.), Seafloor hydrothermal systems: Physical, chemical, biological and geological interactions. American Geophysical Union, pp. 347-356.

Herring, P. J. and Dixon, D. R. 1998. Extensive deep-sea dispersal of postlarval shrimp from a hydrothermal vent. Deep-Sea Research I **45**: 2105-2118.

Jannasch, H. W. 1995. Microbial interactions with hydrothermal fluids. In: Humphris, S. E., Zierenberg, R. A., Mullineaux, L. S. and Thomson, R. E. (eds.), Seafloor hydrothermal systems: Physical, chemical, biological and geological interactions. American Geophysical Union, pp. 273-296.

Jannasch, H. W. and Mottl, M. J. 1985. Geomicrobiology of deep-sea hydrothermal vents. Science **229**: 717-725.

Johnson, H. P. and Embley, R. W. 1990. Axial Seamount: An active ridge axis volcano on the central Juan de Fuca Ridge. Journal of Geophysical Research **95**: 12,689-12,696.

Juniper, K. S. and Tunnicliffe, V. 1997. Crustal accretion and the hot vent ecosystem. Philosophical Transactions of the Royal Society of London Series A **355**: 459-474.

Kaartvedt, S., Van Dover, C. L., Mullineaux, L. S., Wiebe, P. H. and Bollens, S. M. 1994. Amphipods on a deep-sea hydrothermal treadmill. Deep-Sea Research I **41**: 179-195.

Karl, D. M., Wirsen, C. O. and Jannasch, H. W. 1980. Deep-sea primary production at the Galápagos hydrothermal vents. Science **207**: 1345-1347.

Khripounoff, A., Vangriesheim, A., Crassous, P., Segonzac, M., Colaco, A., Desbruyeres, D. and Barthelemy, R. 2001. Particle flux in the Rainbow hydrothermal vent field (Mid-Atlantic Ridge): Dynamics, mineral and biological composition. Journal of Marine Research **59**: 633-656.

Kim, S. L. and Mullineaux, L. S. 1998. Distribution and near-bottom transport of larvae and other plankton at hydrothermal vents. Deep-Sea Research II **45**: 423-440.

Kim, S. L., Mullineaux, L. S. and Helfrich, K. R. 1994. Larval dispersal via entrainment into hydrothermal vent plumes. Journal of Geophysical Research **99**: 12,655-612,665.

Klinkhammer, G. and Hudson, A. 1986. Dispersal patterns for hydrothermal plumes in the South Pacific using manganese as a tracer. Earth and Planetary Science Letters **79**: 241-249.

Lilley, M. D., Feely, R. A. and Trefry, J. H. 1995. Chemical and biochemical transformations in hydrothermal plumes. In: Humphris, S. E., Zierenberg, R. A., Mullineaux, L. S. and Thomson, R. E. (eds.), Seafloor hydrothermal systems: Physical, chemical, biological and geological interactions. American Geophysical Union, pp. 369-291.

Lupton, J. E. 1990. Water column hydrothermal plumes on the Juan de Fuca Ridge. Journal of Geophysical Research **95**: 12,829-12,842.

Lupton, J. E. 1995. Hydrothermal plumes: Near and far field. In: Humphris, S. E., Zierenberg, R. A., Mullineaux, L. S. and Thomson, R. E. (eds.), Seafloor hydrothermal systems: Physical, chemical, biological and geological interactions. American Geophysical Union, pp. 317-346.

Lupton, J. E., Delaney, J. R., Johnson, H. P. and Tivey, M. A. 1985. Entrainment and vertical transport of deep-ocean water by buoyant hydrothermal plumes. Nature **316**: 621-623.

Marcus, N. and Boero, F. 1998. Minireview: The importance of benthic-pelagic coupling and the forgotten role of life cycles in coastal aquatic systems. Limnology and Oceanography **43**: 763-768.

McCollom, T. M. 2000. Geochemical constraints on primary productivity in submarine hydrothermal vent plumes. Deep-Sea Research I **47**: 85-101.

McDuff, R. E. 1995. Physical dynamics of deep-sea hydrothermal plumes. In: Humphris, S. E., Zierenberg, R. A., Mullineaux, L. S. and Thomson, R. E. (eds.), Seafloor hydrothermal systems: Physical, chemical, biological and geological interactions. American Geophysical Union, pp. 357-368.

Metaxas, A. 2001. Behaviour in flow: Perspectives on the distribution and dispersion of meroplanktonic larvae in the water column. Canadian Journal of Fisheries and Aquatic Sciences **58**: 86-98.

Mullineaux, L. S., Wiebe, P. H. and Baker, E. T. 1995. Larvae of benthic invertebrates in hydrothermal vent plumes over Juan de Fuca Ridge. Marine Biology **122**: 585-596.

Murton, B. J., Redbourn, L. J., German, C. R. and Baker, E. T. 1999. Sources and fluxes of hydrothermal heat, chemicals and biology within a segment of the Mid-Atlantic Ridge. Earth and Planetary Science Letters **171**: 301-317.

Polz, M. F., Robinson, J. J., Cavanaugh, C. M. and Van Dover, C. L. 1998. Trophic ecology of massive shrimp aggregations at a Mid-Atlantic Ridge hydrothermal vent site. Limnology and Oceanography **43**: 1631-1638.

Raffaelli, D., Bell, E., Weithoff, G., Matsumoto, A., Cruz-Motta, J. J., Kershaw, P., Parker, R., Parry, D. and Jones, M. 2003. The ups and downs of benthic ecology: considerations of scale, heterogeneity and surveillance for benthic-pelagic coupling. Journal of Experimental Marine Biology and Ecology **285-286**: 191-203.

Robigou, V., Delaney, J. R. and Stakes, D. S. 1993. Large massives sulfide deposits in a newly discovered active hydrothermal system, the High-Rise field, Endeavour Segment, Juan de Fuca Ridge. Geophysical Research Letters **20**: 1887-1890.

Rona, P. A., Palmer, D. R., Jones, C., Chayes, D. A., Czarnecki, M., Carey, E. W. and Guerrero, J. C. 1991. Acoustic imaging of hydrothermal plumes, East Pacific Rise, 21°N, 109°W. Geophysical Research Letters **18**: 2233-2236.

Rona, P. A. and Speer, K. G. 1989. An Atlantic hydrothermal plume: Trans-Atlantic Geotraverse (TAG) area, Mid-Atlantic Ridge crest near 26°N. Journal of Geophysical Research **94**: 13,879-13,893.

Rona, P. A. and Trivett, D. A. 1992. Discrete and diffuse heat transfer at ASHES vent field, Axial Volcano, Juan de Fuca Ridge. Earth and Planetary Science Letters **109**: 57-71.

Roth, S. E. and Dymond, J. 1989. Transport and settling of organic material in a deep-sea hydrothermal plume: Evidence from particle flux measurements. Deep-Sea Research **36**: 1237-1254.

Smith, K. L. J. 1985. Macrozooplankton of a deep sea hydrothermal vent: In situ rates of oxygen consumption. Limnology and Oceanography **30**: 102-110.

Straube, W. L., Deming, J. W., Somerville, C. C., Colwell, R. R. and Baross, J. A. 1990. Particulate DNA in smoker fluids: Evidence for existence of microbial populations in hot hydrothermal systems. Applied Environmental Microbiology **56**: 1140-1147.

Thomson, R. E., Burd, B. J., Dolling, A. G., Gordon, R. L. and Jamieson, G. S. 1992. The deep scattering layer associated with the Endeavour Ridge hydrothermal plume. Deep-Sea Research **39**: 55-73.

Thomson, R. E., Davis, E. E. and Burd, B. J. 1995. Hydrothermal venting and geothermal heating in Cascadia Basin. Journal of Geophysical Research **100**: 6121-6141.

Thomson, R. E., Delaney, J. R., McDuff, R. E., Janecky, D. R. and McClain, J. S. 1992. Physical characteristics of the Endeavour Ridge hydrothermal plume during July 1988. Earth and Planetary Science Letters **111**: 141-154.

Thomson, R. E., Mihaly, S. F., Rabinovich, A. B., McDuff, R. E., Veirs, S. R. and Stahr, F. R. 2003. Constrained circulation at Endeavour ridge facilitates colonization by vent larvae. Nature **424**: 545-549.

Thomson, R. E., Roth, S. E. and Dymond, J. 1990. Near-intertial motions over a mid-ocean ridge: Effects of topography and hydrothermal plumes. Journal of Geophysical Research **95**: 7261-7278.

Trivett, D. A. 1994. Effluent from diffuse hydrothermal venting. 1. A simple model of plumes from diffuse hydrothermal sources. Journal of Geophysical Research **99**: 18,403-18,415.

Trivett, D. A. and Williams, A. J. I. 1994. Effluent from diffuse hydrothermal venting. 2. Measurement of plumes from diffuse hydrothermal vents at the southern Juan de Fuca Ridge. Journal of Geophysical Research **99**: 18,417-18,432.

Tsurumi, M. and Tunnicliffe, V. 2001. Characteristics of a hydrothermal vent assemblage on a volcanically active segment of Juan de Fuca Ridge, northeast Pacific. Canadian Journal of Fisheries and Aquatic Sciences **58**: 530-542.

Tunnicliffe, V. 1991. The biology of hydrothermal vents: Ecology and evolution. Oceanography and Marine Biology: An Annual Review **29**: 319-407.

Tunnicliffe, V. 2000. A documentation of biodiversity characteristics of the hydrothermal vent assemblages at High Rise vent field, Endeavour Segment, Juan de Fuca Ridge. University of Victoria, p. 53.

Tunnicliffe, V., Botros, M., De Burgh, M. E., Dinet, A., Johnson, H. P., Juniper, K. S. and McDuff, R. E. 1986. Hydrothermal vents of Explorer Ridge, northeast Pacific. Deep-Sea Research **33**: 401-412.

Tunnicliffe, V., Garrett, J. F. and Johnson, H. P. 1990. Physical and biological factors affecting the behaviour and mortality of hydrothermal vent tubeworms (vestimentiferans). Deep-Sea Research **37**: 103-125.

Tunnicliffe, V., Juniper, K. S. and Sibuet, M. 2003. Reducing environments of the deep-sea floor. In: Tyler, P. A. (ed.) Ecosytems of the World: The Deep Sea. Elsevier Press, pp. 81-110.

Van Dover, C. L. 2000. The ecology of deep-sea hydrothermal vents. Princeton University Press.

Van Dover, C. L. and Fry, B. 1994. Microorganisms as food resources at deep-sea hydrothermal vents. Limnology and Oceanography **39**: 51-57.

Vereshchaka, A. L. and Vinogradov, G. M. 1999. Visual observations of the vertical distribution of plankton throughout the water column above Broken Spur vent field, Mid-Atlantic Ridge. Deep-Sea Research I **46**: 1615-1632.

Vinogradov, G. M., Vereshchaka, A. L. and Aleinik, D. L. 2003. Zooplankton distribution over hydrothermal vent fields of the Mid-Atlantic Ridge. Oceanology **43**: 656-669.

Vinogradov, G. M., Vereshchaka, A. L., Musaeva, E. I. and Dyakonov, V. Y. 2003. Vertical zooplankton distribution over the Porcupine Abyssal Plain (Northeast Atlantic) in the summer of 2002. Oceanology **43**: 512-523.

Von Damm, K. L. 1995. Controls on the chemistry and temporal variability of seafloor hydrothermal fluids. In: Humphris, S. E., Zierenberg, R. A., Mullineaux, L. S. and Thomson, R. E. (eds.), Seafloor hydrothermal systems: Physical, chemical, biological and geological interactions. American Geophysical Union, pp. 222-247.

Wakeham, S. G., Cowen, J. P., Burd, B. J. and Thomson, R. E. 2001. Lipid-rich ascending particles from the hydrothermal plume at Endeavour Segment, Juan de Fuca Ridge. Geochimica et Cosmochimica Acta **65**: 923-939.

Walker, S. L. and Baker, E. T. 1988. Particle-size distributions within hydrothermal plumes over the Juan de Fuca Ridge. Marine Geology **78**: 217-226.

Wiebe, P. H., Copley, N., Van Dover, C. L., Tamse, A. and Manrique, F. 1988. Deep-water zooplankton of the Guaymas Basin hydrothermal vent field. Deep-Sea Research **35**: 985-1013.

Winn, C. D. and Karl, D. M. 1986. Microorganisms in deep-sea hydrothermal plumes. Nature **320**: 744-746.

Chapter 2

Spatial distribution of zooplankton and nekton above hydrothermal vents on the Endeavour Segment, Juan de Fuca Ridge.

2.1 Introduction

2.1.1 Ecological heterogeneity

Ecologists examine spatial patterns of species or assemblages in order to infer the existence of underlying processes (Legendre and Legendre 1998, Perry et al. 2002). Broad-scale physical processes, such as currents and winds, can create gradients or patchy structures separated by discontinuities (e.g. ocean fronts) in the physical environment (Legendre and Legendre 1998). These broad-scale physical discontinuities can lead to spatial and temporal discontinuities in biological systems (Legendre and Legendre 1998). In short, variation in the environment or, ecological heterogeneity, often leads to variation in organism spatial pattern.

In marine communities, small species with limited mobility (e.g. phytoplankton) are generally aggregated or dispersed by advective processes (Barry and Dayton 1991). Spatial and temporal patterns of pelagic organisms are linked to physical processes that regulate the stability of the water column and the flux of nutrients (Lewis 1979). River plumes, oceanic fronts and areas of upwelling are often associated with distinct changes in organism abundance and biomass (Mackas 1984, Bradford-Grieve et al. 1993, Seguin et al. 1994, Pinel-Alloul 1995, Gallager et al. 1996, Pinca and Dallot 1997, Mianzan and Guerrero 2000, Graham et al. 2001, Sabatini and Martos 2002, Ward et al. 2002). Influx of nutrients and resulting in an increase in primary productivity associated with physical discontinuities are thought to be the main cause of these aggregations.

In the hydrothermal environment, vent effluent is distinct from the surrounding bottom water. In the Pacific, effluent is characterized by higher temperature, lower salinity and increased cloudiness, and is associated with increased microbial activity (Corliss et al. 1979, Cowen et al. 1986, Winn and Karl 1986, Lilley et al. 1995). Aggregations of pelagic organisms over vent areas have been noted in the East Pacific (Berg and Van Dover 1987, Kaartvedt et al. 1994) and the Mid-Atlantic (Van Dover

2000). Some species, like *Isaacsicalanus paucisetus*, *Halice hesmonectes* and *Rimicaris exoculata*, are endemic to vents (Fleminger 1983, Van Dover et al. 1992, Wirsen et al. 1993, Gerbruk et al. 2000), whereas communities at river plume and oceanic front boundaries are not endemic and are instead composed of typical pelagic zooplankton species (e.g. *Calanus*, *Ctenocalanus*). Given that vent effluent is distinct from ambient water, do pelagic organisms increase in abundance in areas of hydrothermal venting?

2.1.2 Video in pelagic studies

There is no unique natural scale at which system processes should be studied thus patches or aggregations can be found on almost every scale of observation (Levin 1992). In zooplankton communities, spatial heterogeneity commonly occurs on a hierarchical continuum of scales (Kolasa and Rollo 1991, Pinel-Alloul 1995). Thus scale is a key concept in the collection, analysis and interpretation of spatial patterns (Hurlbert 1990, Hewitt et al. 1998, Legendre and Legendre 1998, Dungan et al. 2002). To fully explore spatial heterogeneity 'scale' must be decomposed into

1) **extent,** the total area, length, volume included in the study (e.g. sample area) and
2) **grain size,** the size of the individual sampling units which determines the resolution (Kolasa and Rollo 1991, Legendre and Legendre 1998).

While shallow water ecologists have the potential to sample and re-sample intensively over a range of scales, repeated net tows taken at depth in the ocean are painstaking and costly (Raffaelli et al. 2003). To address this issue, many researchers are turning to other methods of sampling: *in situ* viewing from manned submersibles (Mackie and Mills 1983, Vereshchaka and Vinogradov 1999, Vinogradov and Shushkina 2002, Vinogradov et al. 2003), video plankton recorders (Gallager et al. 1996, Graham et al. 2003) and video cameras (Janssen et al. 2000, Priede and Bagley 2000, Tunnicliffe 2000, Bailey and Priede 2002, Henriques et al. 2002, Jones et al. 2003).

One of the few studies to combine continuous observation methods with measurement of environmental variables was Gallager et al. (1996). They used a video plankton recorder in conjunction with temperature, salinity and pressure measurements at Georges Bank (Gulf of Maine) to observe and quantify local concentrations of plankton

with macro- and micro-scale physics. At large scales, zooplankton association with specific water masses of different origins and temperature/density discontinuities dictates spatial pattern. Within each water mass, fine-scale patchiness (on the order of 10s of metres) is associated with regions of vertical stability.

In a video study over High Rise vent field on Endeavour Segment, Tunnicliffe (2000) showed that zooplankton and gelatinous zooplankton abundances are lower in areas where the hydrothermal plume dominates, possibly in response to chemical compounds or microbial activity. Nekton, shrimp and macrourids are highly abundant to the northeast and southwest of venting. Unlike zooplankton, nekton abundance appears to be related to particulate densities.

My study is unique: *In situ* video camera observations allow assessment of horizontal spatial pattern both zooplankton and nekton at a multitude of scales. Combined with simultaneously collected environmental data, I am able to assess how ecological heterogeneity over a vent site influences the spatial pattern of pelagic organisms near the seafloor.

2.1.3 Specific objectives

I use video of the water layer 20 mab, collected in conjunction with navigation and environmental data to assess:

1) spatial pattern of pelagic organisms over a variety of extent and grain sizes at a hydrothermal vent site; and
2) associations between organism spatial pattern and environmental variables characteristic of vent effluent (i.e. does vent effluent play a role in the spatial pattern of organisms).

I assess spatial pattern using autocorrelation and Spatial Analysis Distance IndicEs (SADIE). SADIE is unique among statistical analyses in that it describes and maps local variation and association over the sample area; it determines whether the occurrence of patches and gaps in specific locations (e.g. over a vent field) is random.

I hypothesize that 1) there will be a difference in organism abundance between vent and non-vent areas and 2) local changes in abundance will be associated with vent effluent characteristics.

2.2 Methods

2.2.1 Study sites

The Endeavour Segment (47°56-58'N, 129°06'W) is located in the northern portion of the Juan de Fuca Ridge. It is a seafloor spreading ridge, roughly 250 km west of Vancouver Island (see Figure 1.1). The hydrothermally active portion of Endeavour is nearly 25 km long, 4.5 km wide and is flanked on the west by a series of seamount chains (Delaney et al. 1992). The segment is oriented north-south; currents near the seafloor are driven primarily by tidal action and flow primarily from the south to the north (Garcia-Berdeal 2002, Thomson et al. 2003). The ridge is volcanically elevated to depths of 2000-2250 m and is sediment-free (Delaney et al. 1997). Within the elevated portion of the segment, five large, active, evenly spaced high temperature vent fields and two low temperature fields have been found (Delaney et al. 1997, Johnson 2001). As a system, the Endeavour vents discharge fluid that bears unusually high concentrations of methane and ammonia; this unique chemical signature of the vent fluids and the regular spacing of the vent fields suggest that subsurface fluid flow is occurring among the vents fields (Delaney et al. 1997).

Of interest to my study is a 3.5km long, 0.5km wide section, which includes areas of high (400°C, smoker) and low (10-20°C, diffuse) temperature venting. This area encompasses four known vent fields: High Rise, Clam Bed, Raven and Main Endeavour, plus a section of non-fissured lava (a non-venting area) (Figure 2.1). These four vent fields lie along deep faults that are perpendicular to the length of the spreading centre (Figure 2.2).

High Rise Field is at the northern end of the segment at 47°58'N, 129°05.50'W. High Rise is characterized by high temperature vents, emitting fluid of approximately 330°C over a 210 x 135m area. Fluid is vigorously released through sulphide chimneys restricted to the uplifted block in the centre of the axial valley primarily at the north end

Figure 2.1 Bathymetry map of sample area on Endeavour Segment. High Rise and Main Endeavour Field (MEF) are two of the five high temperature vent fields along the Endeavour Segment. MEF is comprised of north and south sections. Clam Bed has a single smoker vent while Raven has no smokers. Another small vent field, Quebec, lies just to the south of the sample area. Axes are measured in metres; x-axis is measured in an eastward direction, y-axis is measured in a northward direction.

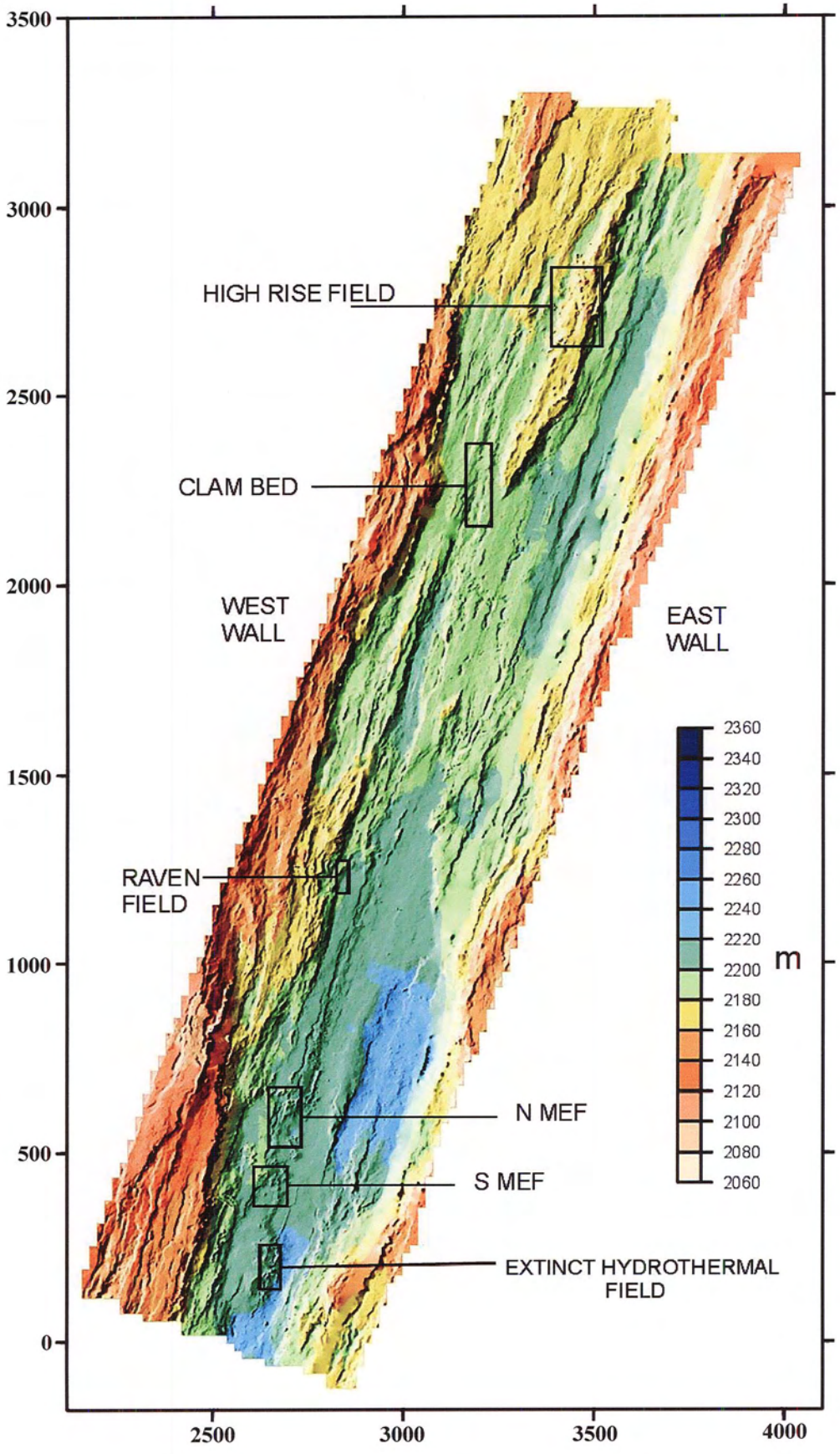
3500
3000
2500
2000
1500
1000
500
0
2500
3000
3500
4000
HIGH RISE FIELD
CLAM BED
WEST WALL
EAST WALL
RAVEN FIELD
N MEF
S MEF
EXTINCT HYDROTHERMAL FIELD
2360
2340
2320
2300
2280
2260
2240
2220
2200
2180
2160
2140
2120
2100
2080
2060
m

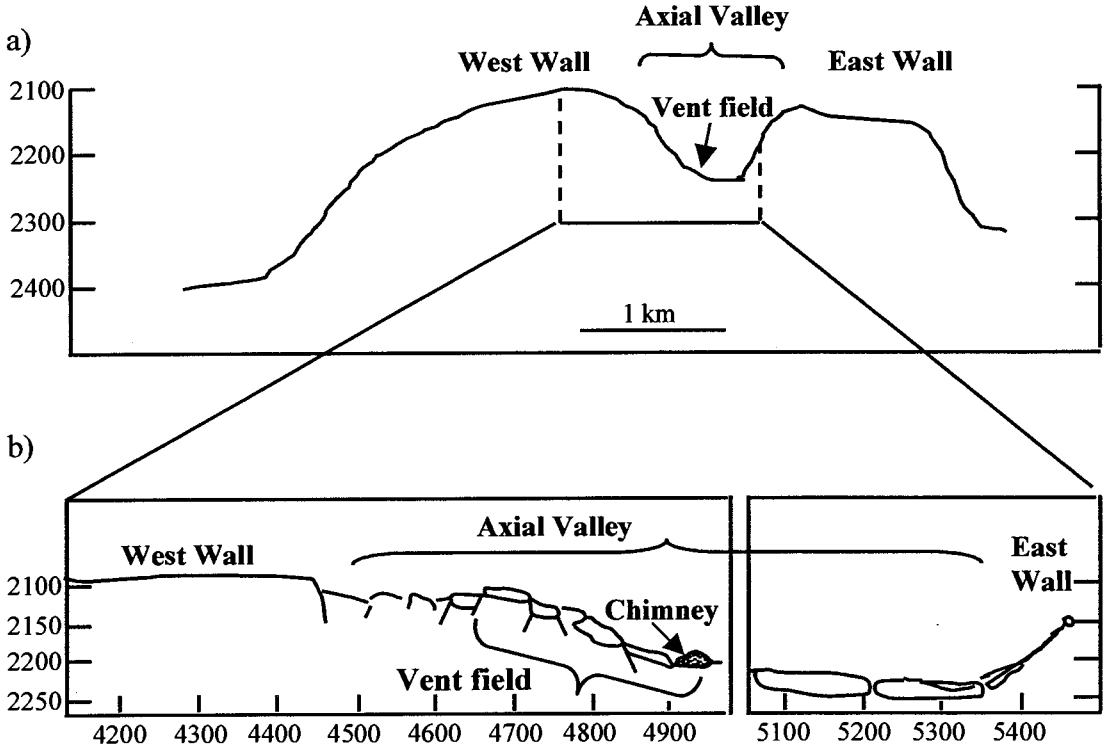

Figure 2.2 a) Cross-section of Endeavour Segment. Vent fields are located on the western half of the axial valley. b) Cross-section of the ridge. Chimneys rise from the flat, fissured basaltic floor of the axial valley. Modified from Delaney et al (1992).

of the field (Robigou et al. 1993, Delaney et al. 1997) (Figure 2.3a). Of the large chimneys, Ventnor was the only one visited during the cruise.

Clam Bed Field, roughly 200 x 74m, is a small field south of High Rise. Clam Bed is primarily diffuse (<30oC) venting. The field is roughly V-shaped: A single white smoker vent (<215°C) is located in the valley near the apex of the 'V' and is dominated by clams. The walls of the valley rise are elevated by 1 m and are characterized by low temperature diffuse venting. Tubeworms dominate vent assemblages along the valley walls while *Calyptogena sp.*, a clam, is dominant in the centre valley (pers. obs.).

Raven Field, discovered during the collection of these data, is a small field (95 x 30m), comprised solely of diffuse vents. Although the vent field community was dominated by tubeworms, the presence of sponges, sea anemones and crabs was also noted (Kurokawa 2000).

Main Endeavour Field (MEF), the southernmost field in the area sampled (47°57'N, 129°06'W), contains more than 100 actively venting sulphide chimneys routinely emitting fluids in excess of 360°C (Delaney et al. 1997) (Figure 2.3b). MEF is the largest of the four vent fields in the sample area (490 x 140m). It is characterized by steep compositional gradients in vent fluids and temperature (Delaney et al. 1997). Effluent released in the northern portion of the field is near ambient seawater salinity whereas vents in the southern portion release less saline, higher temperature fluids with greater concentrations of dissolved gases (Delaney et al. 1997). Lava flows, rather than sediment-covered seafloor, dominate the main venting area (Delaney et al. 1992). Hulk, Dudley, S&M, Milli-Q and Salut vents were visited during the cruise. The basalt floor of the vent field, extending from Dante to Salut supports diffuse venting. Benthic communities at MEF are dominated by tubeworms, polychaetes and limpets.

Vent field boundary coordinates for High Rise and MEF were determined using individual vent locations from the JAS 286 (Kurokawa 2000) and JAS 310 dives (the latter taken in August, 2001) and previously published maps of individual vent fields. I used the maps to determine distances from individual vents to vent field boundaries and then applied these distances to the vent coordinates obtained from the remote operated submersible, JASON, dives to determine vent field boundaries using JASON's coordinate

Figure 2.3 Geological maps of the two high temperature vent fields in the sample area: a) High Rise and b) Main Endeavour Field (MEF). a) is modified from Robigou et al (1993). The coordinate system used by JASON is superimposed on the original coordinates by Robigou et al. Calculations of High Rise vent field coordinates were based on known smoker locations. b) is modified from Delaney et al (1997). Venting is primarily confined to central axis of both vent fields.

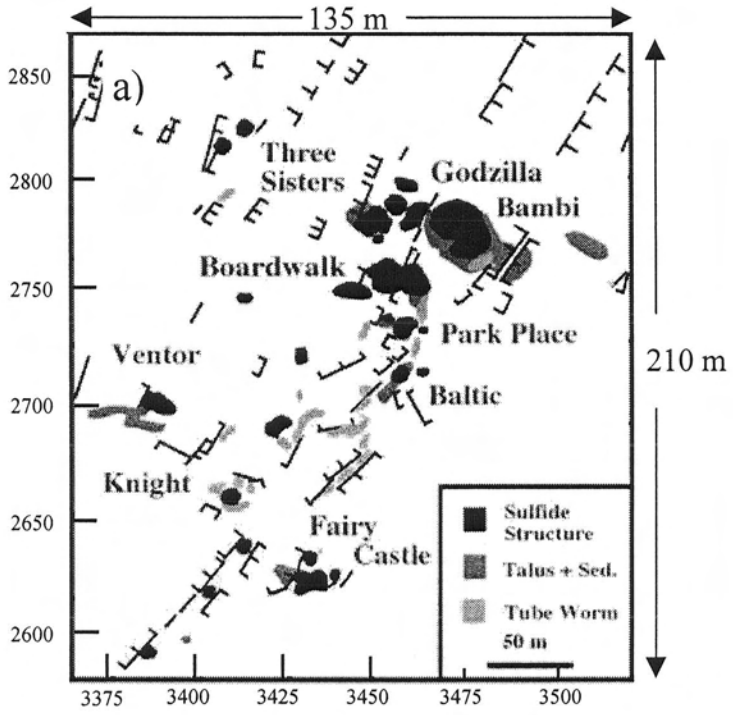
135 m
a)
Three Sisters
Godzilla
Bambi
Boardwalk
Park Place
Ventor
Baltic
Knight
Fairy Castle
Sulfide Structure
Talus + Sed.
Tube Worm
50 m
210 m
2850
2800
2750
2700
2650
2600
3375
3400
3425
3450
3475
3500

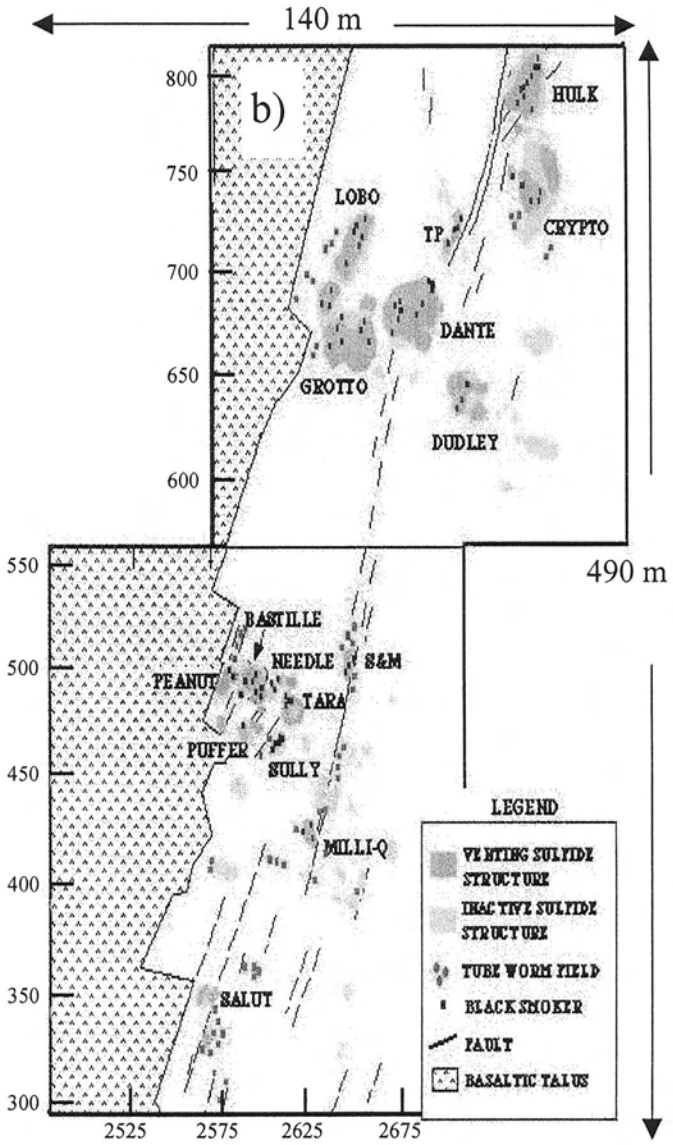
140 m
b)
HULK
LOBO
TP
CRYPTO
DANTE
GROTTO
DUDLEY
490 m
BASTILLE
NEEDLE
S&M
PEANUT
TARA
PUFFER
SULLY
MILLI-Q
SALUT
LEGEND
VENTING SULFIDE STRUCTURE
INACTIVE SULFIDE STRUCTURE
TUBE WORM FIELD
BLACK SMOKER
FAULT
BASALTIC TALUS
800
750
700
650
600
550
500
450
400
350
300
2525
2575
2625
2675

system. Boundary coordinates for Clam Bed and Raven vent fields were estimated from maps of the sample area provided by Paul Johnson, University of Washington.

The 1.5 km stretch separating Raven from Clam Bed appears to be hydrothermally inactive. Sporadic occurrence of brittle stars, anemones and spider crabs is typical of non-venting areas on the Juan de Fuca (Milligan and Tunnicliffe 1994). No venting occurs along the west wall of the Endeavour valley or to the east of MEF and High Rise.

2.2.2 Data Collection

A: Video and water layer

The remotely operated vehicle JASON flew a 3.4 x 0.5 km grid at 20 metres above bottom (mab), over a three day period from 8:47 am October 1 to 0:52 pm October 4, 2000 GMT. The sample area encompassed High Rise, Clam Bed, Raven and MEF as well as the intervening and surrounding non-venting area (Figure 2.4). The area was sampled using 12 transect lines (Table 2.1). Sampling started south of the centre and to the east of line 1. All odd numbered lines were flown from south to north, even numbered lines from north to south. Each line is separated from its neighbour by roughly 50 m. The westernmost line was number 9, line 12 the easternmost. As a result, lines 10-12 are temporally related to line 9, but are spatially nearer to line 1. This juxtaposition influenced how results were analyzed (see Section 2.2.3). Flying at a speed of 0.25 m/s, each transect line took 5-6 hours to complete.

A 'pan and tilt' video camera was mounted on the brow of the submersible. The field of view was estimated to be 0.25 x 0.25 m based on known size ranges of some organisms. A total volume of 2930 m^3 of water was sampled. The camera focused on organisms and particles in the water column directly in front of the submersible. Occasionally, the camera wandered to follow unusual organisms or to check other instrumentation. Typically, these distractions lasted less than one or two minutes and thus were not omitted from analysis.

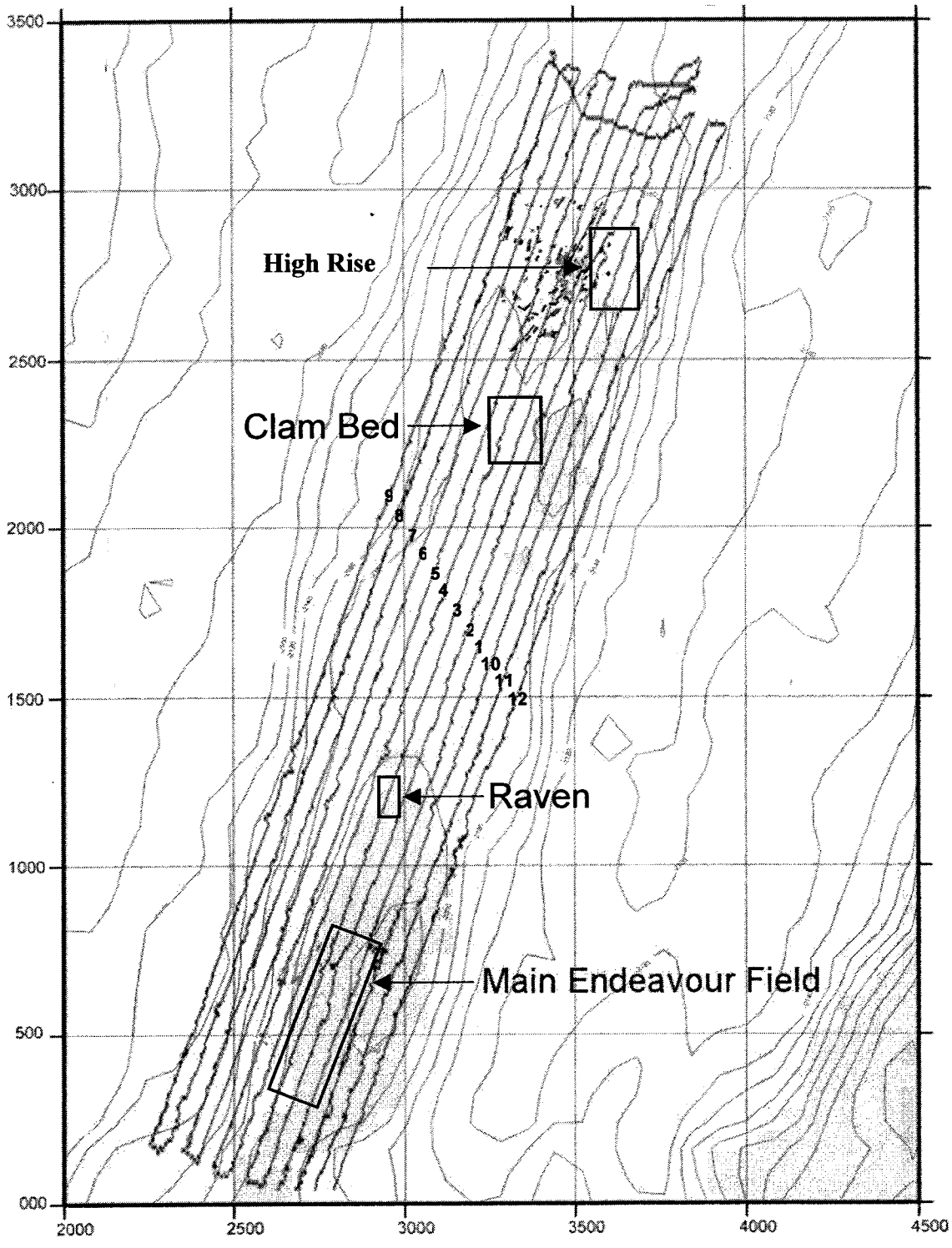

Figure 2.4 Map of area surveyed by JASON. Individual transect lines are labeled. Axes are measured in metres; x-axis is measured in an eastward direction, y-axis is measured in a northward direction.

Table 2.1 Summary of transect data collected in October 2000. Individual transect lines are noted as line #s. The fourth column indicates whether transect lines passed over both vent fields (V) and non-vent area (NV) or solely over non-vent area.

Date	Line #	Start/end time (GMT)	Seafloor character
Oct 1 2000	1	8:47-16:26 (includes 1½ hr gap)	V,NV
	2	17:06-22:00	V,NV
Oct 1-2	3	22:19-3:07	V,NV
	4	3:50-8:36	NV
	5	8:54-13:42	NV
	6	13:54-18:37	NV
	7	18:39-23:29	NV
Oct 3	8	23:37-4:11	NV
	9	4:22-9:02	NV
	10	10:03-14:42	V,NV
	11	14:48-19:31	NV
Oct 3-4	12	19:39-00:52	NV

Navigation and environmental data were collected simultaneously with video. Navigation coordinates (x-y) were obtained every three seconds. Environmental data of the horizontal water layer were collected using a Conductivity-Temperature-Density (CTD) meter and a transmissometer (Table 2.2). Environmental data were collected along the lengths of each transect line with the exception of line 7; only data from the last 350 m of this line were recorded.

Vertical circulation in the oceans is controlled by variations in both temperature and salinity; this is known as thermohaline circulation (Brown et al. 1991). In surface waters, temperature and salinity alone control the density of seawater, but at depth, pressure also becomes important (Brown et al. 1991) thus a number of different temperature and density measurements were collected and calculated.

In situ temperature is the temperature of the seawater measured at its actual depth. Potential temperature is the temperature seawater would attain if brought adiabatically to the surface. Adiabatic changes are those that occur independently of any transfer of heat to or from the surroundings. When a fluid expands, it loses internal energy and its

temperature falls whereas when it is compressed, a fluid gains internal energy and its temperature rises. While this difference in temperature measurements is never more than about 1.5°C, it still has important implications for thermohaline circulation (Brown et al. 1991) and for differentiating between vent and non-vent water. Theta anomaly is the difference in water temperature measured within the sample area minus ambient temperature of water at the same density measured at a position 10km away from the axial valley.

Theta anomaly (°C), **salinity** (practical salinity units or psu) and **light transmissivity** (measured as the percentage of light transmitted between two meters 25 cm apart) were used in analyses to identify vent effluent. Temperature variability, as captured by theta anomaly, is more useful in tracking vent effluent than an absolute temperature measure. Navigation and environmental data were collected and processed by University of Washington researchers (Dr. Paul Johnson) and graduate students (Irene Garcia Berdeal and Matt Pruis).

B: Identifying organisms from videos

The primary source of information for organism spatial pattern was imagery: high resolution (Hi8) video distinguished animals by form and motion. A total of 65 hours of video was collected. A simultaneous net tow complemented visual information and allowed identification of different zooplankton species. The net (125 μm mesh) was held in the submersible arm for the duration of the survey.

Organisms were differentiated using a variety of characteristics: locomotion (e.g. hopping, paddling, swimming), size, shape and colour (Figure 2.5; Table 2.2). Sizes ranged from almost the entire length of the field of view (macrourid fish, roughly 20-25 cm) to large copepods (about 1 cm). Because of the generally low resolution of the videos, I was only able to confidently and consistently identify organisms to broad groups (i.e. small crustaceans or zooplankton, gelatinous zooplankton, etc.) rather than to specific taxonomic levels.

I identified each organism as it appeared on-screen and recorded the abundance (count) and the time at which it appeared. Notes on picture quality (focus, lighting) were kept to distinguish between gaps in abundance and gaps created by unwatchable video.

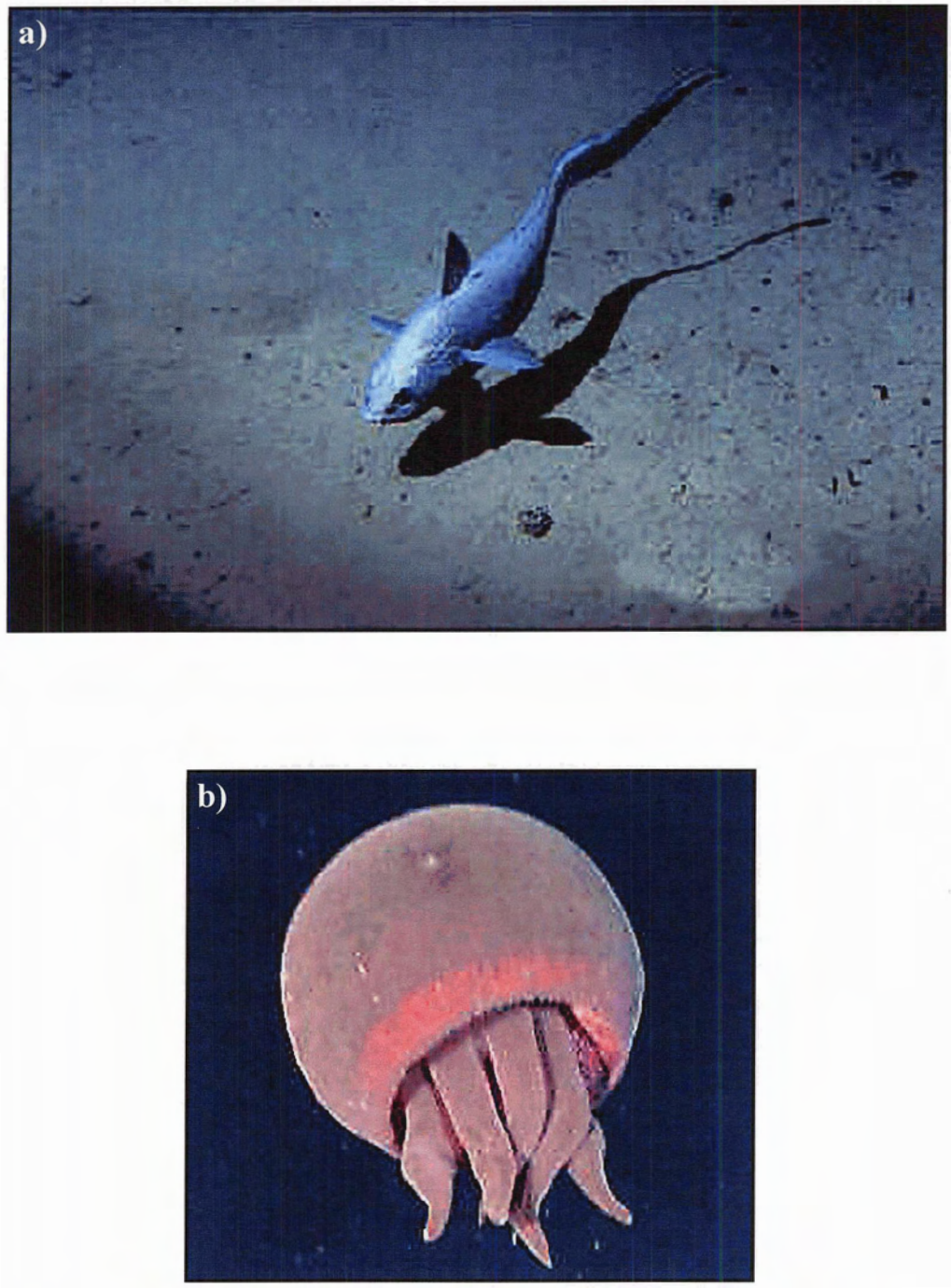

Figure 2.5 Digital images of pelagic organisms seen over vent sites a) macrourid or rattail fish (likely *Coryphaenoides sp.*) and b) *Tiburonia granrojo* (Matsumoto). This photo of *T. granrojo* was captured during the New Millenium Observatory (NeMO) cruise, July-August, 2002.

Table 2.2 Generic organism groups identified from videos. Types of organisms found in each group and how each type of organism was identified are listed. *Identifications are based on Wrobel and Mills (1998).

Group	Types of Organisms	How identified each
Zooplankton	Copepod	-Thoracic jumping, antennae swimming; shape (large)
	Euphausid	-Flapping motion; v-shaped like small shrimp
	Amphipod	-Quick paddling motion
Gelatinous zooplankton*	**Cnidaria** (Hydrozoa, Anthomedusa, Siphonophore)	-Hydrozoa and Anthomedusa - globular and faint, shape and size of umbrella -Siphonophore –strand of connected sparkly globs
	Ctenophore (Order Cyppidia, Order Lampidae, Order Lobata, Order Beroidae)	-Cyppidia – bright silver oval body, two tentacles, woven together and raised vertically -Lampidae – tubular or corseted -Lobata – two round lobes with two buds facing centre -Beroidae – similar to Hydrozoa (head-on), but much brighter; in profile, cucumber-shaped
	Chordate Family Salpidae	-Salp – similar to Beroidae, but more opaque, small silver sphere at base; aggregate forms shaped like cane
	Family Thecosomata	-Larvaceans – bright silver, central sphere surrounded by faint sparkly mucous net (circle within a circle)
	Gastropod Family Heteropoda	-Some elongate and tubular with butterfly wings; a few look like thick Cyppidia with axe shaped bodies (like 2 triangular ears)
Shrimp	*Hymenodora sp.*	-Boomerang shape; pink; paddle using swimmerets or contract thorax and abdomen; if approach head-on, identify by long antennae
Zoarcidae	*Pachycara sp.*	-Ripple (fast swimming motion); tend to halt motionless in water (stand on head; stick-like)
Macrouridae	*Coryphaenoides acrolepis*	-Languorous swimmers; larger than zoarcids; prominent head
Cephalopoda	octopus	-Opaque, globular with large paddle-like appendages
	squid	-Torpedo-shaped, rippling fins
Polychaeta	Family Tomopteridae	-Oval, flat; parapodia visibly moving
Unknown	Unidentifiable organisms	-Debris?; indistinguishable organism (e.g. might be fish or shrimp)

Tapes were watched in order (1-31). Identification of gelatinous zooplankton became more consistent with time therefore, I re-examined the first 10 videos to ensure all gelatinous zooplankton were identified with consistent skill.

Video and environmental data collection did not always overlap. Areas where one or the other is absent (e.g. no environmental data were collected during transition from one line to the next) are omitted from analyses. Simultaneous collection of environmental and video data enabled me to study the link between water characteristics and organism spatial pattern 20 mab.

2.2.3 Analyses

A: General

In order to identify an organism's location in space, I translated the time of occurrence from the video to an x-y coordinate based on the navigation data (which noted both time and position) using a custom program written in Matlab. Because navigation data were collected every 3 seconds, video time and navigation time did not always align. When this occurred, the program calculated the average position using the two nearest times.

Organism and environmental data were then grouped into different-sized, contiguous grains (bins) using Matlab (Table 2.3). Various grain sizes were chosen to reflect the range of swimming abilities of organisms (e.g. fish are relatively fast swimmers, can cover tens or hundreds of metres within a relatively short period time, whereas zooplankton may take hours to cover the same distance). Grain sizes were created based on time intervals, which were roughly equivalent to a particular distance calculated using submersible speed. Mid-point position was calculated for each grain (bin). Over the specified interval size, environmental data were averaged while organism counts were summed. Throughout the text, grain sizes are noted in terms of distance as data were analyzed spatially.

Table 2.3 Grain sizes used to summarize environmental and organism data. Distance is calculated based on submersible speed, which ranged from 0.125-0.25 m/s.

Time interval	Equivalent distance
1 minute	10m
5 minutes	55m
15 minutes	165m
30 minutes	335m

Because different spatial patterns may be evident at different scales, I initially analyzed the data using a variety of extents and grain sizes. Assuming that spatial pattern of pelagic organisms reflects conditions on the seafloor, I divided the sample area into "vent" (all vent fields pooled) and "non-vent" (all area outside the geographically described vent fields) areas. Over the entire extent, I calculated mean and variance for all groups of organisms over vent and non-vent areas. As these analyses did not show statistical differences despite obvious differences in average counts, I further divided the "non-vent" area into "between-vent field" (lines 1-3 which pass over at least one of High Rise and MEF) and "non-vent" (all area outside vent fields and excluding lines 1-3).

At the vent field extent, I limited comparisons to High Rise, Clam Bed and MEF; Raven contained only one 55 m interval (or five 10 m intervals). Only the 55 m and 10 m grain sizes were used to compare average organism counts among vent fields as the two larger grain sizes were often larger than the fields themselves.

To test the hypothesis of no difference in organism abundance among vent, between-vent and non-vent areas, I used a single-factor ANOVA with a post-hoc Tukey test. The ANOVA assumes normality in distribution and equality of variances among groups however, it is a robust test and operates well with considerable heterogeneity of variance if all sample sizes are or are nearly equal or if larger sample variation is associated with the larger samples thus minimizing Type I error (Zar 1984).

Because the ANOVA does not indicate which samples significantly differ, I employed a post-hoc Tukey test which is also relatively robust to departures from its assumptions. The Tukey test identifies sample means that differ by ranking the sample averages and tabulating the pair-wise differences (Zar 1984). For all tests, I used a significance level of α=0.05.

B: Detecting pattern

Video and environmental data constitute series: sequences of observations that are ordered in space. As such, I can look for trends and patterns in the data.

Mapping of spatial data is highly recommended for assessing patterns and for interpreting analysis (Pielou 1977, Diggle 1983, Legendre and Legendre 1998, Perry 1998, Perry et al. 2002). As patchiness can be found at multiple spatial scales, displaying the spatial variation of an ecological variable in the form of a map shows whether the structure is smoothly continuous or marked by sharp discontinuities (Legendre and Legendre 1998). I created contour maps, using Surfer (©Golden Software), of count and environmental data in order to visualize spatial patterns. I used kriging to interpolate between points. Kriging estimates the value at a grid node by drawing a circle around that node and considering the observed points found within that circle using the equation: $y_{node} = \sum w_i y_i$. A weight (w_i) is applied to each observed point within the circle based on the covariance matrix calculated among the *n* observed points (Legendre and Legendre 1998). Using covariances, the weights are statistical in nature instead of geometrical as is the case with other methods (e.g. inverse-distance weighting). Kriging takes into account the grouping of observed points on the map. When two data points are close to each other, the value of the coefficient in the covariance matrix is high thus lowering their respective weights. Kriging is the best interpolation method for data that display anisotropy (relationship between neighbouring points in different geographic directions is not the same) (Legendre and Legendre 1998).

A point pattern describes the physical locations of individual organisms or entities distributed in space (Dutilleul 1993). The purpose of point pattern analysis is: 1) to determine whether or not the geographic distribution of data points (e.g. counts) is random and 2) to describe the type of pattern in order to infer what kind of process may have generated it (Legendre and Legendre 1998). The classification of patterns as regular, random or aggregated may be an over-simplification, but it is a useful one, particularly at early stages of analysis (Diggle 1983).

I employed two different methods to look for patterns in environmental and organism data:

1) spatial autocorrelation and
2) Spatial Analysis Distance IndicEs (SADIE).

These methods are described in detail below.

Spatial autocorrelation

Spatial autocorrelation measures similarity between pairs of points as the distance between points increases (Perry et al. 2002). Nearby pairs of points can either be more similar than expected by chance (positive autocorrelation) or are less alike than expected (negative autocorrelation) (Mackas 1984, Legendre and Legendre 1998). This is particularly important for data series in which the attribute of a value from one location may be influenced by that of a value from a neighbouring location such that nearby values are not independent. In essence, spatial autocorrelation assesses pattern by describing the average change of sample-to-sample similarity with increasing spatial separation.

Autocorrelation is calculated as the series of data is progressively shifted with respect to itself. The autocorrelation coefficient r_x, is calculated as:

$$r_x(k) = \frac{s_x(k)}{\sqrt{s_{x'}^2 s_{x''}^2}}$$

where

$$s_x(k) = \frac{1}{n-k-1} \sum_{n=1}^{n-k} (x_{i+k} - \bar{x}')(x_i - \bar{x}'')$$

and n=total number of points that are paired, k=lag distance, x' and x''=original and lagged series and $s_x(k)$ is the autocovariance of the series. At lag k=0, autocorrelation is equal to 1. At progressively larger distances (e.g. shifting 55m grain data by one lag unit) data points k x 55m apart are compared and similarity between points typically decreases.

Because there is a predominant south-north current, neighbouring points along lines likely display different behaviour than points in different lines (anisotropy). I calculated autocorrelation a) along lines and b) across lines for environmental and organism data. For along-line autocorrelation, each of the 12 transect lines was analyzed individually. Nine arbitrary lines across the width of the sample area were chosen; three in each of the north, middle and south of the sample area (Figure 2.6). Two across-lines included values from either High Rise or MEF (vent lines), all others were considered non-vent lines.

A geostatistical "rule of thumb" is that each lag class should be represented by at least 30-50 pairs of points (Rossi et al. 1992). For along-line comparisons, calculations in which lag exceeded 2800m were omitted because fewer than 25 pairs of counts were compared. Along-line comparisons were made using a maximum of 12 points; while this is far below the geostatistical standard, it does give some idea of how pairs of points along lines behave differently from pairs of points across lines.

Data were de-trended by subtracting the line mean from each data point in a particular transect line. Lines were then grouped into vent (lines 1-3), west-of-vent-field (lines 4-9) and east-of-vent-field (lines 10-12).

Average correlation coefficients for each group of lines were plotted in a correlogram. A correlogram describes the average change of sample-to-sample similarity with increasing spatial separation (Mackas 1984). Because autocorrelation allows detection of structure in a data series (e.g. patch size), correlograms are analyzed primarily by looking at their shape (Legendre and Legendre 1998). Line groupings are based on location within the sample area, whether it passed over at least one of High Rise or MEF and time of data collection. Lines 4 and 5 pass over Clam Bed, but not over High Rise or MEF. Because organisms along these lines did not experience the relatively drastic conditions of those along lines 1-3 (the single smoker vent at Clam Bed is located along line 2 and the rest of the vent field exhibits conditions similar to the surrounding ambient water), lines 4 and 5 were deemed non-vent. Lines 10-12, located adjacent to line 1, were sampled almost 48 hours after line 1. Although line 10 passes over High Rise, this line is grouped with lines 11 and 12 since variation along line 10 may be due to when data was collected.

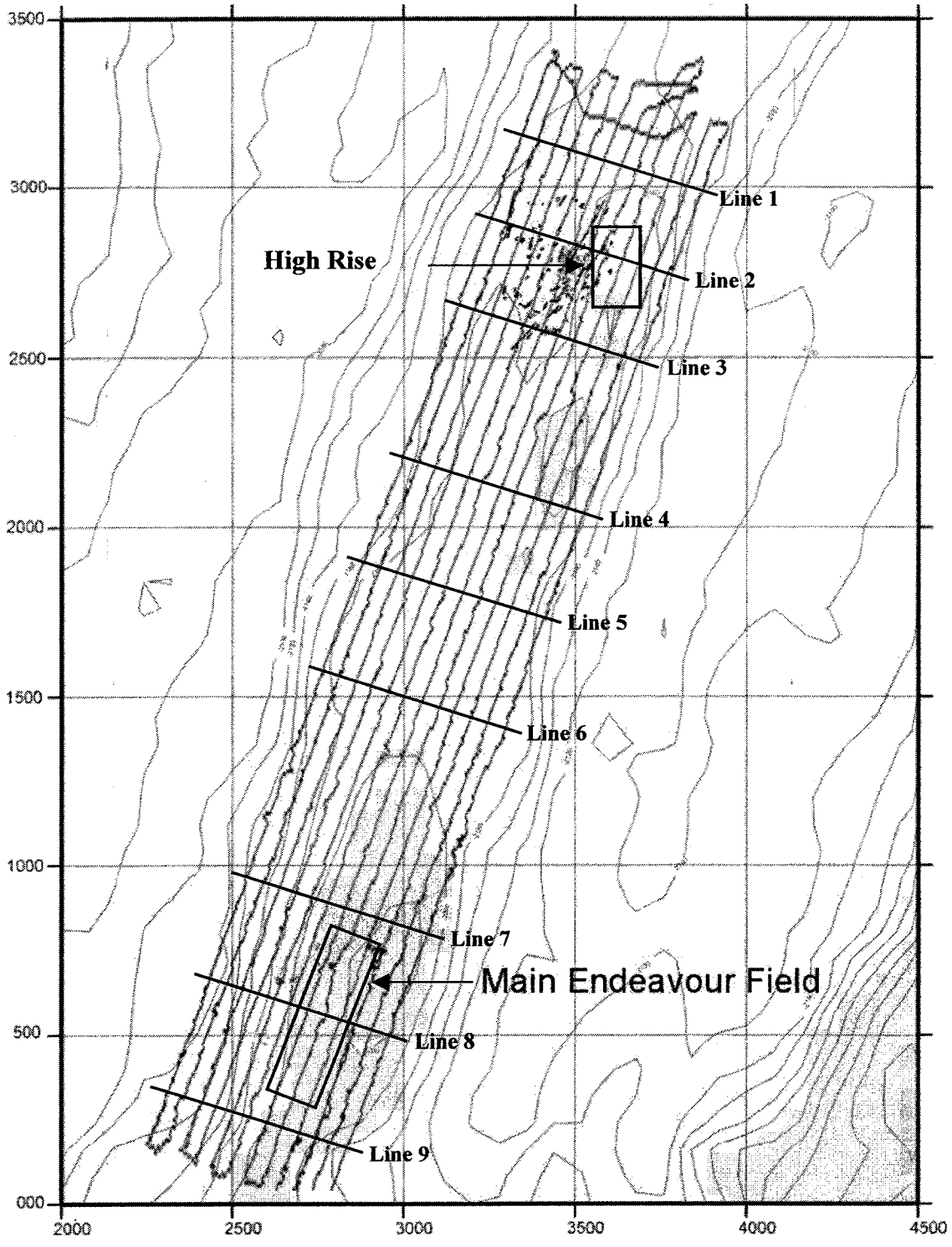

Figure 2.6 Positions of across-lines used in spatial autocorrelation analysis. Axes are measured in metres; x-axis is measured in an eastward direction, y-axis is measured in a northward direction.

De-correlation refers to the breakdown of the relationship between pairs of counts. It occurs when the autocorrelation coefficient first crosses the zero line in a correlogram. The scale of de-correlation refers to the distance, in metres, at which the relationship between pairs of counts breaks down. The scale of de-correlation is used to determine the number of independent events (e.g. patch size) that dictate the number of degrees of freedom in a sample (R. Dewey pers. comm.). By dividing the length of the sample area by the de-correlation distance, I calculated the number of independent events (degrees of freedom) over the entire sample area.

In general, autocorrelation values that fluctuate about the zero line are not significantly different from random (R. Lueck pers. comm.). Lueck and Wolk (1999) suggest a simple method of calculating significance that I employed here. Two-and-a-half and 97.5 percentiles were calculated for random distributions of correlation values. Values that did not fall within the 95% range of values were considered to be significantly different from random. In this study, autocorrelation values for along-line comparisons, which fluctuated about zero and were not significantly different from normal, were used (R. Lueck pers. comm.). Q-Q plots (SPSS) were used to test normality of the data sets. For data sets significantly different from normal (e.g. environmental variables), five random data sets (values ranging from 1 to –1) were generated using Matlab. These random sets were then used to assess significance of along-line autocorrelations. Significance of across-line comparisons was not assessed since the number of comparisons was so small.

SADIE analysis

For each organism group, I also assessed the randomness of their spatial pattern. If patterns observed in point plots or contour maps of organism spatial pattern are not random, then it is possible that one or more measured environmental variables may affect their spatial pattern (Diggle 1983). While autocorrelation can identify relationships (correlation values) between any two points that are significantly different from zero (random), SADIE (Spatial Analysis Distance IndicEs) describes and maps *local* variation of spatial pattern and association. It specifically identifies where, in space, patches and

gaps occur and assesses whether or not the locations of patches and gaps significantly differs from random.

SADIE detects the degree of clustering in spatially referenced data of counts of organisms at different extents and grain sizes, based on a randomization test (for a detailed description, see Perry (1994) and Perry (2003)). The underlying premise is that SADIE regards a set of data as being represented by regions. Within each region, observed counts are either randomly arranged or they form local neighbourhoods of similarly sized counts that are close to one another. These neighbourhoods are termed clusters (Figure 2.7). A group of relatively high density counts that are spatially adjacent is called a *patch cluster* (Figure 2.7b). Similarly, a group of relatively small or zero counts that are spatially close together is called a *gap cluster* (Figure 2.7b). In SADIE, spatial pattern is measured locally, at each sampled unit, through an *index of clustering*. Each unit with a count greater than the overall mean is assigned a *patch cluster index* (v_i), which is positive. Each unit with a count less than the overall mean is assigned a *gap cluster index* (v_j), which is negative. Each index is computed to allow for the size of the count (abundance) at each sample unit. If points are randomly arranged, the cluster index ranges between 1 (v_i) and -1 (v_j). Typically, values >1.50 (v_i) and <-1.50 (v_j) represent a unit with a clustering index that exceeds the 95th percentile for patches or gaps from random spatial patterns. The specific locations of these gap and patch clusters can be plotted using data generated by SADIE. Instead of showing these additional maps to describe the results, I make reference to points of interest using the previously generated contour maps.

The above strength of clustering into patches and gaps is assessed based on randomizations, in which the observed counts are re-arranged among the sample units. SADIE compares the spatial arrangement of clusters (gaps and patches) of the observed sample with other arrangements randomly derived from it. It measures the "distance" each count moves from its initial to its final position: the sum of these individual distances is D, the distance to regularity.

For data in the form of a 2D map, where the x,y coordinates of each individual is known, SADIE moves individual counts simultaneously to fill the allowable space in a regular fashion. Within the sample area, usually rectangular in shape, SADIE uses the

Figure 2.7 Ecological data collected as counts per cell or unit area. a) Map of male tupelo tree data. b) Same data converted to counts. Clustering is assigned as follows: ○ *Patch Cluster*: the large, isolated large value of 2 (top left corner) is ascribed a relatively small patch clustering index (0.88), less than unity, as expected of random arrangements. The second value of 2 (bottom) is also in a patch cluster, but this time is ascribed a relatively high clustering index (2.86) as it exceeds expected unity value (1) for random spatial pattern. □ *Gap Cluster*: similarly for relatively small counts, 0 in the leftmost column is surrounded by relatively large counts and is thus assigned a relatively small gap clustering index (-0.56). The 0 in the 4^{th} column, 5^{th} row is completely surrounded by other zeros thus constituting a gap cluster and is ascribed a relatively large gap cluster index (-1.27). Modified from Perry (2003).

a)

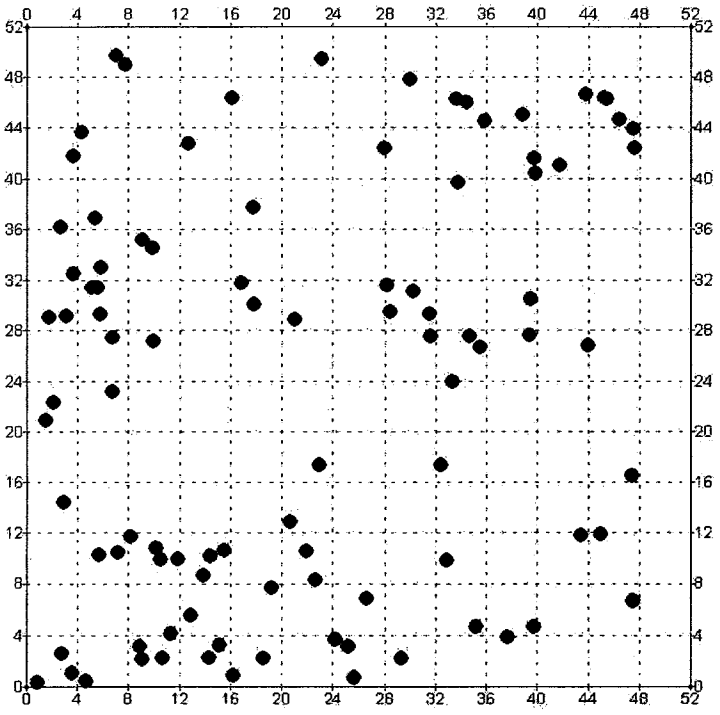
0 4 8 12 16 20 24 28 32 36 40 44 48 52

b)

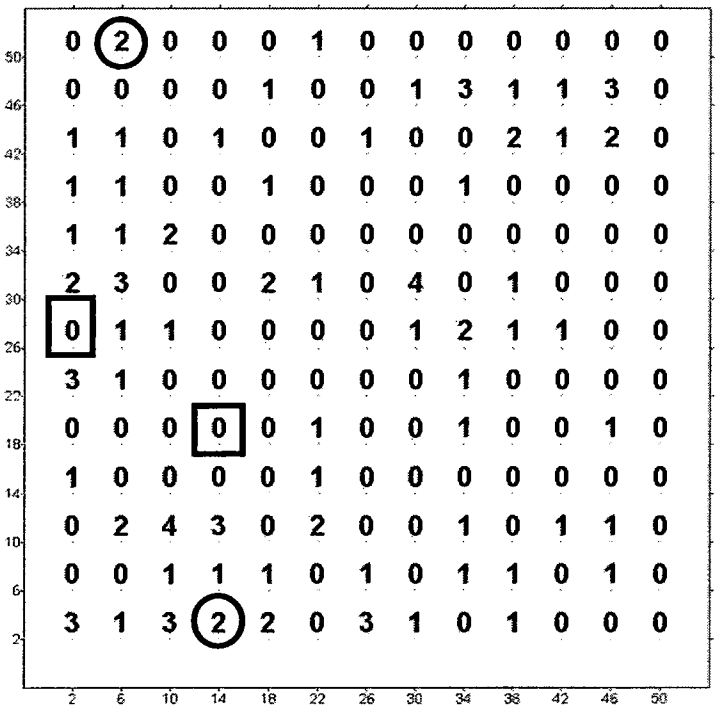
0 2 0 0 0 1 0 0 0 0 0 0 0
0 0 0 0 1 0 0 1 3 1 1 3 0
1 1 0 1 0 0 1 0 0 2 1 2 0
1 1 0 0 1 0 0 0 1 0 0 0 0
1 1 2 0 0 0 0 0 0 0 0 0 0
2 3 0 0 2 1 0 4 0 1 0 0 0
0 1 1 0 0 0 0 1 2 1 1 0 0
3 1 0 0 0 0 0 0 1 0 0 0 0
0 0 0 0 0 1 0 0 1 0 0 1 0
1 0 0 0 0 1 0 0 0 0 0 0 0
0 2 4 3 0 2 0 0 1 0 1 1 0
0 0 1 1 1 0 1 0 1 1 0 1 0
3 1 3 2 2 0 3 1 0 1 0 0 0

Sugihara-Iri algorithm to draw Voronoi tessellations for the counts in the sample area (Figure 2.8). A tessellation is an arrangement of identical polygons in a pattern (e.g. mosaic) without gaps or overlapping areas. The tessellations divide the sample area into N polygons, one for each count, such that any point in a polygon is closer to that count than it is to any other neighbouring count.

A transportation algorithm is then used to move each count from its current position (Figure 2.8a) to one in which the final spatial pattern of counts is uniform (Figure 2.8d). By weighting the contribution of each neighbouring count, the algorithm calculates the new position of each individual count to be at the centroid of the positions of its neighbours (Figure 2.8b and c). In essence, the algorithm moves counts to new positions step by step rather than jumping from an original to a final arrangement. This stepwise progression is more realistic for biological systems. Weighting contribution of each neighbour ensures that gaps are filled as each count is attracted towards more distant neighbours or away from nearest neighbours. The process is iterated until a sufficient degree of regularity in the spatial pattern of counts is achieved (Figure 2.8d).

The program calculates distance to regularity (D_{obs}), the sum total of the distances moved by each count from the initial (observed) arrangement to a final (uniform) arrangement. Assessment of regularity is based on two criteria: The current variation between areas of N polygons should 1) be less than the previous value and 2) differ from it by less than a given constant.

Using a pseudo-random number generator, SADIE then independently and randomly generates and assigns the same number of counts as in the observed sample. Using the procedure outlined above, SADIE calculates the total distance (D_{rand}) for each set of randomly generated counts. Each D_{rand} is stored so that at the end of all of the iterations, an average D_{rand} can be calculated. Because it is a one-sided test of complete spatial randomness, it is possible to calculate the probability that the observed data are no more aggregated than expected from a random permutation of the counts. The number of permutations where $D_{rand} > D_{obs}$ (R) is compared with the total number of permutations (S), such that $P_{rand}=R/S$. $P_{rand} < 0.05$ indicates that the observed arrangement is aggregated (significantly differs from random).

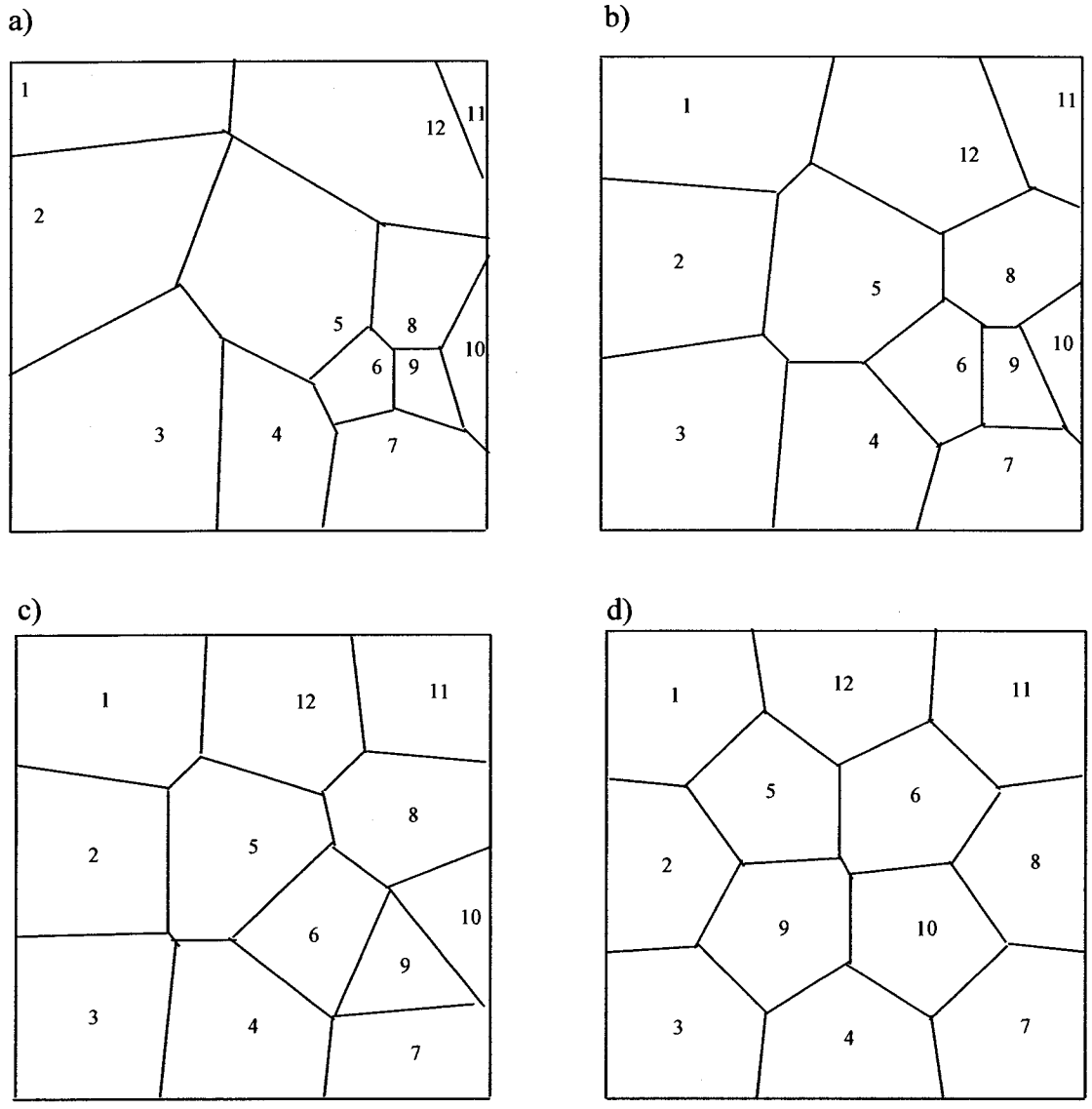

Figure 2.8 Simple example of initial to final arrangement of aphid spatial pattern using SADIE algorithm and Voronoi tessellations (each number represents an individual organism). a) 12 aphids, individually numbered in their initial scaled positions at the start of the SADIE algorithm with the Voronoi tessellation for this arrangement. b) Positions of the 12 aphids after the first iteration of the SADIE algorithm (the position of each aphid has been simultaneously moved). c) Positions of the 12 aphids after four iterations. d) Final positions after 325 iterations or moves. Final positions are as regular as required by the criterion set for the algorithm. After reversal of the scaling, the sum of the distances between the final positions and the corresponding initial positions gives the 'distance to regularity' D. Modified from Perry (1995).

Since the tests may be affected by the degree of replication, an index (I_a) is used to describe the degree of spatial aggregation in the data set and to enable comparisons between data sets. Specifically, the Index of Aggregation (I) is calculated using: $I_a=D_{obs}/E_a$ where E_a=average of the individual D_{rand}/S. Values of $I_a > 1$ are aggregated; values close to 1 indicate randomness and values of $I_a < 1$ indicate regularity.

The sample area as a whole was analyzed using the 165m grain size. Because SADIE can only process <500 records at a time, I divided the sample area into smaller sampling units when using the 55 m grain size (Figure 2.9). I analyzed multiple, overlapping extents using the 55 m grain size to ensure that the patterns detected were not simply a product of the extent at which counts were analyzed. For individual vent fields (High Rise, Clam Bed and MEF), I used both the 55 m and 10 m grain sizes to determine if the spatial arrangement of organisms varied with scale. For each test, I ran the maximum number of randomizations (5967).

C: Correlating patterns

To visualize relationships among environmental variables and organisms, I a) graphed organism abundance and environmental variable versus distance traveled along each transect line and b) created 2-D scatterplots of environmental variables versus organism abundance. This helped to identify which environmental variables to use in cross-correlation analyses.

The purpose of correlation analysis is to establish interdependence between random variables without assuming any explanatory response or causal link between them (Legendre and Legendre 1998). For these data, correlation is used rather than regression for two reasons: 1) both "sets" of variables (organismal and environmental) are random, neither variable can be controlled and 2) the purpose is to explore relationships rather than to model the relationship between variables.

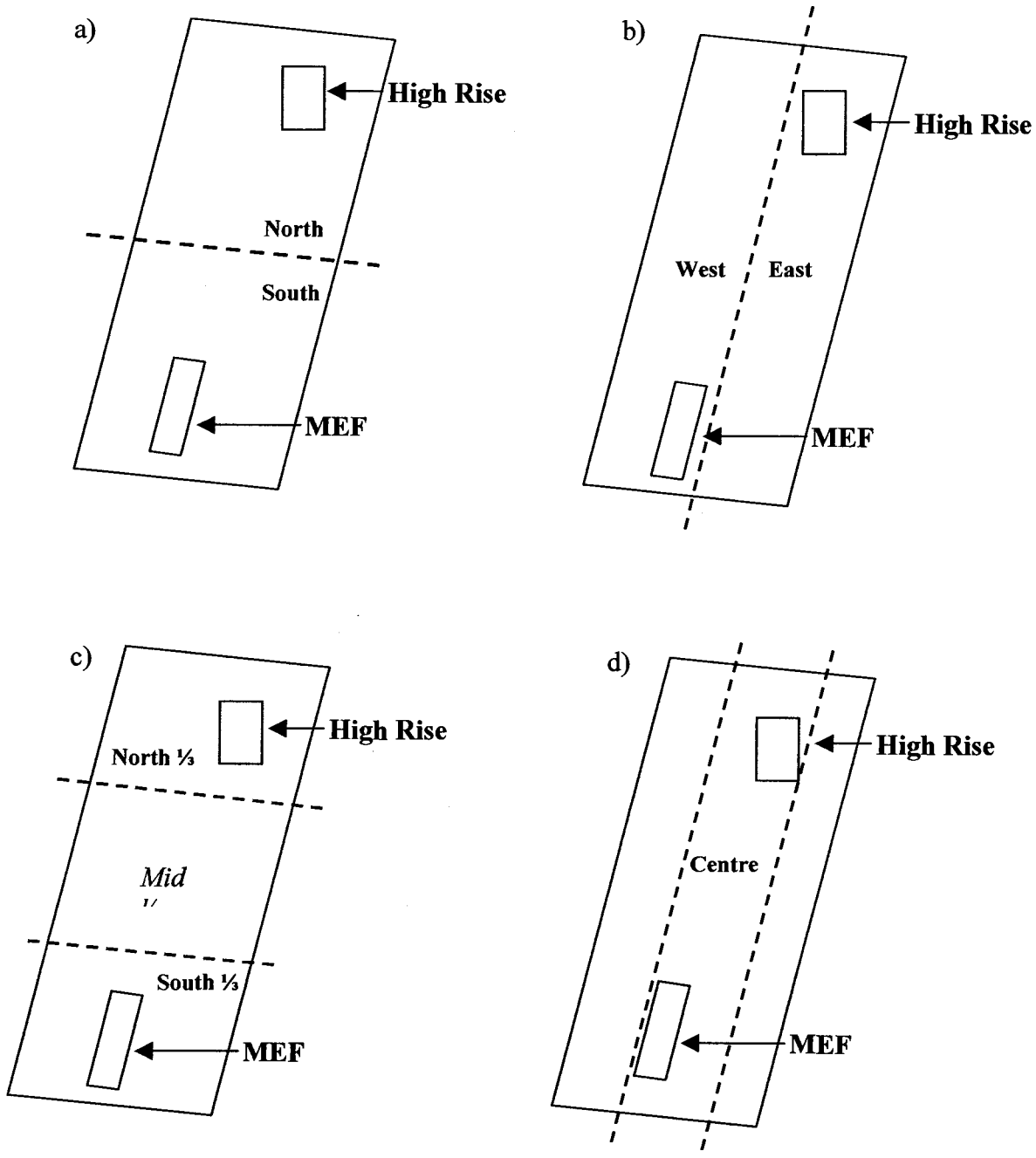

Figure 2.9 Extents used in SADIE analysis at 75m grain a) North-South halves, b) East-West halves, c) North-Middle-South thirds and d) Centre (lines 1-3).

To assess spatial correlation between autocorrelated variables, I used cross-correlation; the same as autocorrelation except that instead of comparing one data series with itself, two data series are compared. The cross-correlation coefficient is calculated as:

$$r_{xy} = \frac{\frac{1}{n}\sum_{n=1}^{n-k} x(n)\, y(n+k)}{s(x)\, s(y)}$$

where x=data set 1, y=data set 2, n=total number of points that are paired and k=lag (Rossi et al. 1992). Because two data sets are used, cross-correlation is generally not symmetrical, the value of the function is not the same if calculated in opposite directions (i.e. one data set moves 'up' or 'down' with respect to the other data set, producing similar, but not the same, distribution of correlation coefficients).

Analyses were performed using the Matlab cross-correlation function, which simultaneously assessed correlation in both directions. Correlation coefficients were plotted versus lag unit along each transect line to visualize relationships. Cross-correlation was used to assess the relationship 1) among environmental variables and 2) between environmental variables and zooplankton spatial pattern along each transect line. This gives an overall idea of how these variables are related over the entire sample area. The significance of the cross-correlation coefficient can be assessed in the same manner as for autocorrelation, where the null hypothesis is that the correlation is not different from zero at lag 'k'.

To assess relationships among organism groups and between environmental variables and gelatinous zooplankton or nekton, I used Pearson's product-moment correlation coefficient (r) at different scales. Upon visual inspection, gelatinous zooplankton autocorrelation and environment autocorrelation did not show similar structure therefore, Pearson's (r) was used instead of cross-correlation. Significance of these associations was tested using degrees of freedom calculated from along-line gelatinous zooplankton autocorrelations. I also used Pearson's (r) to assess correlations between environmental variables and both zooplankon groups over individual vent fields to determine if relationships change with changing extent.

2.3 Results

2.3.1 Environment at 20 mab

A: Whole Area

Contour maps best illustrate environmental conditions of the water layer 20 mab (Figure 2.10). While variables were initially binned over a range of grain sizes (10 m – 335 m), the 55 m grain best illustrates variation in conditions over vent fields and non-vent areas. Larger grain sizes smooth variability while smaller grain sizes create numerous "eddies" that make it difficult to visualize overall patterns in environmental conditions.

The two main vent fields, High Rise and MEF, are easily identified by relatively higher theta anomaly (Figure 2.10a). The north and west halves of the sample area appear slightly warmer overall than the south and east halves.

The south half of the sample area is relatively more saline than the north half, indicative of an increase in depth (>200 m) from north to south (Figure 2.10b). Effluent from High Rise is relatively less saline than the surrounding area, while outflow from MEF is at least as saline as the ambient water. A large patch of relatively high salinity water south of MEF may be effluent advected north from a vent field outside the sample area (Quebec or Beach).

Effluent from MEF is cloudier than surrounding water and also than effluent from High Rise (Figure 2.10c). Small packages of cloudy water are transported southwest of High Rise and west of MEF. It appears that water cloudiness is retained over longer distances than water temperature anomalies. In addition, vent outflow appears to disperse to the west of MEF vents. Two small eddies, south of High Rise, are apparent within the larger effluent plume. Water south of High Rise and over Clam Bed (250 m south of High Rise) is almost as cloudy as effluent found over High Rise. Effluent from Clam Bed, while not very warm, is relatively cloudy suggesting that effluent may be carried south from High Rise. This supports the net current direction from south to north, as described in Thomson et al (2003).

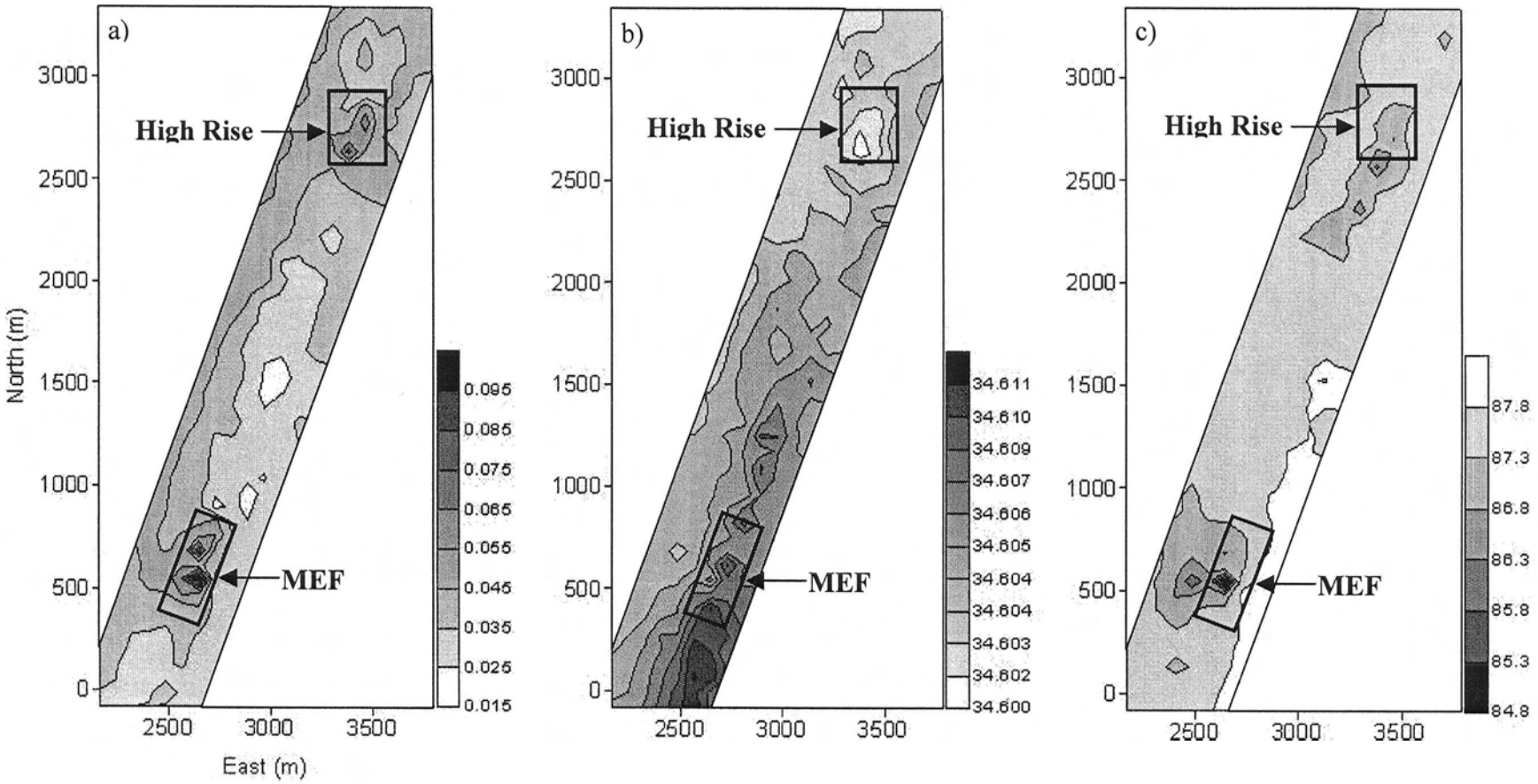

Figure 2.10 Contour maps of environmental conditions of water layer 20 metres above bottom (mab) over the whole sample area: a) theta anomaly, b) salinity and c) light (% transmissivity). Data are averaged over approximately 55 m of observations.

Similar patterns are evident in Figure 2.11. Vent effluent from High Rise and MEF is identified by relatively higher temperature (Figure 2.11a). Both vent fields reach a maximum of 0.12°C difference from ambient water. Vent effluent is not as easily identified using salinity (Figure 2.11b). Effluent from High Rise is less saline than ambient water whereas effluent from MEF is roughly equal to ambient salinity. On the whole, salinity increases with depth from north to south. Similar to the contour plots, light transmissivity is lower over both vent fields, with cloudiest water occurring at MEF (Figure 2.11c).

Similar patterns are evident when distance over the width of the sample area is plotted versus environment variables (Figure 2.12). Theta, salinity and light transmissivity anomalies are evident at both High Rise and MEF. Again, light transmissivity is relatively low west of High Rise, over Clam Bed.

The three environmental variables are plotted versus distance along the length of a transect line that passes over both main vent fields (line 2) and a transect line that passes only over non-vent area (line 8) in Figure 2.13. It is evident that there is greater environmental variability along lines that pass over vent fields. There is a slight increase in water cloudiness at the south end of line 8 (Figure 2.13b) suggesting that effluent, likely from MEF, is advected westward. The overall variability of light transmissivity along line 8 is less than that along line 2.

Correlograms illustrating the relationship between pairs of points along each transect line show similar patterns (e.g. shape, scale of de-correlation) among neighbouring lines thus lines are grouped, in Figure 2.14, into vent (lines 1-3), west-of-vent-field (lines 4-9) and east-of-vent-field lines (lines 10-12). Correlations between temperature anomaly values and light transmissivity values along lines 1-3, which pass over at least one of High Rise and MEF, break down at about 350 m. There is no significant correlation among pairs of points along these lines, suggesting that temperature is relatively variable. There is a slight, but not significant, second positive peak at roughly 2000 m where extreme values, from opposite vent fields, are compared. This second peak is not evident in lines that do not pass over the vent fields. Theta anomaly correlations break down at about 800 m over west-of-vent-field lines and at 1000 m over east-of-vent-field lines.

Figure 2.11 Variation of environmental variables with northward distance a) theta anomaly, b) salinity and c) light transmissivity. Data are from all transect lines. The locations of the two main vent fields, MEF and High Rise, are indicated. Values measured within the vent fields fall within the circles, but not all values within circle are taken over vent fields.

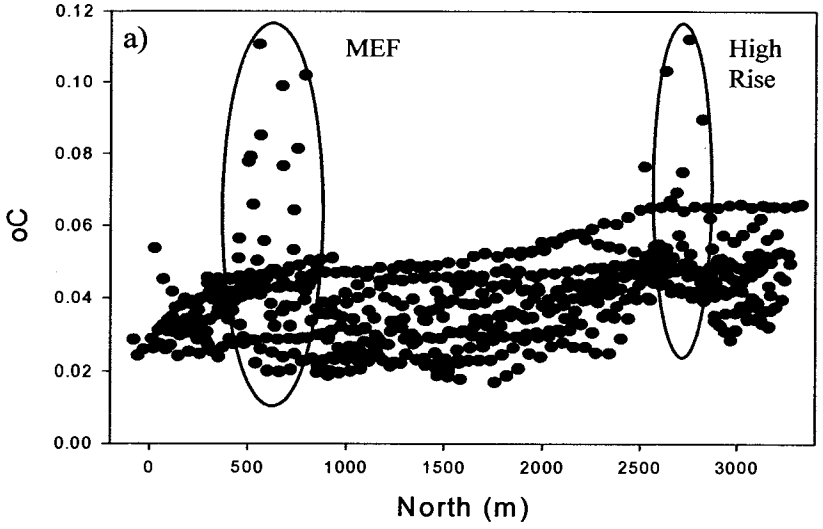
a)
MEF
High Rise
oC
0.12
0.10
0.08
0.06
0.04
0.02
0.00
0
500
1000
1500
2000
2500
3000
North (m)

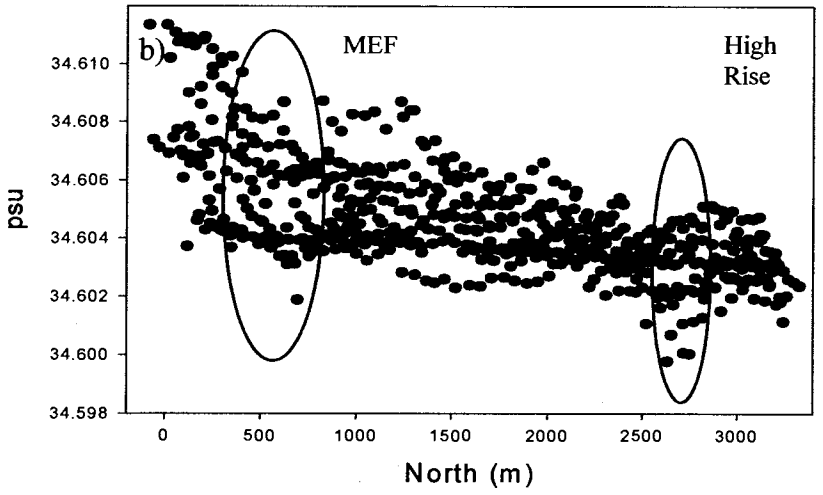
b)
MEF
High Rise
psu
34.610
34.608
34.606
34.604
34.602
34.600
34.598
0
500
1000
1500
2000
2500
3000
North (m)

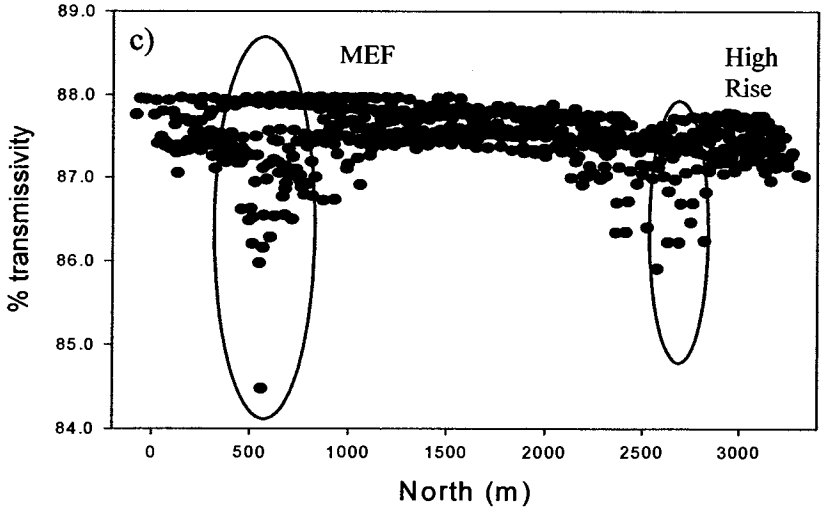
c)
MEF
High Rise
% transmissivity
89.0
88.0
87.0
86.0
85.0
84.0
0
500
1000
1500
2000
2500
3000
North (m)

Figure 2.12 Variation in environmental variables orthogonal to sample lines a) theta anomaly, b) salinity and c) light transmissivity. Data are from all transect lines. Locations of the two main vent fields, MEF and High Rise, are indicated. Values measured within the vent fields fall within the circles, but not all values within circle are taken over vent fields.

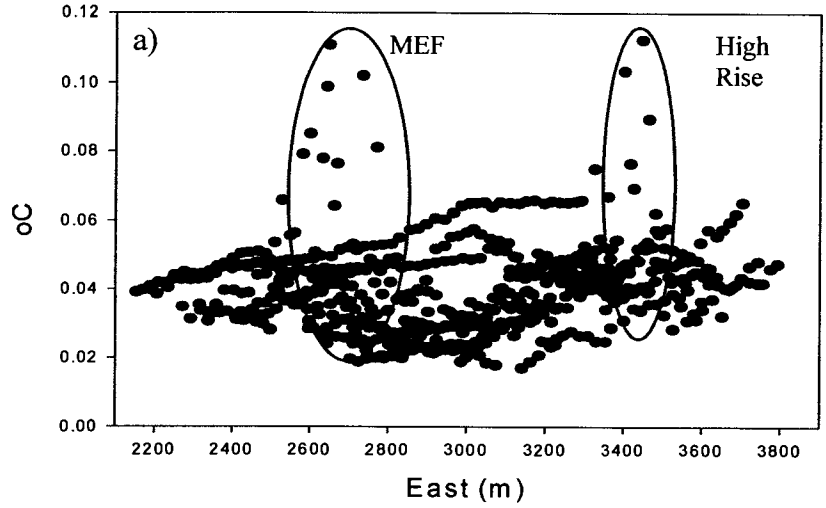
a)
MEF
High Rise
oC
0.12
0.10
0.08
0.06
0.04
0.02
0.00
2200 2400 2600 2800 3000 3200 3400 3600 3800
East (m)

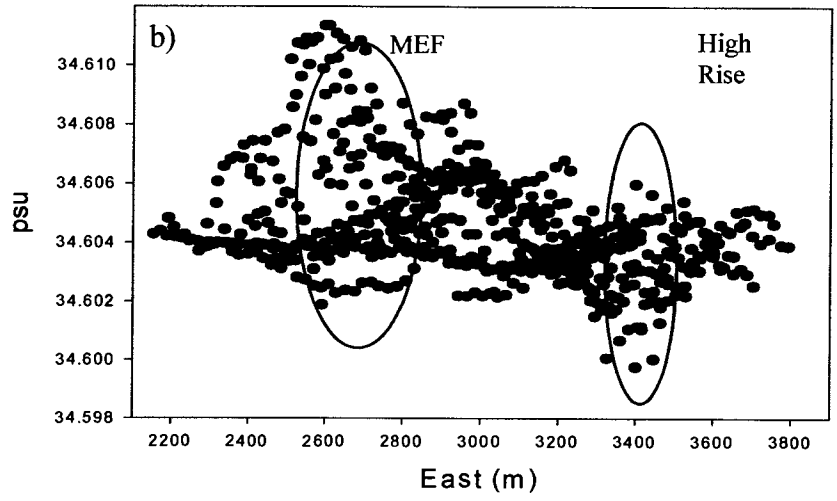
b)
MEF
High Rise
psu
34.610
34.608
34.606
34.604
34.602
34.600
34.598
2200 2400 2600 2800 3000 3200 3400 3600 3800
East (m)

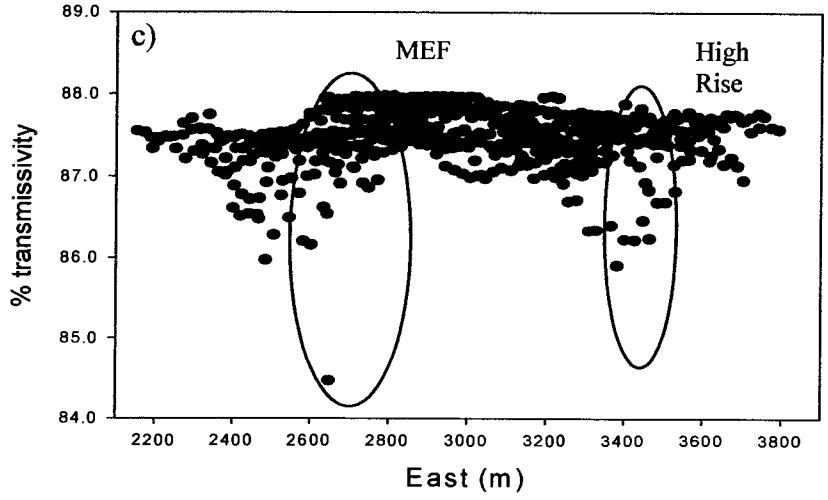
c)
MEF
High Rise
% transmissivity
89.0
88.0
87.0
86.0
85.0
84.0
2200 2400 2600 2800 3000 3200 3400 3600 3800
East (m)

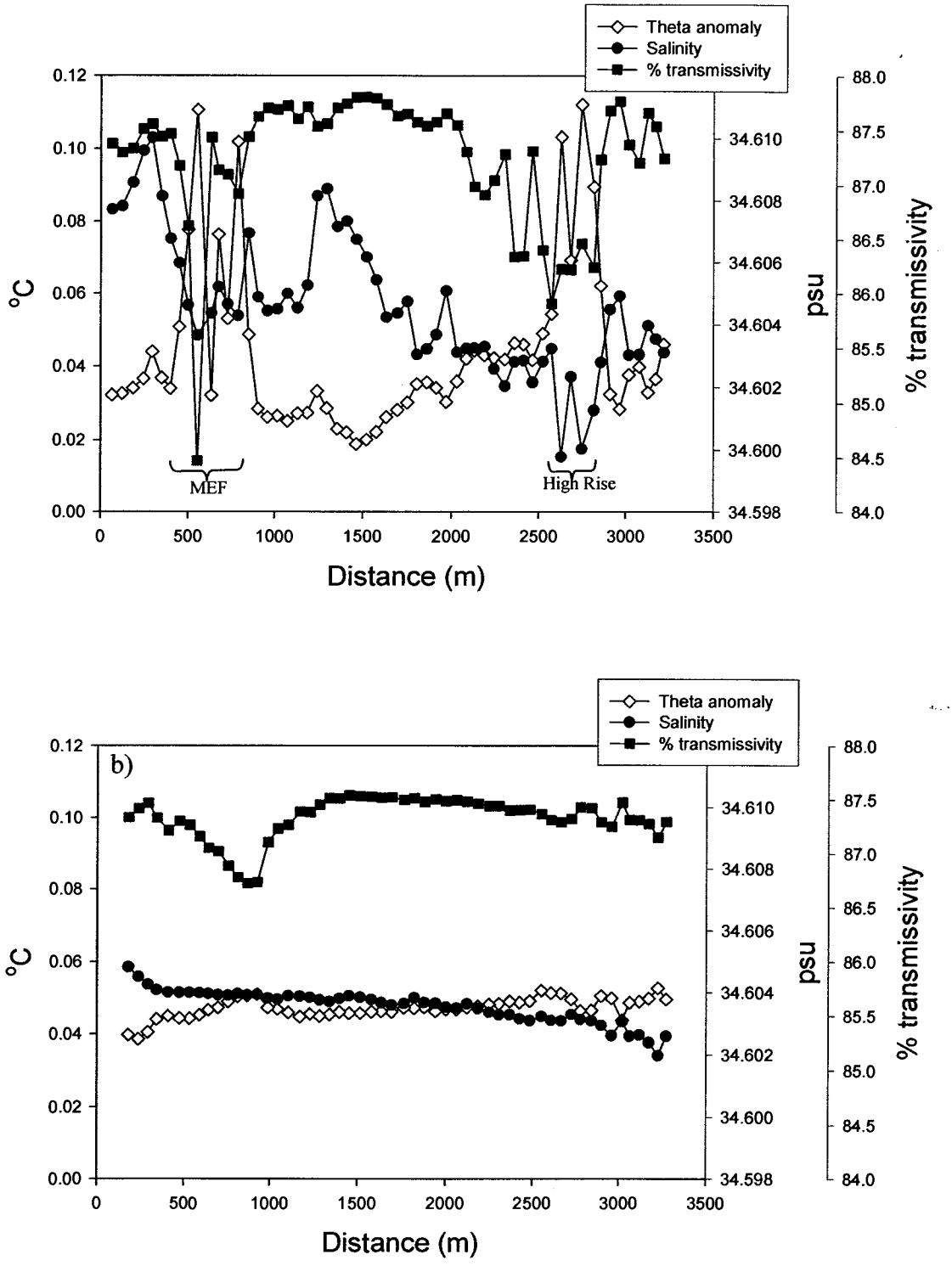

Figure 2.13 Environmental conditions along two transect lines. a) Line 2, from north to south, passes over three of the four vent fields. b) Line 8, from north to south, is non-vent area.

Figure 2.14 Spatial autocorrelograms of a) theta anomaly, b) salinity and c) light transmissivity along vent and non-vent lines. Lines 1-3 are grouped as 'vent', lines 4-9 are grouped as 'west' (west-of-vent-field lines) and lines 10-12 are grouped as 'east' (east-of-vent-field lines). Error bars = +/- SE. Dashed lines indicate lower 2.5%-iles and upper 97.5%-iles, values above and below dashed lines are significantly different from zero.

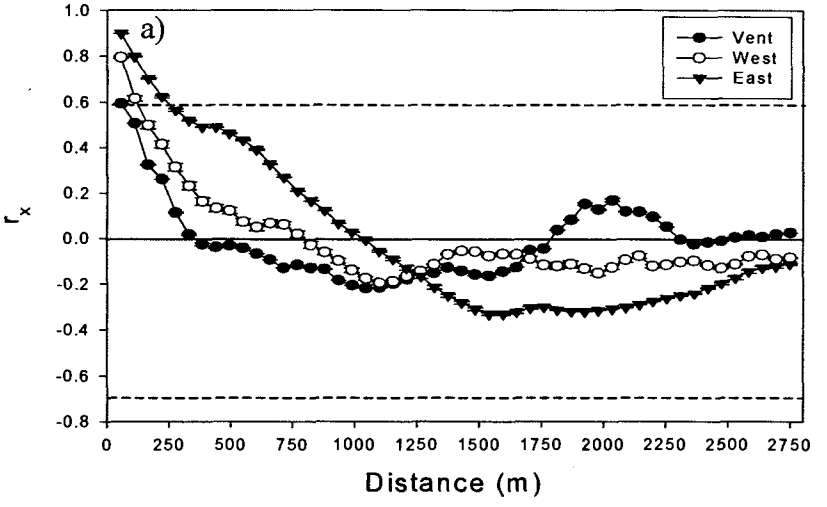
a)
Vent
West
East
r_x
1.0
0.8
0.6
0.4
0.2
0.0
-0.2
-0.4
-0.6
-0.8
0
250
500
750
1000
1250
1500
1750
2000
2250
2500
2750
Distance (m)

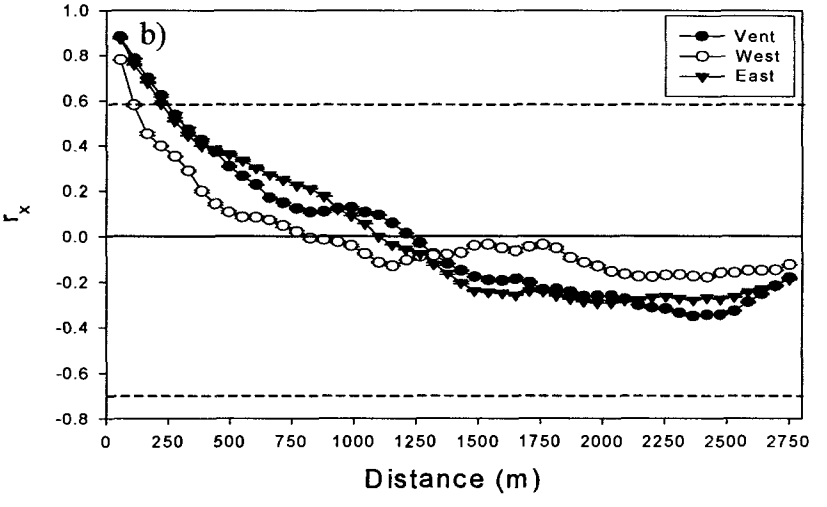
b)
Vent
West
East
r_x
1.0
0.8
0.6
0.4
0.2
0.0
-0.2
-0.4
-0.6
-0.8
0
250
500
750
1000
1250
1500
1750
2000
2250
2500
2750
Distance (m)

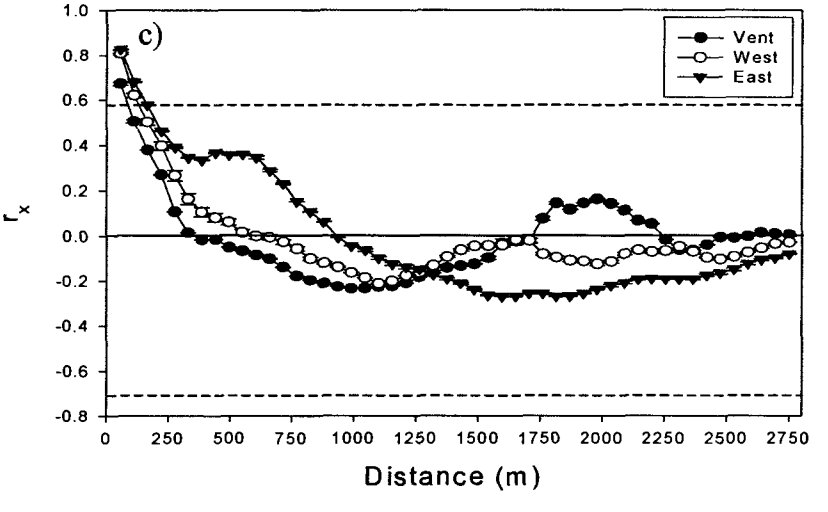
c)
Vent
West
East
r_x
1.0
0.8
0.6
0.4
0.2
0.0
-0.2
-0.4
-0.6
-0.8
0
250
500
750
1000
1250
1500
1750
2000
2250
2500
2750
Distance (m)

Pairs of points 110 m apart (lines 4-9) and 220 m apart (lines 10-12) show significant correlation. Overall, in terms of theta anomaly, lines 1-3 are most variable and lines 10-12 are least (Figure 2.14).

The de-correlation scale for salinity is larger than that for either temperature anomaly or light transmissivity along vent lines (Figure 2.14b). In addition, salinity correlations, along lines 1-3, do not show a second positive correlation peak. Along all three groups of lines, structure is in the form of a gradient; points furthest apart are least related. Significant correlation exists between pairs of points 110 m apart in the west and between pairs of points 220 m apart along eastern and vent lines. Thus there are two salinity gradients: from north to south and from east to west.

De-correlation scales for light transmissivity are similar to those of theta anomaly along the three groups of lines (Figure 2.14c). Significant correlation along vent lines is limited to neighbouring pairs of points, but extends to distances of 110 m and 165 m along west and east lines, respectively. As with theta anomaly, light transmissivity along vent lines displays a second positive correlation peak where transmissivity values from the two main vent fields are compared. Water cloudiness is most variable along vent lines and least variable along east lines.

Across-line autocorrelations are much more variable, in large part because there are few comparisons to make therefore, significance of the autocorrelation coefficients across-lines was not calculated (Figure 2.15). The de-correlation scale for all variables is smaller than for along line comparisons (75-200 m). Theta anomaly de-correlates at larger distances over vent fields than non-vent areas while light transmissivity de-correlates at relatively shorter distances over vent than non-vent areas. Salinity de-correlates at the same distance over all lines.

Theta anomaly and salinity show no significant correlation along vent lines (Figure 2.16a). Significant negative correlation is evident between pairs of points up to about 250 m apart along non-vent west lines (Figure 2.16b). Correlation is strongest along eastern lines (Figure 2.16c). Pairs of points up to 600 m apart show significant correlation. Presence of a relatively steep salinity gradient in the west may be responsible for the lack of correlation at larger distances along non-vent west lines.

Figure 2.15 Spatial correlograms of across-line associations a) theta anomaly, b) salinity and c) light transmissivity over vent and non-vent areas. Error bars = +/- SE. Significance of autocorrelation values was not tested since the number of pairs of points for each comparison is small (≤ 12).

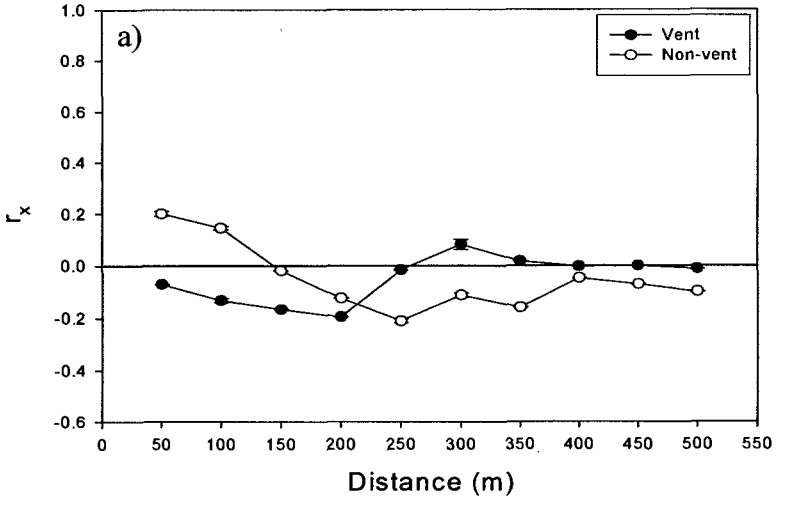
a)
Vent
Non-vent
r_x
1.0
0.8
0.6
0.4
0.2
0.0
-0.2
-0.4
-0.6
0
50
100
150
200
250
300
350
400
450
500
550
Distance (m)

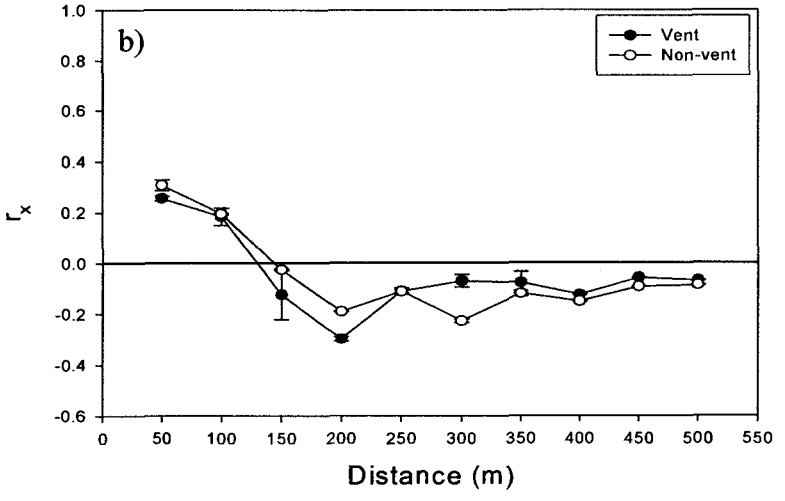
b)
Vent
Non-vent
r_x
1.0
0.8
0.6
0.4
0.2
0.0
-0.2
-0.4
-0.6
0
50
100
150
200
250
300
350
400
450
500
550
Distance (m)

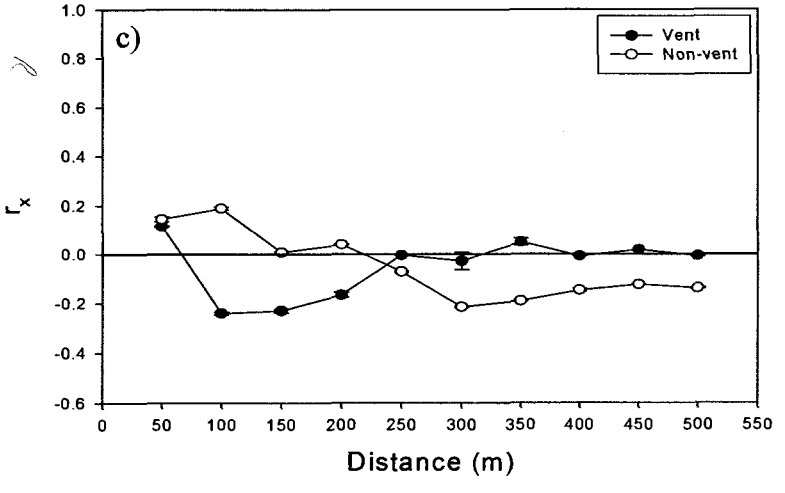
c)
Vent
Non-vent
r_x
1.0
0.8
0.6
0.4
0.2
0.0
-0.2
-0.4
-0.6
0
50
100
150
200
250
300
350
400
450
500
550
Distance (m)

Figure 2.16 Cross-correlograms of theta anomaly and salinity along a) vent lines (1-3), b) west-of-vent-field lines (4-9) and c) east-of-vent-field lines (10-12). Negative and positive refer to the sign of the lag distance 'k'. Error bars = +/- SE. Dashed lines indicate lower 2.5%-iles and upper 97.5%-iles, values above and below dashed lines are significantly different from zero.

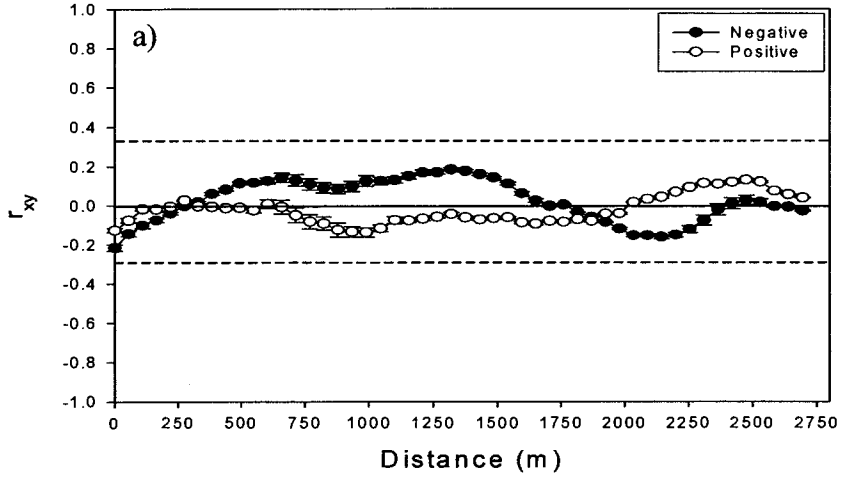
a)
Negative
Positive
1.0
0.8
0.6
0.4
0.2
0.0
-0.2
-0.4
-0.6
-0.8
-1.0
r_{xy}
0
250
500
750
1000
1250
1500
1750
2000
2250
2500
2750
Distance (m)

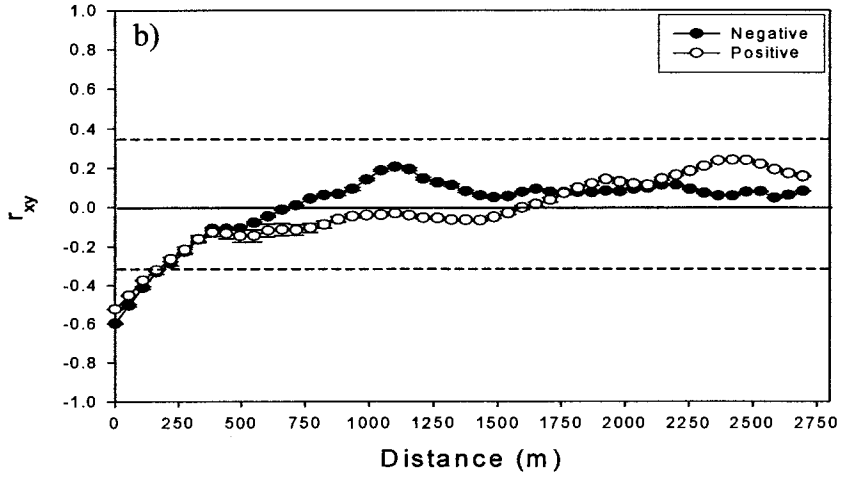
b)
Negative
Positive
1.0
0.8
0.6
0.4
0.2
0.0
-0.2
-0.4
-0.6
-0.8
-1.0
r_{xy}
0
250
500
750
1000
1250
1500
1750
2000
2250
2500
2750
Distance (m)

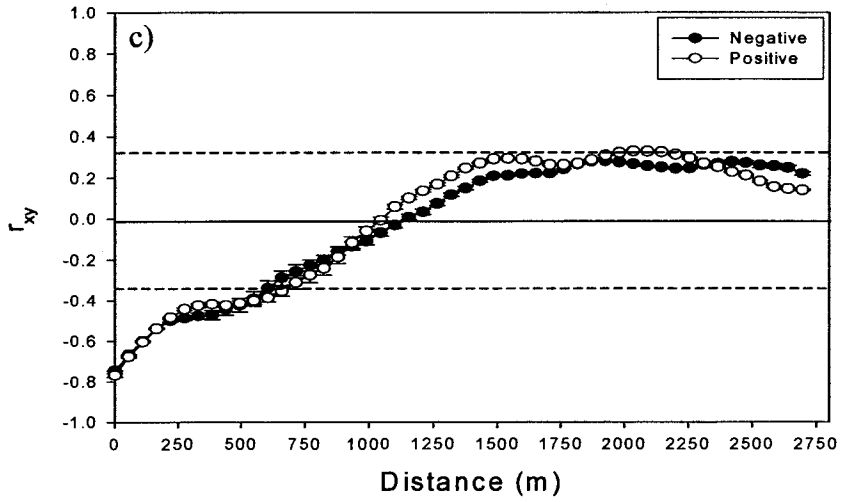
c)
Negative
Positive
1.0
0.8
0.6
0.4
0.2
0.0
-0.2
-0.4
-0.6
-0.8
-1.0
r_{xy}
0
250
500
750
1000
1250
1500
1750
2000
2250
2500
2750
Distance (m)

Significant negative correlation between theta anomaly and light transmissivity is found along all lines (Figure 2.17). Along vent lines, higher temperature corresponds with increased cloudiness up to 225 m distance. Significant correlation along non-vent west lines extends to about 55 m suggesting relatively variable conditions. Along eastern lines, significant negative correlation is found for pairs of points up to 525 m apart. Transport of effluent along lines 1-3 and into the west of the sample area is likely responsible for low correlation over large distances.

Salinity and light transmissivity show significant positive correlation only along eastern lines, up to distances of about 600 m (Figure 2.18). Conditions along these lines are relatively stable. Correlation along all other lines is not significantly different from random, again suggesting transport of effluent and a salinity gradient in the west are likely responsible for the lack of correlation.

Overall, these analyses suggest that conditions along vent and west-of-vent-field lines are more variable than over east-of-vent-field lines. Relatively steep temperature and light transmissivity gradients over the vent fields combined with a steeper salinity gradient in the west result in little significant correlation among environmental variables.

B: Vent fields

Because the vent fields are smaller in extent, the 10 m grain is used to examine environmental variation in their immediate surroundings. At High Rise, temperature anomalies are highest on the east side of the vent field, reaching a maximum of 0.13°C (Figure 2.19). Vent effluent is easily identified at the 10 m grain using temperature anomaly (highs) and salinity (lows). Light transmissivity is low on the east side and appears to be concentrated near two sources, Ventnor and Godzilla (Figure 2.19c). In short, effluent appears to be advected primarily to the south and west.

Effluent from smokers at MEF Hulk, Grotto and Milli Q1, gives discrete signatures at 20 mab (Figure 2.20). Both temperature anomaly and salinity reach greater extremes at MEF than at High Rise. Extremely low values of light transmissivity appear to originate at S&M. Much of the vent effluent appears to be transported to the west with gaps of relatively ambient water between Hulk, Grotto and Milli Q1 (<0.05°C). Unlike High Rise and MEF, Clam Bed (Figure 2.21) does not have high temperature anomalies.

Figure 2.17 Cross-correlograms of theta anomaly and light transmissivity along a) vent lines (1-3), b) west-of-vent-field lines (4-9) and c) east-of-vent-field lines (10-12). Negative and positive refer to the sign of the lag distance 'k'. Error bars = +/- SE. Dashed lines indicate lower 2.5%-iles and upper 97.5%-iles, values above and below dashed lines are significantly different from zero.

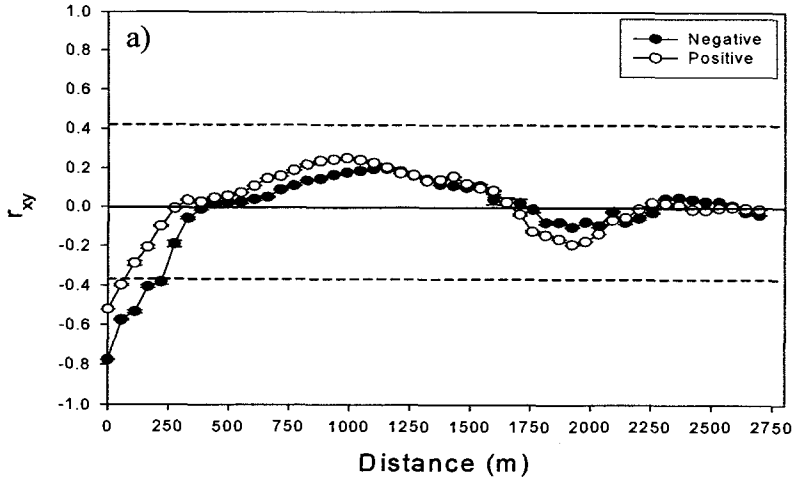
a)
Negative
Positive
1.0
0.8
0.6
0.4
0.2
0.0
-0.2
-0.4
-0.6
-0.8
-1.0
r_{xy}
0
250
500
750
1000
1250
1500
1750
2000
2250
2500
2750
Distance (m)

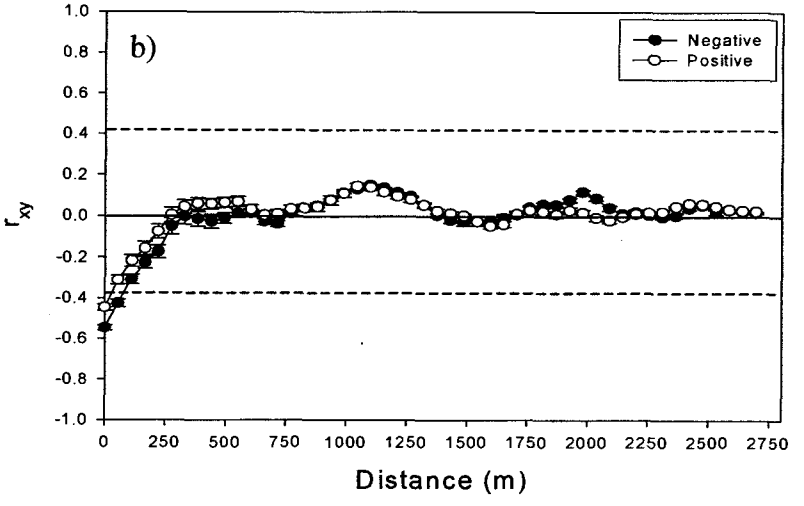
b)
Negative
Positive
1.0
0.8
0.6
0.4
0.2
0.0
-0.2
-0.4
-0.6
-0.8
-1.0
r_{xy}
0
250
500
750
1000
1250
1500
1750
2000
2250
2500
2750
Distance (m)

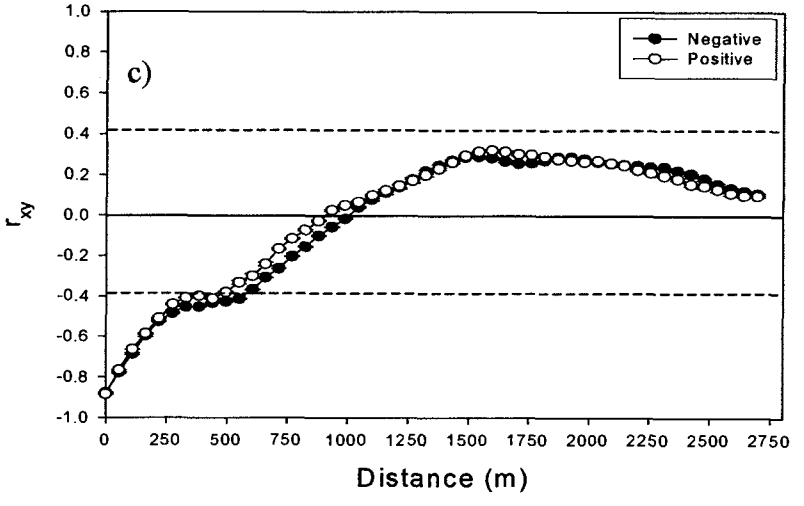
c)
Negative
Positive
1.0
0.8
0.6
0.4
0.2
0.0
-0.2
-0.4
-0.6
-0.8
-1.0
r_{xy}
0
250
500
750
1000
1250
1500
1750
2000
2250
2500
2750
Distance (m)

Figure 2.18 Cross-correlograms of salinity and light transmissivity along a) vent lines (1-3), b) west-of-vent-field lines (4-9) and c) east-of-vent-field lines (10-12). Negative and positive refer to the sign of the lag distance 'k'. Error bars = +/- SE. Dashed lines indicate lower 2.5%-iles and upper 97.5%-iles, values above and below dashed lines are significantly different from zero.

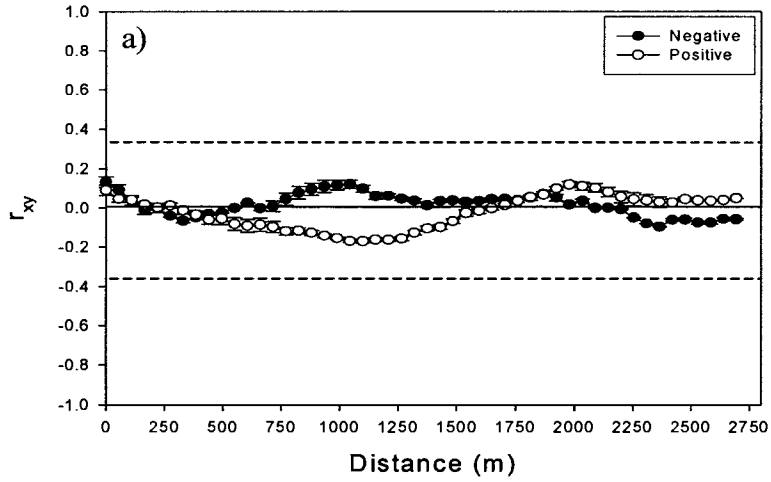
a)
Negative
Positive
1.0
0.8
0.6
0.4
0.2
0.0
-0.2
-0.4
-0.6
-0.8
-1.0
r_{xy}
0
250
500
750
1000
1250
1500
1750
2000
2250
2500
2750
Distance (m)

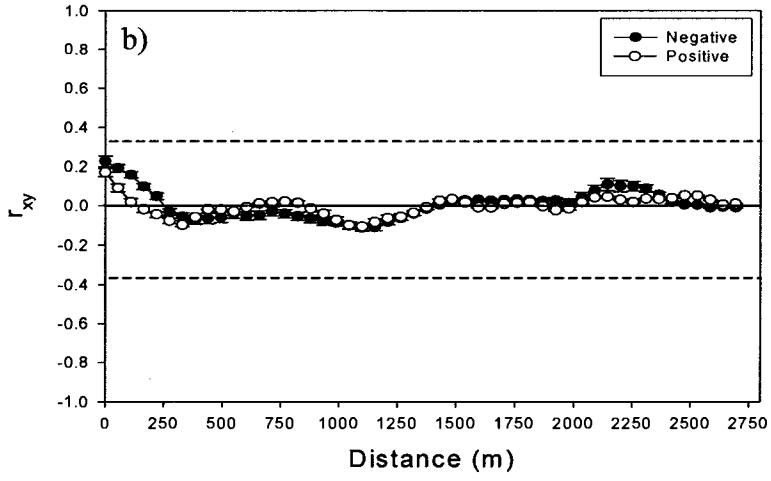
b)
Negative
Positive
1.0
0.8
0.6
0.4
0.2
0.0
-0.2
-0.4
-0.6
-0.8
-1.0
r_{xy}
0
250
500
750
1000
1250
1500
1750
2000
2250
2500
2750
Distance (m)

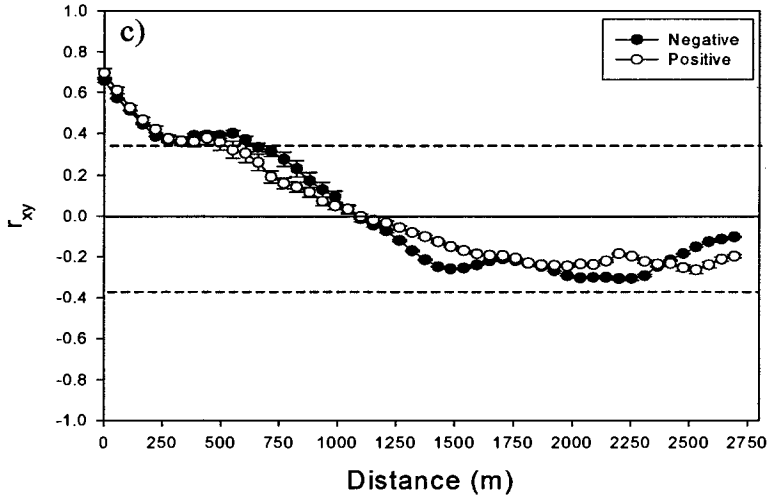
c)
Negative
Positive
1.0
0.8
0.6
0.4
0.2
0.0
-0.2
-0.4
-0.6
-0.8
-1.0
r_{xy}
0
250
500
750
1000
1250
1500
1750
2000
2250
2500
2750
Distance (m)

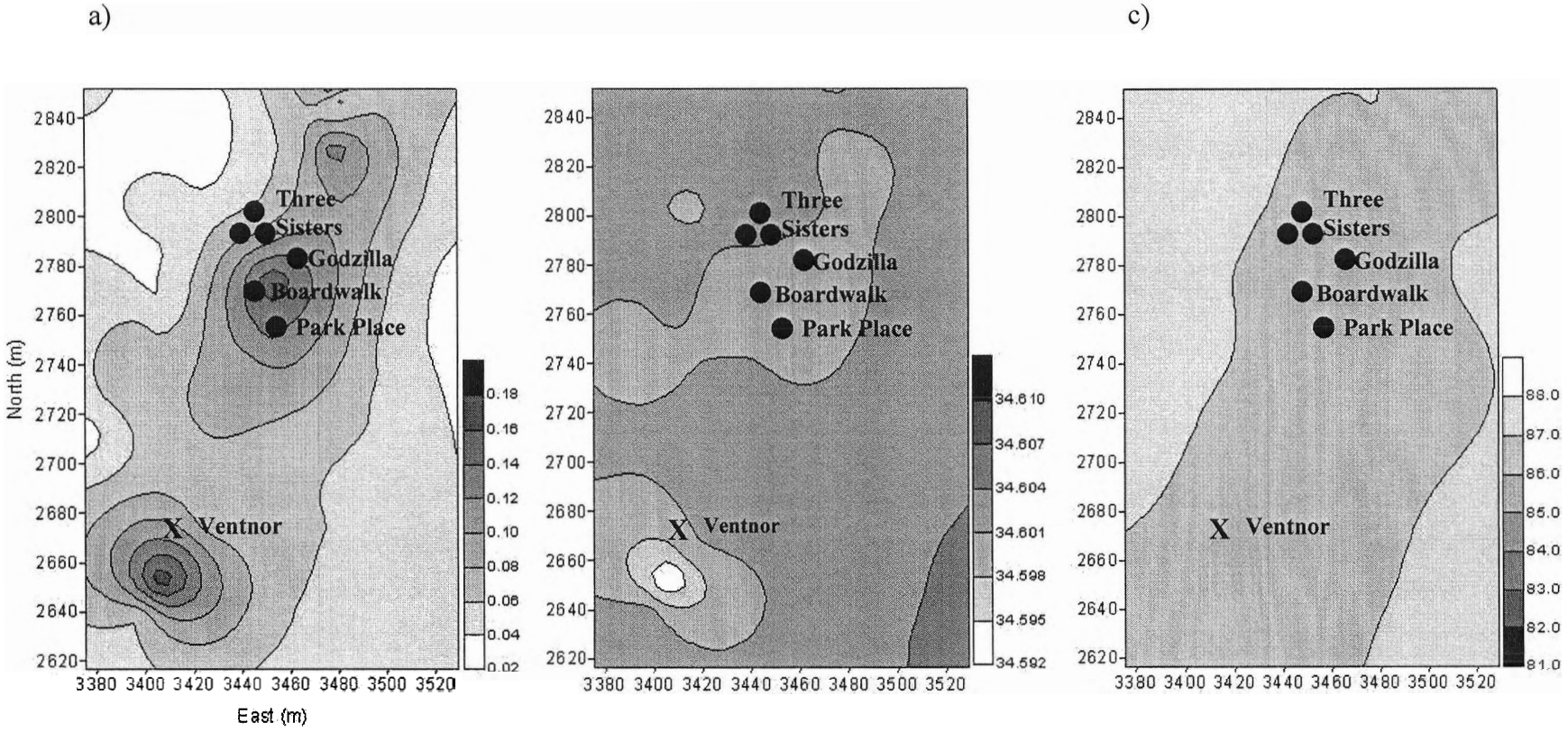

Figure 2.19 Contour plots of environmental variables a) theta anomaly, b) salinity and c) light transmission at 20 mab over High Rise using 10 m grain. Position of Ventnor (X), a smoker, is based on coordinates from JASON dives. Locations of other smokers (●), Godzilla, Boardwalk, Park Place and the three Sisters are calculated from vent locations in Robigou et al (1993).

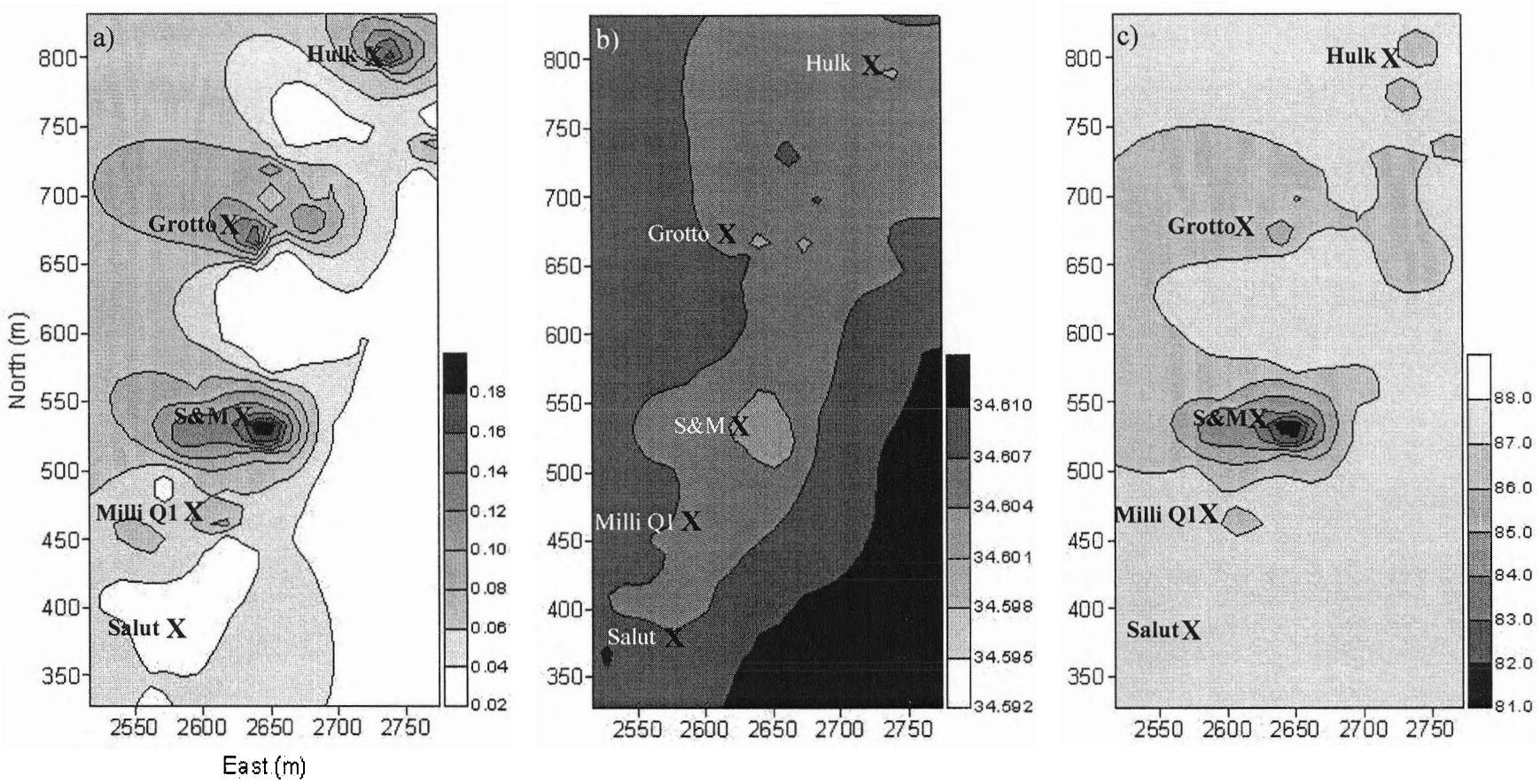

Figure 2.20 Contour plots of environmental variables a) theta anomaly, b) salinity and c) light transmission at 20 mab over Main Endeavour Field using 10 m grain. Locations of individual vents are indicated (X).

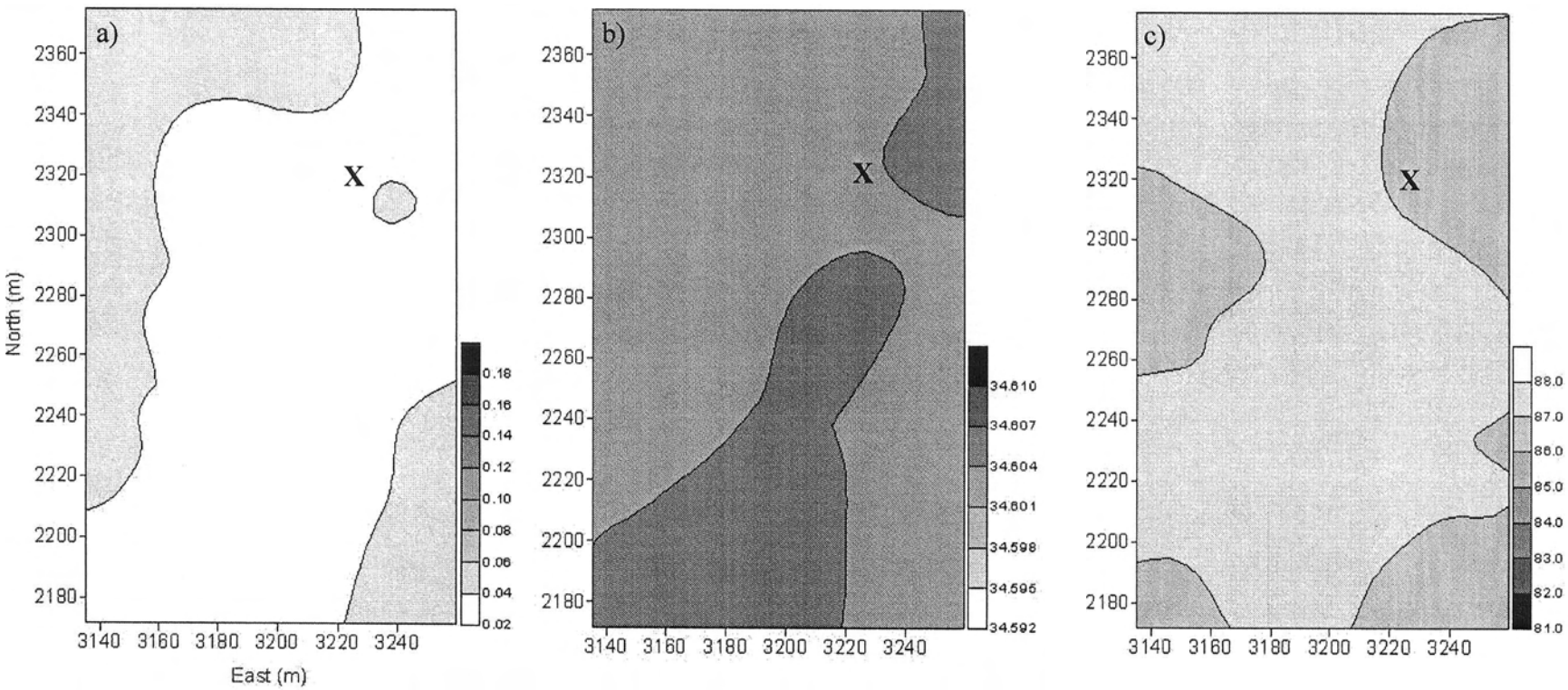

Figure 2.21 Contour plots of environmental variables a) theta anomaly, b) salinity and c) light transmission at 20 mab over Clam Bed using 10 m grain. Location of single smoker vent indicated (X).

Interestingly, the cloudiest water in the vent field is in the northeast corner, 5-10 m from the single smoker source. Cloudiness is the only feature of vent effluent from all fields that is retained in the water over distances of hundreds of metres; both temperature and salinity differences tend to dissipate on smaller scales.

Conditions at Raven are near ambient. Water is slightly warmer (hundredths of a degree) and cloudier (tenths of a percent) in the south. There is no change in salinity over the vent field.

As is evident in Table 2.4, environmental variables are all highly correlated at High Rise and MEF. Associations between temperature anomaly and salinity and between salinity and light transmissivity are slightly weaker at MEF than at High Rise. There is no significant association between salinity and light transmissivity at Clam Bed. Correlation between theta anomaly and light transmissivity at Clam Bed suggests that cloudy effluent from High Rise is carried over Clam Bed.

Table 2.4 Summary of significant correlations over vent fields at 10 m grain. All correlations significant at p=0.01.

	High Rise	**MEF**	**Clam Bed**
Temperature anomaly - Salinity	-0.810	-0.440	-0.496
Temperature anomaly – Light transmissivity	-0.644	-0.799	-0.381
Salinity – Light transmissivity	0.820	0.453	-

2.3.2 Video Imagery

A: General Observations

Roughly one organism was encountered every seven seconds of video over the 64.1 hours of almost continuous video. Video was usually clear (dark blue). Cloudy water, particularly over vent fields, was smoky and white. In only one video segment, about 10s, was the water so cloudy (dark brown) that no organisms and few particles were observed. This occurred over MEF. All organisms were visible in cloudy areas though the depth of field was smaller. As a result, abundances of some organisms (e.g. zooplankton, ctenophores) may be slightly underestimated.

Camera focus was generally clear however, on occasion the focus changed and particles became so blurry that everything appeared as large white triangles. In these instances, it was impossible to differentiate organisms from particles.

Organisms often passed the camera at the edge of the field of view, making accurate identification difficult. Shrimp and large ctenophores often approached the camera "head-on" appearing as large silver blobs. Only those that either swam away (shrimp) or shifted their approach angle (revealing some internal structure, e.g. ctenophores) were counted. Overall, I likely underestimated the abundance of most organisms with the exception of macrourids. Macrourids were the easiest group to identify given their large size and distinctive locomotion.

B: General Summary

Over the entire sample area, zooplankton are the most abundant group, accounting for more than 75% of organisms observed on the videos (Table 2.5).

Table 2.5 Comparison of video and net tow data. Total abundance for each group of organisms is listed with relative abundance in parentheses.

Group	Video		Net tow	
Zooplankton	**21657**	**(0.75)**	**469**	**(0.921)**
Copepod	21284	(0.982)	465	(0.992)
Euphausiid	340	(0.016)	1	(0.002)
Amphipod	33	(0.002)	3	(0.006)
Gelatinous zooplankton	**4814**	**(0.17)**	**1**	**(0.002)**
Nekton	**729**	**(0.03)**	0	0
Shrimp	380	(0.52)	0	0
Zoarcid fish	245	(0.34)	0	0
Macrourid fish	104	(0.14)	0	0
Tomopterids	**6**	**(0.0002)**	0	0
Cephalopods	**5**	**(0.0002)**	0	0
Unknown/Other	**1639**	**(0.06)**	**39**	**(0.077)**
Total	**28 850**		**509**	

Groups of gelatinous zooplankton appear to vary in abundance within the sample area. Gelatinous zooplankton occur in low abundance over vent fields. Beroidae, Lobata and Salpidae increase in abundance with distance from vents. Small ctenophores (Cyppidia) are most abundant along lines 11 and 12. Macrourids are most abundant along lines that passed through vent fields; line 3 have the highest count while lines 7 and 8 (west of vent fields) have the fewest. Tomopterid polychaetes are seen primarily in non-vent areas. Debris and questionable identifications of known organism groups are classified as 'unknowns'.

Table 2.5 summarizes notable differences in observations between video and net tow. Given the size of the net and the duration of the net tow, the net likely clogged after the first few hours of sampling. Most obvious is that no nekton and only one jellyfish are caught in the net. One ampharetid polychaete (*Amphisamytha sp.*) is collected in the net; no tomopterid polychaetes were found. Video is better for sampling large or fragile organisms.

Using video data, I summarize the distributions of counts for all organisms using frequency histograms (Figure 2.22). A single grain size (55 m) is used to keep exploratory analyses simple.

Both zooplankton (2-89) and gelatinous zooplankton (1-25) show relatively wide ranges of counts (Figure 2.22a). Nekton distribution is skewed towards small counts throughout the sample area (Figure 2.22b). Shrimp show the highest abundance (9) of the three nekton groups at this grain.

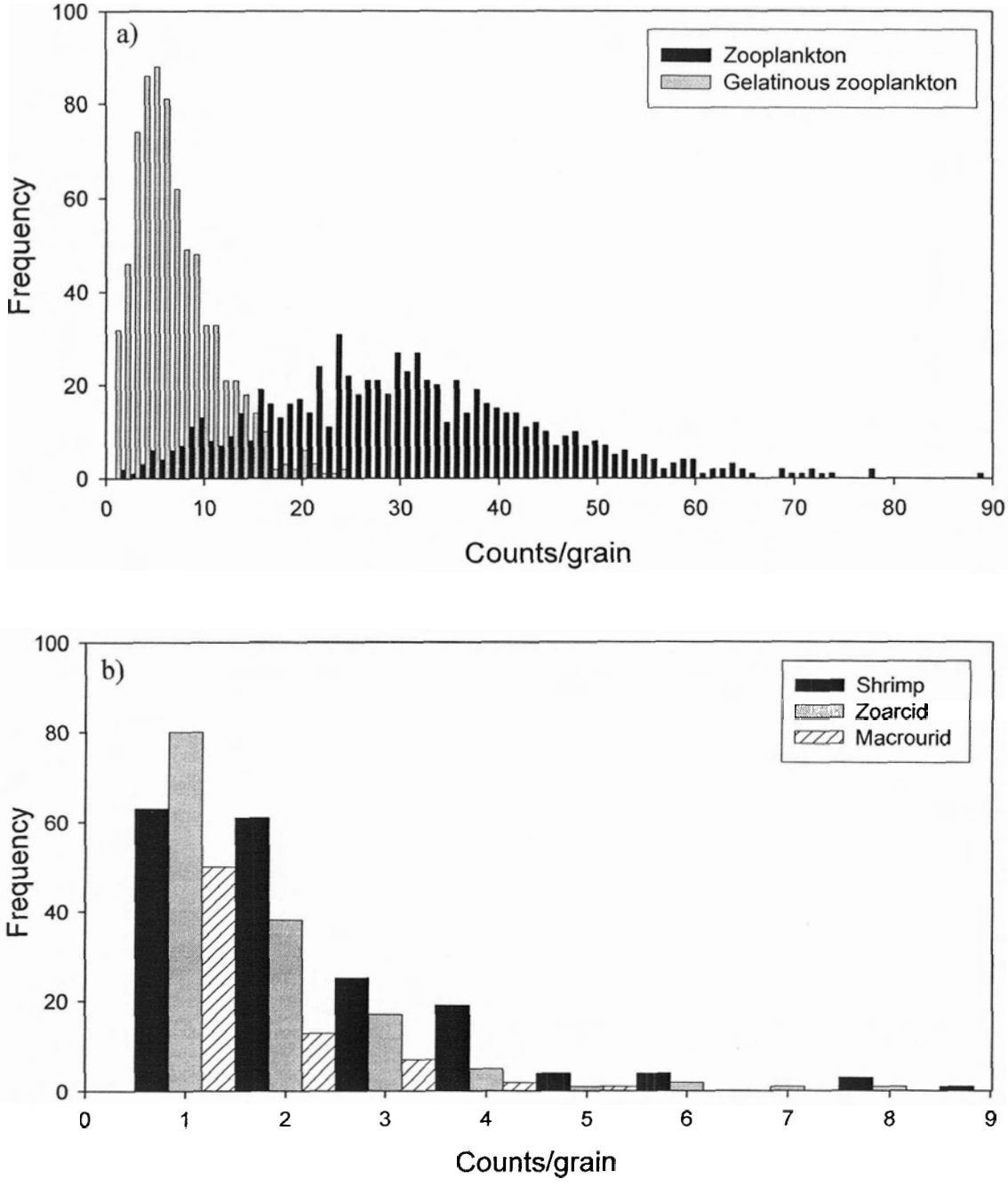

Figure 2.22 Frequency histograms of a) zooplankton and gelatinous zooplankton and b) nekton (shrimp, zoarcids, macrourids) counts per 55 m grain.

Abundance per m^3 or 100 m^3 was calculated for each organism group over vent and non-vent (hereafter divided into between-vent and non-vent) areas using the 55 m grain (Table 2.6). All groups appear to be more abundant in non-vent areas. At this grain, zooplankton are least abundant over vent fields and most abundant in the non-vent area between the vent fields. Macrourids appear to be relatively abundant over vent fields.

Table 2.6 Abundance per m^3 or $100m^3$ of each organism group over vent and non-vent areas. Numbers were calculated using 55 m grain size.

	Zooplankton /m^3	**Gelatinous zooplankton /m^3**	**Shrimp /$100m^3$**	**Zoarcid /$100m^3$**	**Macrourid /$100m^3$**
Vent	5.8	1.3	10	5	4
Between vent	11	1.7	10	9	2
Non-vent	9.6	2.2	20	10	5
Total	9.5	2.1	20	10	5

To summarize the effect of changing grain size, mean and variance values were calculated for each group of organisms over vent, between vent and non-vent areas (Table 2.7). Overall, variance decreases with decreasing grain size as the number of samples taken within the same area increases.

Zooplankton were most abundant between vent fields at all grain sizes, except 335 m. Gelatinous zooplankton and zoarcids are most abundant in non-vent areas at all grain sizes. Shrimp abundance varies depending on grain size; they are most abundant over vent fields at 335 m, between-vent areas at 165 m and non-vent areas at 55 m. Macrourids are slightly more abundant in vent fields (335 m) or between-vent fields (225 and 55 m).

Comparisons of mean values of organisms over vent, between-vent and non-vent areas are summarized in Table 2.8. Zooplankton abundance is significantly different between vent and non-vent and between vent and 'between-vent field' areas at all grain sizes. Only at the 55 m grain is there a distinction between non-vent areas (non-vent area west of the vent fields versus non-vent area between the vent fields). Significant differences are found in comparisons of gelatinous zooplankton abundance with greatest difference evident at the smallest grain (10 m). None of the nekton show significant

Table 2.7 Summary of general statistics of organism abundance over vent and non-vent areas at different grain sizes. AVG=average number of organisms per grain size. VAR=variance per grain. V=vent, B=between vent fields and N=non-vent. Number of grains within each area are given in parentheses. NA=not applicable.

Grain size	Zooplankton		Gelatinous zooplankton		Shrimp		Zoarcids		Macrourids	
	AVG	VAR	AVG	VAR	AVG	VAR	AVG	VAR	AVG	VAR
335m										
Vent (9)	115	2762	24.8	143.9	3.4	12.5	0.7	0.5	1.2	3.2
Between vent field (12)	194.8	4048	34.8	80.7	3.3	2.5	1.8	4.7	0.3	0.4
Non-vent (83)	196.8	4599	44.6	521.7	2.5	8.1	2.2	5	1.6	1.6
165m										
Vent (25)	63.5	766.7	13.3	44.1	1.4	3.4	0.5	0.7	0.4	1.3
Between vent field (27)	109.4	969.1	17.4	24.8	1.9	1.9	0.9	0.7	0.5	0.5
Non-vent (156)	99.5	1314.8	23	142.7	1.7	2.9	1.2	1.9	0.2	0.7
55m										
Vent (59)	20.1	126	4.6	6.3	0.3	0.5	0.2	0.2	0.1	0.1
Between vent field (83)	36.7	131.9	5.7	5.3	0.5	0.4	0.3	0.3	0.1	0.1
Non-vent (488)	32.4	188.7	7.6	19.2	0.6	0.7	0.4	0.5	0.2	0.2
10m										
Vent (242)	3.9	8.9	0.9	0.8	NA	NA	NA	NA	NA	NA
Between vent field (319)	6.9	13.7	1.2	1						
Non-vent (2602)	6.6	16.4	1.5	1.9						

Table 2.8 Summary of density comparisons among vent fields (V), between-vent areas (B) and non-vent areas (N). Grain size refers to grain at which difference is significant. * indicates significance at $p<0.05$. ** indicates significance at $p<0.01$.

Taxon	Total Abundance (# individuals)			Grain size	Which comparisons differ
	Vent (V)	Between (B)	Non-vent (N)		
Zooplankton	1167	3046	17444	335 m	V/B*, V/N**
				165 m	V/B**, V/N**
				55 m	V/B**, V/N**, B/N*
				10 m	V/B**, V/N**
Gelatinous zooplankton	264	471	4079	335 m	V/N*
				165 m	V/N**, B/N*
				55 m	V/N**, B/N**
				10 m	V/B*, V/N**, B/N**
Shrimp	19	54	307	335 m	None
				165 m	
				55 m	
				10 m	
Zoarcid	12	24	209	335 m	None
				165 m	
				55 m	
				10 m	
Macrourid	6	6	92	335 m	None
				165 m	
				55 m	
				10 m	

differences in abundances among the different areas. Shrimp show some difference at 55 m grain between two areas (vent/between $p=0.06$) although these are not significant. Zoarcids also show no significant difference at any grain, although at 165 m vent/non-vent comparison is close ($p=0.055$). Macrourids show no significant differences in abundance at any grain.

To compare among vent fields, I calculated mean and variance for zooplankton and gelatinous zooplankton only as there were too few counts of any nekton group over any of the vent fields (Table 2.9). Raven was also not included in the analysis as it has only a maximum of five 10 m grains. Zooplankton abundance at High Rise and at MEF was significantly lower from that at Clam Bed at both 55 m and 10 m grains ($p<0.01$). Gelatinous zooplankton abundance also differed among vent fields. At both 75 and 10 m grains, abundance at High Rise is significantly higher than at MEF ($p<0.01$). Gelatinous zooplankton abundance at Clam Bed did not differ significantly from either High Rise or MEF abundances.

Table 2.9 Summary of general statistics of organism abundance over vent fields at different grain sizes. AVG=average number of organisms per grain size. VAR=variance per grain. Number of grains within each area are given in parentheses.

Grain size	**Zooplankton**		**Gelatinous zooplankton**	
	AVG	**VAR**	**AVG**	**VAR**
55 m				
High Rise (16)	18.2	107	6.1	8.6
MEF (25)	16.2	73.1	4.7	5.5
Clam Bed (12)	29.2	166.5	3.5	3.6
10 m				
High Rise (57)	4.6	12.6	1.2	0.9
MEF (129)	5.4	9.9	0.9	0.7
Clam Bed (47)	6.4	5.3	0.4	0.3
Raven (5)	3.3	7.7	0.7	0.5

2.3.3 Spatial patterns

A: Overall spatial pattern

In this section, I describe the overall spatial pattern of organisms, by group, using qualitative (visual) methods, autocorrelation and SADIE. I then assess the spatial pattern of zooplankton and gelatinous zooplankton over vent fields using SADIE; only these groups have sufficient sample size for analyses over vent fields. Overall, different organism groups show different patterns throughout the entire sample area.

Zooplankton

Contour maps of zooplankton spatial pattern using the four grain sizes are shown in Figure 2.23. They exhibit a distinct pattern irrespective of grain size: areas of relatively low abundance are apparent over High Rise and MEF and relatively high abundance in the centre. The pattern is most obvious at the 55 m and 10 m grains. Within the centre of the sample area, zooplankton abundance appears to be highly variable. In all maps, there is a large patch of high zooplankton abundance between 1000-2000 m north and 2800-3100 m east.

This pattern is also evident in Figure 2.24. Maximum zooplankton abundance occurs in the middle of the sample area thus illustrating a curvilinear relationship with distance (north and east).

Zooplankton counts along vent lines (lines 1-3) show relatively high correlation at short distances (Figure 2.25a). Along vent lines, pairs of counts up to 165 m apart are significantly correlated. Significant correlation occurs between pairs of counts up to 110 m apart along lines west-of-vent-fields and up to 165 m apart along lines east-of-vent-fields. The influence of the vent fields is evident in the appearance of a negative correlation peak between 800-1200 m; autocorrelation includes comparisons of low counts that are in and around High Rise and MEF with high counts near the middle of the sample area. A positive peak is evident at roughly 2000 m where low counts in and around High Rise and MEF are compared. These patterns are relatively constant; no additional structure is evident when lag size is decreased.

The shape of the east-of-vent-field line is dominated by line 10. As line 10 passes over High Rise, low High Rise counts are compared with high counts north of MEF

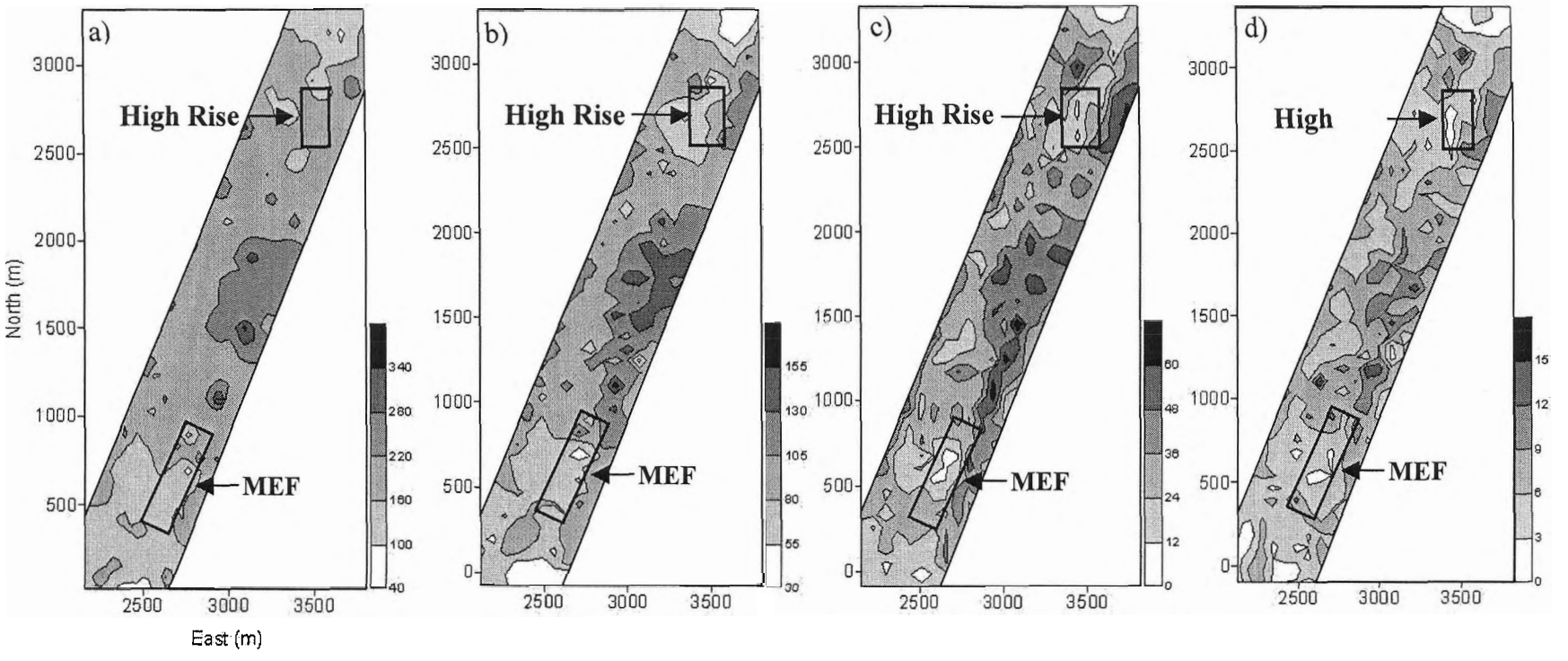

Figure 2.23 Contour plots of zooplankton abundance at 20 mab throughout whole sample area using: a) 335 m, b) 165 m, c) 55 m and d) 10 m grains. Scale indicates zooplankton abundance in each grain.

Figure 2.24 Variation in zooplankton abundance along the a) length and b) width of the sample area. Data are from all transect lines.

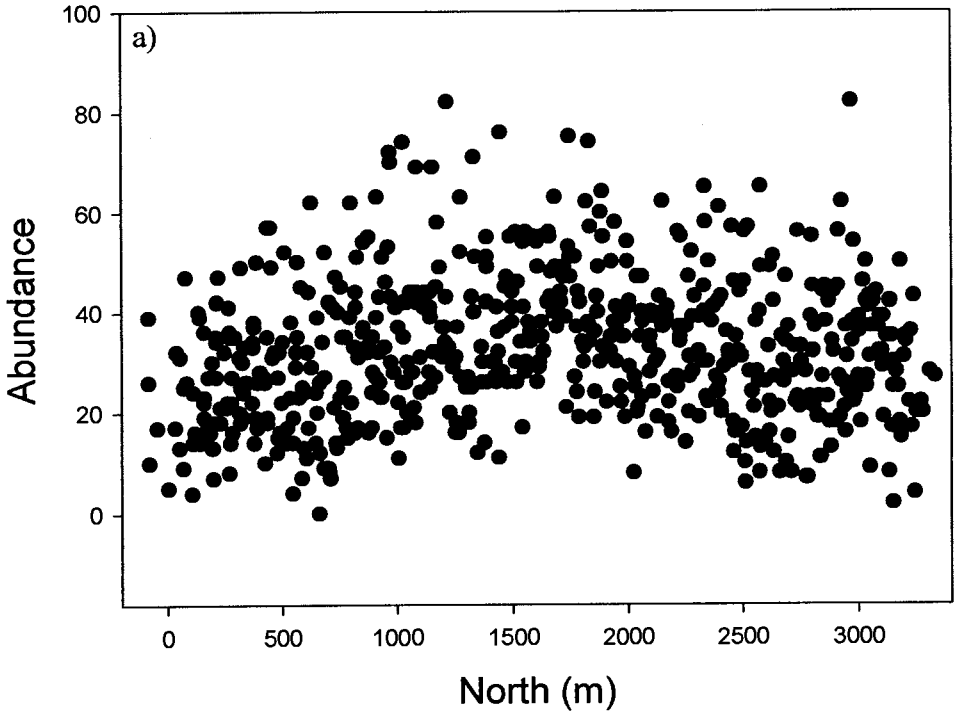
a)
Abundance
100
80
60
40
20
0
0
500
1000
1500
2000
2500
3000
North (m)

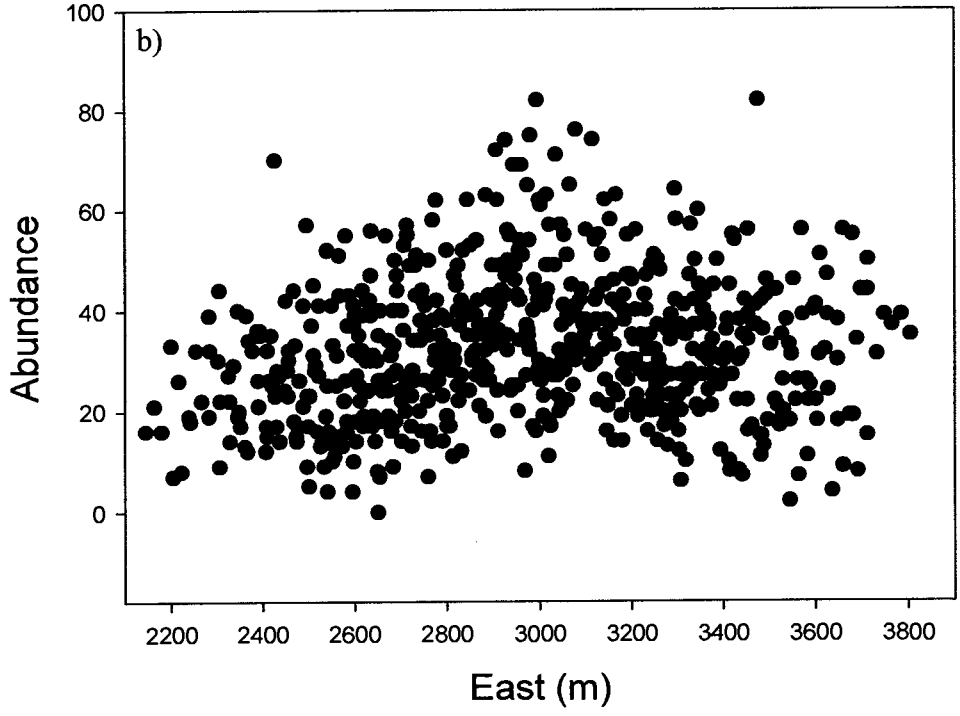
b)
Abundance
100
80
60
40
20
0
2200
2400
2600
2800
3000
3200
3400
3600
3800
East (m)

Figure 2.25 Spatial autocorrelograms of zooplankton abundance a) along-lines (transect lines) and b) across-lines (orthogonal to transect lines). Error bars = +/- SE. For a), Lines 1-3 are grouped as 'vent', lines 4-9 are grouped as 'west' (west-of-vent-field lines) and lines 10-12 are grouped as 'east' (east-of-vent-field lines). Dashed lines indicate lower 2.5%-iles and upper 97.5%-iles, values above and below dashed lines are significantly different from zero. Significance of values in b) was not tested since the number of pairs of points for each comparison is small (≤ 12).

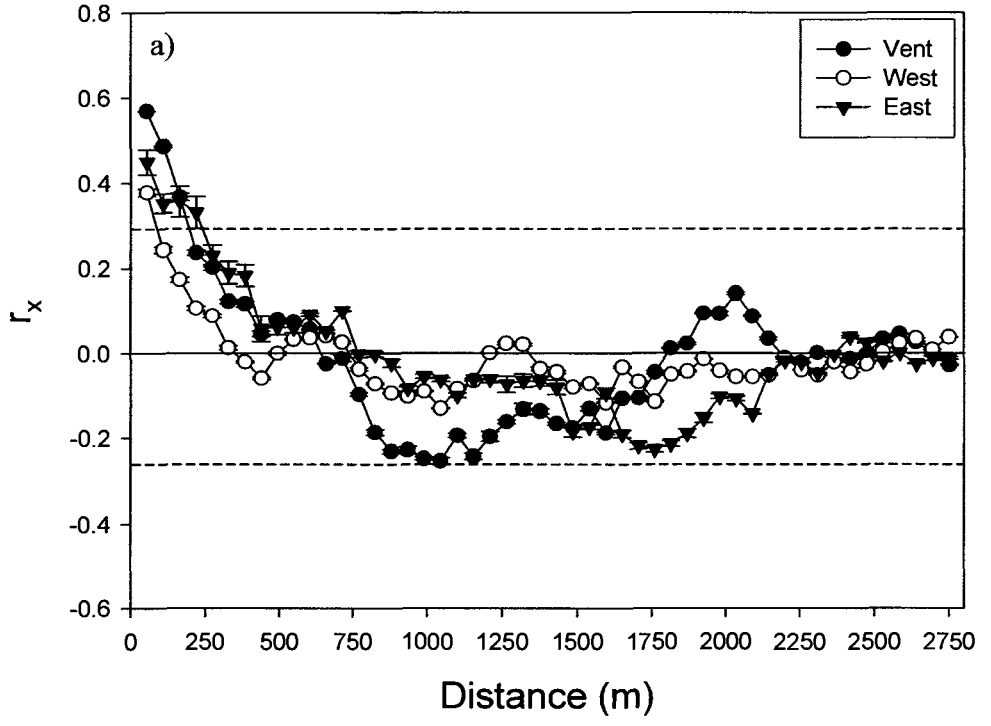
a)
Vent
West
East
0.8
0.6
0.4
0.2
0.0
-0.2
-0.4
-0.6
r_x
0
250
500
750
1000
1250
1500
1750
2000
2250
2500
2750
Distance (m)

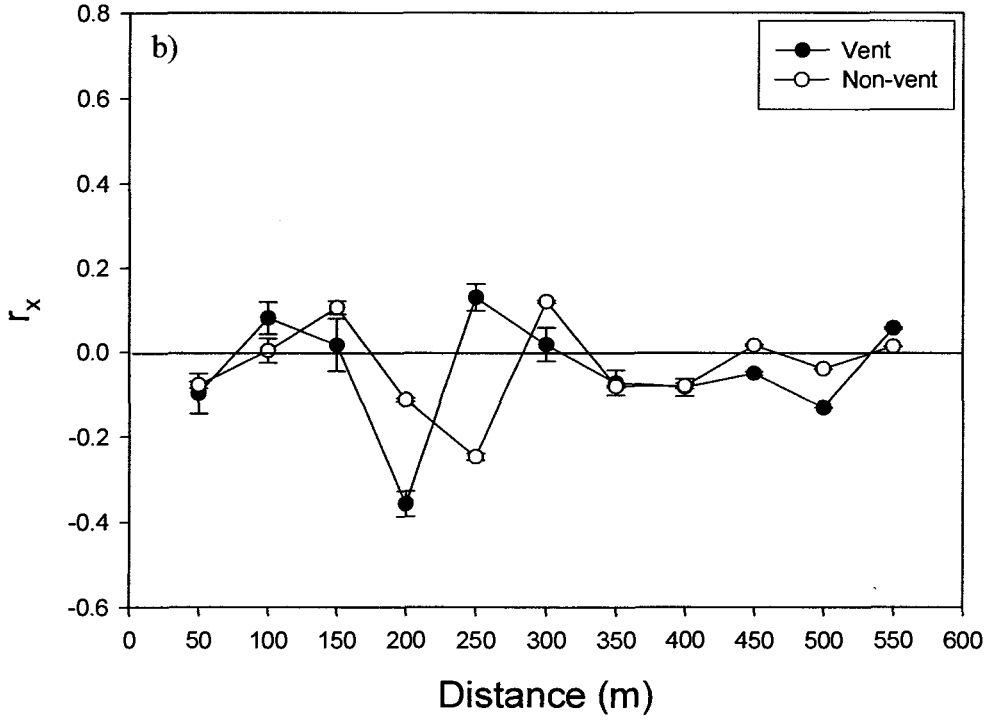
b)
Vent
Non-vent
0.8
0.6
0.4
0.2
0.0
-0.2
-0.4
-0.6
r_x
0
50
100
150
200
250
300
350
400
450
500
550
600
Distance (m)

causing a negative correlation peak (1750 m). As is the case along vent lines (1-3), the shape of the autocorrelation curve for line 10 is driven primarily by the presence of High Rise vent field thus temporal difference between lines 1 and 10 does not appear to affect zooplankton counts.

On average, de-correlation occurs at about 570 m. The number of independent events is roughly six per line (the total length of the line divided by the distance at which de-correlation occurs) or 72 (6 x 12 lines) over the whole area.

Because the scale at which independent events occur along lines at the 55 m grain is roughly 570 m, decreasing the grain size to 10 m does not increase the number of independent events. Increasing grain size to 165 m or 335 m runs the risk of not detecting all six of the independent events. Thus of the four grain sizes, the 55 m grain size is the most efficient in detecting pattern. As a result, I limit future analyses of zooplankton patterns, throughout the entire sample area, to the 55 m grain.

Across-line comparisons de-correlate at smaller scales (50-100 m) than along-line comparisons (Figure 2.25b). Because there are so few counts to compare, little structure is evident. Interestingly, unlike the along-line comparisons, neighbouring counts are negatively correlated; a high count in one transect line is compared with a relatively low count in the next transect line.

Using SADIE, clustering is shown to be significant at all extents (Table 2.10). The middle third of the sample area is the least patchy (I_a =1.6). This section contains the area of highest zooplankton abundance. Both the centre and west sections have relatively high overall clustering and have relatively high gap clustering indices (v_i) compared to their patch clustering indices (v_j). These statistics quantify patchiness that is evident in Figure 2.23c. As seen this figure, pattern along the central length of the sample area is dominated by the gaps in abundance over High Rise and MEF. In addition, the western half of the sample area contains patches of relatively low abundance in comparison to patches in the east. Gap clusters occurring in the northern and southern halves of the sample area (Table 2.10) coincide with the locations of the two main vent fields, again confirming the pattern seen in the contour maps (Figure 2.23c). In short, this pattern is significantly different from random (Table 2.10, all $p<0.01$). Gaps and patches apparent

above the vent fields and in the middle portion of the area, respectively, are significantly different from a random spatial pattern of counts.

Table 2.10 Summary of SADIE statistics for zooplankton over sub-divisions of the entire extent at 55 m grain. I_a=index of aggregation (strength of clustering in gaps and patches). P_a=probability that clustering is not significantly different from random. v_i=gap cluster index and v_j=patch cluster index. Only average gap and patch clustering indices are shown. All v_i and v_j values are significant ($p<0.01$).

Area	I_a (P_a)	AVG v_i	AVG v_j
North	4.218 (0.0002)	4.207	-3.889
South	4.284 (0.0002)	3.749	-4.461
West	4.56 (0.0002)	4.051	-5.158
East	3.961 (0.0002)	3.701	-3.958
North 1/3	2.062 (0.0012)	1.9	-1.951
Mid 1/3	1.607 (0.0131)	1.633	-1.608
South 1/3	2.957 (0.0002)	2.898	-3.046
Centre	3.205 (0.0002)	2.498	-3.48

Gelatinous zooplankton

Gelatinous zooplankton are most abundant in the eastern half of the sample area at the 55 m grain (Figure 2.26). Gelatinous zooplankton abundance is low in the central area. A single, large gap appears to extend from north of MEF, through the vent field, into the southern most portion of the sample area.

Plots of gelatinous zooplankton abundance along the length and width of the sample area also show that abundance slightly increases primarily to the east (Figure 2.27).

Like zooplankton, gelatinous zooplankton show little along-line structure; correlation coefficients fluctuate about the zero line (Figure 2.28a). Along lines east of the vent fields, significant correlation is limited to pairs of points 55 m apart, while significant correlation extends to pairs of points 110 m apart in the west. Significant correlation exists only between pairs of counts 110 m apart along vent lines; pairs of

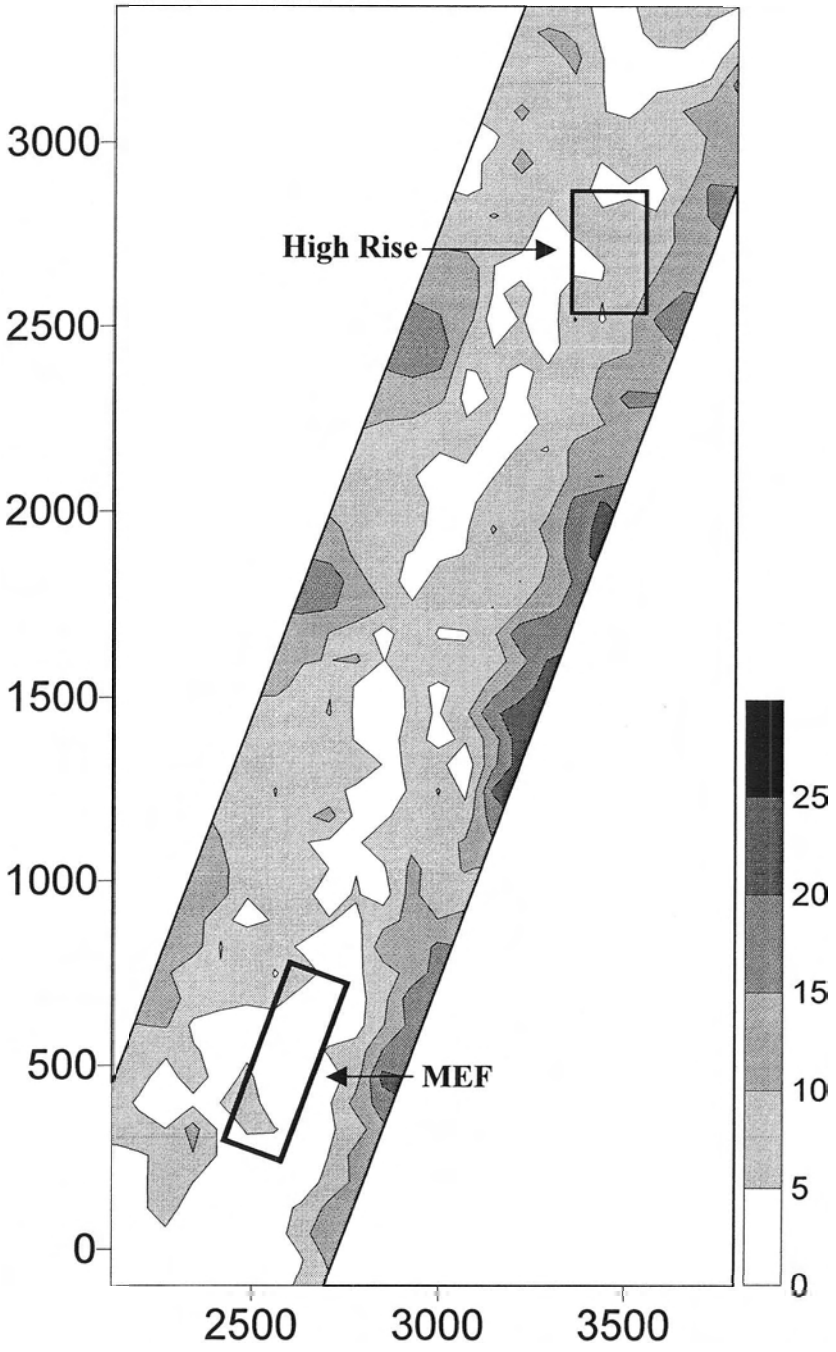

Figure 2.26 Contour plots of gelatinous zooplankton abundance at 20 mab over the entire sample area using 55 m grain size. Scale indicates gelatinous zooplankton abundance in each grain.

Figure 2.27 Variation in gelatinous zooplankton abundance along the a) length and b) width of the sample area. Data are from all transect lines.

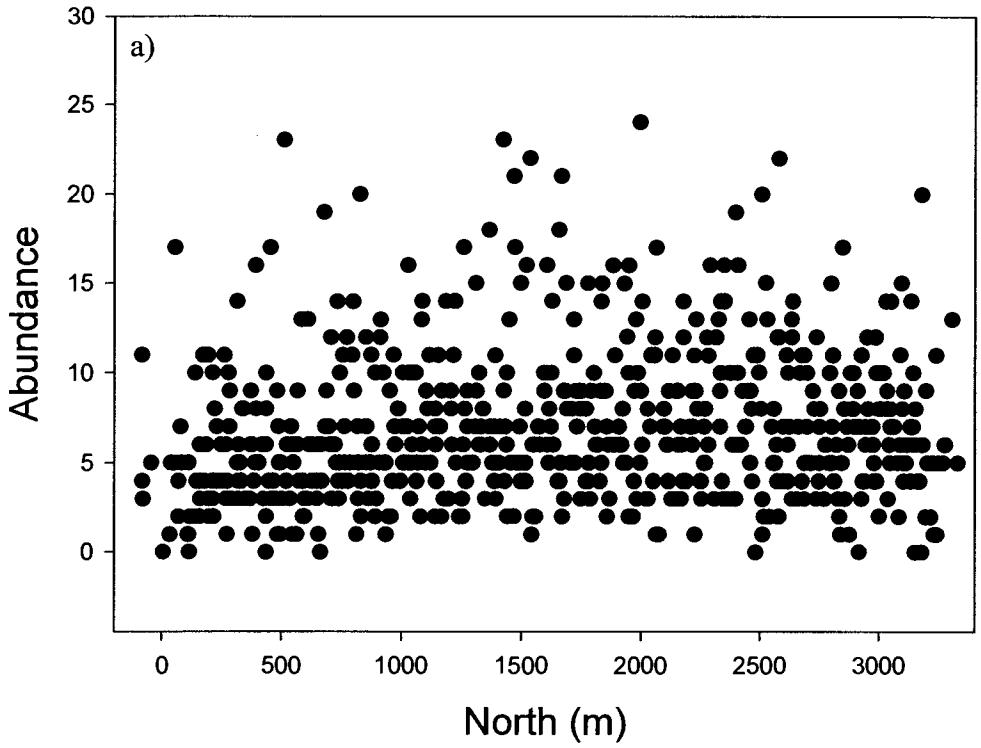
a)
Abundance
North (m)
0
5
10
15
20
25
30
0
500
1000
1500
2000
2500
3000

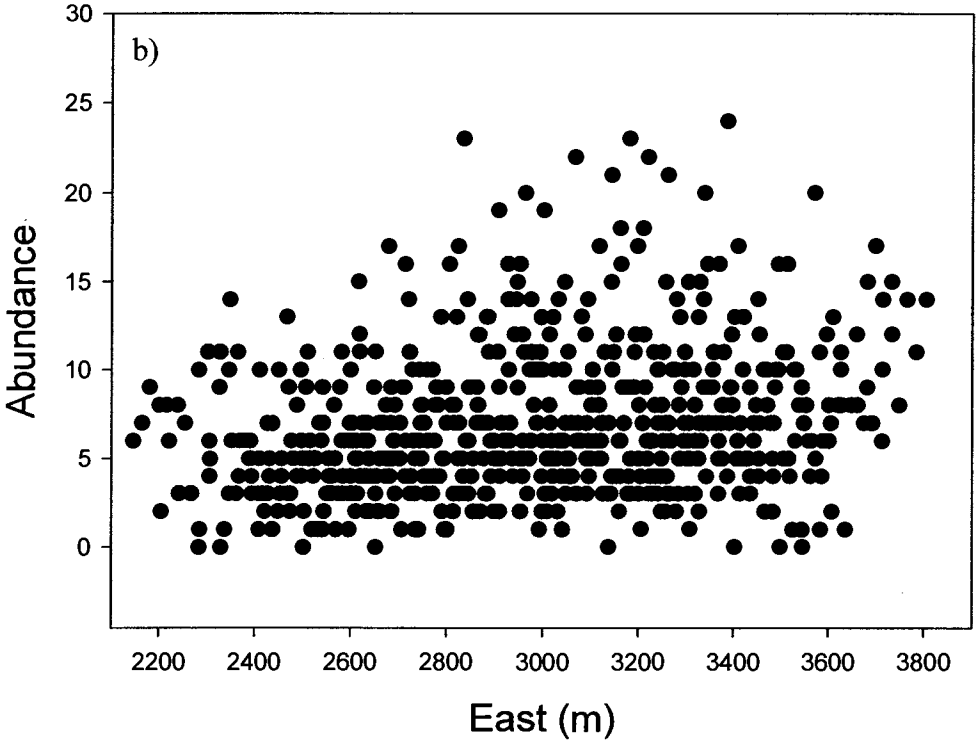
b)
Abundance
East (m)
0
5
10
15
20
25
30
2200
2400
2600
2800
3000
3200
3400
3600
3800

Figure 2.28 Spatial autocorrelograms of gelatinous zooplankton abundance a) along-lines (transect lines) and b) across-lines (orthogonal to transect lines). Error bars = +/- SE. For a), Lines 1-3 are grouped as 'vent', lines 4-9 are grouped as 'west' (west-of-vent-field lines) and lines 10-12 are grouped as 'east' (east-of-vent-field lines). Dashed lines indicate lower 2.5%-iles and upper 97.5%-iles, values above and below dashed lines are significantly different from zero. (Because the distribution of values is slightly skewed, but not significantly different from normal, the 2.5%-ile and 97.5%-ile lines are not even about the zero line.) Significance of values in b) was not tested since the number of pairs of points for each comparison is small (≤ 12).

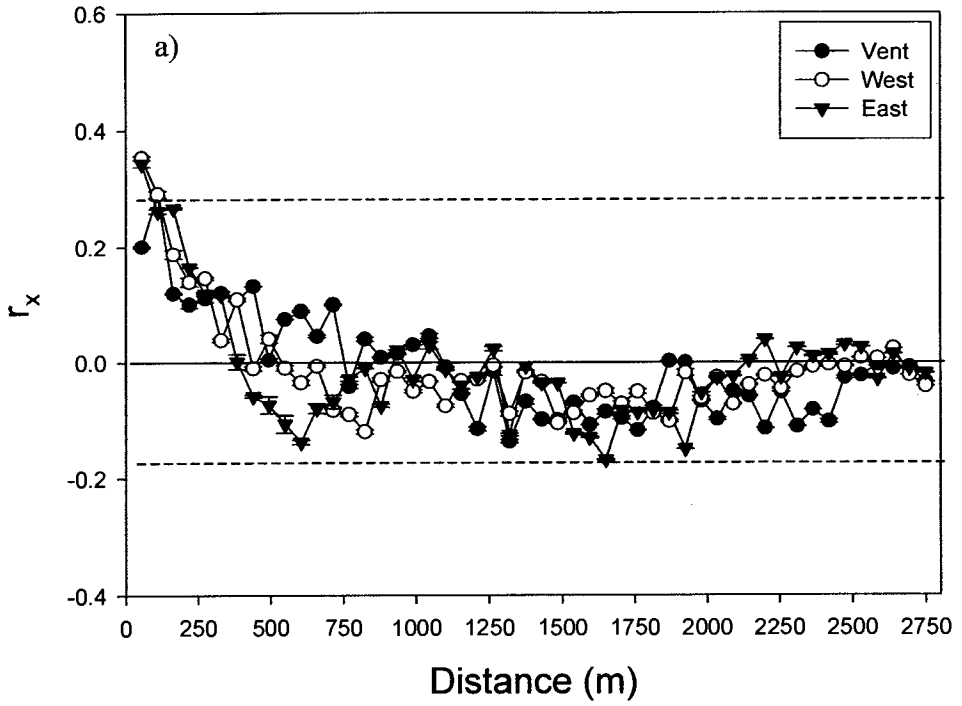
a)
Vent
West
East
0.6
0.4
0.2
0.0
-0.2
-0.4
r_x
0
250
500
750
1000
1250
1500
1750
2000
2250
2500
2750
Distance (m)

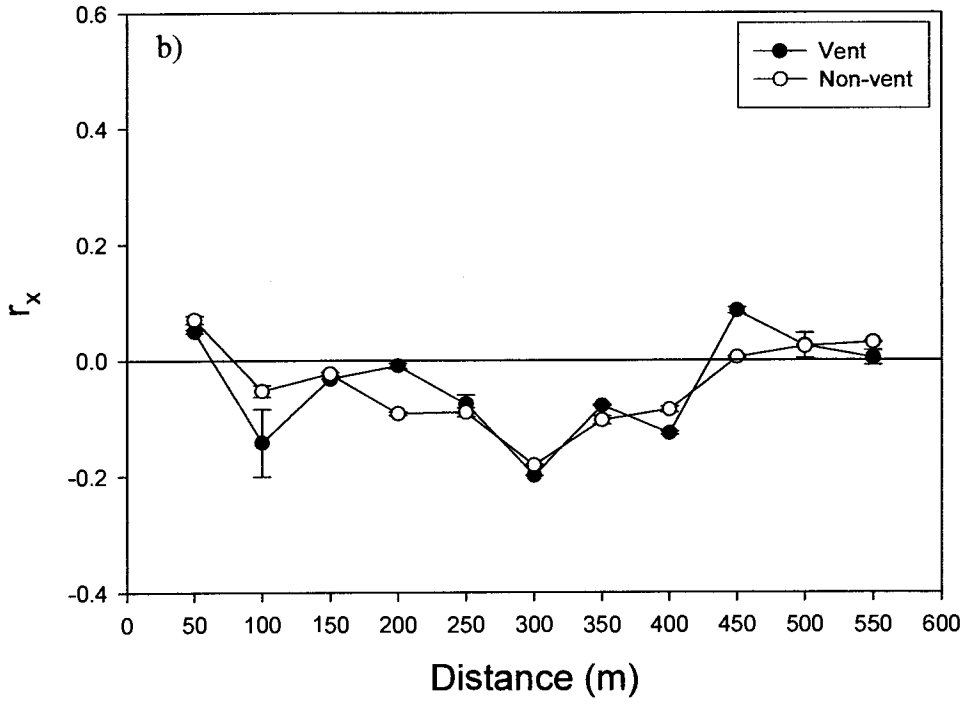
b)
Vent
Non-vent
0.6
0.4
0.2
0.0
-0.2
-0.4
r_x
0
50
100
150
200
250
300
350
400
450
500
550
600
Distance (m)

counts 110 m apart are more strongly correlated than neighbouring counts. De-correlation occurs at roughly 530 m. As a result, like zooplankton, there are six independent events per line and 72 independent events throughout the entire sample area. Thus spatial analyses and figures using the 55 m grain are shown.

Correlation across-lines tends to break down at roughly the same scale as across line comparisons for zooplankton (Figure 2.28b). Unlike zooplankton, correlations at the smallest lag distance, 50 m, are mostly positive. This suggests that counts in adjacent lines are relatively similar.

Gelatinous zooplankton spatial pattern shows significant clustering, primarily in the form of gaps (Table 2.11). The highest gap cluster index is in the centre, which is evident as a long gap in Figure 2.26. An elongated patch of relatively high gelatinous zooplankton counts is found along the easternmost side of the area which is likely responsible for the similarity between patch (v_i) and gap (v_j) clustering values in the east, north and middle sections. Overall, gelatinous zooplankton are less abundant over the central length of the sample area where most of the venting occurs.

Table 2.11 Summary of SADIE statistics for gelatinous zooplankton over sub-divisions of the entire extent at 55 m grain. I_a=index of aggregation (strength of clustering in gaps and patches). P_a=probability that clustering is not significantly different from random. v_i=gap cluster index and v_j=patch cluster index. Only average gap and patch clustering indicies are shown. All v_i and v_j values are significant ($p<0.01$).

Area	I_a (P_a)	AVG v_i	AVG v_j
North	2.152 (0.0008)	1.911	-2.146
South	4.003 (0.0002)	3.566	-3.992
West	4.359 (0.0002)	4.051	-4.607
East	2.367 (0.0008)	2.135	-2.389
North 1/3	1.903 (0.0023)	1.753	-1.913
Mid 1/3	1.791 (0.004)	1.577	-1.761
South 1/3	2.885 (0.0002)	2.549	-2.95
Centre	4.403 (0.0002)	3.505	-5.174

Nekton

Nekton are less abundant than either zooplankton group. A larger grain size was used in nekton spatial analyses because:

1) in the majority of the sample area, nekton are either present in very low numbers (1 or 2) or are absent
2) they are better swimmers than zooplankton and are able to move more quickly over longer distances.

Therefore the 165 m grain size was used for analyses of nekton spatial patterns.

Shrimp appear more abundant in north and on the west side of the sample area at the 165 m grain size (Figure 2.29a). Using Pearson's product moment correlation, shrimp abundance appears to slightly, but significantly, increase in the north ($r=0.19$, $p<0.001$). Shrimp are particularly abundant in and around High Rise and Clam Bed.

Zoarcids are more abundant in the south, especially north of MEF, including the area over Raven (Figure 2.29b). In contrast to shrimp, zoarcids show a slight, but significant increase toward the south (Pearson's $r=0.15$, $p<0.02$) and in fact appear to be most abundant where there are few shrimp and macrourids.

Macrourids, like shrimp, are relatively more abundant in the north half, especially over Clam Bed (Figure 2.29c). There are two patches of relatively high abundance in the middle and north of MEF, near Raven. Macrourids are virtually absent from MEF and surrounding area.

Unlike zooplankton, each nekton count is treated as an independent value as nekton are relatively low in abundance. Counts are likely independent; nekton can choose to be in an area where there are other conspecifics or avoid areas with unsuitable conditions. However, for the sake of simplicity, independence of observations was assumed.

As with both zooplankton groups, nekton show significant clustering throughout the entire sample area (Table 2.12). All three groups have higher average gap clustering indices (v_j). As is evident in Figure 2.29, nekton are either present (abundance=1) or absent in the majority of the sample area. Patch clusters of shrimp and macrourids are concentrated over the vent fields while zoarcids cluster to the north and south of MEF.

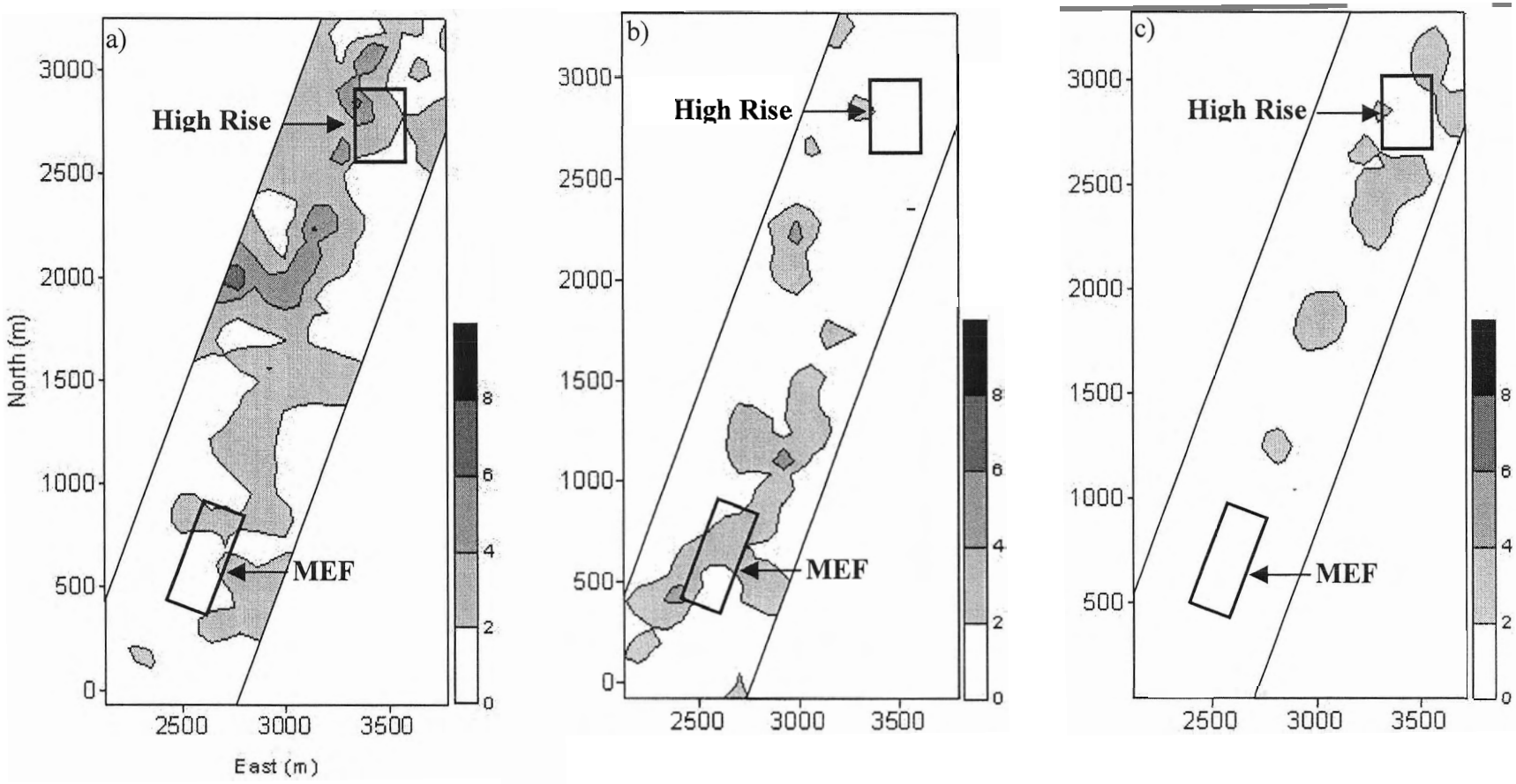

Figure 2.29 Contour maps of a) shrimp, b) zoarcid and c) macrourid abundance 20 mab throughout whole sample area at 165m grain. Scale indicates nekton abundance in each grain.

Table 2.12 Summary of SADIE statistics for nekton at 165 m grain. I_a=index of aggregation (strength of clustering in gaps and patches). P_a=probability that clustering is not significantly different from random. v_i=gap cluster index and v_j=patch cluster index. All v_i and v_j values are significant ($p<0.05$).

Group	Extent	I_a (P_a)	AVG v_i	AVG v_j
Shrimp	Whole area	2.970 (0.002)	2.366	-3.132
Zoarcid	Whole area	2.162 (0.0064)	1.896	-2.106
Macrourid	Whole area	2.818 (0.002)	2.399	-2.898

B: Spatial pattern over vent fields

Because the extent of the sample area is reduced, I only use the 10 m grain size map spatial pattern over vent fields. Use of the smaller grain size identifies pattern within pattern (i.e. small patches and gaps occurring within large patches and gaps). High Rise, Clam Bed and MEF are used in the following analyses. Raven is omitted as only one transect line passes through the vent field.

Zooplankton

Among vent fields, zooplankton are most abundant over Clam Bed, the smallest of the three mapped fields (Figure 2.30). Some degree of clustering is evident within each of the three vent fields. Clustering at High Rise is significant (I_a=1.881, Table 2.13). Gap clustering is more intense than patch clustering.

At MEF, zooplankton are least abundant along the central length of the vent field (Figure 2.30b). This gap extends the length of the vent field, occurring over the majority of individual vents. Spatial pattern at MEF significantly differs from random (Table 2.13).

At Clam Bed, gaps and patches are not significantly aggregated (Figure. 2.30c). Based on SADIE analysis, zooplankton spatial pattern at this site is random.

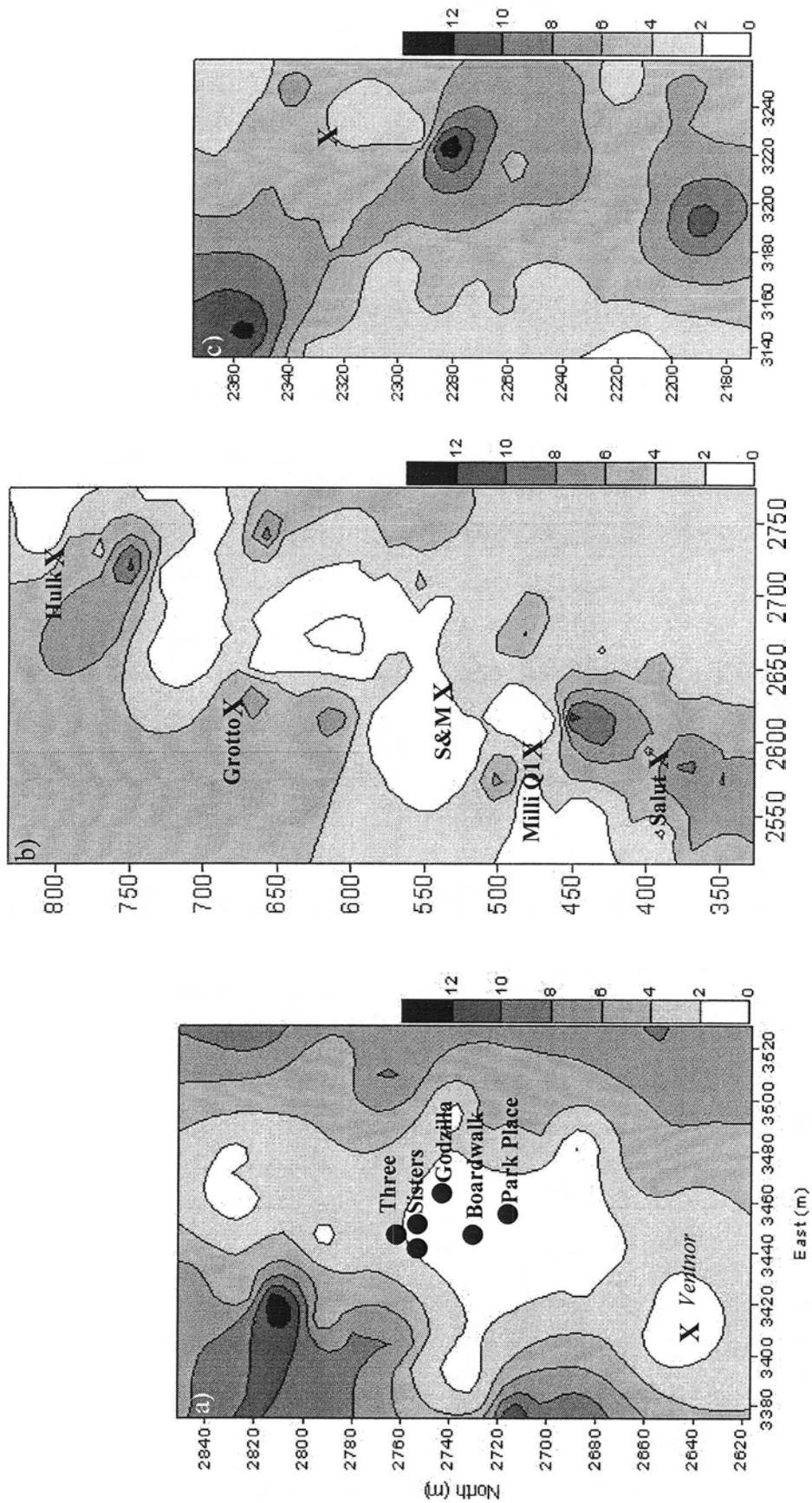

Figure 2.30 Contour maps of zooplankton abundance over a) High Rise, b) MEF and c) Clam Bed at 10 m grain. Individual vents are indicated (X).

Table 2.13 Summary of SADIE statistics for zooplankton over three of the four vent fields using 10 m grain. I_a=index of aggregation (strength of clustering in gaps and patches). P_a=probability that clustering is not significantly different from random. v_i=gap cluster index and v_j=patch cluster index. Only significant ($p<0.05$) patch and gap clustering indices (v_i and v_j) are shown.

Area	I_a (P_a)	AVG v_i	AVG v_j
High Rise	1.881 (0.0008)	1.831	-1.859
MEF	1.641 (0.039)	1.910	-
Clam Bed	1.036 (0.3568)	-	-

Gelatinous zooplankton

Among vent fields, abundance of gelatinous zooplankton is lowest over MEF (6) and highest over High Rise (11). A large patch of relatively high numbers of gelatinous zooplankton at is evident over High Rise (Figure 2.31a). At MEF, gelatinous zooplankton are concentrated along the northern and eastern boarders (Figure 2.31b). Clam Bed is characterized by a relatively large cluster of low counts through the centre of the vent field (Figure 2.31c).

Despite relatively low abundance, gelatinous zooplankton spatial pattern is statistically significantly different from random over all three vent fields (Table 2.14). At High Rise and Clam Bed, patch and gap clustering are relatively equal (v_i and v_j have similar absolute values). Only at MEF does gap clustering significantly exceed patch clustering. As with zooplankton, gelatinous zooplankton are virtually absent along the length of MEF, where most of the venting occurs.

Table 2.14 Summary of SADIE statistics for gelatinous zooplankton over three of the four vent fields using 10 m grain. I_a=index of aggregation (strength of clustering in gaps and patches). P_a=probability that clustering is not significantly different from random. v_i=gap cluster index and v_j=patch cluster index. Only significant ($p<0.05$) patch and gap clustering indices (v_i and v_j) are shown.

Area	I_a (P_a)	AVG v_i	AVG v_j
High Rise	1.669 (0.0027)	1.788	-1.727
MEF	1.57 (0.006)	-	-1.575
Clam Bed	1.645 (0.0034)	1.675	-1.659

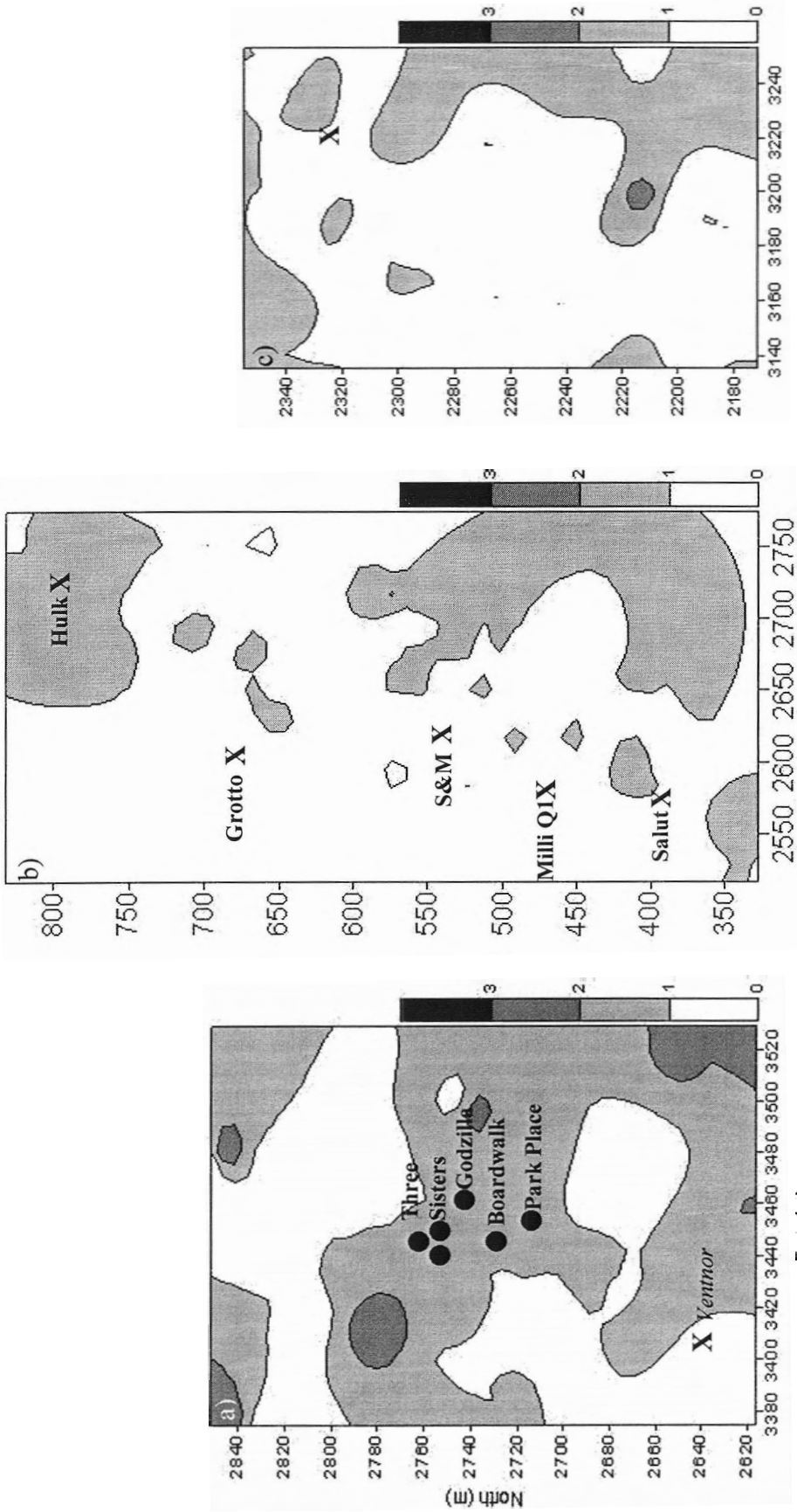

Figure 2.31 Contour maps of gelatinous zooplankton abundance above a) High Rise, b) MEF and c) Clam Bed at 10 m grain. Individual vents are indicated (X).

2.3.4 Co-variation of patterns – Inter-taxon comparisons

Correlations among groups of organisms may hint at underlying biological processes, such as predation, competition and sharing food resources, that may influence organism spatial pattern. Over the entire sample area, zooplankton and gelatinous plankton are significantly correlated at 165 m (r=0.575) and 55 m (r=0.42) grains (335 m and 10 m grains are not used in these comparisons) (Table 2.15). Zooplankton also show significant correlation with zoarcids at 165 m (r=0.291) and 55 m (r=0.197). Gelatinous plankton and zoarcids were also significantly correlated at these grains (165 m, r=0.241; 55 m r=0.114). Among nekton, only shrimp and macrourids show significant correlation, the strength of which decreases with decreasing grain size (at 165 m, r=0.275; at 55 m, r=0.157).

When the entire extent is divided into vent, between-vent and non-vent areas, some correlations are no longer significant. Fewer groups are significantly correlated over vent fields. Only zooplankton and gelatinous zooplankton show significant correlation at both grains (165 m r=0.483; 55 m, r=0.413) while shrimp and macrourids are significantly correlated only at the 165 m grain (r=0.444) (Table 15). In the area between vent fields, significant correlations between zooplankton and gelatinous zooplankton (r=0.383) and between zooplankton and shrimp (r=0.413) were found at 165 m grain. No significant correlations were found among any organisms between the vent fields at the 55 m grain. Significant correlations were also found in the non-vent areas particularly between zooplankton and gelatinous zooplankton (165 m, r=0.508; 55m, r=0.43), and zooplankton and zoarcids (165 m, r=0.324; 55 m, r=0.202). Gelatinous zooplankton and zoarcids (r=0.176) and shrimp and macrourids (r=0.288) showed significant correlation at 165 m.

Table 2.15 Summary of correlations among organism groups. Grain sizes at which association is significant are indicated. Associations significant at p=0.05 are indicated by '*'; associations significant at p=0.01 are indicated by '**'. Calculated degrees of freedom (df): zooplankton (72) and gelatinous zooplankton (72).

	Gelatinous zooplankton	Shrimp	Zoarcid	Macrourid
Whole area				
Zooplankton	165m**, 55m**	-	165m**, 55m**	-
Gelatinous zoopl.	X	-	165m**, 55m**	-
Shrimp	-	X	-	165m**, 55m**
Zoarcid	-		X	-
Vent fields				
Zooplankton	165m*, 55m**	-	55m**	-
Gelatinous zoopl.	X	-	-	-
Shrimp	-	X	-	165m*
Zoarcid	-	-	X	-
Between fields				
Zooplankton	165m**	-	165m**	-
Gelatinous zoopl.	X	-	-	-
Shrimp	-	X	-	-
Zoarcid	-	-	X	-
Non-vent area				
Zooplankton	165m**, 55m**	-	165m**, 55m*	-
Gelatinous zoopl.	X	-	165m*, 55m*	-
Shrimp	-	X	-	165m**
Zoarcid	-	-	X	-

Essentially, there are two "groups" of associated organisms: 1) zooplankton, gelatinous zooplankton and zoarcids and 2) shrimp and macrourids.

2.3.5 Co-variation of patterns - Spatial pattern and environmental variables

A: Whole area

In this section, I discuss co-variation of patterns over the whole area and then over individual vent fields. Environmental associations are assessed over vent fields only with respect to zooplankton (both small crustaceans and gelatinous).

Zooplankton

Zooplankton abundance shows some association with theta anomaly (Figure 2.32a). Maximum zooplankton counts are found between anomalies of 0.02-0.04°C, primarily in non-vent areas. Additional evidence of an association between zooplankton

Figure 2.32 Correlation between theta anomaly and zooplankton abundance a) in vent, between-vent and non-vent areas, b) along line 2 and c) along line 8 (non-vent area only).

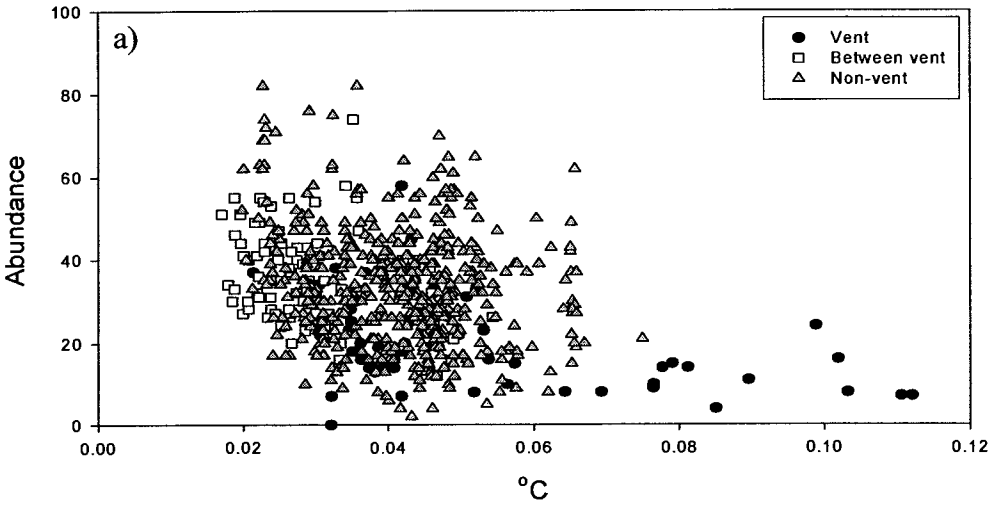
a)
Vent
Between vent
Non-vent
Abundance
°C

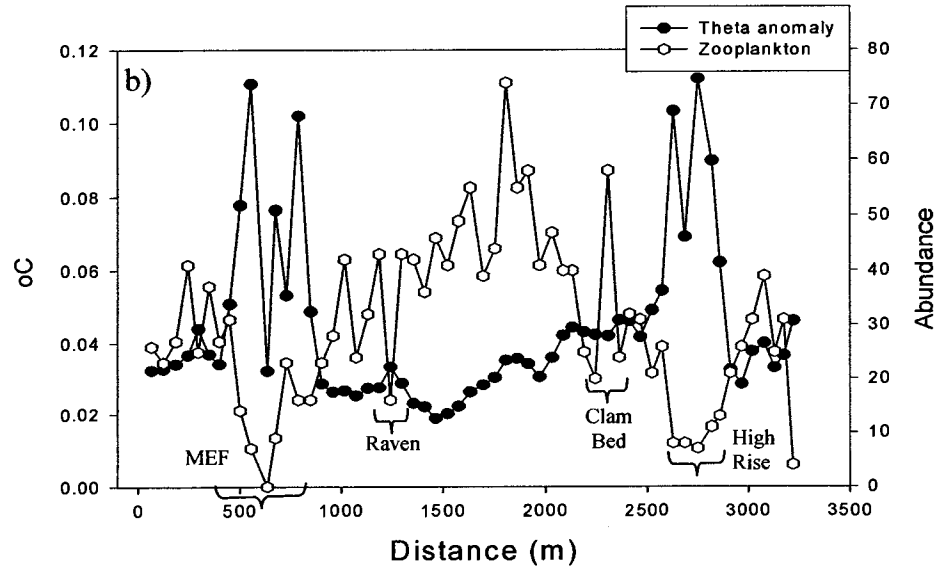
b)
Theta anomaly
Zooplankton
oC
Abundance
MEF
Raven
Clam Bed
High Rise
Distance (m)

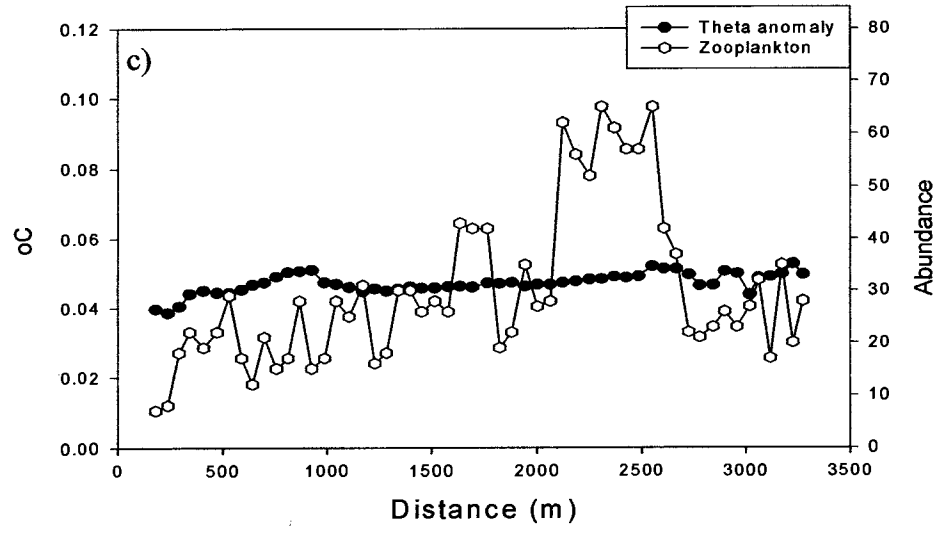
c)
Theta anomaly
Zooplankton
oC
Abundance
Distance (m)

abundance and temperature anomaly of vent effluent is seen in Figure 2.32b Along line 2, increases in theta anomaly above High Rise and MEF coincide with decreases in zooplankton abundance. This trend appears much stronger over High Rise, where there is less fluctuation in temperature within the vent field. Along line 8, which does not pass over any vent field, zooplankton abundance fluctuates irrespective of theta anomaly, peaking between 2000-2600 m, about 150 m west of Clam Bed (Figure 2.32c). Thus zooplankton abundance appears to be strongly associated with theta anomaly only over vent fields.

Although effluent is no longer distinguishable in terms of theta anomaly along line 8, the peak in zooplankton abundance may still be influenced by vent effluent. This idea will be addressed in the discussion.

Little association is evident between abundance and salinity (Figure 2.33a). At High Rise and MEF, an overall drop in zooplankton coincides with an overall drop in salinity, suggesting some association (Figure 2.33b). However, between the two fields, zooplankton increase despite no change in salinity. Overall, the decrease in zooplankton over vent fields is not likely associated with salinity as salinity is mostly a proxy for depth. As with theta anomaly, abundance along line 8 shows little relationship with salinity (Figure 2.33c)

Some association between increased water cloudiness and decreased abundance is evident in Figure 2.34a, although the relationship is not as strong as for theta anomaly. In the cloudiest water, almost 30 zooplankton were counted in a 55 m interval. This suggests that while water cloudiness may contribute to underestimation of zooplankton, it is not solely responsible for low counts. Consistent with this, zooplankton abundance remains lower in relatively clear areas over vent fields than that in non-vent areas. Decreases in light transmissivity over High Rise and MEF also coincide with decreases in zooplankton abundance (Figure 2.34b).

Conversely, at Clam Bed, water is relatively cloudy (light transmissivity decreases), but zooplankton abundance increases. It may be relevant that there is no increase in temperature at Clam Bed despite a decrease in light transmissivity. Along line 8, zooplankton abundance fluctuates despite relatively stable light transmissivity (Figure

Figure 2.33 Correlation between salinity and zooplankton abundance a) in vent, between-vent and non-vent areas b) along line 2 and c) line 8 (non-vent area only).

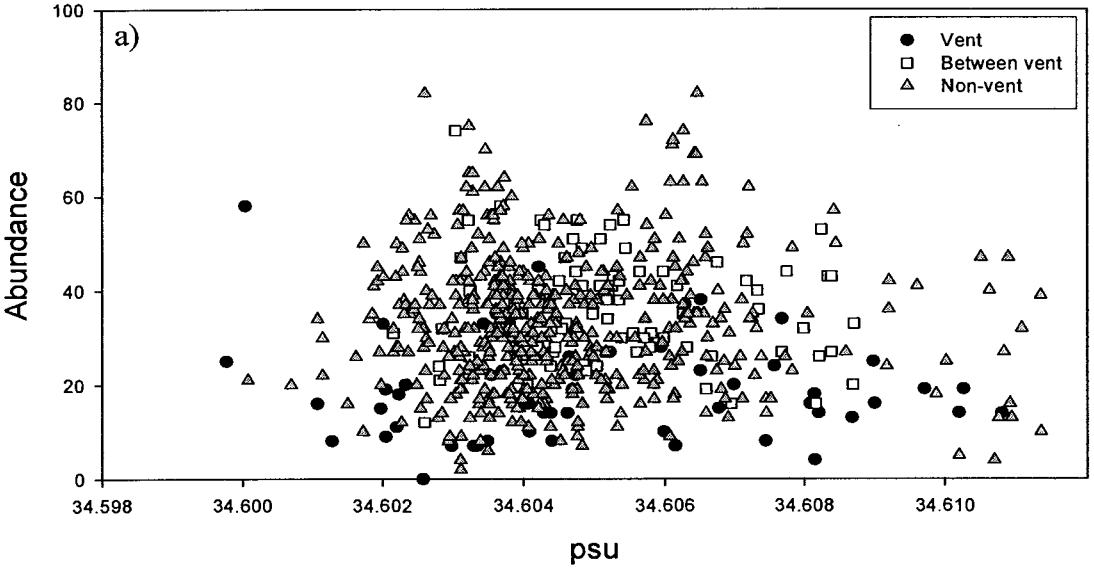
a)
Vent
Between vent
Non-vent
Abundance
psu
100
80
60
40
20
0
34.598
34.600
34.602
34.604
34.606
34.608
34.610

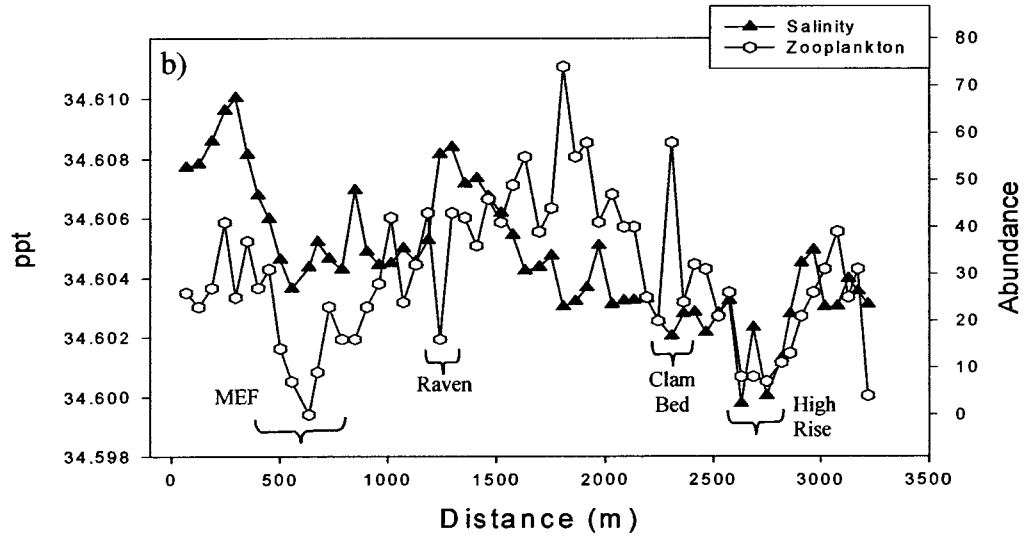
b)
Salinity
Zooplankton
ppt
Abundance
Distance (m)
MEF
Raven
Clam Bed
High Rise
34.610
34.608
34.606
34.604
34.602
34.600
34.598
80
70
60
50
40
30
20
10
0
0
500
1000
1500
2000
2500
3000
3500

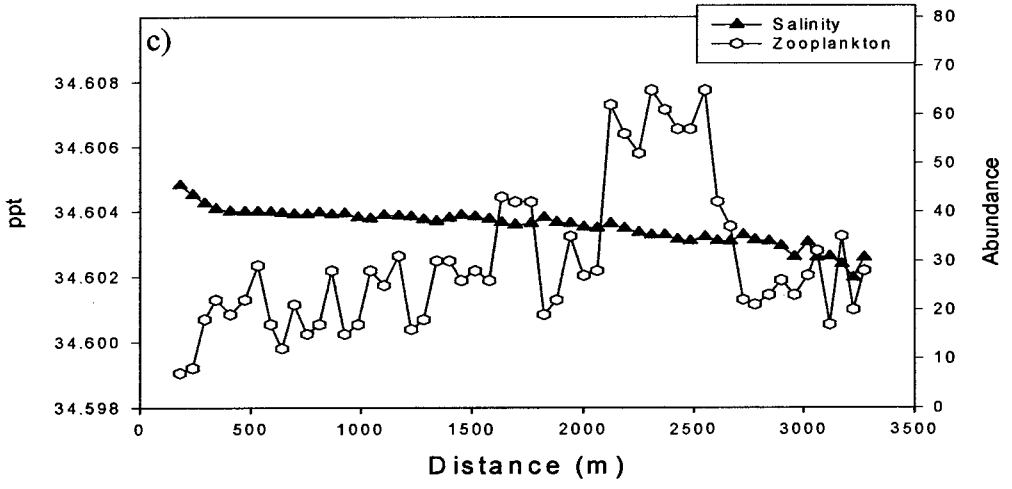
c)
Salinity
Zooplankton
ppt
Abundance
Distance (m)
34.608
34.606
34.604
34.602
34.600
34.598
80
70
60
50
40
30
20
10
0
0
500
1000
1500
2000
2500
3000
3500

Figure 2.34 Correlation between light transmissivity and zooplankton abundance a) in vent, between-vent and non-vent areas, b) along line 2 and c) line 8 (non-vent area only).

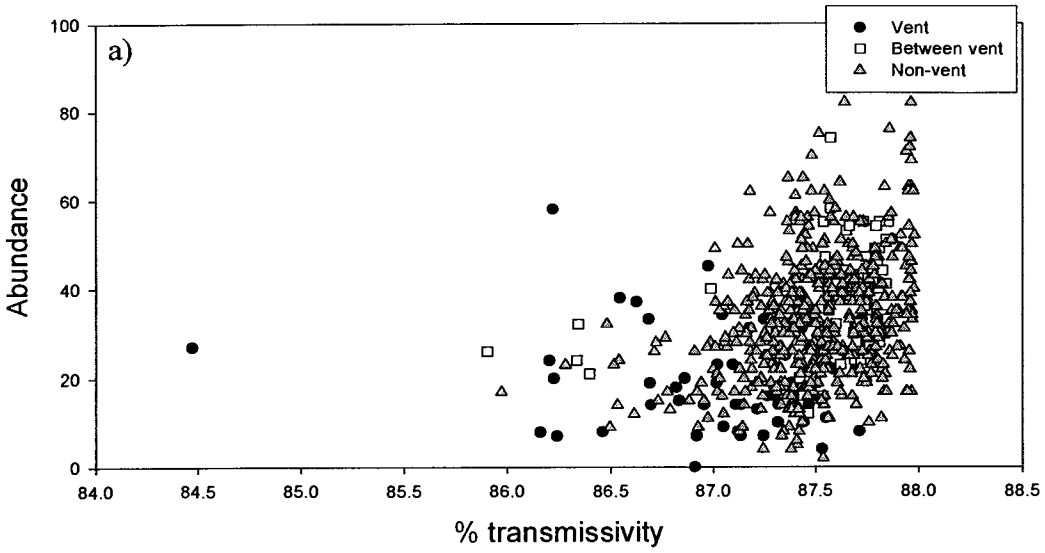
a)
Vent
Between vent
Non-vent
Abundance
% transmissivity

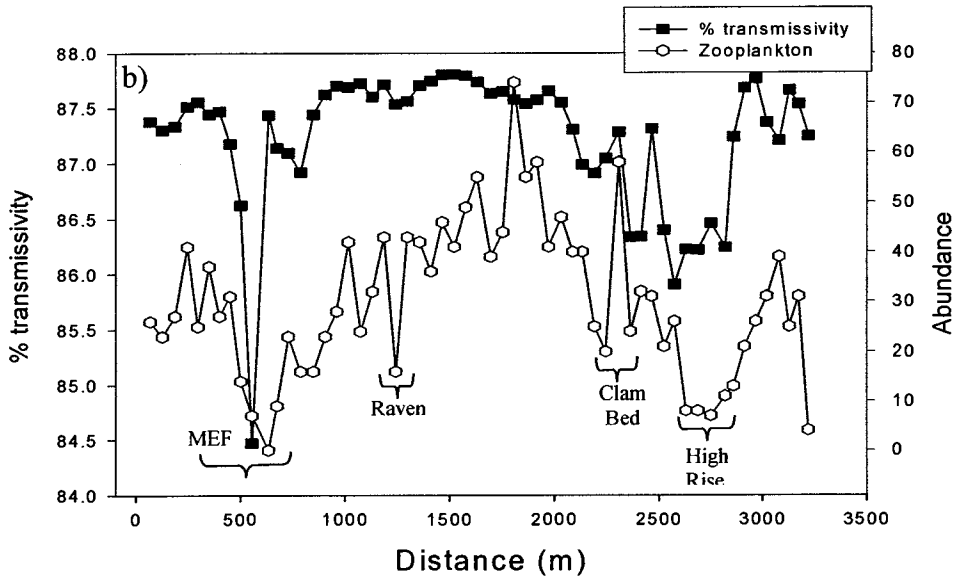
b)
% transmissivity
Zooplankton
% transmissivity
Abundance
MEF
Raven
Clam Bed
High Rise
Distance (m)

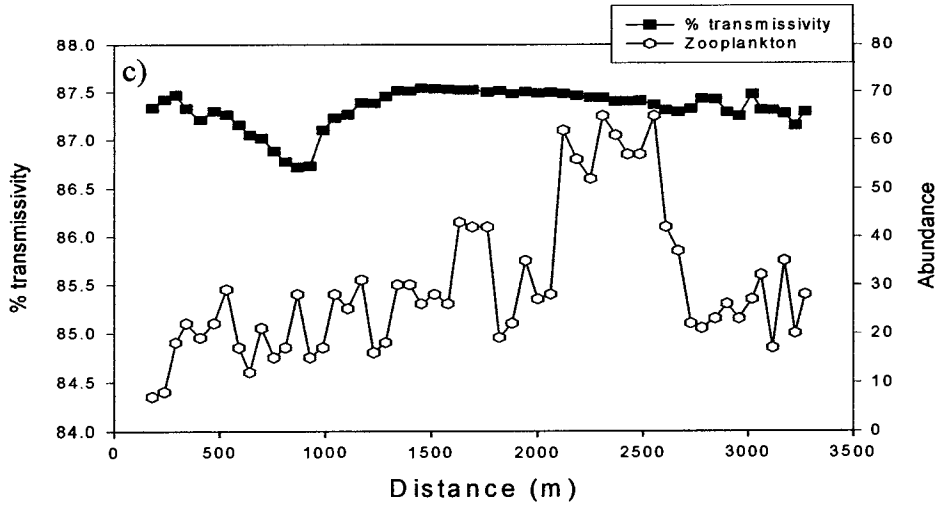
c)
% transmissivity
Zooplankton
% transmissivity
Abundance
Distance (m)

2.34c). While a small increase in turbidity occurs slightly north of 1000 m, the coinciding drop in zooplankton abundance is no greater than that before or after the change in water conditions. This suggests that water cloudiness, particularly over vent fields, may influence zooplankton abundance.

Zooplankton show significant negative correlation with theta anomaly up to distances of 110 m along vent lines (Figure 2.35). No significant correlation is evident along either set of non-vent lines. However, large variation among averaged coefficients along lines 10-12 is dominated by line 10; the shape of the cross-correlogram for line 10 is similar to lines 1-3. If line 10 is included with lines 1-3, significant correlation extends to distances of 165 m (in negative direction) and 225 m (in positive direction). Line 10 passes over High Rise and is therefore technically a vent line, but because it is sampled roughly 48 hours after line 1, it is treated separately. Because the relationship between theta anomaly and zooplankton abundance along line 10 is similar to that along lines 1-3, the effect of temperature on zooplankton abundance is consistent over space and time.

Because association between zooplankton abundance and salinity is not significantly different from random along any of the lines, no figure is shown.

Strong, significant positive correlation between zooplankton abundance and light transmissivity occurs along lines 1-3 over 55 m in negative direction and 110 m in positive direction (Figure 2.36). As with theta anomaly, line 10 is similar in shape to lines 1-3 (not shown) thus the effect of water cloudiness on zooplankton abundance is also consistent in space and time.

Based on qualitative examination and cross-correlation analysis, theta anomaly and light transmissivity levels characteristic of vent effluent appear to adversely affect zooplankton abundance.

Gelatinous zooplankton

Like zooplankton, gelatinous zooplankton abundance shows some association with theta anomaly. Over vent fields, where temperature is higher, fewer organisms are found (Figure 2.37a). From Figure 2.37b, there does not appear to be a clear relationship between salinity and abundance in different areas. Gelatinous zooplankton are most abundant at middle salinity ranges, from 34.602-34.607 psu. Gelatinous zooplankton

Figure 2.35 Cross-correlograms of zooplankton abundance and theta anomaly along a) vent lines (1-3), b) west-of-vent-field lines (4-9) and c) east-of-vent-field lines (10-12). Negative and positive refer to the sign of the lag distance 'k'. Error bars = +/- SE. Dashed lines indicate lower 2.5%-iles and upper 97.5%-iles, values above and below dashed lines are significantly different from zero.

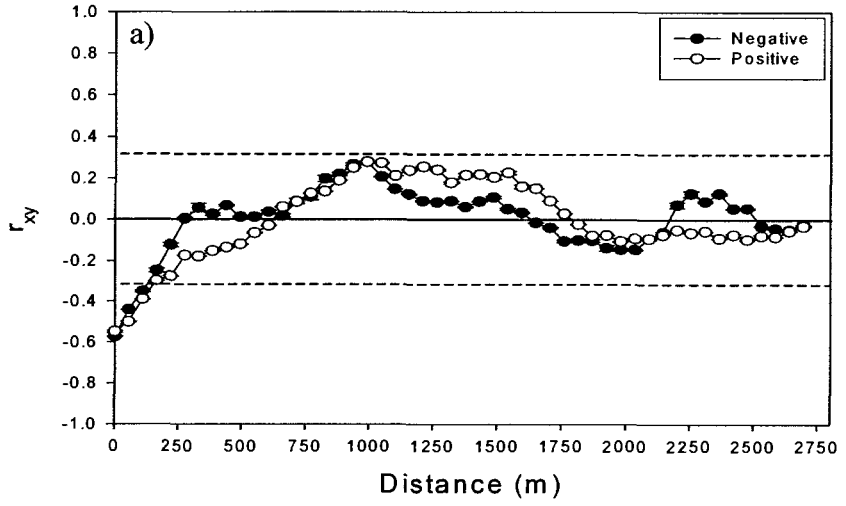
a)
Negative
Positive
1.0
0.8
0.6
0.4
0.2
0.0
-0.2
-0.4
-0.6
-0.8
-1.0
r_{xy}
0
250
500
750
1000
1250
1500
1750
2000
2250
2500
2750
Distance (m)

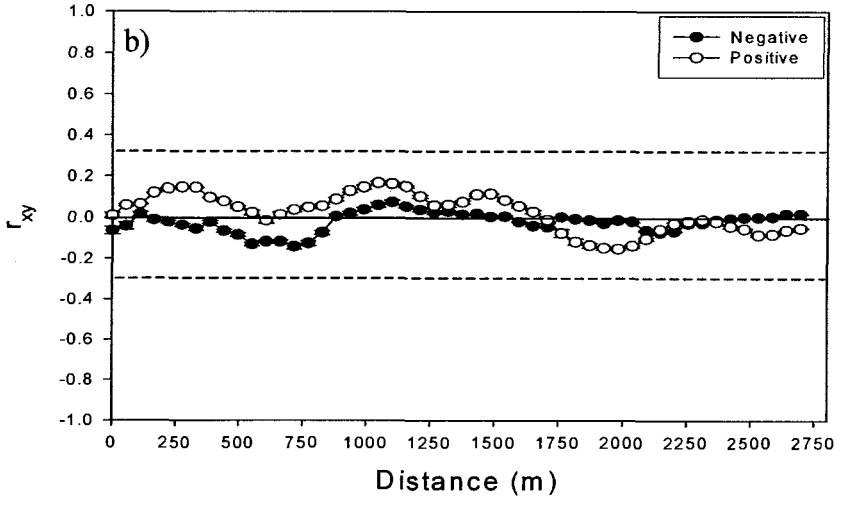
b)
Negative
Positive
1.0
0.8
0.6
0.4
0.2
0.0
-0.2
-0.4
-0.6
-0.8
-1.0
r_{xy}
0
250
500
750
1000
1250
1500
1750
2000
2250
2500
2750
Distance (m)

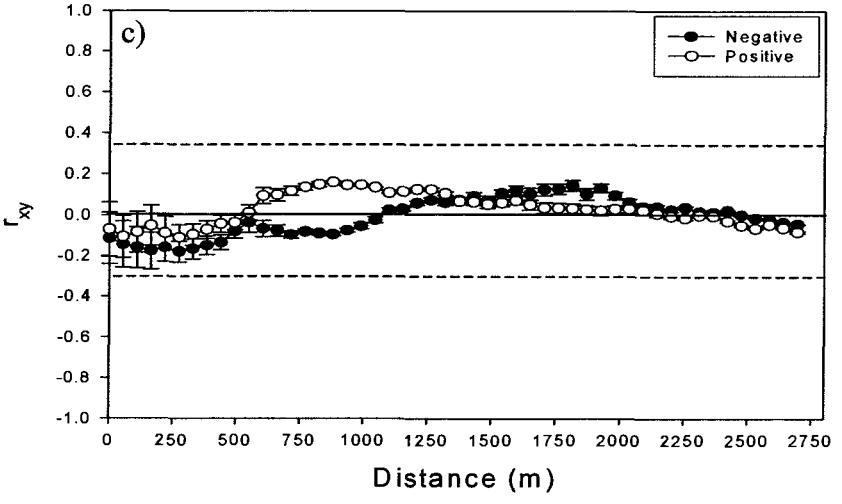
c)
Negative
Positive
1.0
0.8
0.6
0.4
0.2
0.0
-0.2
-0.4
-0.6
-0.8
-1.0
r_{xy}
0
250
500
750
1000
1250
1500
1750
2000
2250
2500
2750
Distance (m)

Figure 2.36 Cross-correlograms of zooplankton abundance and light transmissivity along a) vent lines (1-3), b) west-of-vent-field lines (4-9) and c) east-of-vent-field lines (10-12). Negative and positive refer to the sign of the lag distance 'k'. Error bars = +/- SE. Dashed lines indicate lower 2.5%-iles and upper 97.5%-iles, values above and below dashed lines are significantly different from zero.

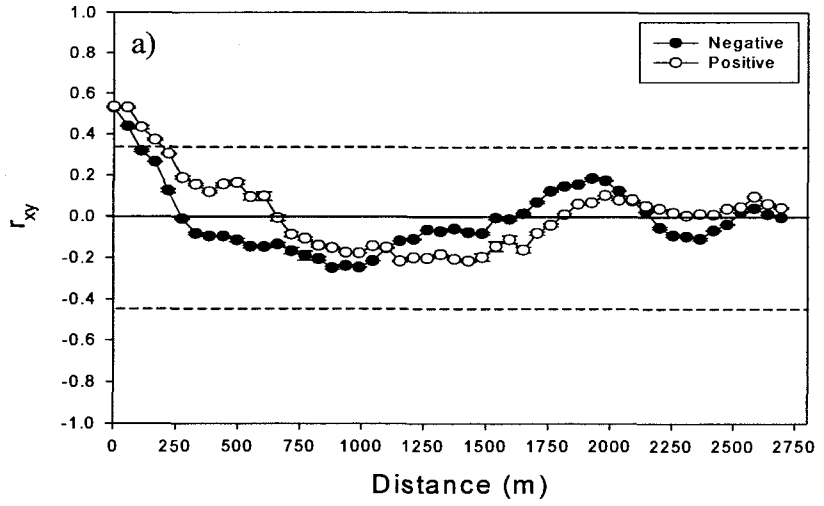
a)
Negative
Positive
r_{xy}
1.0
0.8
0.6
0.4
0.2
0.0
-0.2
-0.4
-0.6
-0.8
-1.0
0
250
500
750
1000
1250
1500
1750
2000
2250
2500
2750
Distance (m)

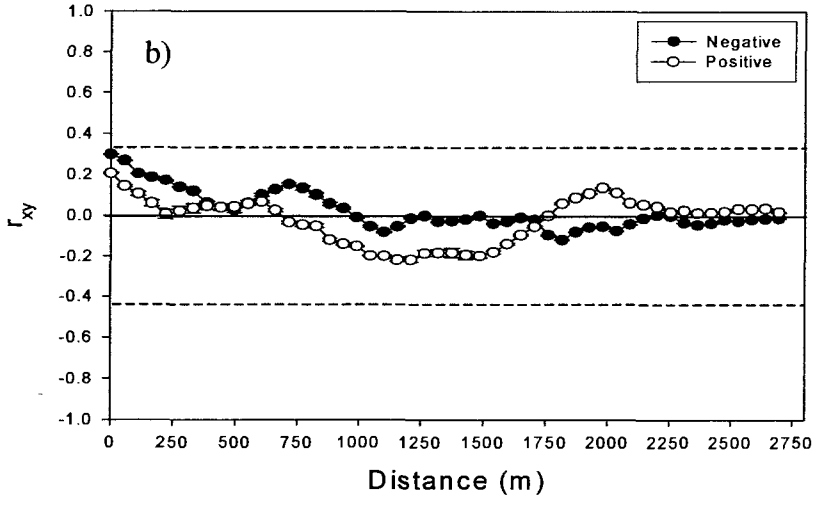
b)
Negative
Positive
r_{xy}
1.0
0.8
0.6
0.4
0.2
0.0
-0.2
-0.4
-0.6
-0.8
-1.0
0
250
500
750
1000
1250
1500
1750
2000
2250
2500
2750
Distance (m)

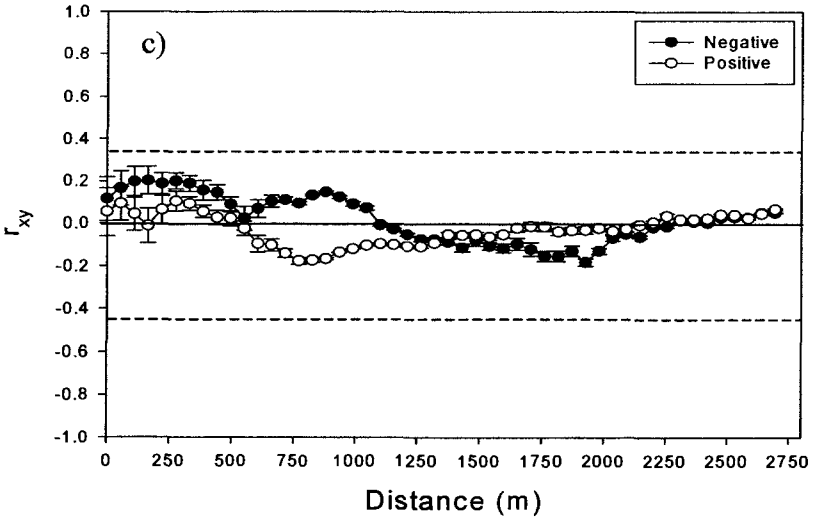
c)
Negative
Positive
r_{xy}
1.0
0.8
0.6
0.4
0.2
0.0
-0.2
-0.4
-0.6
-0.8
-1.0
0
250
500
750
1000
1250
1500
1750
2000
2250
2500
2750
Distance (m)

Figure 2.37 Scatterplots of gelatinous zooplankton abundance versus a) theta anomaly, b) salinity and c) % light transmissivity in vent, between-vent and non-vent areas.

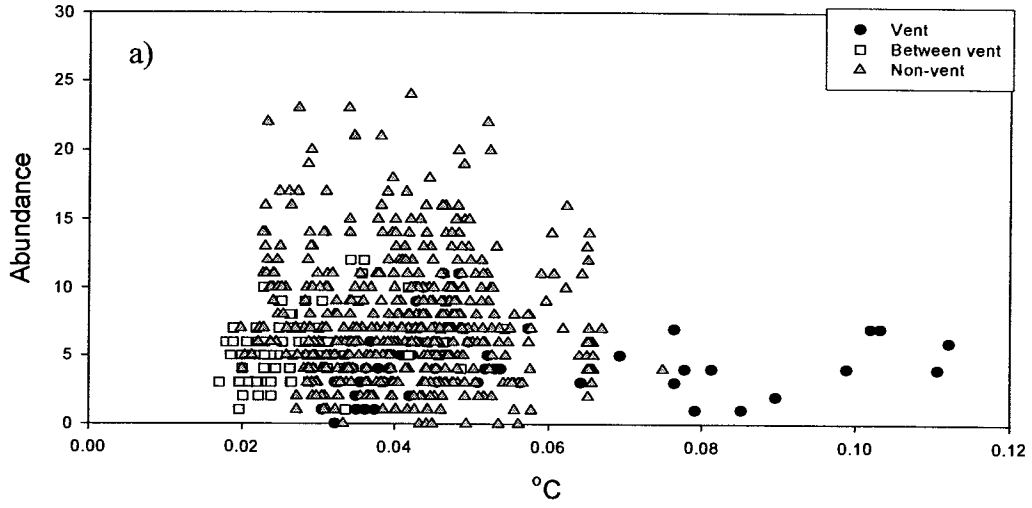
a)
Vent
Between vent
Non-vent
Abundance
0
5
10
15
20
25
30
0.00
0.02
0.04
0.06
0.08
0.10
0.12
°C

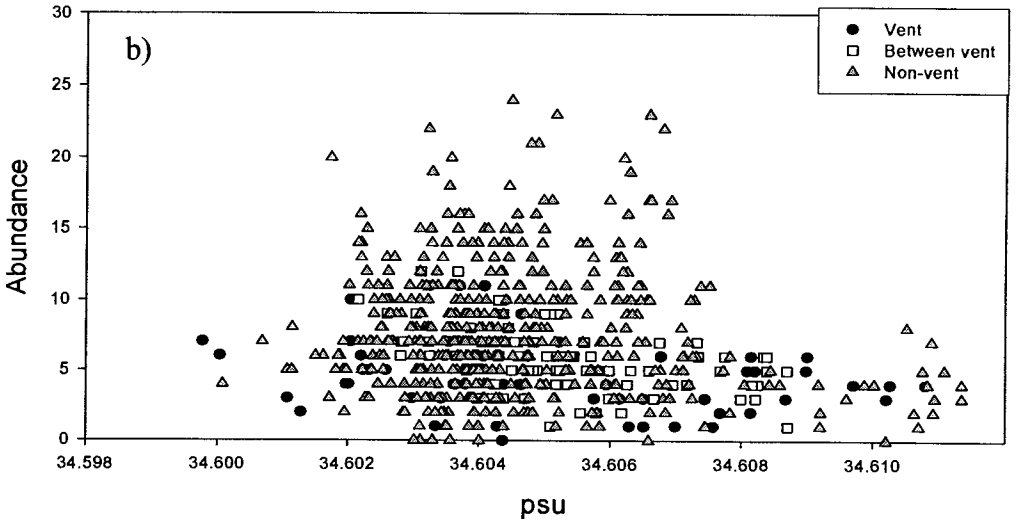
b)
Vent
Between vent
Non-vent
Abundance
0
5
10
15
20
25
30
34.598
34.600
34.602
34.604
34.606
34.608
34.610
psu

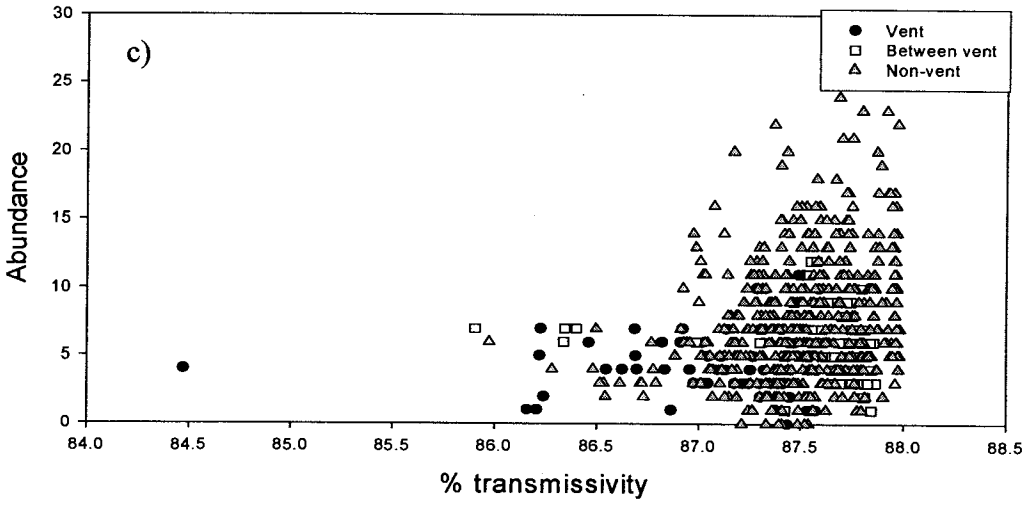
c)
Vent
Between vent
Non-vent
Abundance
0
5
10
15
20
25
30
84.0
84.5
85.0
85.5
86.0
86.5
87.0
87.5
88.0
88.5
% transmissivity

abundance also varies with light transmissivity (Figure 2.37c). Cloudy water over vent fields and between vent areas have relatively low abundance, while relatively clear water over non-vent areas harbours the highest abundances (Figure 2.37c). Because effluent from High Rise and MEF is predominantly carried away from lines 11 and 12, water along these lines is relatively clear. In short, gelatinous zooplankton are most abundant where there is little effluent.

Gelatinous zooplankton abundance shows significant positive correlation with light transmissivity over the entire sample area (Table 2.16). No significant correlations are found over vent fields, likely due to the paucity of gelatinous zooplankton observations. Gelatinous zooplankton abundance shows significant positive correlation with theta anomaly and significant negative correlation with salinity over between-vent areas. Significant positive correlation is found between abundance and light transmissivity over non-vent areas. Overall, light transmissivity appears to be influential in gelatinous zooplankton spatial pattern.

Table 2.16 Summary of correlation between gelatinous zooplankton spatial pattern and environmental variables. All correlations are assessed using 55 m grain. Associations significant at p=0.05 are indicated by '*'; associations significant at p=0.01 are indicated by '**'. df=6 per line or 72 over the whole area (number of independent observations as calculated from along line correlograms).

Extent and variable	Gelatinous zooplankton
Whole area	
Temperature anomaly	-
Salinity	-
Light transmissivity	0.239**
Vent fields	
Temperature anomaly	-
Salinity	-
Light transmissivity	-
Between vent fields	
Temperature anomaly	0.321**
Salinity	-0.475**
Light transmissivity	-
Non-vent	
Temperature anomaly	-
Salinity	-
Light transmissivity	0.279**

Nekton

Over the entire extent, shrimp show little association with environmental variables (Table 2.17). Shrimp abundance shows significant negative correlation with salinity over the entire area as a whole and in non-vent areas. This supports earlier results that shrimp occur in greater concentrations in the north, where salinity is lower. Vent effluent appears to have no significant effect on shrimp abundance at 20 mab over the vent fields.

Zoarcids are the only nekton group that shows significant correlation with any environmental variables (light transmissivity) over vent fields (Table 2.17). Of the nekton, zoarcids are also the only group that are less abundant over vent fields. Overall, zoarcids and zooplankton show similar environmental association. Theta anomaly and water cloudiness appear to adversely affect zoarcid spatial pattern.

Table 2.17 Summary of correlations between nekton spatial pattern and environmental variables. All correlations were assessed at 165 m grain. Associations significant at p=0.05 are indicated by '*'; associations significant at p=0.01 are indicated by '**'.

Extent and variable	Shrimp	Zoarcid	Macrourid
Whole area			
Temperature anomaly	-	-0.178**	0.193**
Salinity	-0.142*	-	-0.205**
Light transmissivity	-	0.222**	-
Vent fields			
Temperature anomaly	-	-	-
Salinity	-	-	-
Light transmissivity	-	0.437*	-
Between vent fields			
Temperature anomaly	-	-	-
Salinity	-	-	-
Light transmissivity	-	-	-
Non-vent			
Temperature anomaly	-	-0.237**	0.212**
Salinity	-0.19*	-	-0.177*
Light transmissivity	-	0.16*	-

Macrourids show significant positive correlation with theta anomaly and negative association with salinity (Table 2.17) over the sample area as a whole. As is seen in

Figure 2.29c, macrourids are most abundant around High Rise and Clam Bed where theta anomalies are slightly higher than ambient and salinity is slightly lower. This suggests that effluent from High Rise and Clam Bed may be influential in macrourid spatial pattern.

B: Vent fields

Zooplankton

To assess if associations between zooplankton abundance and environmental variables change with changing scale, Pearson's product moment correlation (r) is employed to look at correlations over three vent fields at the 10 m grain.

Abundance showed significant negative correlation with theta anomaly at both High Rise and MEF (Table 2.18). The correlation at MEF is not as strong as at High Rise; this is evident in Figure 2.32b, where abundance at MEF fluctuates even within the vent field. As over the whole area, zooplankton abundance decreases over vent fields where temperature anomaly increases.

At High Rise, salinity and zooplankton abundance show significant correlation (Table 2.18). Zooplankton are more abundant in water with relatively ambient salinity levels.

Light transmissivity shows significant correlation with abundance over High Rise and Clam Bed at this grain; zooplankton abundance decreases with increasing turbidity. Because temperature anomaly is not significantly correlated with abundance at Clam Bed, this suggests that, at small scales, light transmissivity, independent of temperature anomaly, may influence zooplankton abundance. As on larger scales, theta anomaly and light transmissivity also negatively affect zooplankton abundance at small scales.

Table 2.18 Summary of significant correlations between zooplankton abundance and environmental variables over three vent fields at the 10 m grain. Associations significant at p=0.05 are indicated by '*'; associations significant at p=0.01 are indicated by '**'.

Vent Field	Environmental variable	Correlation 10m
High Rise	Temperature anomaly	-0.407**
	Salinity	0.293*
	% transmissivity	0.366**
MEF	Temperature anomaly	-0.211*
	Salinity	-
	% transmissivity	-
Clam Bed	Temperature anomaly	-
	Salinity	-
	% transmissivity	0.328*

Gelatinous zooplankton

At the vent field extent, gelatinous zooplankton show significant correlation only with theta anomaly at Clam Bed (Table 2.19). Effluent at Clam Bed is only slightly warmer than ambient suggesting that conditions over this vent field may be more physiologically tolerable.

At small scales, few correlations are significant because gelatinous zooplankton are so few. Thus as environmental variables fluctuate, there appears to be little associated fluctuation in gelatinous zooplankton abundance.

Table 2.19 Summary of significant correlations between gelatinous zooplankton abundance and environmental variables over three vent fields at the 10 m grain. Associations significant at p=0.05 are indicated by '*'; associations significant at p=0.01 are indicated by '**'.

Vent Field	Environmental variable	Correlation 10m
High Rise	Theta anomaly	-
	Salinity	-
	% transmissivity	-
MEF	Theta anomaly	-
	Salinity	-
	% transmissivity	-
Clam Bed	Theta anomaly	0.357*
	Salinity	-
	% transmissivity	-

2.4 Discussion

This study of the spatial pattern of pelagic organisms near the seafloor with respect to hydrothermal effluent is unique in a couple of ways.

1) The horizontal spatial pattern of zooplankton as well as gelatinous zooplankton and nekton is assessed. Most studies of pelagic organisms at vents focus on either zooplankton or vent larvae.
2) Horizontal dipersion or spatial pattern is assessed at different scales. In studies of ecological heterogeneity, it is essential to explore relationships between organisms and their environment at multiple scales. Zooplankton studies often focus on vertical spatial pattern rather than horizontal. Environmental characteristics near the seafloor at vents are influenced primarily by the laterally spreading plume. Thus in studying the influence of vent effluent on the spatial pattern of pelagic organisms in and around vent fields it is important to assess horizontal spatial patterns.

Previous studies of pelagic organisms at vents have speculated on the association between vent effluent and organism spatial pattern. This is the first study in which the results demonstrate such a link.

2.4.1 Use of video

Video provides a more comprehensive picture of pelagic organism spatial pattern near the seafloor than net tows. The two main benefits are:

1) video captures organisms that are normally absent in net tows, like gelatinous zooplankton and nekton (Table 2.5), that are important components of the deep-sea ecosystem (Mackie and Mills 1983, Burd and Thomson 2000, Graham et al. 2001, Graham et al. 2003); and
2) video allows analysis of spatial structure on a variety of scales in order to assess how relationships between organisms and environment change.

A major drawback of the videos is the lack of resolution. Gelatinous zooplankton species are often visually indistinguishable. Different functional groups of organisms, which may have different abilities to identify and tolerate the rapidly changing conditions at vents, are lumped into one group. Similarly, zooplankton groups (calanoids, cyclopoids, siphonostomes) are also impossible to distinguish in the videos. Some species of copepods may be better able to tolerate conditions over vent fields and may thus be more abundant. Despite these drawbacks, my work has shown that the combination of video and net tows is the best method of sampling plankton within tens of metres of the bottom in and near hydrothermal vent fields.

There are inherent problems in sampling the pelagic environment with a submersible: large bow wave may push organisms out of the area or organisms may sense the approaching vehicle (e.g. detect submersible headlights or changes in pressure), swim away and thus avoid being sampled. Maneuvering the submersible around individual vents is also difficult. Visibility is lower over vent fields and chimneys can extend tens of metres into the water column. Because nets must either be held by the submersible arm or somehow attached to the submersible, number of nets and net size (diameter, length, mesh size) are constrained. Large nets, more useful for sampling larger zooplankton and nekton species are currently not practical to use. Therefore, gaps in organism abundance may be apparent in net tow samples, but rather than being indicative of what is actually there (or not there, as the case may be), gaps may be the result of inefficient sampling. In short, trying to cover the sample area with net tows would be impossible within the same timeframe.

There is no unique scale in nature at which aggregation occurs; thus it is important to look at more than one scale to determine how relationships between organisms and their environment change (Levin 1992). Conventional gear (nets and pumps) preclude such analysis, particularly at smaller scales, as samples are integrated over greater scales than those necessary to resolve spatial patterns (Gallager et al. 1996). Video is superior in this respect as patterns can be assessed at a variety of extents and grains.

2.4.2 Spatial patterns

Abiotic

In general, at smaller scales (grain and extent), environmental variation is usually less pronounced (Diggle 1983). While this generalization is applicable over non-vent areas, I found that this is not the case over vent fields. Greater variation is detected at smaller scales (Figures 2.19 and 2.20). Temperature and salinity anomalies dissipate rapidly due to mixing with ambient water. Relatively steep theta anomaly and light transmissivity gradients appear to be good indicators of location of effluent sources.

Plume-induced currents, caused by strong venting at MEF and Mothra, draw water northward into the axial valley (Thomson et al. 2003). Tidal currents account for at least half of flow variability. Flow reversals are common in autumn, occurring every few weeks, persisting for a few days. Periods of cross-axis flow are also common and are linked to eddy circulation. In my study, effluent from High Rise, appears to be primarily carried south and west along lines 1-3 (Figures 2.10 and 2.19). More striking is that effluent signature from MEF is evident along line 8 (Figures 2.10, 2.13 and 2.20), 250 m west of the vent field. Trivett (1994) emphasizes the importance of tides in dispersing diffuse plumes. Kim and Mullineaux (1998) and Kaartvedt et al (1994) also speculate on the importance of tidal action near the seafloor in the transport of vent larvae. Based on my results, it appears that predominant northward current and tidal action are important in dispersing vent effluent at 20 mab. This likely influences spatial patterns of pelagic organisms within the axial valley.

Biotic

No single pattern is shared by all organism groups. The most obvious pattern is in terms of abundance over vent and non-vent areas: organisms are more abundant, per cubic metre, over non-vent areas.

For each group, the same spatial patterns are found at multiple scales using a variety of qualitative and statistical methods (contour maps, abundance versus distance along the length and width of the sample area, spatial autocorrelation and SADIE). Spatial patterns of the different groups are relatively simple:

1. zooplankton are least abundant over the two main vent fields and most abundant in the central non-vent area between the vent fields;
2. gelatinous zooplankton are least abundant along the three central lines that pass over vent fields and are most abundant in the eastern half of the sample area;
3. shrimp are most abundant in the north;
4. zoarcids are most abundant in the south (north of MEF); and
5. macrourids are most abundant in and around High Rise and Clam Bed.

For zooplankton and macrourids, spatial pattern appears to be significantly influenced by location of the vents. Influence of vent outflow on all groups of organisms will be addressed in the next section.

Over the sample area as a whole, spatial patterns are remarkably similar at different grain sizes. As is evident from zooplankton maps (Figure 2.23), spatial pattern is similar at large (335 m) and small (10 m) grain sizes. Based on autocorrelation analysis, pattern is best detected using the 55 m grain; patches and gaps, on the order of 500 m, occur throughout the sample area (Figure 2.25). This suggests that, of the four grain sizes, the 55 m grain size is the minimum grain required in order to detect spatial pattern in the distribution of near seafloor zooplankton along the Endeavour Segment.

Pattern is most easily detected along the length of the sample lines rather than across. Difference in collection time may cause some variation between points that are on neighbouring lines. Advective processes, such as currents and tides, which are oriented along the length of the sample area, likely play a significant role in the orientation of spatial patterns.

Within individual vent fields, spatial pattern of both zooplankton and gelatinous zooplankton appears to change with changing grain size; small gaps and patches occur within large gaps (i.e. pattern within pattern). More intense variation on smaller scales in both the environment and in organism spatial pattern is detectable at the smaller grain size (10 m).

Using a relatively new spatial analysis method (SADIE), I am able to determine that spatial pattern of pelagic organisms over the axial valley is not random. Complete spatial randomness assumes: 1) the intensity of points over the sampling plane does not vary and 2) that there are no interactions among points (Diggle 1983). At some scales, processes such as growth, reproduction and mortality can influence spatial pattern (Legendre and Legendre 1998) therefore, complete spatial randomness seems highly unlikely. Nevertheless, it is essential to show that structure is not random in order to infer if any and what kind of variables (e.g. vent effluent) may play a role in generating pattern (Diggle 1983, Legendre and Legendre 1998). In this respect, SADIE is unique. It describes and maps variation on a local scale. Based on these analyses, I determined that the location of zooplankton gaps over High Rise and MEF is significantly different from random. Significant non-random results are also found for the other four groups of organisms over the entire sample area and for zooplankton and gelatinous zooplankton over most vent fields. Because organism spatial pattern is non-random, at a *variety of scales* and *in particular locations*, organism spatial pattern is likely affected by environmental characteristics associated with venting.

2.4.3 Influence of vent outflow

From this study, it is evident that the spatial pattern of pelagic organisms at 20 mab may be affected by the presence of the vents. Burd et al (1992), Burd and Thomson (1994, 1995) and Vinogradov et al (2003), suggest that zooplankton decrease in abundance in the plume "core", where effluent signature is likely to be strongest, but no environmental data are collected by the author at the same scale. Based on the correlations between zooplankton abundance and environmental variables, it is apparent from my study that zooplankton are less abundant in areas where effluent signature is strongest.

Gaps over vent fields could result from 1) depletion of plankton 'particles' by entrainment into the rising effluent or 2) active plume avoidance. Rapid, continuous discharge of effluent may carry zooplankton vertically with the rising plume, resulting in relatively low counts of zooplankton within the vicinity of individual smokers. At the orifice, effluent from smokers is expelled at a rate ranging from 25-90 cm/s (Rona and Trivett 1992). The rate of plume rise at 20 mab can reach up to 10 cm/s (Little et al. 1987). Entrainment of ambient water is on the order of 0.06-0.1 cm/s in the laterally spreading plume (Trivett 1994) while vertical entrainment near a vent orifice can be on the order of 10 cm/s (Rona and Trivett 1992). As the buoyant plume rises, the rate of entrainment decreases as the velocity of the rising plume decreases (McDuff 1995) thus mixing rates at 20 mab are likely lower than those at the orifice. Copepods however, are not inanimate particles; exploitation of eddies and other physical hydrographic features allows copepods to be more than passively drifting plankton, giving an individual control over its movement and population dispersal (Mauchline 1998, Buskey et al. 2002). In response to an approaching predator, a copepod elicits a rapid escape behaviour as small-scale hydrodynamic conditions shift (e.g. pressure, turbulence (Buskey et al. 2002, Buskey and Harline 2003)). Similar response-inducing conditions may be encountered at the edges of the spreading plume, where entrainment of ambient water occurs. Although significant differences exist in threshold shear values that elicit escape reactions in different species of copepods (Fields and Yen 1997), in general, calanoid copepod escape reaction can approach 100 body lengths per second (Mauchline 1998). In effect, a 1 mm copepod could potentially jump a distance of 10 cm in one second. Because zooplankton are not highly abundant within either of the two main vent fields, this suggests that they are likely able to detect turbulence associated with the rising plume and avoid vertical advection (i.e. the escape response is elicited prior to reaching the rapidly rising plume core). The size of the zooplankton gaps suggests that the area of influence is larger than the area of plume entrainment. In short, entrainment of copepods into the rising plumes at 20 mab may not play a significant role in creating gaps in zooplankton abundance above the two main vent fields. Thus thermal and/or chemical discontinuities associated with vent effluent are more likely to affect zooplankton spatial pattern within and near vent fields.

Theta anomalies over the vent fields are not pronounced (0.1-0.18°C). Sabatini and Martos (2002) found that copepod biomass peaked in stratified waters away from a thermal discontinuity (e.g. an ocean front). Anomalies in their study were on the order of 2-3°C. In my study, the steepness of the temperature gradient, or how quickly temperature changes over very small scales, may be important. The ability to detect environmental heterogeneity depends on the scale of measurement, whereas an organism's ability to respond to patchiness depends on how an organism perceives its environment (Wiens, 1989). Zooplankton in a relatively constant environment, like the abyssal depths, may be more sensitive to small changes in temperature and salinity than zooplankton at surface or mid-depths. Zooplankton, in effect, may be responding to changes in temperature on micro-scales, but the effect is seen on larger scales (tens of metres).

In benthic studies, vent effluent temperature is often used as a proxy for sulphide concentration (Van Dover 2000) as higher temperature effluent is relatively more sulphide rich (Johnson et al. 1988). Vent effluent is rich in chemical, metal and mineral species, e.g. mostly H_2S, but also HS- and H_2SO_4, Fe, Mn, He, CH_4, low O_2 (Von Damm, 1995). Relatively high theta anomalies and low light transmissivity over the vent fields may indicate relatively toxic vent effluent; high in sulphide, low in oxygen. Sulphide is highly reduced and can poison aerobic respiration even at low concentrations (Felbeck et al. 1985). Because most copepods often forage using chemoreception (Mauchline 1998), it is likely that they can detect adverse conditions at vents. Thus sulphide concentration, rather than theta anomaly, may be more important in excluding zooplankton from vent fields.

Zooplankton abundance gradually increases with distance from vents to form aggregations (Figure 2.23). These aggregations are not randomly dispersed. Along line 9, which is furthest from any vent field, no large patches or gaps are evident. Zooplankton abundance is relatively constant; counts typically range from 20-50 per 55 m grain (Figure 2.38). Along line 8 (Figures 2.32-2.34, 2.38), a large patch of zooplankton is evident west of Clam Bed. Counts along line 8 typically range between 20-40, but west of Clam Bed, counts jump to 60 for about 500 m (Figures 2.32-2.34, 2.38). In this area, vent effluent signature is no longer detectable and environmental conditions appear

relatively constant. I speculate that biological, rather than physical factors, may play a role in enhancing local concentrations of zooplankton.

Increased organism abundance is often associated with areas of physical discontinuities (e.g. fronts, upwelling, river plumes, neutrally buoyant plume) where nutrient-rich waters are introduced to an otherwise depauperate area (Burd et al. 1992, Bradford-Grieve et al. 1993, Burd and Thomson 1994, 1995, Mianzan and Guerrero 2000, Graham et al. 2001, Sabatini and Martos 2002). In upwelling areas on the New Zealand coast, Bradford-Grieve et al (1993) found that zooplankton abundance is significantly lower at the source of upwelling and gradually increases downstream. Weaker swimming species capitalize on the cold, nutrient-rich upwelled water as it moves away from its source. A similar situation may be occurring over the hydrothermal vent site. Roth and Dymond (1989) find more than 95% of the organic matter collected 21 m directly above smoker vent in MEF is of chemosynthetic origin. In the rising plume, microbial biomass and particulate DNA concentration substantially increase relative to background water (Corliss et al. 1979, Cowen et al. 1986, Winn and Karl 1986, Lilley et al. 1995). This suggests that, within the vicinity of the vent fields, microbial productivity may be enhanced above background levels.

Gowing and Wishner (1992) find that copepods above an eastern tropical Pacific seamount feed on particles colonized by bacteria, a food resource that is not common in the open deep sea. Some deep sea copepods (e.g. *Spinocalanus sp.*), typically generalist feeders, are able to specialize opportunistically on this resource. Gowing and Wishner (1992) also find encapsulated metal-precipitating bacteria, similar to those found at hydrothermal vents, in guts of copepods. Fransz and Gonzalez (1995), and Nielsen and Sabatini (1996) speculate that *Oithona similis* is the primary link between microbial production and higher zooplankton in the open ocean. It is worth noting that, in my study, individuals of both of these genera were captured in the net tow. Burd et al (2002) also found that zooplankton associated with the neutrally buoyant plume feed on chemosynthetic products derived from the neutrally buoyant plume. Thus it is evident from previous work that zooplankton, including copepod species captured in this study, may be capable of feeding on bacteria associated with hydrothermal effluent.

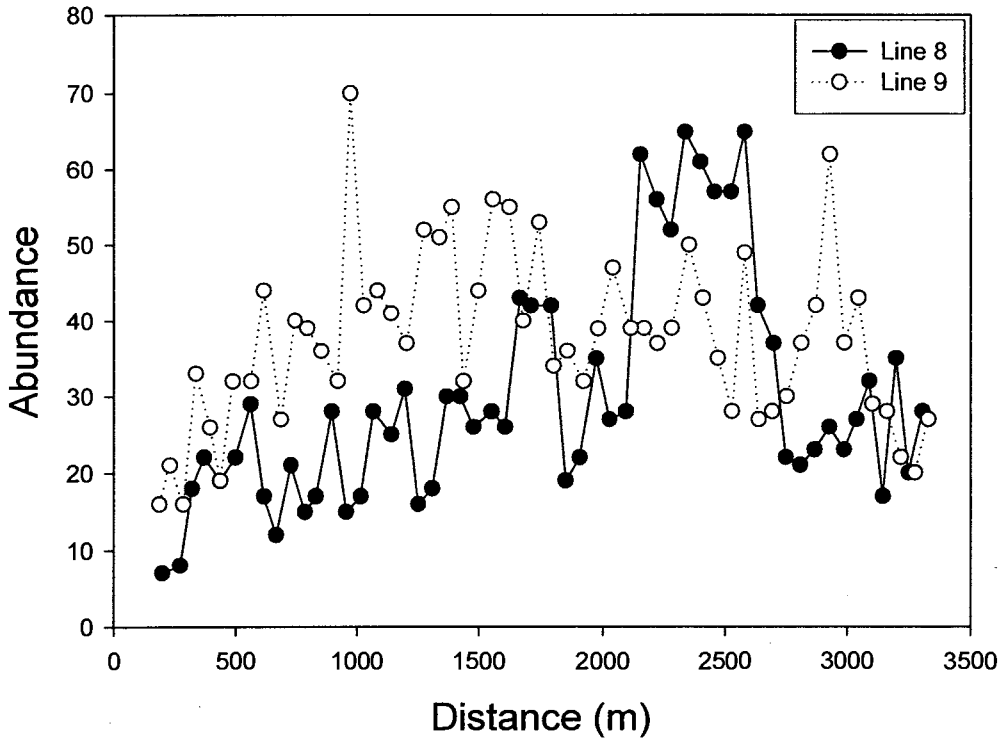

Figure 2.38 Comparison of zooplankton abundance along lines 8 and 9. Line 9 is furthest from any vent field. A patch of increased zooplankton abundance appears along line 8, west of Clam Bed. Patch size is roughly 500 m.

Zooplankton abundance increases as temperature and chemical anomalies dissipate with horizontal distance from vents. There are patches of relatively high zooplankton abundance (e.g. in the central area, west of Clam Bed on line 8, north of MEF on line 10). Although zooplankton densities in this study are not of the same magnitude as those found at ocean fronts (e.g. 6000 individuals/m^3, (Sabatini and Martos 2002)) or upwelling areas (e.g. 500-6000 individuals/m^3, (Bradford-Grieve et al. 1993)), zooplankton densities west of Clam Bed (17.3 individuals/m^3) and in the centre of the sample area (11 individuals/m^3) are greater than those found by Berg and Van Dover (1987) over vent fields on the East Pacific Rise (maximum 6.7 individuals/m^3). Berg and Van Dover find zooplankton densities over vent fields are one to two magnitudes greater than those over non-vent areas. In my study, whether this increase is specifically due to resources available at vents is difficult to say as no region far from the vents is sampled. There are obvious changes in abundance on local scales within the sample area (Figure 2.38), particularly in areas where effluent signature is weak (e.g. Line 8). Increased microbial activity associated with vent effluent, which has lost much of its temperature/salinity/light signature, may be responsible for these localized increases in zooplankton abundance. Zooplankton that are already in the axial valley may be able to take advantage of vent resources, i.e. feed on microbes associated with effluent. While vent productivity may not sustain densities of zooplankton on the order of that found at ocean fronts or upwelling areas, increased microbial productivity associated with the laterally spreading plume may be responsible for *localized* increases in zooplankton abundance.

This study also shows that gelatinous zooplankton are associated with zooplankton, but appear to be more limited in their overall spatial pattern. Typically at fronts or areas of physical discontinuities, gelatinous zooplankton abundance increases (Mianzan and Guerrero 2000, Graham et al. 2001). Gelatinous zooplankton are attracted to increased zooplankton concentrations within the vicinity of these discontinuities (Graham et al. 2001). Vinogradov et al. (2003) describe densities of 0.06-0.08 individuals/m^3 of gelatinous zooplankton above Rainbow vent field in the Mid-Atlantic at the upper border of neutrally buoyant plume (1800-2200m). In my study, I find densities of 1.3 individuals/m^3 over vents and 2.2 individuals/m^3 over non-vent areas. Cnidarians

seen in the videos, such as *Crossota, Pantachogon* and *Halicreas*, are found at similar depths in the northwest Pacific by Vinogradov and Shushkina (2002). Salps, which are most abundant along the eastern transect lines, are often found at gyres and current borders where there are large amounts of detritus-related bacteria and protozoans (Vinogradov and Shushkina 2002). Burd and Thomson (2000) also find that increases in gelatinous zooplankton are associated with significant increases in zooplankton abundance above the neutrally buoyant plume. Similarly, in this study, gelatinous zooplankton are likely feeding on locally enhanced zooplankton abundance. Areas of relatively high abundance of both groups show some overlap in the east (Figure 2.26), hence the correlation between the two groups. However, gelatinous zooplankton appear less physiologically tolerant of areas most influenced by venting (centre). Gelatinous zooplankton are weak swimmers, unable to dart in and out of intolerable conditions, and may thus avoid rapidly changing conditions by remaining on the east side of sample area where conditions are most constant. Abundance of prey and slightly more physiologically tolerable conditions in the eastern half of the sample area likely affect gelatinous zooplankton spatial pattern.

Zoarcid abundance increases in areas roughly similar to that of zooplankton (Figure 2.29). Voight (2000) found adult and juvenile zoarcids in areas of intense venting, suggesting zoarcids can tolerate adverse vent conditions. Shank et al (1998) also found an increase in zoarcid abundance in association with an increase in microbial activity at EPR. Because zoarcids typically scavenge or feed on zooplankton (Janssen et al. 2000), it seems unlikely that they are directly capitalizing on increased microbial production. Based on this study, zoarcids are likely attracted to increased zooplankton abundance that may be associated with microbial activity.

Shrimp and macrourids appear least affected by effluent. They can quickly swim in and out of vent field areas, where conditions are most variable and likely least tolerable. Both groups appear to be negatively correlated with salinity however, this is likely not a cause and effect relationship, especially as macrourids are known to inhabit waters that are deeper than in this study. Shrimp are known scavengers (Butler 1980), but in particular, deep sea shrimp are also capable of feeding on dormant zooplankton (Yamaguchi et al. 2002). In this study, shrimp are abundant near High Rise and also in

the west of the sample area. Perhaps they are feeding on the abundant vent benthos at High Rise and Clam Bed however, no shrimp have ever been seen on the seafloor in either of these areas (Tunnicliffe pers. comm.). Shrimp may instead be feeding on zooplankton that are relatively abundant in the north-west. What causes the shrimp to remain concentrated in the north half of the sample area rather than dispersing into the south half is not clear.

Macrourids may be attracted to High Rise and Clam Bed by the abundance of shrimp. Macrourids primarily scavenge, but are also capable of feeding on other fish and shrimp (McLellan 1977). Macrourids have also been observed feeding on tubeworms (Tunnicliffe et al. 1990). Therefore, in this study, macrourids are likely using the abundant benthic biomass at vents as a food resource. Previous studies have shown macrourids are capable of locating bait within minutes of its arrival on the seafloor by tracking the odour upstream (McLellan 1977, Priede and Bagley 2000, Henriques et al. 2002, Ross et al. 2003). Macrourids within the axial valley are likely attracted to or may cue to the vents using the vent effluent. In this study, macrourids show significant positive correlation with temperature anomaly. Based on what is known about macrourid foraging behaviour, theta anomaly may be a proxy for the smell of the effluent (sulphide) or the smell of the organisms themselves. Smell, rather than temperature, is likely what attracts macrourids to the vent fields.

2.5 Conclusions

Hydrothermal vents provide enhanced resources for microbial activity and alter deep sea circulation through the release of heated effluent therefore, it is necessary to study the effect of these benthic processes on the pelagic environment.

1. Patterns of organism abundance are relatively simple. These patterns are identifiable at multiple scales suggesting that the presence of the vent fields is a strong influence on near seafloor spatial pattern of pelagic organisms.

2. Zooplankton abundance decreases in areas of intense venting. Zooplankton may be responding to relatively high sulphide concentrations, as indicated by theta anomalies, and turbulence associated with the rising plume.

3. Gelatinous zooplankton appear less tolerant of vent effluent than zooplankton. High abundance of gelatinous zooplankton is primarily limited to the eastern side of the sample area where environmental conditions are relatively ambient. Gelatinous zooplankton spatial pattern appears to be correlated with turbidity.

4. Nekton are better swimmers than zooplankton and are likely able to move in and out of unattractive conditions relatively rapidly. Zoarcids are most abundant in the south. Shrimp are abundant in the north and west. Macrourids are most abundant in the north, particularly around High Rise and Clam Bed.

5. An interesting paradox emerged: vent effluent may be responsible for localized enhancement of zooplankton, but not over vent fields. I speculate that a possible cause of these localized increases may be microbial activity associated with laterally spreading effluent. Zooplankton may be able to capitalize on this resource only in areas where effluent signature is weakest.

6. Zoarcids and gelatinous zooplankton appear to aggregate in areas where zooplankton are relatively abundant.

7. Shrimp and macrourids may be attracted to the abundant benthos associated with the vent fields. Whether shrimp are responding to environmental or biological cues is unclear. Macrourids however, are likely attracted to the vents by smell, either sulphide-rich effluent or benthic organisms themselves.

Based on my study, it appears that vents play some role in benthic-pelagic coupling in the deep sea. Pelagic organisms appear to be able to utilize resources at vents (e.g. microbes in effluent, abundant benthic biomass) and do so by aggregating in areas where resources are enhanced above background levels. Thus pelagic organisms within the axial valley aggregate on local scales apparently in response to vent productivity.

2.6 References

Bailey, D. M. and Priede, I. G. 2002. Predicting fish behaviour in response to abyssal food falls. Marine Biology **141**: 831-840.

Barry, J. P. and Dayton, P. K. 1991. Physical heterogeneity and the organization of marine communities. In: Kolasa, J. and Pickett, S. T. A. (eds.), Ecolgical Heterogeneity. Springer-Verlag, pp. 270-320.

Berg, C. J. J. and Van Dover, C. L. 1987. Benthopelagic macrozooplankton communities at and near deep-sea hydrothermal vents in the eastern Pacific Ocean and the Gulf of California. Deep-Sea Research **34**: 379-401.

Bradford-Grieve, J. M., Murdoch, R. C. and Chapman, B. E. 1993. Composition of macrozooplankton assemblages associated with the formation and decay of pulses within an upwelling plume in greater Cook Strait, New Zealand. New Zealand Journal of Marine and Freshwater Research **27**: 1-22.

Brown, J., Colling, A., Park, D., Phillips, J., Rothery, D. and Wright, J. 1991. Seawater: Its composition, properties and behaviour. Pergammon Press.

Burd, B. J. and Thomson, R. E. 1994. Hydrothermal venting at Endeavour Ridge: Effect on zooplankton biomass throughout the water column. Deep-Sea Research I **41**: 1407-1423.

Burd, B. J. and Thomson, R. E. 1995. Distribution of zooplankton associated with the Endeavour Ridge hydrothermal plume. Journal of Plankton Research **17**: 965-997.

Burd, B. J. and Thomson, R. E. 2000. Distribution and relative importance of jellyfish in a region of hydrothermal venting. Deep-Sea Research I **47**: 1703-1721.

Burd, B. J., Thomson, R. E. and Calvert, S. E. 2002. Isotopic composition of hydrothermal epiplume zooplankton: evidence of enhanced carbon recycling in the water column. Deep-Sea Research I **49**: 1877-1900.

Burd, B. J., Thomson, R. E. and Jamieson, G. S. 1992. Composition of a deep scattering layer overlying a mid-ocean ridge hydrothermal plume. Marine Biology **113**: 517-526.

Buskey, E. J. and Harline, D. K. 2003. High-speed video analysis of the escape response of the copepod *Acartia tonsa* to shadows. Journal of Plankton Research **204**: 28-37.

Buskey, E. J., Lenz, P. H. and Hartline, D. K. 2002. Escape behaviour of planktonic copepods in response to hydrodynamic disturbances: high speed video analysis. Marine Ecology Progress Series **235**: 135-146.

Butler, T. H. 1980. Shrimps of the Pacific Coast of Canada.

Corliss, J. B., Dymond, J., Gordon, L. I., Edmond, J. H., von Herzen, R. P., Ballard, R. D., Williams, K. D., Bainbridge, A., Crane, R. and van Andel, T. H. 1979. Submarine thermal springs on the Galapagos Ridge. Science **203**: 1073-1083.

Cowen, J. P., Massoth, G. J. and Baker, E. T. 1986. Bacterial scavenging of Mn and Fe in a mid- to far-field hydrothermal vent plum. Nature **322**: 169-171.

Delaney, J. R., Kelley, D. S., Lilley, M. D., Butterfield, D. A., McDuff, R. E., Baross, J. A., Deming, J. W., Johnson, H. P. and Robigou, V. 1997. The Endeavour hydrothermal system I: Cellular circulation above an active cracking front yiedls large sulfide structures, "fresh" vent water and hyperthermophilic Archaea. RIDGE Events **July**: 11-20.

Delaney, J. R., Robigou, V. and McDuff, R. E. 1992. Geology of a vigorous hydrothermal system on the Endeavour Segment, Juan de Fuca Ridge. Journal of Geophysical Research **97**: 19,663-19,682.

Diggle, P. J. 1983. Statistical analysis of spatial point patterns. Academic Press.

Dungan, J. L., Perry, J. N., Dale, M. R. T., Legendre, P., Citron-Pousty, S., Fortin, M.-J., Jakomulska, A., Miriti, M. and Rosenberg, M. S. 2002. A balanced view of scale in spatial statistical analysis. Ecography **25**: 626-640.

Dutilleul, P. 1993. Modifying the t test for assessing the correlation between two spatial processes. Biometrics **49**: 305-314.

Felbeck, H., Powell, M. A., Hand, S. C. and Somero, G. N. 1985. Metabolic adaptations of hydrothermal vent animals. Bulletin of the Biological Society of Washington **6**: 261-272.

Fields, D. M. and Yen, J. 1997. The escape behaviour of marine copepods in response to a quantifiable fluid mechanical disturbance. Journal of Plankton Research **19**: 1289-1304.

Fleminger, A. 1983. Description and phylogeny of Isaacsicalanus paucisetus n. gen., n. sp., (Copepoda: Calanoida: Spinocalanidae) from an East Pacific hydrothermal vent site (21°N). Proceedings of the Biological Society of Washington **96**: 605-622.

Fransz, H. G. and Gonzalez, S. R. 1995. The production of Oithona similis (Copepoda: Cyclopoida) in the Southern Ocean. ICES Journal of Marine Science **52**: 549-555.

Gallager, S. M., Cabell, S. D., Epstein, A. W., Solow, A. and Beardsley, R. C. 1996. High-resolution observations of plankton spatial distributions correlated with hydrography in the Great South Channel, Georges Bank. Deep-sea Research II **43**: 1627-1663.

Gerbruk, A. V., Southward, E. C., Kennedy, H. and Southward, A. J. 2000. Food sources, behaviour and distribution of hydrothermal vent shrimps at the Mid-Atlantic Ridge. Journal of Marine Biological Association UK **80**: 485-499.

Gowing, M. M. and Wishner, K. F. 1992. Feeding ecology of benthopelagic zooplankton on an eastern tropical Pacific seamount. Marine Biology **112**: 451-467.

Graham, W. M., Martin, D. L. and Martin, J. C. 2003. *In situ* quantification and analysis of large jellyfish using a novel video profiler. Marine Ecology Progress Series **254**: 129-140.

Graham, W. M., Pages, F. and Hamner, W. M. 2001. A physical context for gelatinous zooplankton aggregations: a review. Hydrobiologia **451**: 199-212.

Henriques, C., Priede, I. G. and Bagley, P. M. 2002. Baited camera observations of deep-sea demersal fishes of the northeast Atlantic Ocean at 15-28°N off West Africa. Marine Biology **141**: 307-314.

Hewitt, J. E., Thrush, S. F., Cummings, V. J. and Turner, S. J. 1998. The effect of changing sampling scales on our ability to detect effects of large-scale processes on communities. Journal of Experimental Marine Biology and Ecology **227**: 251-264.

Hurlbert, S. H. 1990. Spatial distribution of the montane unicorn. Oikos **58**: 257-271.

Janssen, F., Treude, T. and Witte, U. 2000. Scavenger assemblages under differing trophic conditions: a case study in the deep Arabian Sea. Deep-sea Research II **47**: 2999-3026.

Johnson, K. S., Childress, J. J. and Beehler, C. L. 1988. Short-term temperature variability in the Rose Garden hydrothermal vent field: an unstable deep-sea environment. Deep-Sea Research **35**: 1711-1721.

Jones, E. G., Tselepides, A., Bagley, P. M., Collins, M. A. and Priede, I. G. 2003. Bathymetric distribution of some benthic and benthopelagic species attracted to baited cameras and traps in the deep eastern Mediterranean. Marine Ecology Progress Series **251**: 75-86.

Kaartvedt, S., Van Dover, C. L., Mullineaux, L. S., Wiebe, P. H. and Bollens, S. M. 1994. Amphipods on a deep-sea hydrothermal treadmill. Deep-Sea Research I **41**: 179-195.

Kim, S. L. and Mullineaux, L. S. 1998. Distribution and near-bottom transport of larvae and other plankton at hydrothermal vents. Deep-Sea Research II **45**: 423-440.

Kolasa, J. and Rollo, C. D. 1991. The heterogeneity of heterogeneity: A glossary. In: Kolasa, J. and Pickett, S. T. A. (eds.), Ecological Heterogeneity. Springer-Verlag, pp. 1-23.

Kurokawa, T. 2000. Direct and indirect measurements of the thermal budget of two large hydrothermal systems on the Juan de Fuca Ridge. University of Washington, p. 135.

Legendre, P. and Legendre, L. 1998. Numerical Ecology. Elsevier.

Levin, S. A. 1992. The problem of pattern and scale in ecology. Ecology **73**: 1943-1967.

Lewis, W. M. J. 1979. Zooplankton community analysis. Springer-Verlag.

Lilley, M. D., Feely, R. A. and Trefry, J. H. 1995. Chemical and biochemical transformations in hydrothermal plumes. In: Humphris, S. E., Zierenberg, R. A., Mullineaux, L. S. and Thomson, R. E. (eds.), Seafloor hydrothermal systems: Physical, chemical, biological and geological interactions. American Geophysical Union, pp. 369-291.

Little, S. A., Stolzenbach, K. D. and Von Herzen, R. P. 1987. Measurements of plume flow from a hydrothermal vent field. Journal of Geophysical Research **92**: 2587-2596.

Lueck, R. G. and Wolk, F. 1999. An efficient method for determining significance of covariance estimates. Journal of Atmospheric and Oceanic Technology **16**: 773-775.

Mackas, D. L. 1984. Spatial autocorrelation of plankton community composition in a continental shelf ecosystem. Limnology and Oceanography **29**: 451-471.

Mackie, G. O. and Mills, C. E. 1983. Use of the Pisces IV submersible for zooplankton studies in coastal waters of British Columbia. Canadian Journal of Fisheries and Aquatic Sciences **40**: 763-776.

Mauchline, J. 1998. The biology of Calanoid copepods. Academic Press.

McDuff, R. E. 1995. Physical dynamics of deep-sea hydrothermal plumes. In: Humphris, S. E., Zierenberg, R. A., Mullineaux, L. S. and Thomson, R. E. (eds.), Seafloor hydrothermal systems: Physical, chemical, biological and geological interactions. American Geophysical Union, pp. 357-368.

McLellan, T. 1977. Feeding strategies of the macrourids. Deep-Sea Research **24**: 1019-1036.

Mianzan, H. W. and Guerrero, R. A. 2000. Environmental patterns and biomass distribution of gelatinous macrozooplankton. Three study cases in the South-western Atlantic Ocean. Scientia Marina **64**: 215-224.

Milligan, B. N. and Tunnicliffe, V. 1994. Vent and nonvent faunas of Cleft segment, Juan de Fuca Ridge, and their relations to lava age. Journal of Geophysical Research **99**: 4777-4786.

Nielsen, T. G. and Sabatini, M. 1996. Role of cyclopoid copepods *Oithona* spp. in North Sea plankton communities. Marine Ecology Progress Series **139**: 79-93.

Perry, J. N. 1994. Spatial analysis by distance indices. http://www.rothamsted.bbsrc.ac.uk/pie/sadie/SADIE_home_page_1.htm.

Perry, J. N. 1998. Measures of spatial pattern for counts. Ecology **79**: 1008-1017.

Perry, J. N. 2003.
http://www.rothamsted.bbsrc.ac.uk/pie/sadie/SADIE_home_page_1.htm.

Perry, J. N., Liebhold, A. M., Rosenberg, M. S., Dungan, J., Miriti, M., Jakomulska, A. and Citron-Pousty, S. 2002. Illustrations and guidelines for selecting statistical methods for quantifying spatial pattern in ecological data. Ecography **25**: 578-600.

Pielou, E. C. 1977. Mathematical Ecology. John Wiley and Sons.

Pinca, S. and Dallot, S. 1997. Zooplankton community structure in the Western Mediterranean sea related to mesoscale hydrodynamics. Hydrobiologia **356**: 127-142.

Pinel-Alloul, B. 1995. Spatial heterogeneity as a multi-scale characteristic of zooplankton community. Hydrobiologia **300/301**: 17-42.

Priede, I. G. and Bagley, P. M. 2000. *In situ* studies on deep-sea demersal fishes using autonomous unmanned lander platforms. Oceanography and Marine Biology: An Annual Review **38**: 357-392.

Raffaelli, D., Bell, E., Weithoff, G., Matsumoto, A., Cruz-Motta, J. J., Kershaw, P., Parker, R., Parry, D. and Jones, M. 2003. The ups and downs of benthic ecology: considerations of scale, heterogeneity and surveillance for benthic-pelagic coupling. Journal of Experimental Marine Biology and Ecology **285-286**: 191-203.

Robigou, V., Delaney, J. R. and Stakes, D. S. 1993. Large massives sulfide deposits in a newly discovered active hydrothermal system, the High-Rise field, Endeavour Segment, Juan de Fuca Ridge. Geophysical Research Letters **20**: 1887-1890.

Rona, P. A. and Trivett, D. A. 1992. Discrete and diffuse heat transfer at ASHES vent field, Axial Volcano, Juan de Fuca Ridge. Earth and Planetary Science Letters **109**: 57-71.

Ross, M. F., Bailey, D. M., Wagner, H. J. and Priede, I. G. 2003. Olfactory, gustatory and tactile searching behaviour by the deep-sea grenadier fish, *Coryphaenoides armatus*. 10th Deep-Sea Biology Symposium.

Rossi, R. E., Mulla, D. J., Journel, A. G. and Franz, E. H. 1992. Geostatistical tools for modeling and interpreting ecological spatial dependence. Ecological Monographs **62**: 277-314.

Roth, S. E. and Dymond, J. 1989. Transport and settling of organic material in a deep-sea hydrothermal plume: Evidence from particle flux measurements. Deep-Sea Research **36**: 1237-1254.

Sabatini, M. and Martos, P. 2002. Mesozooplankton features in a frontal area off northern Patagonia (Argentina) during spring 1995 and 1998. Scientia Marina **66**: 215-232.

Seguin, G., Errhif, A. and Dallot, S. 1994. Diversity and structure of pelagic copepod populations in the frontal zone of the eastern Alboran sea. Hydrobiologia **292/293**: 369-377.

Shank, T. M., Fornari, D. J., Von Damm, K. L., Lilley, M. D., Haymon, R. M. and Lutz, R. A. 1998. Temporal and spatial patterns of biological community development at nascent deep-sea hydrothermal vents (9°50'N, East Pacific Rise). Deep-Sea Research II **45**: 465-515.

Thomson, R. E., Mihaly, S. F., Rabinovich, A. B., McDuff, R. E., Veirs, S. R. and Stahr, F. R. 2003. Constrained circulation at Endeavour ridge facilitates colonization by vent larvae. Nature **424**: 545-549.

Trivett, D. A. 1994. Effluent from diffuse hydrothermal venting. 1. A simple model of plumes from diffuse hydrothermal sources. Journal of Geophysical Research **99**: 18,403-418,415.

Tunnicliffe, V. 2000. A documentation of biodiversity characteristics of the hydrothermal vent assemblages at High Rise vent field, Endeavour Segment, Juan de Fuca Ridge. University of Victoria, p. 53.

Tunnicliffe, V., Garrett, J. F. and Johnson, H. P. 1990. Physical and biological factors affecting the behaviour and mortality of hydrothermal vent tubeworms (vestimentiferans). Deep-Sea Research **37**: 103-125.

Van Dover, C. L. 2000. The ecology of deep-sea hydrothermal vents. Princeton University Press.

Van Dover, C. L., Kaartvedt, S., Bollens, S. M., Wiebe, P. H., Martin, J. W. and France, S. C. 1992. Deep-sea amphipod swarms. Nature **358**: 25-26.

Vereshchaka, A. L. and Vinogradov, G. M. 1999. Visual observations of the vertical distribution of plankton throughout the water column above Broken Spur vent field, Mid-Atlantic Ridge. Deep-Sea Research I **46**: 1615-1632.

Vinogradov, G. M., Vereshchaka, A. L. and Aleinik, D. L. 2003. Zooplankton distribution over hydrothermal vent fields of the Mid-Atlantic Ridge. Oceanology **43**: 656-669.

Vinogradov, G. M., Vereshchaka, A. L., Musaeva, E. I. and Dyakonov, V. Y. 2003. Vertical zooplankton distribution over the Porcupine Abyssal Plain (Northeast Atlantic) in the summer of 2002. Oceanology **43**: 512-523.

Vinogradov, M. E. and Shushkina, E. A. 2002. Vertical distribution of gelatinous macroplankton in the North Pacific observed by manned submersibles *Mir*-1 and *Mir*-2. Journal of Oceanography **58**: 295-303.

Voight, J. 2000. A review of predators and predation at deep-sea hydrothermal vents. Cahier de Biologie Marine **41**: 155-166.

Ward, P., Whitehouse, M., Meredith, M., Murphy, E., Shreeve, R., Korb, R., Watkins, J., Thorpe, S., Woodd-Walker, R., Brierley, A., Cunningham, N., Grant, S. and Bone, D. 2002. The Southern Antarctic Circumpolar Current Front: physical and biological coupling at South Georgia. Deep-Sea Research I **49**: 2183-2202.

Winn, C. D. and Karl, D. M. 1986. Microorganisms in deep-sea hydrothermal plumes. Nature **320**: 744-746.

Wirsen, C. O., Jannasch, H. W. and Molyneaux, S. J. 1993. Chemosynthetic microbial activity at Mid-Atlantic Ridge hydrothermal vent sites. Journal of Geophysical Research **98**: 9693-9703.

Yamaguchi, A., Watanabe, Y., Ishida, H., Harimoto, T., Furusawa, K., Suzuki, S., Ishizaka, J., Ikeda, T. and Mac Takahashi, M. 2002. Structure and size distribution of plantkon communities down to the greater depths in the western North Pacific Ocean. Deep-sea Research II **49**: 5513-5529.

Zar, J. H. 1984. Biostatistical analysis. Prentice-Hall Inc.

Chapter 3

Characteristics of zooplankton assemblages in the near-bottom water layers on the Juan de Fuca and Explorer Ridges.

3.1 Abstract

Previous work suggests that although vent production may play a role in enhancing zooplankton assemblages hundreds of metres above vent fields, little is known about how vents influence near-bottom zooplankton and nekton in the NE Pacific.

In this study, net tows above non-vent areas, diffuse vents and smoker vents on the Juan de Fuca and Explorer Ridges were used to characterize zooplankton assemblages at 20 metres above bottom and near the seafloor (1-7 m above bottom). Simultaneous video was collected to complement net tow samples. Species composition and abundance were recorded for all groups where possible. Characteristics of copepod assemblages, such as ratio of females to males, juveniles to adults and dead (exoskeleton) to live, were recorded.

Video is useful for capturing large pelagic organisms. Video and net tows capture similar numbers of copepods over non-vent and smoker vent areas. Because small mesh nets are used, cyclopoids and poecilostomatoids are well-represented. The 63 μm net consistently captures larger, more diverse samples. Given the difficulty of sampling in the deep sea, multiple sampling methods are useful.

Seventy-two copepod species are found, including representatives from different biotopes: epipelagic, mesopelagic, bathypelagic/abyssal and benthic. Composition of non-vent, diffuse vent and smoker vent assemblages is not distinct. Twenty-four species occur in all assemblage types. Diffuse vent assemblages are least diverse (34 species) and smoker vent assemblages are most diverse (57 species). *Oithona similis* dominates all 20 mab samples whereas near-bottom diffuse vent assemblages are dominated by dirivultids.

Copepod densities range from 0.7-3.5 individuals/m^3 over smoker vent and non-vent sites to 14.6 individuals/m^3 over diffuse vent sites.

Typical of benthopelagic studies, most copepod species are predominantly female; the exception is *Oithona similis*, which are male-dominated. *Neocalanus plumchrus* copepodites (stage II and III) are relatively abundant over diffuse vents suggesting that vent effluent may induce stage V copepodites to emerge from diapause, molt and mate. Dirivultid copepodites are relatively abundant over non-vent areas, supporting the idea that species like *Stygiopontius quadrispinosus* develop in the water column.

Based on my work, there is some evidence to suggest that vents represent a significant source of food for pelagic copepods near the seafloor within the axial valley. Copepods appear to play a role in the utilization and transfer of carbon from vents to the deep sea.

3.2 Introduction

If composition and abundance of benthopelagic zooplankton are driven by the availability of food resources, it is possible that pelagic zooplankton may be attracted to chemosynthetically-derived resources at vents. Vertical advection of benthic debris and free-living bacteria associated with vent effluent may represent a relatively abundant resource in the otherwise depauperate deep sea.

3.2.1 Pelagic organisms near the seafloor

In marine environments, zooplankton biomass and abundance decrease exponentially with depth (Wishner 1980a). The exception to this rule is the relative increase in zooplankton biomass and abundance near the seafloor within the benthic boundary layer. In general, zooplankton are attracted to increased availability of resources associated with seafloor sediments (Angel 1990). Zooplankton depend on sinking photosynthetically-derived material, marine detritus in the form of marine snow, faecal pellets, resuspended sediment, crustacean moults and larger carcasses, and also on bacterial mats colonizing seafloor sediments (Wishner 1980a, Gowing and Wishner 1992, Gili et al. 2000). However, the contribution of living benthic particles (e.g. from vents) to pelagic systems is a process that is also likely to influence the dynamics of water column populations and communities (Raffaelli et al. 2003). This aspect of benthic-pelagic coupling remains poorly studied.

3.2.2 Vent environment

Several characteristics of vent effluent could potentially influence pelagic organisms near the seafloor. At hydrothermal vents, hot, mineral effluent is expelled through discrete openings and through cracks in the seafloor in the form of a plume. As this plume of warm water rises, it entrains and mixes with ambient seawater. Effluent released from discrete openings, or smoker vents, often rises to altitudes of 100-200 m above the seafloor. Effluent released through cracks in the seafloor, or diffuse vents, remains trapped within 50 m of the seafloor. Unlike typical benthic boundary layers, turbulence is greater at 50 m above bottom than at the seafloor as the result of mixing effluent and ambient water (Trivett 1994). Effluent is horizontally transported hundreds of metres downstream from the source by prevailing currents and tidal action (Thomson et al. 1990, Trivett 1994).

Vent outflow is rich in metals (e.g. Mn and Fe) and H_2S (Von Damm 1995). Bacterial chemosynthesis, fueled by high concentrations of gases, such as H_2S, CH_4 and NH_4 (Jannasch and Mottl 1985) and reduced metals (Klinkhammer and Hudson 1986), generate organic matter in the advecting plume (Roth and Dymond 1989, Cowen et al. 1990, McCollom 2000). Chemical and metal species are oxidized through biologically mediated reactions and are then precipitated and sink to the seafloor (Lilley et al. 1995). The ascending flux of vent particulate organic matter at some vent sites (e.g. Endeavour) is six times greater over vent fields than in non-vent areas and is roughly equivalent to the downward fluxes at similar oceanic depths (Wakeham et al. 2001).

3.2.3 Pelagic organisms at vents

Copepod and amphipod swarms above vents on the East Pacific Rise (EPR) are the focus of some of the early studies on near-bottom plankton assemblages (Smith 1985, Berg and Van Dover 1987, Van Dover et al. 1992, Kaartvedt et al. 1994). The first comprehensive study of zooplankton and larvae over vent and non-vent areas is by Berg and Van Dover (1987). They find benthopelagic zooplankton communities at vents enriched in both abundance and biomass with respect to non-vent areas. Bathypelagic and epibenthic copepods dominate their samples.

Since then, most zooplankton studies have focused on composition, abundance and biomass of assemblages hundreds of metres above the bottom. Wiebe et al (1988) find no significant increase in zooplankton assemblages in the water column 100-200 m above vent fields in the Guyamas Basin. Conversely, in a series of papers, Burd et al (1992) and Burd and Thomson (1994, 1995, 2000) find increased abundance and biomass of zooplankton, primarily copepods, and gelatinous zooplankton associated with the neutrally buoyant plume from Main Endeavour Field on the Endeavour Segment, Juan de Fuca Ridge. Surface and mid-depth copepod species appear to be attracted to bacterial biomass synthesized within or vertically advected by the rising plume (Cowen et al. 2001, Burd et al. 2002).

More recent work by Vereshchaka and Vinogradov (1999) and Vinogradov et al (2003), using *in situ* submersible observations and vertical net tows, suggests the opposite occurs over vents along the Mid-Atlantic Ridge. Zooplankton show no significant increase in abundance in the near-bottom layers or near plumes; zooplankton abundance appears to be more closely related to surface production.

In short, there is yet no clear picture of how vents influence near-bottom zooplankton assemblages.

3.2.4 Specific objectives

In this paper, I characterize zooplankton assemblages in terms of composition and abundance over venting and non-venting seafloor within the axial valleys. Pelagic species that are able to tolerate variable conditions at vents are likely to be more abundant at vents than species that have narrower physiological tolerances. Assuming zooplankton assemblages reflect conditions on the seafloor, I hypothesize that diffuse vent and smoker vent copepod assemblages will be more similar to each other than either is to non-vent assemblages.

Based on benthic assemblages, I hypothesize that pelagic organisms will be more abundant over diffuse vents than smoker vents. Benthic organisms cluster around cracks in the seafloor where microbial production is enhanced above background levels and environmental conditions are less extreme (Van Dover and Fry 1994). If pelagic organisms can utilize vent production, it is likely that they will aggregate in areas where

environmental conditions are less extreme if they are not specifically adapted to this environment.

Comparisons with other benthopelagic studies in vent and abyssal areas are used to speculate about the possible importance of vents as food resources for near-bottom pelagic organisms.

3.3 Methods

3.3.1 Site descriptions

All samples were collected on the New Millenium Observatory (NeMO) and CANRIDGE cruises in July and August, 2002 on the Juan de Fuca and Explorer Ridges. Sample sites and number of samples are listed on Figure 3.1. Number of samples and locations of sample collection were dictated by dive schedules and were limited by poor weather.

Axial Seamount

Axial Seamount rises to an altitude of roughly 1000 m above the bottom. Volcanically and hydrothermally active, the seamount lies at the intersection of the Cobb-Eickelberg Seamount Chain and the Juan de Fuca Ridge at 45°57'N, 130°01'W (Johnson and Embley 1990). The summit is 1450 m below the surface and is characterized by a large rectangular 100 m deep caldera, 8 km long by 4 km wide and is oriented northwest to southeast (Feely et al. 1990).

Net tow samples were collected from ASHES vent field in the southwest quadrant of the caldera (Table 3.1). Extensive chimney formations and extremely hot fluid emissions characterize ASHES vent field; the field is roughly 100 m long by 400 m wide (Feely et al. 1990). Southward and northward flowing currents converge west of Axial, flowing away from the ridge, and thus determine the fate of hydrothermal fluid that exits from the summit of Axial (Johnson and Embley 1990). Thermal anomalies from Axial vent outflow are restricted to a 200 m thick layer above the caldera; these anomalies are generally smaller than those associated with other hydrothermal fields on the Juan de Fuca Ridge (Baker et al. 1990).

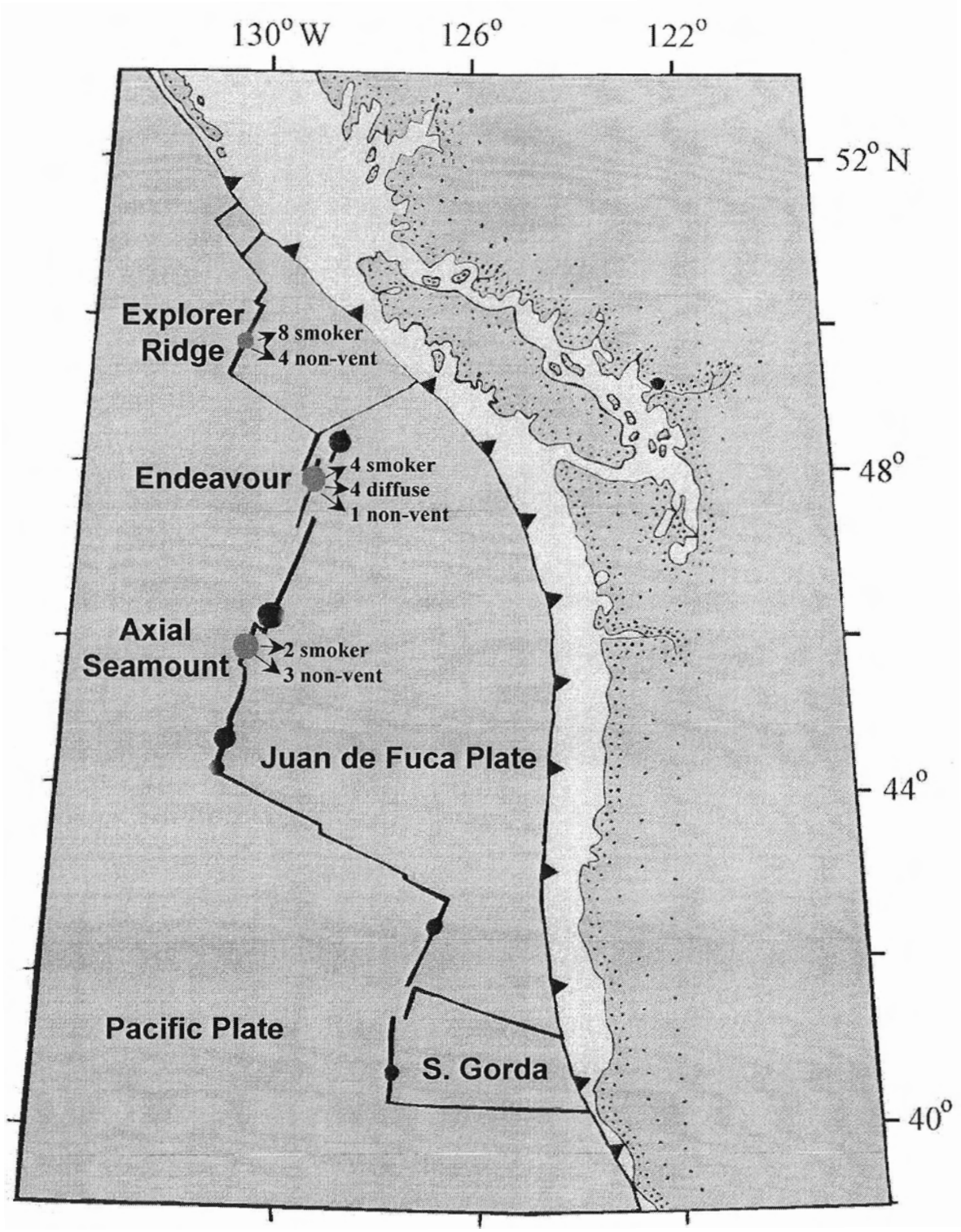

Figure 3.1 Location of net tows along Explorer-Juan de Fuca-Gorda Plate spreading ridge. Samples were collected from Explorer and from Endeavour Segment and Axial Seamount on the Juan de Fuca Ridge. Numbers of samples collected from each area and over the different site types (non-vent, diffuse vent and smoker vent) are indicated.

Table 3.1 Summary of net sample information. Altitudes are noted as metres above bottom (mab). Net samples collected using submersible claw are denoted as '**hh**' (hand held). Pump (**p**) samples are also indicated. * Where two mesh sizes are listed, two simultaneous samples were collected. For these samples, combined sample volume is indicated. Sample location and duration were dictated by dive schedules. Total number of samples collected was limited by poor weather.

Region	Sample #	Mesh size (μm)*	Location	Seafloor character	Depth	Altitude (mab)	Duration	Sample volume	Video taken
Axial	R661	63	Mid-caldera	Non-vent	1530m	2-3	44 min	109 m^3	-
	R666	63, 180	ASHES	Smoker	1773m	~2m above chimney	31 min	132 m^3	-
	R667	63, 180	Transit	Non-vent	1799m	20-25	32 min	146 m^3	Yes
Endeavour	R682	63, 180	Clam Bed	Diffuse	2173m	20	30 min	64 m^3	Yes
	R682 **p**	180	Clam Bed	Diffuse	2173m	20	36 min	0.3 m^3	-
	R682 **hh**	180	Clam Bed	Diffuse	2190m	1-7	31 min	66 m^3	Yes
	R683	63, 180	Bastille, MEF	Smoker	2180m	~2m above chimney	30 min	64 m^3	Yes
	R683 **hh**	180	Easter Island	Diffuse	2199m	2-5	30 min	64 m^3	Yes
	R683 **p**	180	Easter Island	Diffuse	2199m	2-5	31 min	0.21 m^3	-
	R684	180	South of Clam Bed	Non-vent	2175m	20	25 min	27 m^3	-
	R685	63, 180	MEF	Smoker	2178m	20	30 min	104 m^3	Yes
Explorer	R664	63, 180	Magic Mountain	Non-vent	1800-1878m	2-20	70 min	128 m^3	-
	R665	63, 180	W of Magic Mountain	Non-vent	1821m	2-5	31 min	66 m^3	-
	R668	63, 180	Einstein	Smoker	1790m	5	30 min	128 m^3	-

Table 3.1 continued.

Region	Sample #	Mesh size (μm)*	Location	Seafloor character	Depth	Altitude (mab)	Duration	Sample volume	Video taken
Explorer	R669	63, 180	Majestic Mound	Smoker	1788 m	~2m above chimney	30 min	128 m^3	-
	R670	63, 180	Zooarium	Smoker	1791m	~2m above chimney	31 min	128 m^3	-
	R670 **p1**	180	Zooarium	Smoker	1792m	~2m above chimney	30 min	0.23 m^3	-
	R670 **p2**	180	Zooarium	Smoker	1799m	~2m above chimney	42 min	0.40 m^3	-

Endeavour Segment

Endeavour Segment (47°57'N, 129°06'W) is a 300 km long, 10 km wide oceanic spreading zone, oriented northeast to southwest on the Juan de Fuca Ridge (Delaney et al. 1992). Most of the venting is confined to a narrow, 10 km long, 2000-2400 m deep section along the west wall of the valley (Delaney et al. 1997). The valley itself is bounded by 100-150 m high walls (Delaney et al. 1992). Strong venting in the south and central area creates plume-induced currents that pull ambient water northward into the axial valley, although flow reversals are common (Thomson et al. 2003).

Net tow samples were collected from two vent fields, Clam Bed and Main Endeavour, near the centre of the segment (Table 3.1). Clam Bed is a small vent field comprising one high and numerous low temperature vents. Roughly 75 x 200 m, the centre of Clam Bed is in a shallow v-shaped valley and is characterized by the bivalve, *Calyptogena pacifica*. Valley edges rise a couple of metres above the seafloor and are characterized by tubeworm bushes clustered around numerous cracks emitting low temperature fluid.

Main Endeavour Field (MEF), roughly 1.5 km south of Clam Bed, contains more than 100 actively venting sulphide chimneys routinely emitting fluids in excess of 360°C (Delaney et al. 1997). MEF is characterized by steep compositional gradients in vent fluids and temperature. Effluent released in the northern portion of the field is near ambient seawater salinity whereas vents in the southern portion release less saline, higher temperature fluids with greater concentrations of dissolved gases (Delaney et al. 1997).

Explorer

While the vents along this ridge have remained relatively unexplored since preliminary work in the 1980s, in July-August 2002, the NeMO cruise found 30 active vents, emitting fluid 20-311°C at four different sites (Embley 2002). Much of the venting is confined to Magic Mountain (49°46'N, 139°16'W), a topographic high located outside the primary rift valley at a depth of 1870 m (Tunnicliffe et al. 1986). Net tow samples were collected above smoker vents on Magic Mountain and during transits between vent fields (Table 3.1).

Benthic assemblages are sporadic. Only some smoker vents within the vent fields are colonized by benthic organisms (Embley 2002). Swarms of adult pycnogonids characterize Magic Mountain vents (Embley 2002).

Non-vent areas

In this study, "non-vent area" refers to sections of unfissured, non-venting lavas within 1 km of vent fields. Typically, brittle stars, anemones and spider crabs are sporadically dispersed along non-venting seafloor on the Juan de Fuca (Milligan and Tunnicliffe 1994).

3.3.2 Data collection and processing

Two plankton nets, 30 cm diameter by 90 cm long, were mounted between two bars at the front end of the ROPOS submersible (Figure 3.2). Net cod ends were attached to a rod that extended from the top bar back to the submersible to keep nets extended while towing. One 180 μm and one 63 μm mesh net were used for most dives (Table 3.1). The 180 μm net was usually mounted on the port side with the exception of one dive (R682) when it was mounted on the starboard side.

Stiffening rods were sewn along the outside of the net mouth fabric allowing the net mouths to be opened or closed on command. When the net mouths were opened, nets were towed horizontally at 0.5-0.8 knots in straight lines along the length of the vent field, above an individual smoker vent or in transit between vent fields ranging from 30-80 minutes (Table 3.1). Upon completion of each tow, net mouths were remotely closed and the nets were cinched roughly two-thirds down the length of each net using a rope.

A third net of the same dimensions and 180 μm mesh was held in the robotic claw and used to collect most near-bottom samples. Manipulations of the net opened and closed the net mouth. The net was stowed during transit.

Five pump samples were also collected over vent and non-vent areas at Endeavour and Explorer (Table 3.1). The McLane pump® was designed for large volume *in situ* collection of suspended or dissolved particulates in aqueous environments onto a filter. Mesh filters of 180 μm were used. The pump was positioned downstream from the filter

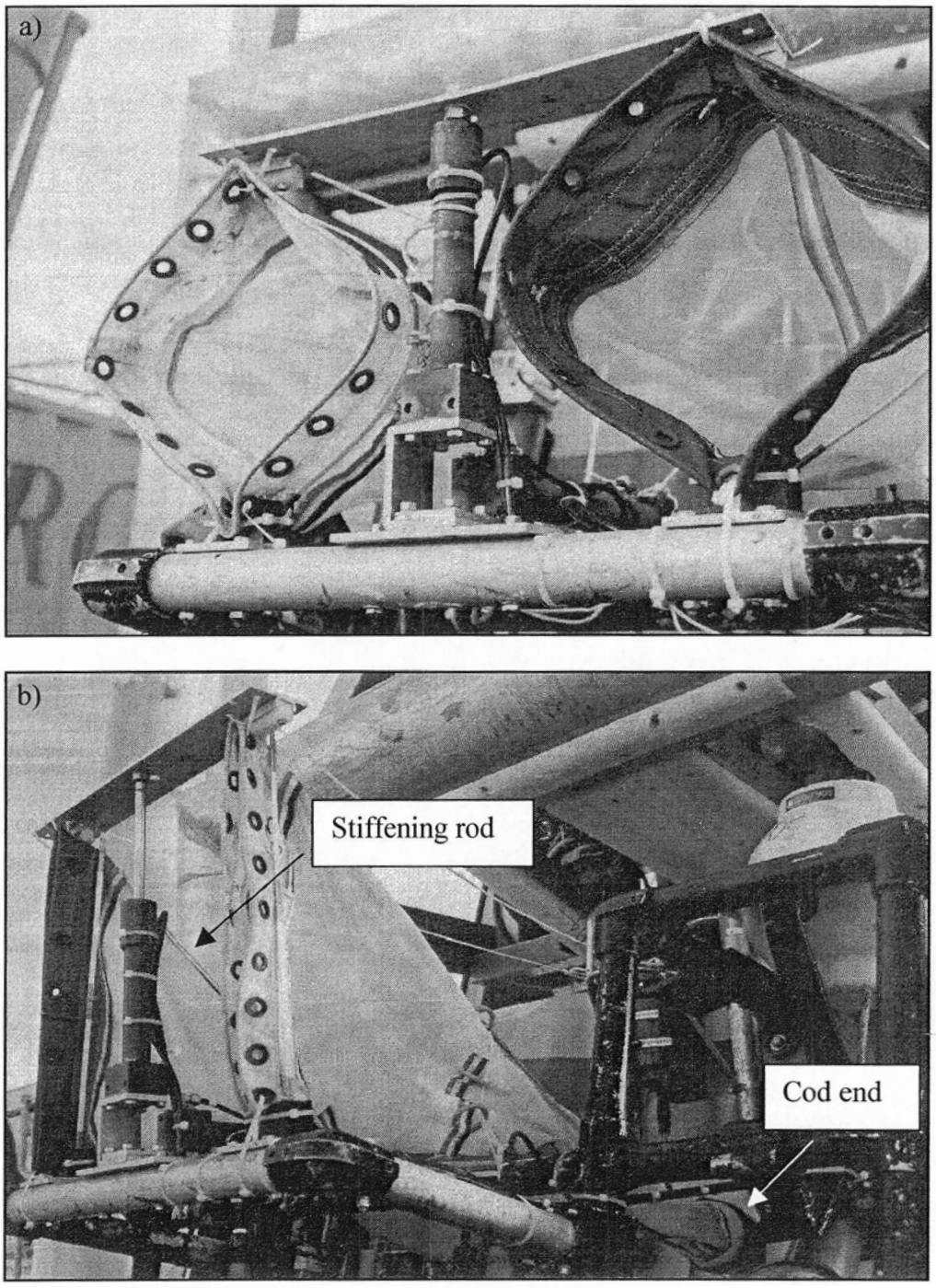

Figure 3.2 Configuration of nets mounted on ROPOS submersible, a) shows both nets in open position and b) shows closed nets, not cinched. In a) 63 μm net (white mouth) is on the port side, 180 μm net (dark mouth) is on the starboard side. In b) 180 μm net is on the port side, 63 μm net is on the starboard side. Nets are attached to a stiffening rod, ensuring the nets are fully extended.

to avoid contamination of the sample by material that originates in the pump. The pump was positioned approximately 1 m below the mounted nets.

Nets and filters were removed immediately upon return of the submersible and rinsed using filtered seawater. Samples were preserved using 95% ethanol to ensure larvae remained intact.

Samples were initially pre-sorted (i.e. organisms were separated from debris) and then sorted a second time to identify organisms to species where possible. Voucher specimens of copepods were identified by an expert (M. Galbraith, Institute of Ocean Sciences).

Copepods were identified at least to genus; most were identified to species. Abundance, number of females and males (adult and late stage copepodites), number of gravid females and number of early stage copepodites (I-IV) were recorded for each sample. Calanoid copepodites that could not be identified to species were grouped as 'miscellaneous calanoid copepodites'. As in Wishner (1980b), intact exoskeletons (e.g. molts) were also counted. Counts were converted to densities using net mouth area and distance of net tow.

Video of the horizontal water layer was taken during some net tows (Table 3.1). Videos were used to compare relative abundance of copepods with net tows and to identify larger pelagic organisms (e.g. gelatinous zooplankton, shrimp, fish) that were not captured in the nets, but were present in the water layer. Video resolution was low therefore, organisms were identified to general groups (e.g. zooplankton (crustaceans), gelatinous plankton, shrimp, zoarcid and macrourid fish). Copepods were distinguished from other zooplankton based on their means of locomotion (e.g. hopping, paddling).

3.3.3 Analyses

A paired t-test was used to compare abundance and diversity of copepod assemblages collected in the 63 μm and 180 μm nets. If a significant difference was found, data from the two nets were pooled to give a better idea of overall assemblage abundance and composition.

To compare species richness among non-vent, diffuse vent and smoker vent sites, rarefaction curves were created using EcoSim 7.8. The program uses a computer-

sampling algorithm of rarefaction, in which a specified number of individuals are randomly drawn from a community sample. The process is iterated to generate a mean and a variance of species diversity. The maximum of 1000 iterations were performed.

Cluster analysis was used to determine if zooplankton assemblages from different sample areas were distinct (PCOrd ver. 4.0). Clustering was assessed using species presence/absence data. To determine if net mesh size influenced assemblage composition, 63 μm and 180 μm samples from each location were analyzed individually. A second cluster analysis was performed on pooled data to determine if clustering was based on site type (vent or non-vent) or on geographic location. Clustering was assessed using an unweighted pair-group method using arithmetic averages (UPGMA) and a Bray-Curtis similarity index.

3.4 Results

3.4.1 Methodologies

Video versus nets

In both net and video samples, the majority of organisms 'captured' are copepods (Table 3.2). The water layer above diffuse vent fields is relatively cloudy and has more particulates over the entire extent. In the near-bottom videos over diffuse vents, small zooplankton are difficult to see. Above smokers, water cloudiness is confined to relatively small, discrete areas and likely did not influence zooplankton counts.

Above smoker vent and non-vent sites, similar numbers of zooplankton are captured using video and nets (Table 3.2). However, over diffuse vents, zooplankton captured in nets outnumber those seen in video by almost 9:1. (Table 3.2). The large discrepancy between video and net samples above diffuse vent fields is likely due to juvenile copepods (copepodites). Their small size make it difficult to distinguish them from particulates suspended in the water above diffuse sites.

Video captures larger zooplankton and fast swimming nekton better than nets (Table 3.2). Gelatinous zooplankton are virtually absent from the nets tows, yet are relatively abundant in the videos. Shrimp are relatively abundant at non-vent and diffuse vent sites; zoarcids are most abundant in non-vent areas while macrourids are seen only in vent areas. None of these nekton groups are captured in net tows (Table 3.2).

Table 3.2 Comparison of video and net tow abundance data. Nets over non-vent, diffuse vent and smoker vent areas sample roughly the same volume of water (~33 m^3). Numbers in parentheses indicate number of simultaneously collected samples from each site type. The non-vent sample was collected from Axial Valley. Three of the four diffuse samples were collected over Clam Bed. The fourth diffuse vent near-bottom (n-b) sample was collected from Easter Island, an area of diffuse venting within Main Endeavour Field. The two 20 mab Clam Bed samples were collected using one 180 μm net and one 63 μm net. The two near-bottom diffuse samples were collected using the 180 μm hand held net. All four smoker samples were collected over Main Endeavour vent field; two samples were collected using the 180 μm net and two samples were collected using the 63 μm net.

	Non-vent		**Diffuse 20 mab**		**Diffuse n-b**		**Smoker**		**Total**	
	Video (1)	Net (1)	Video (1)	Net (2)	Video (2)	Net (2)	Video (2)	Net (4)	**Video**	**Net**
Zooplankton	136	118	98	937	79	944	108	292	**421**	**2291**
Gelatinous zoopl.	66	1	39	0	41	1	94	0	**240**	**2**
Shrimp	5	0	5	0	5	0	2	0	**17**	**0**
Zoarcid	8	0	2	0	0	0	4	0	**14**	**0**
Macrourid	0	0	1	0	1	0	2	0	**4**	**0**
Tomopterid	0	0	0	1	1	0	0	0	**1**	**1**
Unknown	51	0	16	0	44	0	35	0	**146**	**0**
Total	268	119	161	938	171	945	245	292	**843**	**2294**

Relatively high numbers of 'unknowns' are a drawback of video analysis. Organisms approaching the video camera head-on, especially gelatinous zooplankton, are often difficult to distinguish from large particles.

In short, video and net tow methods complement each other well. Video is more effective at capturing larger pelagic organisms whereas net tows are more effective closer to the seafloor and in areas where particulates and debris are abundant in the water column. Large pelagic organisms are examined in more extensive video data from another study (Chapter 2); here I will comment only on net tows.

Net tow data (Net versus net)

In general, the 63 μm net captured more copepods than the 180 μm net (Figure 3.3a). Two anomalies are evident: 1) the high number of copepods (663) caught in the 180 μm net at 20 mab over a diffuse vent and 2) the relatively low number of copepods in a large sample volume collected from Axial (R661). During dive R682, the 180 μm net caught 663 copepods whereas the 63 μm net caught 273 copepods. Despite this, a paired t-test comparing the number of copepods caught in each dive showed no significant difference ($t=0.439$, $p=0.204$). During dive R661, a relatively large volume of water is sampled while few copepods are caught. Because there is no associated 180 μm net sample from this site to determine if this is an unusual sample or if this is an accurate measure of copepod abundance at the site, this sample is omitted from further analysis.

There is a significant difference in the number of copepod species caught with the 63 μm and 180 μm nets ($t=0.748$, $p=0.013$). Figure 3.3b shows that the 63 μm net captures more species than the 180 μm net.

Samples appear to cluster according to net size (Figure 3.4). All 180 μm net diffuse vent samples, 20 mab and near-bottom, and one 180 μm non-vent sample cluster with the 63 μm net samples. These samples are relatively speciose.

These analyses suggest that while there is no significant difference in the size of samples collected by the two nets, there is a significant difference in the composition of the samples. Therefore, pooling simultaneously collected samples will result in a better overall picture of copepod assemblage composition.

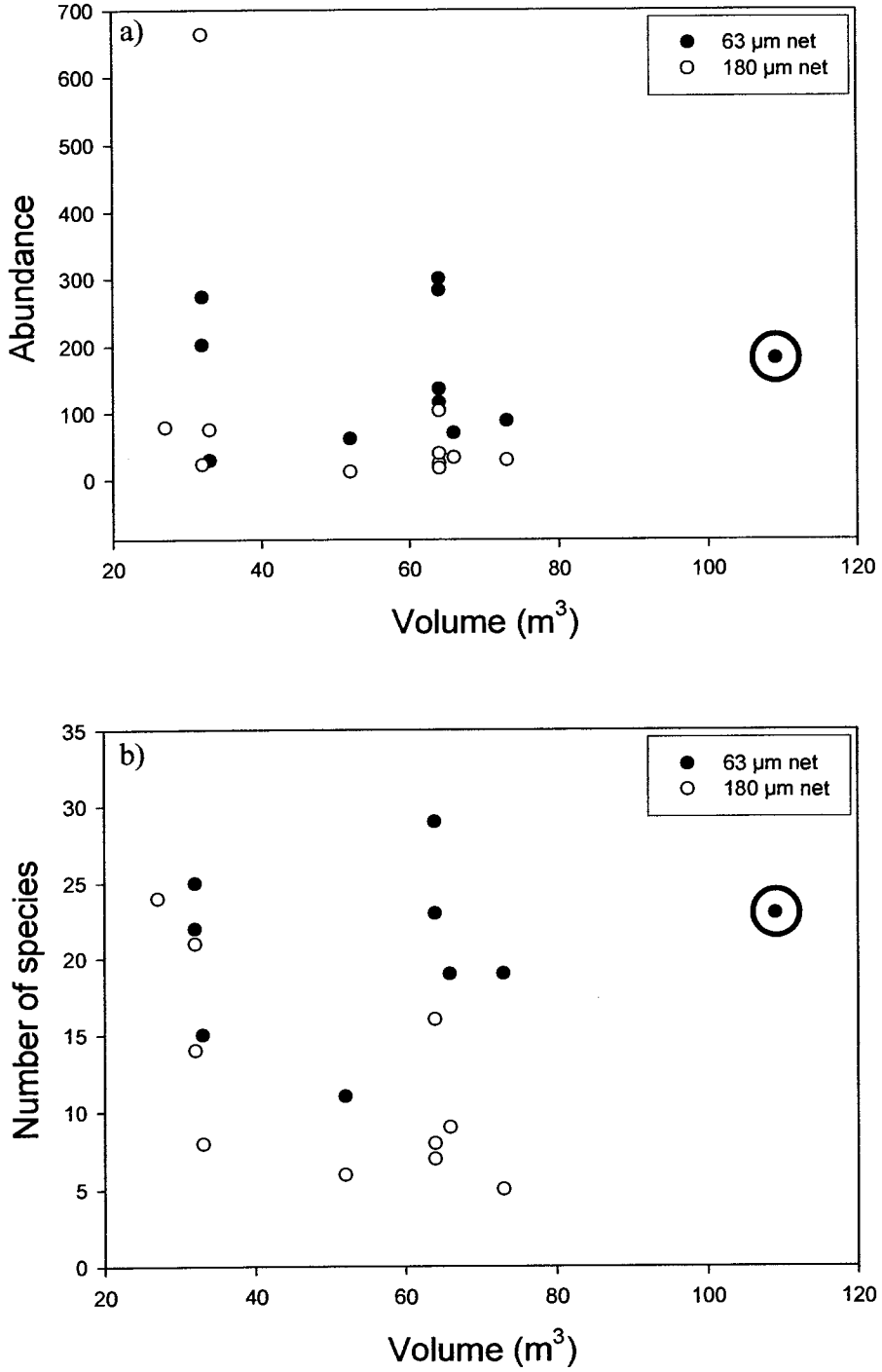

Figure 3.3 Scatterplots of a) copepod abundance and b) number of copepod species collected in 63 and 180 µm nets versus volume sampled. Circled point is non-vent sample R661 that is omitted from further analysis.

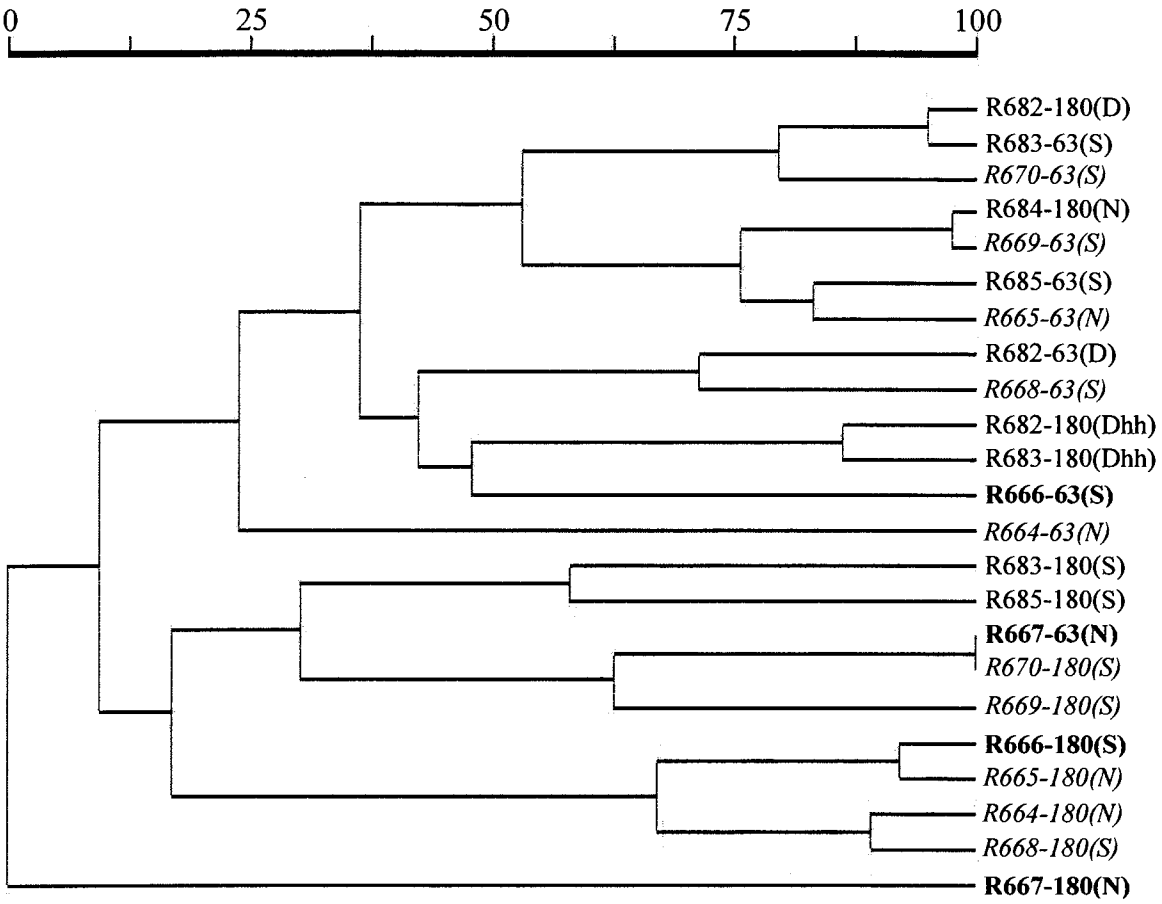

Figure 3.4 Cluster dendrogram of species presence/absence based on net type. Percent similarity is indicated on axis above dendrogram. Site types are listed in parentheses after the dive number: non-vent (N), diffuse vent 20 mab (D), diffuse vent near-bottom (Dhh) and smoker vent (S). Both net mesh size and site type are indicated for each sample. Endeavour, **Axial** and *Explorer* sites are indicated by font type.

Net versus pump samples

Nets outperform the McLane pump. Nets sample larger volumes of water over the same period of time (Table 3.1). Nets capture large, diverse samples (Table 3.3). Only copepods are caught in the pump samples; numbers of copepods caught range from zero to two. The maximum number of species caught in any pump sample is two. Pump samples will therefore be excluded from further analysis.

3.4.2 Assemblage characteristics

Benthic organisms, such as vent gastropods and polychaetes, are relatively abundant in smoker vent and near-bottom diffuse vent samples (Table 3.3). Juvenile gastropods are found in only one non-vent sample. Pycnogonids are only found in samples from Explorer. Two adult pycnogonids are found in samples above a smoker vent in Zooarium vent field whereas 44 juveniles are found above a smoker vent in Majestic Mound vent field (Table 3.3).

Pelagic copepods and ostracods are found at all site types (Table 3.3). Pelagic ostracods (Podocopida) are more abundant than the vent ostracod, *Euphilomedes climax*, in all but the near-bottom diffuse vent samples.

Copepods are the most abundant and most speciose organisms in all samples and are therefore, considered in greater detail.

Copepods are most dense over diffuse vents at 20 mab (14.6 individuals/m^3) (Table 3.4). Copepod densities over smoker vents (0.7-3.5 individuals/m^3) and non-vent areas (0.8-2.9 individuals/m^3) are considerably lower. Near-bottom densities over diffuse vents are intermediate (Table 3.4).

Abundance is highly variable even within site types (Table 3.4). Highest abundance is found in diffuse vent samples (R682) at 20 mab while relatively few copepods are found in samples taken 20 mab along the central axis, where the majority of venting occurs, over MEF (R685) (Table 3.4).

Table 3.3 Total abundance of different groups of organisms caught in net tows above vent and non-vent areas. Number of net tows at each site type is listed in parentheses. In second column, 'mab' refers to metres above bottom. In third column, 'nb' refers to near-bottom. All vent organisms are identified to species. Vent organisms are considered to be obligate vent species. Epibenthic organisms have been found in vent samples, but may not be obligate. *Microsetella rosea* is a pelagic harpacticoid commonly found in tubeworm grabs. Pelagic organisms are not endemic to vents and are found only in the water column. *indicates that these vent gastropods are juveniles.

	Non-vent (7)	**Diffuse 20 mab (2)**	**Diffuse nb (2)**	**Smoker (12)**
Vent organisms				
gastropod	19*	-	46	30
polychaete	-	-	10	2
pycnogonid	-	-	-	46
nemertean	-	-	-	1
tanaid	-	-	-	1
ostracod	2	-	24	1
copepod	30	4	139	49
Epibenthic organisms				
asellote isopod	-	1	-	1
amphipod	3	-	30	4
Microsetella rosea	11	41	-	71
Pelagic organisms				
fish larva	-	1	-	-
jellyfish	1	-	1	2
tomopterid polychaete	1	1	-	-
chaetognath	-	1	-	6
ostracod	7	4	6	19
euphausiid	-	-	2	1
copepod	583	891	224	975

Table 3.4 Total abundance of copepods from each sample location. Net size is indicated (63 μm net, 180 μm net, 180 μm hand-held net (hh)) in parentheses. Where more than one mesh size is listed, two simultaneous net samples are collected. Abundance and number of species collected in these nets are pooled. Copepod densities are listed as number of individuals per m^3.

Site Type	Region	Sample	# Species	Abundance	Volume (m^3)	#ind/m^3
Non-vent	Axial	R667 (63/180)	22	117	146	0.8
	Endeavour	R684 (180)	24	79	27	2.9
	Explorer	R664 (63/180)	29	324	128	2.5
		R665 (63/180)	22	104	66	1.6
Diffuse 20 mab	Endeavour	R682 (63/180)	38	936	64	14.6
Diffuse	Endeavour	R682 (hh)	26	240	33	7.3
near-bottom	Endeavour	R683 (hh)	21	123	32	3.8
Smoker	Axial	R666 (63/180)	23	103	131	0.79
	Endeavour	R683 (63/180)	30	225	64	3.5
		R685 (63/180)	14	73	104	0.7
	Explorer	R668 (63/180)	36	386	128	3
		R669 (63/180)	18	155	128	1.2
		R670 (63/180)	18	153	128	1.2

Seventy-two species of copepods from 22 families are collected in net tows (Table 3.5). Most species are present at all three site types. The majority of species are suspension feeders or detritivores (Yamaguchi et al. 2002). Only a few carnivorous species, *Heterorhabdus tanneri* and *Aetideopsis* sp., are present.

Adult *Pseudocalanus* sp. are the only group that appeared to be limited to either non-vent or smoker sites (Table 3.5). No adult *Pseudocalanus* are found over diffuse vents.

Most species that are found at only one site (e.g. *Pseudochirella obtuse, Centropages abdominalis*) are rare, usually one or two organisms. The exception is *Acartia longiremis*; 120 individuals of this species are found at a single non-vent site at Explorer.

Table 3.5 Occurrence of copepod species at non-vent (N), diffuse vent 20 mab (D(20)), diffuse vent near-bottom (D(nb)) and smoker vent (S) sites. Vent species are indicated (V). Calanoids are organized by Family. *indicates only one individual of this species was found in all samples. Second column indicates community to which species typically belongs (V=vent, Eb=epibenthic, Ep=epipelagic (0-50 m), M=mesopelagic (50-175 m), B=bathypelagic (175-3000 m), A=abyssal (below 3000 m)) as indicated in Rose (1933), Brodskii (1967), Mauchline (1998) and Heron and Frost (2000).

Species		N	D (20)	D (nb)	S
Dirivultid					
Stygiopontus quadrispinosus	V	●	●	●	●
Aphotopontius forcipatus	V	●	●	●	●
Benthoxynus spiculifer	V	●	●	●	
Unknown sp 1	?				*
Unknown sp 2	?				*
Misophriopsid					
Misophriopsis longicauda	V		●	●	●
Harpacticoid					
Uptionyx verenae	V		●	●	
Microsetella rosea	Eb	●	●		●
Unknown sp 1	?	●	●		
Unknown sp 2	?	●			●
Unknown sp 3	?	●	●	●	
Cyclopoid					
Barathricola rimensis	V				●
Corycaeus anglicus	Ep		●		
Oithona atlantica		●	●		●
Oithona similis	Ep	●	●	●	●
Oithona spinorostris		●	●		●
Conaea rapax	?B	●			●
Oncaea canadensis	Ep-B	●			●
Oncaea glabra	Ep	●	●		●
Oncaea ivlevi		●			●
Oncaea prolata/grossa	Ep-B	●	●	●	●
Oncaea sp.		●	●	●	●
Sapphirina sp.	Ep		●	●	●
Monstrilloid					
Monstrilla sp.					*
Calanoid					
Acartia longiremis	Ep	●			
Aetideopsis rostrata	B	●	●	●	●
Pseudochirella obtuse	B/A				*
Neocalanus cristatus	Ep/M/B	●	●	●	●
Neocalanus flemingeri	Ep/M/B		*	●	
Neocalanus plumchrus	Ep/M/B	●	●	●	●
Calanus marshallae	Ep/M/B	●			
Calanus pacificus	Ep	●	●	●	●
Centropages abdominalis	Ep		●		

Table 3.5 continued.

Species		N	D (20)	D (nb)	S
Calanoids continued					
Eucalanus bungii	Ep/M/B	●	●		●
Heterorhabdus tanneri	B	*			
Lucicutia ellipsoides	B/A				*
Lucicutia grandis	B/A	●		●	
Lucicutia sp.		●	●		●
Metridia brevicaudatus	B/A				*
Metridia curticauda	B/A	●			●
Metridia lucens	Ep-B	●			●
Metridia pacifica	Ep-B	●	●	●	●
Metridia princeps	B/A				*
Mormonilla minor	B	●	●	●	●
Mormonilla phasma	B	●	●	●	●
Paracalanus parvus	Ep	●	●	●	●
Xanthocalanus sp.	B/A	●	●	●	●
Epilabdidocera laongipedata	Ep	●	●		
Clausocalanus arcuicornis	Ep		*		
Clausocalanaus lividus					●
Clausocalanus mastigophora		●			●
Clausocalanus sp.		●	●	●	●
Mesocalanus tenuicornis		●	●		
Microcalanus pygmaeus	Ep-B	●	●	●	●
Mimocalanus cultifer			●	●	
Pseudocalanus mimus	Ep	●			●
Pseudocalanus minutus	Ep	●			●
Pseudocalanus newmani	Ep				●
Pseudocalanus sp.		●			●
Spinocalanus abyssalis	A	●			
Spinocalanus brevicaudatus	Ep-A	●	●	●	●
Spinocalanus horridus	A	●	●	●	●
Spinocalanus longicornis	A	●			●
Spinocalanus similis	B/A		●	●	●
Scaphocalanus brevicornis	B	●	●		●
Scaphocalanus major	B		*		
Scaphocalanus subbrevicornis	B/A	*			
Scolithricella emarginata	B	●	●	●	
Scolithricella minor	Ep	●			●
Scolithricella ovata	B				*
Scolithricella sp.		●	●	●	●
Unknown calanoid sp 1	?				*

Many species are relatively rare. Only a few groups or species represent more than 10% of the copepods in a sample; typically these species are *Oithona similis, Oncaea* sp. and miscellaneous calanoid copepodites. A total of 34 species are found in diffuse vent samples (20 mab and near-bottom) whereas 55 and 57 species are found in non-vent and smoker vent samples respectively. *Oithona similis* is the most abundant species at the majority of sites. Relative abundance of this species ranges from 22-33%.

Non-vent sites are characterized by *Oithona similis* and *Oncaea* sp. (Figure 3.5a). *Acartia longiremis* is highly abundant in one non-vent sample collected from Explorer, but is not found in any other sample.

Oithona similis is also relatively abundant over diffuse vent sites at 20 mab, but is virtually absent in near-bottom samples (Figure 3.5b). *Paracalanus parvus* however, is relatively abundant in both 20 mab and near-bottom samples from diffuse vents. *P. parvus* represents <10% of the copepods captured at non-vent and smoker sites (Figure 3.5a and c). Miscellaneous calanoid copepodites, such as stages I-IV of *P. parvus, Spinocalanus* sp. and *Pseudocalanus* sp., are also relatively abundant in both 20 mab and near-bottom diffuse vent samples (Figure 3.5b). Although not highly abundant, *Corycaeus anglicus* is only found in diffuse vent 20 mab samples (Figure 3.5b). Benthic dirivultid species, such as *Stygiopontius quadrispinosus* and *Aphotopontius forcipatus*, each represent >20% of the copepods in near-bottom diffuse vent samples (Figure 3.5b).

Similar to non-vent samples, smoker samples are dominated by *Oithona similis* and *Oncaea* sp. (Figure 3.5c). *Pseudocalanus* sp. are more abundant in smoker samples than in any others. None of the dirivultid species are relatively abundant above smoker vents (Figure 3.5c). The harpacticoid, *Microsetella rosea*, is most abundant in smoker samples (Figure 3.5).

Based on the net tow data, rarefaction curves are calculated for each site type (Figure 3.6). At any given abundance, non-vent and smoker vent assemblages have a higher expected number of species than diffuse vent assemblages, 20 mab or near-bottom.

Distinct non-vent, diffuse vent and smoker vent assemblages are not evident from cluster analysis (Figure 3.7). Only the two near-bottom diffuse vent samples cluster together. Different site types from different regions appear to randomly cluster. This

Figure 3.5 Relative abundance of copepod species in a) non-vent, b) diffuse vent and c) smoker vent samples. Species that are most abundant and species that are unique to some areas are used. These species represent 86% (non-vent), 92.6% (diffuse vent 20 mab), 76.6% (diffuse vent near-bottom) and 84% (smoker vent) of the total number of copepod species collected from each site type. Misc. copepodites consist only of stage I-IV calanoid copepodites.

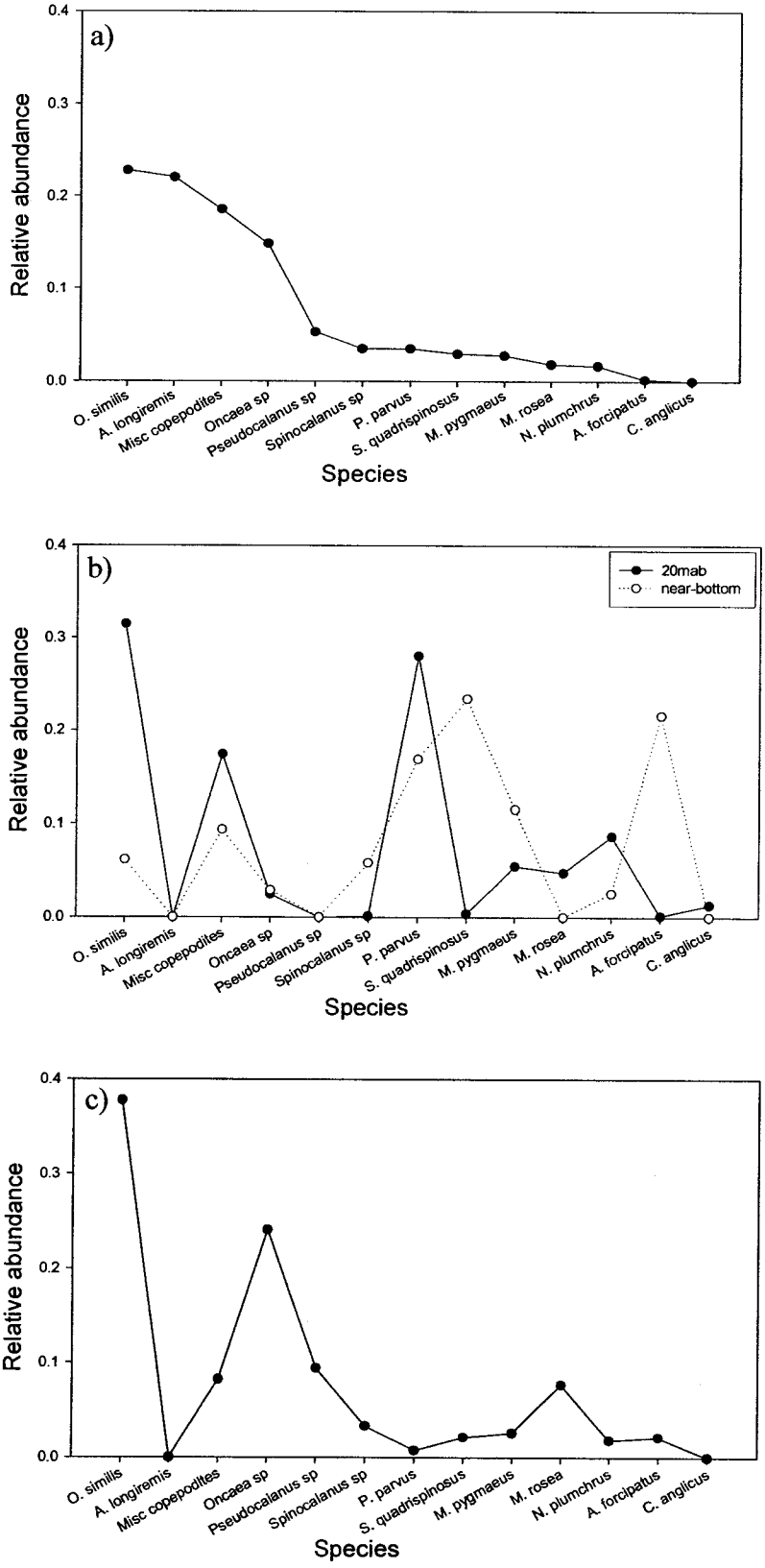
a)
b)
c)
Relative abundance
0.0
0.1
0.2
0.3
0.4
20mab
near-bottom
O. similis
A. longiremis
Misc copepodites
Oncaea sp
Pseudocalanus sp
Spinocalanus sp
P. parvus
S. quadrispinosus
M. pygmaeus
M. rosea
N. plumchrus
A. forcipatus
C. anglicus
Species

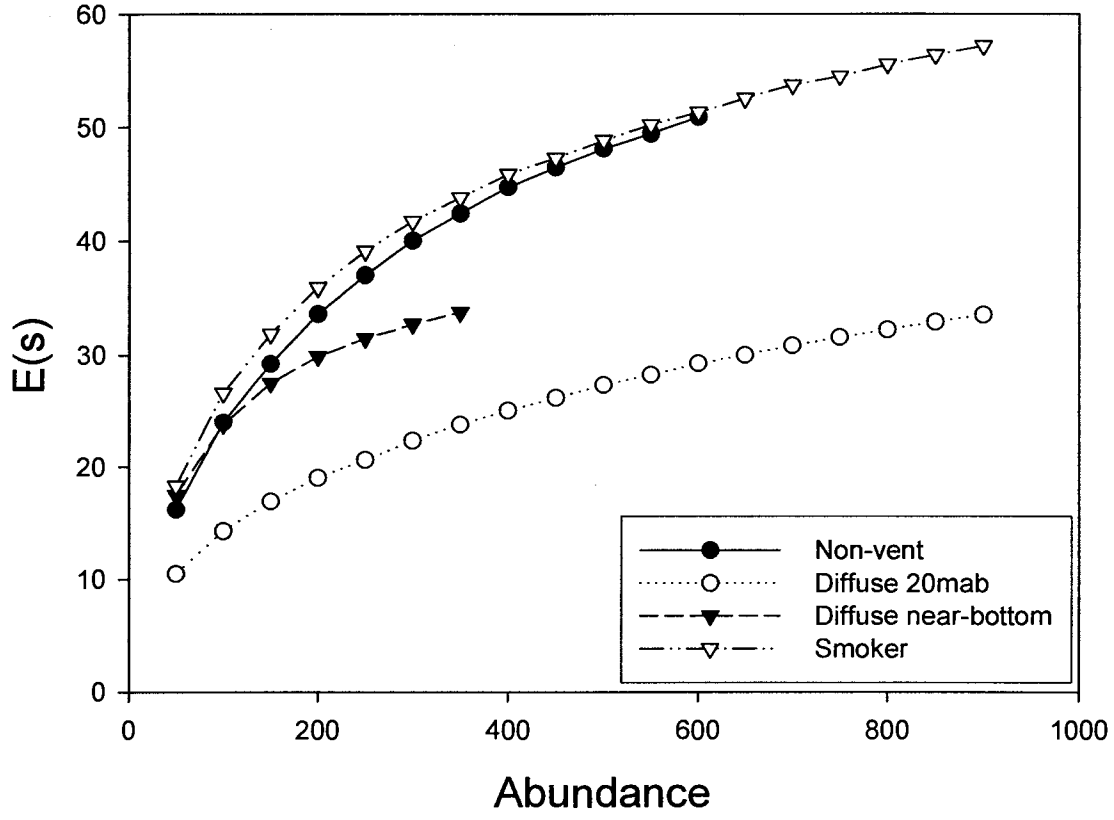

Figure 3.6 Rarefaction curves of three site types non-vent, diffuse vent and smoker vent. E(s) is the expected number of species in a sample of a given size.

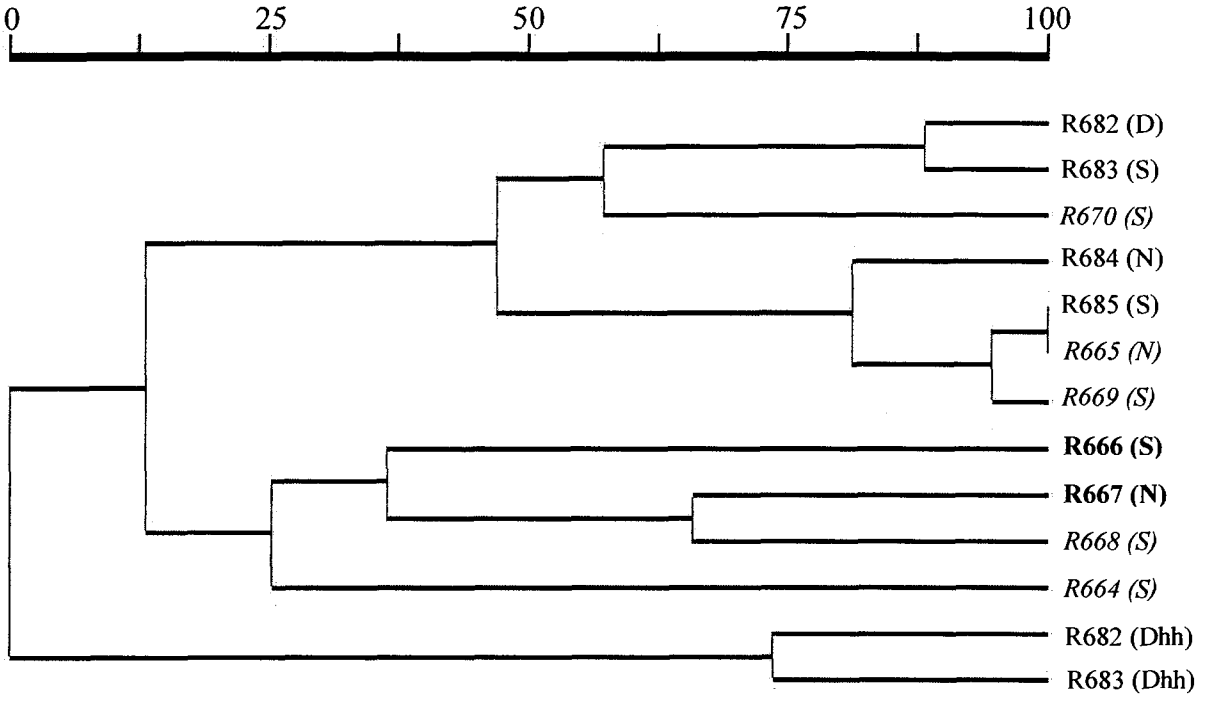

Figure 3.7 Cluster dendrogram of species presence/absence based on site type. With the exception of R684, two net samples are collected at each location and results are pooled. Percent similarity is indicated on axis above dendrogram. Site types are listed in parentheses after the dive number: non-vent (N), diffuse vent 20 mab (D), diffuse vent near-bottom (Dhh) and smoker vent (S). Endeavour, **Axial** and *Explorer* sites are indicated by font type.

lack of relationship is also seen when rare species, i.e. species that only occur in one or two samples, are removed.

3.4.3 Copepod assemblage characteristics

Copepod assemblages are predominantly female (Table 3.6). Over diffuse vent sites, dirivultids are >95% female. Over non-vent and smoker vent sites, *Stygiopontius quadrispinosus* males are slightly more abundant, although overall, *S. quadrispinosus* is less abundant at these site types (Table 3.6).

Like *Stygiopontius quadrispinosus*, the relative abundance of *Paracalanus parvus* females and males is different depending on site type (Table 3.6). Slightly more males are found in near-bottom diffuse vent samples while in all vent and non-vent 20 mab samples females are more abundant.

Two species, *Oithona similis* and *Corycaeus anglicus*, are dominated by males (Table 3.6). Because of relatively large sample sizes, I used the normal approximation to the binomial test ($n>25$) to determine if the proportion of females in male-dominated *O. similis* assemblages is significantly different from expected (i.e. proportion of each sex is 0.5) (Zar 1984). The proportion of *O. similis* females over non-vent areas, diffuse vents (20 mab) and smoker vents significantly differs from expected ($p<0.05$ at all three site types).

Gravid females are present in seven of the 23 samples. A total of 13 female dirivultids are gravid. Eight are found over diffuse vent sites (six *Stygiopontius quadrispinosus*, one *Aphotopontius forcipatus* and one *Benthoxynus spiculifer*) and five are found over smoker vent sites (all *S. quadrispinosus*). Gravid *Microsetella rosea*, a harpacticoid, are found in low abundance over all three site types. Gravid *Mormonilla sp.*, a bathypelagic calanoid, and *Oncaea ivlevi*, a poecilostomatoid, are found in low abundance over smoker vent sites.

For most copepod groups, adults are more abundant than juveniles (Table 3.7). Adult cyclopoids and harpacticoids are consistently more abundant over all site types. Adult dirivultids are most abundant in the water column above vents. Dirivultid copepodites, mostly *Stygiopontius quadrispinosus* and a few *Aphotopontius forcipatus*, are more abundant in non-vent samples (Table 3.7).

Table 3.6 Ratio of females to males for most abundant species. Species in which sexes appeared to be easy to differentiate are included. Total number of females and males of each species from each site type are listed. Adults that are poorly preserved or missing urosome segments are not included. Ratios less than zero (males are more abundant than females) are bolded.

	Non-vent			**Diffuse vent 20 mab**			**Diffuse vent near-bottom**			**Smoker vent**		
Species	female	male	ratio	female	male	ratio	female	male	ratio	female	male	ratio
Stygiopontius quadrispinosus	1	3	**0.3**	1	0	1:0	53	2	26.5	5	6	**0.8**
Aphotopontius forcipatus	2	0	2:0	0	0	-	56	3	18.7	12	0	12:0
Oithona similis	76	125	**0.6**	93	114	**0.82**	2	15	**0.13**	84	206	**0.4**
Oncaea sp.	28	29	**0.97**	10	4	2.5	3	2	1.5	70	50	1.4
Corycaeus anglicus	0	0	-	0	10	**0:10**	0	0	-	0	0	-
Microcalanus pygmaeus	14	4	3.5	20	15	1.3	10	4	2.5	12	8	1.5
Neocalanus cristatus	2	0	2:0	1	0	1:0	2	0	2:0	2	0	2:0
Neocalanus plumchrus	5	0	5:0	13	0	13:0	2	0	2:0	4	1	4
Paracalanus parvus	13	1	13	16	5	3.2	3	16	**0.19**	2	0	2:0
Pseudocalanus mimus	1	1	1	16	4	4	0	0	-	8	5	1.6
Pseudocalanus minutes	4	1	4	0	0	-	0	0	-	1	0	1:0
Pseudocalanus newmani	0	0	-	0	0	-	0	0	-	18	4	4.5
Spinocalanus sp.	7	6	1.2	0	0	-	6	2	3	19	6	3.2

Table 3.7 Ratios of juveniles to adults for groups of copepods. 'Cyclopoid' comprises both cyclopoids (e.g. *Oithona sp.*) and poecilostomatoids (e.g. *Oncaea sp.*). Copepodites in stages I-V are used as "juveniles". Ratios greater than zero (juveniles are more abundant than adults) are bolded.

	Non-vent			**Diffuse vent 20 mab**			**Diffuse vent near-bottom**			**Smoker vent**		
	juvenile	adult	ratio	juvenile	adult	ratio	juvenile	adult	ratio	juvenile	adult	ratio
Dirivultid	24	6	**4.8**	3	1	**3**	11	125	0.09	19	28	0.68
Harpacticoid	0	17	0:17	1	39	0.03	3	13	0.23	3	73	0.04
Cyclopoid	48	285	0.17	73	226	0.32	2	26	0.08	160	423	0.38
Calanoid	199	190	**1.05**	384	73	**5.26**	35	17	**2.06**	222	137	**1.62**
Overall	305	516	0.59	541	396	**1.37**	128	237	0.54	386	703	0.55

Interestingly, calanoid copepodites are consistently more abundant than adults at all sites (Table 3.7). In diffuse vent 20 mab samples, calanoid copepodites outnumber adults by 5 to 1.

Live copepods outnumber exoskeletons at all sites (Table 3.8). Some samples contained no copepod exoskeletons.

3.5 Discussion

3.5.1 Use of multiple sampling methods

At all sites, copepods are the most abundant organisms; this is evident from both video and net data. Nets are better at capturing small organisms not easily distinguished on video (e.g. copepodites) whereas video is better at capturing large organisms that are fragile (e.g. gelatinous zooplankton) or that easily avoid nets (e.g. fish and shrimp). Because the nets are mounted on the submersible, net dimensions are limited.

Mounting the nets on the submersible proves to be both good and bad. First, while the stiffening rods sewn around the outside of the net mouths allows the net mouth to be opened and closed remotely, this configuration prevents the net mouths from opening to their fullest extent (30 cm diameter; Figure 3.2). This may affect the filtering efficiency of the nets. Second, the sampling efficiency of the 180 μm net appears to differ depending on which side of the submersible it is mounted. The 180 μm net performed exceptionally well when mounted on the starboard side (R682). This suggests that flow around ROPOS is not symmetrical. Third, the nets are fully stretched by attaching the cod ends to a rod. This proves advantageous as it prevents the nets from drooping while the submersible changed direction or slowed. Overall, mounting nets on the submersible is a relatively effective method for collecting simultaneous samples of copepod assemblages.

The two mesh sizes produce different results. Overall, the 63 μm net appears to sample more efficiently; samples are usually larger and more speciose than those collected using the 180 μm net. It is possible that a positional or opening factor is the cause of the relatively poor performance of the 180 μm net. In general, the 180 μm net catches a larger proportion of large copepods (e.g. *Neocalanus* sp.) while the 63 μm net

Table 3.8 Ratios of exoskeletons to live copepods for different copepod groups. 'Cyclopoid' comprises both cyclopoids (e.g. *Oithona sp.*) and poecilostomatoids (e.g. *Oncaea sp.*).

	Non-vent			**Diffuse vent 20 mab**			**Diffuse vent near-bottom**			**Smoker vent**		
	exoskeleton	live	ratio	exoskeleton	live	ratio	exoskeleton	live	ratio	exoskeleton	live	ratio
Dirivultid	0	29	0:29	2	4	0.5	14	139	0.1	2	47	0.04
Harpacticoid	2	17	0.12	2	42	0.05	3	13	0.23	1	76	0.01
Cyclopoid	43	333	0.13	73	310	0.24	2	28	0.07	67	583	0.11
Calanoid	16	389	0.04	76	580	0.13	10	183	0.05	30	359	0.08
Overall	61	735	0.08	153	936	0.16	29	363	0.08	117	1093	0.11

catches a larger proportion of small copepods (e.g. cyclopoids, copepodites). Because relatively small mesh sizes are used, small copepods, like *Oithona* and *Oncaea*, were relatively well-sampled in comparison to most benthopelagic studies in which mesh sizes of >220 μm are typical (Marlowe and Miller 1975, Fulton 1983, Saltzman and Wishner 1997, Vinogradov 1997, Christiansen et al. 1999, Goldblatt et al. 1999, Vinogradov et al. 2003, Vinogradov et al. 2003). Combining samples from the two nets creates a more complete picture of assemblage composition than either net does alone.

Because only a limited number of samples can be taken during a dive, complementary methods of sampling pelagic organisms over vents are productive. Video is useful for capturing large pelagic organisms that are not caught in small nets. The 63 μm net tends to outperform the 180 μm net when mounted on the brow of the submersible. The smaller mesh net captures larger samples with more species, particularly small copepod species, such as *Oithona* and *Oncaea*, which are typically undersampled in most zooplankton studies. An additional net held in the submersible claw allows 1) simultaneously sampling of different heights above bottom and 2) near-bottom sampling (1-2 mab). Future studies of pelagic organisms over vents should therefore, employ multiple sampling methods.

3.5.2 Diversity and density comparisons

Diversity

Ocean Station Papa (Station P) is located northwest of the Juan de Fuca Ridge system at 50°N, 145°W (Marlowe and Miller 1975). A number of studies have looked at species composition and vertical distribution of copepods to depths of 500 m at Station P (Marlowe and Miller 1975, Fulton 1983, Miller et al. 1984, Miller and Clemons 1988, Goldblatt et al. 1999, Mackas and Tsuda 1999). How do assemblage composition and densities at the surface compare with that from vent and non-vent sites? Typically, *Neocalanus, Eucalanus, Metridia, Calanus, Pseudocalanus, Microcalanus* and *Oithona* account for 80-90% of the total number of copepods in the upper 150-250 m at Station P (Goldblatt et al. 1999). At vent and non-vent sites on the Juan de Fuca and Explorer Ridges, *Neocalanus, Pseudocalanus, Microcalanus* and *Oithona* account for almost 50%

of the total number of individuals; *Oithona similis* alone represents between 30-40% of copepods at these sites. Because no benthopelagic samples from Station P exist, I also compare my results with previous studies over vent, abyssal plain and continental shelf areas in the Pacific, Atlantic and Mediterranean (Table 3.9). As is typical of deep sea, copepod assemblages over vent and non-vent areas on the Juan de Fuca and Explorer Ridges are highly speciose; at least 72 copepod species are present (Table 3.5). Only Wishner (1980b) found higher numbers of copepod species (>100). Fewer species of pelagic organisms are found in near-bottom samples on continental shelves (Table 3.9).

Density

Over the first 500 m depth at Station P, densities in July and August range from 12-250 individuals/m^3 (Fulton 1983). Peak densities are found in June when *Neocalanus sp.* are dominant. While in my study, the highest copepod densities at diffuse vent sites (14.6 individuals/m^3) appear to fall within the lower end of the range at Station P, densities at smoker vent and non-vent sites are far below surface levels (0.7-3.5 individuals/m^3).

Similar vent and non-vent copepod densities are found over the East Pacific Rise and Guyamas Basin by Berg and Van Dover (Table 3.9). The exception is the 20 mab diffuse vent sample from Clam Bed where copepod density reaches 14.6 individuals/m^3. Whether this sample is anomalous or is indicative of assemblage size is unclear as only one pair of samples is collected at 20 mab over a diffuse vent. Maximum copepod densities at 20 mab over vent and non-vent areas in this study exceed densities typically found in the deep sea by a an order of magnitude (Table 3.9). This may suggest that pelagic food resources are more readily available in non-vent areas within the axial valley than in typical deep sea areas.

In general, near-bottom zooplankton densities are higher over continental shelves than abyssal plains or vent areas (Table 3.9). Greater availability of food resources in the form of sinking phytodetritus is often sited as a likely explanation for this trend (Angel 1990, Marcus and Boero 1998). In this study, copepod densities over both vent and non-vent areas fall within the ranges found by Wildish et al (1992) suggesting that copepods may be responding to elevated food resources within the axial valley. In short, vent-

Table 3.9 Comparison of near-bottom zooplankton densities from vent, deep sea and continental shelf sites. Copepod densities are listed for most studies, the exception is Chevrier et al (1991) in which amphipod densities are indicated. Total number of species are listed with number of copepod species, if known, in parentheses. Densities over vents are bolded. * indicates studies in which a Macer-GIROQ epibenthic sled, consisting of an upper and lower net, is used.

Study	Location		Depth (m)	MAB	Net size (mouth)	Mesh size	Volume (m^3)	#/m^3	Number of species
Vent									
Present study	Juan de Fuca	*Non-vent*	1500-2000	2-20	0.07m^2	63	27-109	0.8-2.9	97 (72)
		Vent		1-20		and	32-66	**0.7-14.6**	
						180			
	Explorer	*Non-vent*	1700	20			33-64	1.6-2.5	
		Vent		20			64	**1.2-3**	
Berg and Van Dover (1987)	East Pacific Rise	*Non-vent*	2560-2600	1-23	0.4m^2	183	25-101	0.5-2.2	Not given ('extraordinary' diversity of copepods is noted)
		Vent					4.7-76	**0.8-5.5**	
	Guyamas Basin	*Non-vent*	2000	1-5			69.5	0.5	
		Vent					61-80	**1.5-6.7**	
Wiebe et al. (1988)	Guyamas Basin		2000	100-200	1m^2	183	464-710	2.7	(67)
Deep sea plains									
Wishner (1980b)	San Diego Trough		1100-1200	10-100	0.15m^2	183	350-1480	1.1-1.9	(>100)
	Ecuador Trench (Pacific)		2400-3000	10-100					
Christiansen et al. (1999)	West European Basin (Atlantic)		4500	0-100	1m^2	333	1800 per net	0.4	(17 copepod families)
Continental shelf									
Chevrier et al. (1991)*	Bay of Fundy (Atlantic)		119	0.33-0.73	2m^2	500	5048 (lower net)	419.97 (lower net)	48 (lower net)
				1-1.5			4795 (upper net)	29.55 (upper net)	33 (upper net)

Table 3.9 continued.

Study	Location	Depth (m)	MAB	Net size (mouth)	Mesh size	Volume (m^3)	#/m^3	Number of species
Continental shelf continued								
Wildish et al. (1992)*	Browns Bank (NW Atlantic)	64-240	0.33-0.73 1-1.5	$2m^2$	500	111-444	0-34.6 (lower net) 1.41-16.9 (upper net)	126
Cartes (1998)*	La Merenguera Canyon (NW Mediterranean)	1125-1355	0.1-1.5	$2m^2$	500	742-1381	6	Not given

derived resources may be available to pelagic organisms not only above vents, but also above non-vent areas within a couple of kilometres of the vent source.

3.5.4 Assemblage characteristics

Diversity

This study could not distinguish among non-vent, diffuse vent and smoker vent assemblage composition (Figure 3.6). Although copepod assemblages over vent and non-vent areas on the Juan de Fuca and Explorer Ridges are highly diverse, of the 72 species found, one-third are common to all 20 mab samples (Figure 3.8). One species, *Oithona similis*, dominates all 20 mab assemblages (Table 3.10). A total of 30 species are unique to only one site type (Figure 3.8). Most occur in small numbers in one sample. The exception is *Acartia longiremis*; 120 specimens are found in one non-vent sample from Explorer. Composition of non-vent and smoker assemblages appears to be relatively similar; four of the five most abundant copepod species over non-vent sites are also abundant over smoker sites (Table 3.10). In total, 17 copepod species are common to both non-vent and smoker vent assemblages (Figure 3.8). This may suggest that while smoker vent samples are collected while passing through buoyant effluent, little lateral spreading of rising smoker effluent occurs and conditions above smoker vents may not be as toxic as initially thought.

No specialized fauna appear to live within the benthic boundary layer at vent and non-vent areas on the Juan de Fuca and Explorer Ridges. Fauna from both benthic and pelagic realms are found within 20 m of the bottom.

Epipelagic species

Oithona similis is the most abundant species over most site types: Why is *O. similis* so dominant?

Cyclopoids and poecilostomatoids are typically undersampled in zooplankton studies (Paffenhofer 1993, Bottger-Schnack 1995, Fransz and Gonzalez 1995, Nielsen and Sabatini 1996, Saltzman and Wishner 1997). *Oithona similis* is usually considered to be an epipelagic dominant (0-50 m), often replaced by *Oncaea* sp. in the meso- and bathypelagic zones of the NW Pacific (Yamaguchi et al. 2002). However, Saltzman and

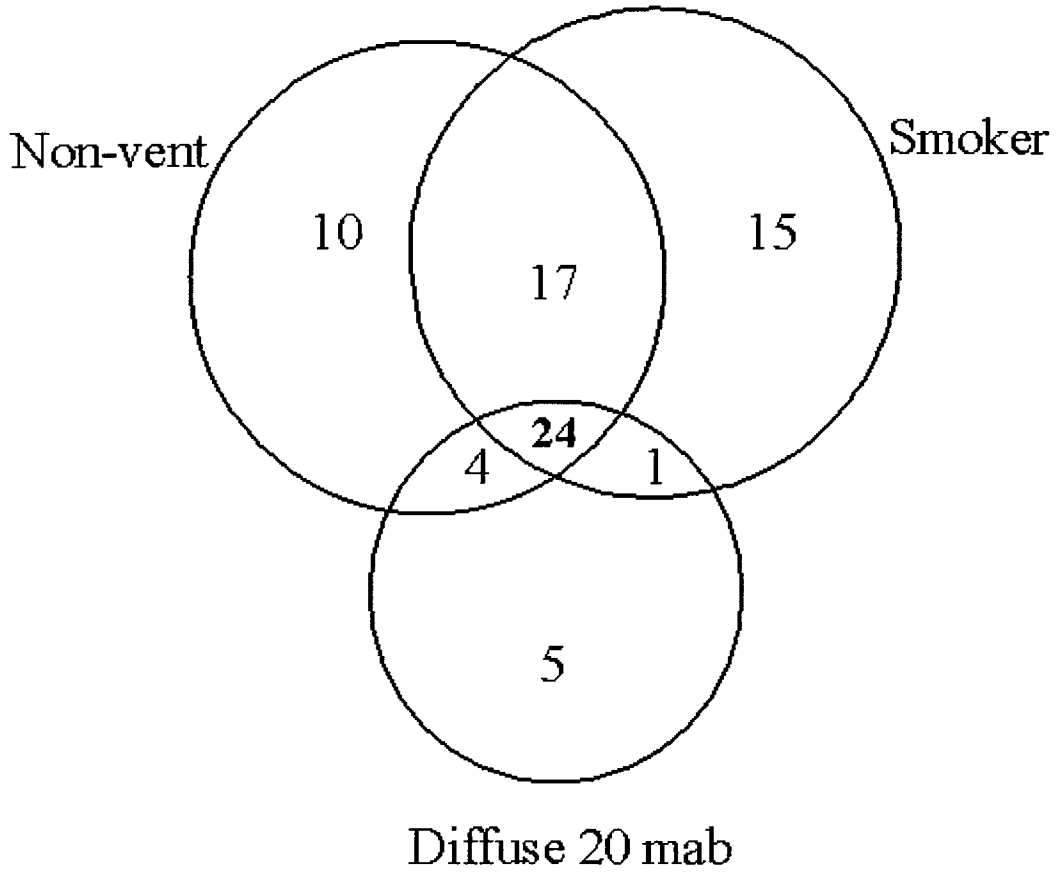

Figure 3.8 Venn diagram illustrating overlap in copepod species composition among non-vent, diffuse vent (20 mab only) and smoker vent sites. Size of circles is representative of total number of species found at each site type; smoker vent samples have the most species (57), followed by non-vent samples (55) and diffuse vent samples (34). Most species are shared among the different site types (24). In addition, non-vent and smoker vent samples share 17 species in common whereas non-vent and diffuse vent samples share four species and smoker vent and diffuse vent samples only share one species in common. Smoker vent samples have the highest number of unique species (15), followed by non-vent samples (10) and diffuse vent samples (5).

Table 3.10 Similarities and differences among non-vent, diffuse vent and smoker vent copepod assemblages. Diversity refers to total number of copepod species. Miscellaneous (misc.) copepodites are stage I-IV calanoid copepodites.

	Non-vent	**Diffuse vent (20mab)**	**Diffuse vent (near-bottom)**	**Smoker vent**
Diversity	55	34	34	57
Density (ind/m^3)	0.8-2.9	14.6	3.8-7.3	0.7-3.5
Most abundant species (represent >6% of total number of copepods)	*Oithona similis* *Acartia longiremis* Misc. copepodites *Oncaea sp.* *Pseudocalanus sp.*	*Oithona similis* *Paracalanus parvus* Misc. copepodites *Neocalanus plumchrus* *Microcalanus pygmeaus*	*Stygiopontius quadrispinosus* *Aphotopontius forcipatus* *Paracalanus parvus* *Microcalanus pygmaeus* Misc. copepodites	*Oithona similis* *Oncaea sp.* *Pseudocalanus sp.* Misc. copepodites *Microsetella rosea*
Sex ratio (F:M)	1.1	1.2	3.3	0.8
Development stage (Adult:Copepodite)	0.6	1.4	0.5	0.5

Wishner (1997) found *Oithona* sp. and *Oncaea* sp. to be abundant not only in the epipelagic, but also at the base of the oxygen minimum zone at depths of 600-1000 m. *O. similis* may be relatively abundant in most habitats, including deep sea, but because sampling net mesh sizes are often large (>220 μm), *O. similis* appears to be absent from or relatively rare in most samples (Paffenhofer 1993).

Oithona similis is tolerant of large temperature ranges; this species is abundant in polar (Coyle et al. 1990, Fransz and Gonzalez 1995) and in subtropical waters (Morgan et al. 2003). *Oithona* sp. also appear to be tolerant of low oxygen conditions (Saltzman and Wishner 1997). Tolerance of wide temperature ranges and low oxygen conditions may, in part, explain why they are the most abundant group. *O. similis* is often thought to be associated with microbial-based production, providing a trophic link between bacteria and higher pelagic organisms (Fransz and Gonzalez 1995, Nielsen and Sabatini 1996, Nakamura and Turner 1997). This suggests that *O. similis* may not only be able to tolerate extreme conditions at vents, but that it may also be able to feed on the enhanced concentrations of microbes associated with hydrothermal effluent.

Mesopelagic species

In this study, adults and diapausing copepodite stage Vs (CV) of all three species are found. CVs of *Neocalanus plumchrus, N. cristatus* and *Eucalanus bungii* enter a diapausing or overwintering stage by the onset of summer in the NE Pacific (Miller et al. 1984, Miller and Clemons 1988, Coyle et al. 1990). Typically, diapausing *N. cristatus* and *N. plumchrus* are found below 250 m and *E. bungii* are principally found between 250-500 m (Miller et al. 1984, Miller and Clemons 1988). In benthopelagic studies, the role of sinking phytodetrital material as a deep sea food resource is emphasized. The presence of CV and adult *Neocalanus* sp. and *E. bungii* above vents may suggest that surface production is transported to the deep sea in the form of diapausing copepods.

Bathypelagic species

Species, such as *Mormonilla sp.* and *Spinocalanus sp.*, are typically found in the deep sea (Saltzman and Wishner 1997, Auel and Hagen 2002, Yamaguchi et al. 2002) and are present in the majority of vent and non-vent samples. Gowing and Wishner

(1992) find bacteria in the guts of *Spinocalanus* sp. above a seamount in the Pacific. This suggests that *Spinocalanus*, at the very least, may be able to feed on microbes associated with vent effluent. If so, deep sea copepod species, in addition to species like *Oithona similis*, may play a role in the transport vent productivity into deep sea.

Amphibenthopelagic

Vereshchaka (1995) describes the distribution of decapods over seamounts and continental slopes. Based on the habits of different species, Vereshchaka groups species according to their distribution, behaviour and feeding. Amphibenthopelagic species periodically live in all three biotopes: pelagic, benthopelagic and benthic. The harpacticoid, *Microsetella rosea,* may fit into this category. *M. rosea* is typically described as a pelagic species (Rose 1933) and is found in surface samples in the NE Pacific (Marlowe and Miller 1975). In my study, *M. rosea* is abundant in the 63 μm net samples from all three site types. Hundreds or even thousands of *M. rosea* individuals are often found in benthic samples from Endeavour (V. Tunnicliffe, pers. comm.). This suggests that *M. rosea* is highly tolerant of the vent environment and may be able to feed on resources produced at the vents (e.g. detritus, bacteria). *M. rosea*, like the bathypelagic species, may play a role in carbon transfer from vents to the deep sea.

Hypobenthopelagic

Hypobenthopelagic species (Vereshchaka 1995) are primarily benthic, but spend part of their life cycle in the water column near the seafloor. Dirivultids appear to fit into this category.

In the NE Pacific, dirivultids are typically found as free-living adults at vents (Tsurumi et al. 2003). In this study, adult dirivultids are also found in large numbers a couple of metres above diffuse vents. The presence of early stage copepodites, likely stage II or III, particularly over non-vent areas confirms a suspected deep sea phase (Ivanenko 1998) to the dirivultid life cycle.

Density

Diffuse vent 20 mab assemblages have the highest copepod densities (Table 3.10). Diffuse vents typically have higher benthic biomass than smoker vents or non-vent sites (Van Dover 2000, Giere et al. 2003). Free-living chemosynthetic bacteria suspended within the vent effluent support thriving populations of benthic organisms (Van Dover and Fry 1994). Toxic conditions at the orifice of black smokers and lack of substratum surface area may limit numbers of individuals on smoker vents (Giere et al. 2003). In non-vent areas, benthos is primarily limited by lack of food resources (Tyler 1995). Copepods, like benthic organisms, may be more tolerant of conditions over diffuse vents, particularly at 20 mab, than conditions over smoker vents. Copepods, such as *Oithona similis, Spinocalanus* sp. as well as various copepodites, may be able to feed on chemosynthetic microbial production associated with the vent effluent (Gowing and Wishner 1992, Fransz and Gonzalez 1995, Nielsen and Sabatini 1996, Nagata et al. 2000, Finlay and Roff 2003).

Benthopelagic zooplankton density increases with proximity to the seafloor (Chevrier et al. 1991, Wildish et al. 1992, Vereshchaka 1995), but in this study, copepod density is lower in near-bottom diffuse vent samples than in 20 mab samples (Table 3.10). Pelagic copepods over diffuse vents may avoid the seafloor because of variable chemical and physical conditions (e.g. increased turbulence associated with venting, anoxic conditions, relatively rapid temperature gradients). Vertically and horizontally spreading effluent transports chemosynthetic bacteria away from the vent source (Cowen and German 2003). Thus vent-derived resources are potentially available to pelagic organisms tens of metres above the seafloor. Species such as *Oithona similis* and *Spinocalanus sp.* that may be able to feed on chemosynthetic bacteria likely do not need to be as closely associated with the vent source as do benthic organisms. Thus relatively tolerable environmental conditions and enhanced food resources associated with venting may explain why copepods are more abundant at 20 mab over diffuse vents than at 20 mab over non-vent areas and smoker vents, respectively.

Sex ratios

One distinguishing feature of most benthopelagic assemblages is the predominance of female copepods (Wishner 1980b, Christiansen et al. 1999). In this study, non-vent and diffuse vent samples are also female-dominated (Table 3.10). The exception occurs over smoker vents where males are more abundant (Table 3.10) although this is likely due to the abundance of *Oithona similis* in smoker vent samples. In all samples, males of some cyclopoid species (e.g. *O. similis, Corycaeus anglicus* and *Oncaea ivlei*) are consistently more abundant than females. Male-dominated assemblages are not uncommon in the field (M. Voordouw, pers. comm.). Sex ratios may be biased by differential mortality (Vacquier 1961) or because females and males congregate in different areas of a habitat (M. Voordouw, pers. comm.).

Development stage

As in previous benthopelagic studies (Wishner 1980b, Christiansen et al. 1999), calanoid copepodites in this study are more abundant than adults in all samples (Table 3.7). At 20 mab over diffuse vent sites, *Neocalanus plumchrus* is one of the most abundant species (Table 3.10). Of the 82 *N. plumchrus* in these samples, over half are stage II or stage III copepodites. Finding CIIs and CIIIs in samples in July and August is unusual (D. Mackas, pers. comm.). One possibility is that conditions at vents may induce CVs to break diapause, molt, mate and reproduce in early summer resulting in a second annual cohort at depth (D. Mackas, pers. comm.). Typically, *N. plumchrus* adults reproduce below depths of 250 m in early spring (Miller et al. 1984). Newly hatched nauplii migrate from these depths to the surface waters to feed (Miller et al. 1984, Miller and Clemons 1988). Nauplii develop into copepodites and pass through copepodite stages I-IV at the surface (Miller et al. 1984). Stage Vs develop at the surface and then migrate to depth during the early summer where they enter into diapause (Miller et al. 1984). CVs develop into adults in early spring and reproduce at depth.

However, early emergence from diapause is not uncommon. Miller (1984) reported that some diapause breaking and spawning occurs at depth throughout the summer and fall although he did not report any juveniles, likely because the mesh size of the nets was too large (333 μm) to adequately sample small populations of copepodites.

Temperature and chemical cues are thought to induce emergence from diapause (Dahms 1995). Slight increases in temperature and relatively high levels of sulphide (or low oxygen) associated with vent effluent may induce diapausing copepods to emerge and reproduce. Thus breaking of diapause and spawning at depth in response to vent effluent may explain the presence of early copepodite stages of *Neocalanus plumchrus* in vent samples.

In contrast to calanoids, cyclopoid and harpacticoids adults are consistently more abundant than copepodites (Table 3.7). It is unclear whether this is typical of cyclopoid and harpacticoid benthopelagic assemblages as most studies use larger mesh nets and thus undersample these species (Paffenhofer 1993, Bottger-Schnack 1995). Because the copepodites of the cyclopoid and harpacticoid species found in this study are so small (e.g. on the order of 0.1-0.3 mm), they may be too small to be effectively sampled. However, dirivultid copepodites, which are roughly the same size as many cyclopoid copepodites, are abundant in some samples, suggesting that low capture efficiency may not be the only explanation for low copepodite abundance. Species such as *Oithona similis* and some *Oncaea sp.* can reproduce year-round (Fransz and Gonzalez 1995, Nielsen and Sabatini 1996) resulting in mixing of age classes. Thus copepodites may not constitute a large percentage of cyclopoid and harpacticoid populations. In short, the presence of more adults cyclopoids and harpacticoids may be typical.

Dirivultid copepodites are thought to develop in the water column as few copepodites are found in bottom samples (Ivanenko 1998). In this study, a total of 57 dirivultid copepodites and 13 gravid dirivultid females are found above vents. This lends further support to the hypothesis that copepodites hatch and develop in the water column. Interestingly, the highest number of dirivultid copepodites is found over non-vent areas. This supports the hypothesis that copepodites are transferred between vent fields as copepodites rather than as adults.

Exoskeletons

In previous deep sea benthopelagic studies, copepod exoskeletons outnumber live copepods by a factor of two to six (Wishner 1980b, Christiansen et al. 1999). However, sampling 100 m above vents in the Guyamas Basin, Wiebe et al (1988) found copepod

exoskeletons represented only 31 and 10% of the live copepods captured in two samples. In this study, exoskeletons represented 8-14% of the total copepod catch. Harding (1973) found that decomposition of exoskeletons increases at elevated temperatures. Because water temperature at 20 mab over vents is typically elevated by only 0.1-0.2°C (Chapter 2) temperature likely does not play much of a role in exoskeleton decomposition above vents. Böttger-Schnack (1990) and Christiansen et al (1999) suggest differences in species mortality and in growth rates may be responsible for variable proportions of exoskeletons. At this point, it is unclear why copepod exoskeletons are relatively rare in the water column above vent and non-vent areas within the axial valleys.

3.6 Conclusions

1. Video is better than nets at capturing large pelagic organisms, such as gelatinous zooplankton and nekton.
2. Small mesh nets capture relatively large numbers of small copepods (e.g. cyclopoids, poecilostomatoids and harpacticoids) suggesting these groups may be more deeply distributed than typically thought.
3. Mounted 63 μm net captures larger and more diverse samples than the 180 μm net although net position on the submersible may influence filter efficiency.
4. Copepod assemblage composition above non-vent, diffuse vent and smoker vent sites is not distinct. Copepods are most abundant over diffuse vents, but are generally more speciose over non-vent areas and smoker vents.
5. Vent and non-vent copepod assemblages on the Juan de Fuca and Explorer Ridges are highly diverse (72 species). One third of the species are common to non-vent, diffuse vent and smoker vent 20 mab samples. A total of 30 species are unique to one site type.
6. Comparisons with previous studies show that copepods are enhanced over vent fields, especially at 20 mab over diffuse vents. Densities over non-vent areas within the axial valley are also slightly higher than those over abyssal plains, suggesting that there is an overall increase in copepod abundance over and near vent sites.

7. All 20 mab assemblages are dominated by *Oithona similis*. In near-bottom diffuse vent samples, *O. similis* is replaced by the dirivultids, *Stygiopontius quadrispinosus* and *Aphotopontius forcipatus*. Most adult pelagic copepod species are less abundant in near-bottom samples.
8. Calanoid species in vent and non-vent samples are predominantly female. Other species, primarily cyclopoid, are sometimes male-dominated. *Oithona similis* males are more abundant than females at all sites.
9. Copepodites are not consistently more abundant than adults. Cyclopoid and harpacticoid adults are more abundant than copepodites. Calanoid copepodites are more abundant than adults at all sites. At 20 mab over diffuse vents, *Neocalanus plumchrus* copepodites are relatively abundant. Dirivultid copepodites are relatively abundant in non-vent samples.
10. In contrast to many previous benthopelagic studies, few exoskeletons are found over vent and non-vent sites.

This study highlights the importance of complementary sampling methods and the use of small mesh nets in characterizing benthopelagic assemblages. Small cyclopoid and poecilostomatoid copepods, which are usually under-sampled in conventional net tows, are abundant. Copepod abundance is enhanced over vent fields, especially 20 mab over diffuse vents, suggesting that pelagic copepods present in the deep sea may be attracted to and capable of utilizing vent-derived resources.

3.7 References

Angel, M. V. 1990. Life in the benthic boundary layer: connections to the mid-water and sea floor. Philosophical Transactions of the Royal Society of London A **331**: 15-28.

Auel, H. and Hagen, W. 2002. Mesozooplankton community structure, abundance and biomass in the central Arctic Ocean. Marine Biology **140**: 1013-1021.

Baker, E. T., McDuff, R. E. and Massoth, G. J. 1990. Hydrothermal venting from the summit of a ridge axis seamount: Axial Volcano, Juan de Fuca Ridge. Journal of Geophysical Research **95**: 12,843-12,854.

Berg, C. J. J. and Van Dover, C. L. 1987. Benthopelagic macrozooplankton communities at and near deep-sea hydrothermal vents in the eastern Pacific Ocean and the Gulf of California. Deep-Sea Research **34**: 379-401.

Bottger-Schnack, R. 1995. Summer distribution of micro- and small meso-zooplankton in the Red Sea and Gulf of Aden, with special reference to non-calanoid copepods. Marine Ecology Progress Series **118**: 81-102.

Böttger-Schnack, R. 1990. Community structure and vertical distribution of cyclopoid copepods in the Red Sea, I. Central Red Sea, autumn 1980. Marine Biology **106**: 473-485.

Brodskii, K. A. 1967. Calanoida of the Far Eastern Seas and Polar Basin of the USSR. Israel Program for Scientific Translation Ltd.

Burd, B. J. and Thomson, R. E. 1994. Hydrothermal venting at Endeavour Ridge: Effect on zooplankton biomass throughout the water column. Deep-Sea Research I **41**: 1407-1423.

Burd, B. J. and Thomson, R. E. 1995. Distribution of zooplankton associated with the Endeavour Ridge hydrothermal plume. Journal of Plankton Research **17**: 965-997.

Burd, B. J. and Thomson, R. E. 2000. Distribution and relative importance of jellyfish in a region of hydrothermal venting. Deep-Sea Research I **47**: 1703-1721.

Burd, B. J., Thomson, R. E. and Calvert, S. E. 2002. Isotopic composition of hydrothermal epiplume zooplankton: evidence of enhanced carbon recycling in the water column. Deep-Sea Research I **49**: 1877-1900.

Burd, B. J., Thomson, R. E. and Jamieson, G. S. 1992. Composition of a deep scattering layer overlying a mid-ocean ridge hydrothermal plume. Marine Biology **113**: 517-526.

Cartes, J. E. 1998. Dynamics of the bathyal benthic boundary layer in the northwestern Mediterranean: depth and temporal variations in macrofaunal-megafaunal communities and their possible connections within deep-sea trophic webs. Progress in Oceanography **41**: 111-139.

Chevrier, A., Brunel, P. and Wildish, D. J. 1991. Structure of a suprabenthic shelf sub-community of gammaridean Amphipoda in the Bay of Fundy compared with similar sub-communities in the Gulf of St. Lawrence. Hydrobiologia **223**: 81-104.

Christiansen, B., Druke, B., Koppelmann, R. and Weikert, H. 1999. The near-bottom zooplankton at the abyssal BIOTRANS site, northeast Atlantic: composition, abundance and variability. Journal of Plankton Research **21**: 1847-1863.

Cowen, J. P., Bertram, M. A., Wakeham, S. G., Thomson, R. E., Lavelle, J. W., Baker, E. T. and Feely, R. A. 2001. Ascending and descending particle flux from hydrothermal plumes at Endeavour Segment, Juan de Fuca Ridge. Deep-Sea Research I **48**: 1093-1120.

Cowen, J. P. and German, C. 2003. Biogeochemical cycling in hydrothermal plumes. In: Halbach, P. E., Tunnicliffe, V. and Hein, J. R. (eds.), Energy and mass transfer in marine hydrothermal systems. Dahlem University Press, pp. 303-316.

Cowen, J. P., Massoth, G. J. and Feely, R. A. 1990. Scavenging rates of dissolved manganese in a hydrothermal vent plume. Deep-Sea Research **37**: 1619-1637.

Coyle, K. O., Paul, A. J. and Ziemann, D. A. 1990. Copepod populations during the spring bloom in Alaskan subarctic embayment. Journal of Plankton Research **12**: 759-797.

Dahms, H.-U. 1995. Dormancy in the Copepoda - an overview. Hydrobiologia **306**: 199-211.

Delaney, J. R., Kelley, D. S., Lilley, M. D., Butterfield, D. A., McDuff, R. E., Baross, J. A., Deming, J. W., Johnson, H. P. and Robigou, V. 1997. The Endeavour hydrothermal system I: Cellular circulation above an active cracking front yiedls large sulfide structures, "fresh" vent water and hyperthermophilic Archaea. RIDGE Events **July**: 11-20.

Delaney, J. R., Robigou, V. and McDuff, R. E. 1992. Geology of a vigorous hydrothermal system on the Endeavour Segment, Juan de Fuca Ridge. Journal of Geophysical Research **97**: 19,663-619,682.

Embley, R. W. 2002. Ring of Fire. http://oceanexplorer.noaa.gov/explorations/02fire/logs/yr_sum/yr_sum.html

Feely, R. A., Geiselmand, T. L., Baker, E. T. and Massoth, G. J. 1990. Distribution and composition of hydrothermal plumes particles from the ASHES vent field at Axial Volcano, Juan de Fuca Ridge. Journal of Geophysical Research **95**: 12,855-12,873.

Finlay, K. and Roff, J. 2003. Ontogenic changes in diet of coastal marine copepods. 3rd International Zooplankton Production Symposium.

Fransz, H. G. and Gonzalez, S. R. 1995. The production of Oithona similis (Copepoda: Cyclopoida) in the Southern Ocean. ICES Journal of Marine Science **52**: 549-555.

Fulton, J. 1983. Seasonal and annual variations of net zooplankton at Ocean Station "P", 1956-1980. Department of Fisheries and Oceans, p. 65.

Giere, O., Borowski, C. and Prieur, D. 2003. Biological productivity in hydrothermal systems. In: Halbach, P. E., Tunnicliffe, V. and Hein, J. R. (eds.), Energy and mass transfer in marine hydrothermal systems. Dahlem University Press, pp. 211-234.

Gili, J. M., Pages, F., Bouillon, J., Palanques, A., Puig, P., Heussner, S., Calafat, A., Canals, M. and Monaco, A. 2000. A multidisciplinary approach to the understanding of hydromedusan populations inhabiting Mediterranean submarine canyons. Deep-Sea Research I **47**: 1513-1533.

Goldblatt, R. H., Mackas, D. L. and Lewis, A. G. 1999. Mesozooplankton community characteristics in the NE subarctic Pacific. Deep-Sea Research II **46**: 2619-2644.

Gowing, M. M. and Wishner, K. F. 1992. Feeding ecology of benthopelagic zooplankton on an eastern tropical Pacific seamount. Marine Biology **112**: 451-467.

Harding, G. C. H. 1973. Decomposition of marine copepods. Limnology and Oceanography **18**: 670-673.

Heron, G. A. and Frost, B. W. 2000. Copepods of the family Oncaeidae (Crustacea: Poecilostomatoida) in the northeast Pacific Ocean and inland coastal waters of Washington State. Proceedings of the Biological Society of Washington **113**: 1015-1063.

Ivanenko, V. N. 1998. Deep-sea hydrothermal vent Copepoda (Siphonostomatoida, Dirivultidae) in plankton over the Mid-Atlantic Ridge (29°N), morphology of their first copepodid stage. Zoologichesky Zhurnal **77**: 1249-1256.

Jannasch, H. W. and Mottl, M. J. 1985. Geomicrobiology of deep-sea hydrothermal vents. Science **229**: 717-725.

Johnson, H. P. and Embley, R. W. 1990. Axial Seamount: An active ridge axis volcano on the central Juan de Fuca Ridge. Journal of Geophysical Research **95**: 12,689-12,696.

Kaartvedt, S., Van Dover, C. L., Mullineaux, L. S., Wiebe, P. H. and Bollens, S. M. 1994. Amphipods on a deep-sea hydrothermal treadmill. Deep-Sea Research I **41**: 179-195.

Klinkhammer, G. and Hudson, A. 1986. Dispersal patterns for hydrothermal plumes in the South Pacific using manganese as a tracer. Earth and Planetary Science Letters **79**: 241-249.

Lilley, M. D., Feely, R. A. and Trefry, J. H. 1995. Chemical and biochemical transformations in hydrothermal plumes. In: Humphris, S. E., Zierenberg, R. A., Mullineaux, L. S. and Thomson, R. E. (eds.), Seafloor hydrothermal systems: Physical, chemical, biological and geological interactions. American Geophysical Union, pp. 369-291.

Mackas, D. L. and Tsuda, A. 1999. Mesozooplankton in the eastern and western subarctic Pacific: community structure, seasonal life histories and interannual variability. Progress in Oceanography **43**: 335-363.

Marcus, N. and Boero, F. 1998. Minireview: The importance of benthic-pelagic coupling and the forgotten role of life cycles in coastal aquatic systems. Limnology and Oceanography **43**: 763-768.

Marlowe, C. J. and Miller, C. B. 1975. Patterns of vertical distribution and migration of zooplankton at Ocean Station "P". Limnology and Oceanography **20**: 824-844.

Mauchline, J. 1998. The biology of Calanoid copepods. Academic Press.

McCollom, T. M. 2000. Geochemical constraints on primary productivity in submarine hydrothermal vent plumes. Deep-Sea Research I **47**: 85-101.

Miller, C. B. and Clemons, M. J. 1988. Revised life history analysis for large grazing copepods in the subarctic Pacific Ocean. Progress in Oceanography **20**: 293-313.

Miller, C. B., Frost, B. W., Batchelder, H. P., Clemons, M. J. and Conway, R. E. 1984. Life histories of large, grazing copepods in a subarctic ocean gyre: *Neocalanus plumchrus, Neocalanus cristatus* and *Eucalanus bungii* in the Northeast Pacific. Progress in Oceanography **13**: 201-243.

Milligan, B. N. and Tunnicliffe, V. 1994. Vent and nonvent faunas of Cleft segment, Juan de Fuca Ridge, and their relations to lava age. Journal of Geophysical Research **99**: 4777-4786.

Morgan, C. A., Peterson, W. T. and Emmett, R. L. 2003. Onshore-offshore variations in copepod community structure off the Oregon coast during the summer upwelling season. Marine Ecology Progress Series **249**: 223-236.

Nagata, T., Fukuda, H., Fukuda, R. and Koike, I. 2000. Bacterioplankton distribution and production in deep Pacific waters: Large-scale geographic variations and possible coupling with sinking particle fluxes. Limnology and Oceanography **45**: 426-435.

Nakamura, Y. and Turner, J. T. 1997. Predation and respiration by the small cyclopoid copepod *Oithona similis*: How important is feeding on ciliates and heterotrophic flagellates? Journal of Plankton Research **19**: 1275-1288.

Nielsen, T. G. and Sabatini, M. 1996. Role of cyclopoid copepods *Oithona* spp. in North Sea plankton communities. Marine Ecology Progress Series **139**: 79-93.

Paffenhofer, G.-A. 1993. On the ecology of marine cyclopoid copepods (Crustacea, Copepoda). Journal of Plankton Research **15**: 37-55.

Raffaelli, D., Bell, E., Weithoff, G., Matsumoto, A., Cruz-Motta, J. J., Kershaw, P., Parker, R., Parry, D. and Jones, M. 2003. The ups and downs of benthic ecology: considerations of scale, heterogeneity and surveillance for benthic-pelagic coupling. Journal of Experimental Marine Biology and Ecology **285-286**: 191-203.

Rose, M. 1933. Faune de France: Copépdes Pélagiques. Fédération Française des Sociétés de Sciences Naturelles.

Roth, S. E. and Dymond, J. 1989. Transport and settling of organic material in a deep-sea hydrothermal plume: Evidence from particle flux measurements. Deep-Sea Research **36**: 1237-1254.

Saltzman, J. and Wishner, K. F. 1997. Zooplankton ecology in the eastern tropical Pacific oxygen minimum zone above a seamount: 2. Vertical distribution of copepods. Deep-Sea Research I **44**: 931-954.

Smith, K. L. J. 1985. Macrozooplankton of a deep sea hydrothermal vent: In situ rates of oxygen consumption. Limnology and Oceanography **30**: 102-110.

Thomson, R. E., Mihaly, S. F., Rabinovich, A. B., McDuff, R. E., Veirs, S. R. and Stahr, F. R. 2003. Constrained circulation at Endeavour ridge facilitates colonization by vent larvae. Nature **424**: 545-549.

Thomson, R. E., Roth, S. E. and Dymond, J. 1990. Near-intertial motions over a mid-ocean ridge: Effects of topography and hydrothermal plumes. Journal of Geophysical Research **95**: 7261-7278.

Trivett, D. A. 1994. Effluent from diffuse hydrothermal venting. 1. A simple model of plumes from diffuse hydrothermal sources. Journal of Geophysical Research **99**: 18,403-18,415.

Tsurumi, M., de Graaf, R. C. and Tunnicliffe, V. 2003. Distributional and biological aspects of copepods at hydrothermal vents of the Juan de Fuca Ridge, north-east Pacific ocean. Journal of the Marine Biological Association of UK **83**: 469-477.

Tunnicliffe, V., Botros, M., De Burgh, M. E., Dinet, A., Johnson, H. P., Juniper, K. S. and McDuff, R. E. 1986. Hydrothermal vents of Explorer Ridge, northeast Pacific. Deep-Sea Research **33**: 401-412.

Tyler, P. A. 1995. Conditions for the existence of life at the deep-sea floor: An update. Oceanogr Mar Biol Annu Rev **33**: 221-244.

Vacquier, V. J. 1961. Hydrostatic pressure has a selective effect on the copepod *Tigriopus*. Science **135**: 724-725.

Van Dover, C. L. 2000. The ecology of deep-sea hydrothermal vents. Princeton University Press.

Van Dover, C. L. and Fry, B. 1994. Microorganisms as food resources at deep-sea hydrothermal vents. Limnology and Oceanography **39**: 51-57.

Van Dover, C. L., Kaartvedt, S., Bollens, S. M., Wiebe, P. H., Martin, J. W. and France, S. C. 1992. Deep-sea amphipod swarms. Nature **358**: 25-26.

Vereshchaka, A. L. 1995. Macroplankton in the near-bottom layer of continental slopes and seamounts. Deep-Sea Research I **42**: 1639-1668.

Vereshchaka, A. L. and Vinogradov, G. M. 1999. Visual observations of the vertical distribution of plankton throughout the water column above Broken Spur vent field, Mid-Atlantic Ridge. Deep-Sea Research I **46**: 1615-1632.

Vinogradov, G. M., Vereshchaka, A. L. and Aleinik, D. L. 2003. Zooplankton distribution over hydrothermal vent fields of the Mid-Atlantic Ridge. Oceanology **43**: 656-669.

Vinogradov, G. M., Vereshchaka, A. L., Musaeva, E. I. and Dyakonov, V. Y. 2003. Vertical zooplankton distribution over the Porcupine Abyssal Plain (Northeast Atlantic) in the summer of 2002. Oceanology **43**: 512-523.

Vinogradov, M. E. 1997. Some problems of vertical distribution of meso- and macroplankton in the ocean. Advances in Marine Biology **32**: 2-166.

Von Damm, K. L. 1995. Controls on the chemistry and temporal variability of seafloor hydrothermal fluids. In: Humphris, S. E., Zierenberg, R. A., Mullineaux, L. S. and Thomson, R. E. (eds.), Seafloor hydrothermal systems: Physical, chemical, biological and geological interactions. American Geophysical Union, pp. 222-247.

Wakeham, S. G., Cowen, J. P., Burd, B. J. and Thomson, R. E. 2001. Lipid-rich ascending particles from the hydrothermal plume at Endeavour Segment, Juan de Fuca Ridge. Geochimica et Cosmochimica Acta **65**: 923-939.

Wiebe, P. H., Copley, N., Van Dover, C. L., Tamse, A. and Manrique, F. 1988. Deep-water zooplankton of the Guaymas Basin hydrothermal vent field. Deep-Sea Research **35**: 985-1013.

Wildish, D. J., Wilson, A. J. and Frost, B. 1992. Benthic boundary layer macrofauna of Browns Bank, northwest Atlantic, as potential prey of juvenile benthic fish. Canadian Journal of Fisheries and Aquatic Sciences **49**: 91-98.

Wishner, K. F. 1980a. The biomass of the deep-sea benthopelagic plankton. Deep-Sea Research **27A**: 203-216.

Wishner, K. F. 1980b. Aspects of the community ecology of deep-sea, benthopelagic plankton, with special attention to Gymnopleid copepods. Marine Biology **60**: 179-187.

Yamaguchi, A., Watanabe, Y., Ishida, H., Harimoto, T., Furusawa, K., Suzuki, S., Ishizaka, J., Tsutomu, I. and Masayuki, M. T. 2002. Community and trophic structures of pelagic copepods down to greater depths in the western subarctic Pacific (WEST-COSMIC). Deep-Sea Research I **49**: 1007-1025.

Zar, J. H. 1984. Biostatistical analysis. Prentice-Hall Inc.

Chapter 4

Summary

In this chapter, I bring together results from Chapters 2 and 3 and review relevant literature to consider the hypothesis that vents represent a significant food resource for near-bottom pelagic organisms.

4.1 Background

Vent biologists have long speculated about the importance of hydrothermal vents in the deep sea. Because vent effluent provides resources that support thriving benthic communities, many vent biologists have thought that vents should represent a significant food resource for deep sea pelagic organisms (Winn and Karl 1986, Mullineaux and France 1995, Kim and Mullineaux 1998, Van Dover 2000). Previous studies of copepod and amphipod swarms associated with vents on the East Pacific Rise (Smith 1985, Van Dover et al. 1992, Kaartvedt et al. 1994); shrimp swarms associated with vents on the Mid-Atlantic Ridge (Herring and Dixon 1998, Polz et al. 1998, Gerbruk et al. 2000); and deep scattering layers of zooplankton associated with the neutrally buoyant plume above Endeavour Segment (Burd et al. 1992, Thomson et al. 1992, Burd and Thomson 1994, Burd and Thomson 1995, Burd and Thomson 2000, Cowen et al. 2001, Burd et al. 2002) and Broken Spur vent field on the Mid-Atlantic Ridge (Vereshchaka and Vinogradov 1999) have all supported this hypothesis.

However, more recent work by Vinogradov et al. (2003) in the water column above vents in the Mid-Atlantic suggests otherwise. Over six vent fields, ranging in depth from 800-3050 m, Vinogradov et al. found no increase in gelatinous zooplankton (larvaceans, ctenophores, siphonophores, medusae), chaetognath, decapod and fish biomass in association with the neutrally buoyant plumes. Gelatinous zooplankton appeared to be relatively abundant near-bottom (20-500 m above bottom or mab) and about 800 m below surface however, they speculate that this is likely not due to the presence of the vents as similar increases in gelatinous zooplankton abundance are found over the Porcupine Abyssal Plain (Vinogradov et al. 2003). In short, the debate is far from being resolved.

My study uniquely contributes to this debate. I use environmental, video and net tow data to look at the effect of vent effluent on pelagic organisms near the seafloor (20 mab) at multiple scales over various sites. My results suggest that vents do enhance abundance of pelagic organisms near the seafloor (Figure 4.1):

1. overall, within axial valley;
2. on local scales over non-vent areas; and
3. over diffuse vents.

Pelagic organisms, especially copepods and gelatinous zooplankton, are least abundant over high temperature vent fields, where venting is most intense.

4.2 Paradox of the vents

These results present an interesting paradox. Benthic organisms at vents are most abundant within a couple of metres of the vent source, relying on vent-derived resources for food. If vent-derived resources are important for near-bottom pelagic organisms, it follows that they too should be relatively abundant over vent fields. From this study, near-bottom pelagic organisms are found to be most abundant over non-vent areas yet I speculate that these aggregations may be in response to elevated microbial concentrations associated with vent effluent. It is likely that the very effluent that plays a role in limiting pelagic organism dispersion (i.e. due to toxic or turbulent conditions) may also attract pelagic organisms within the axial valley.

In the following paragraphs, I use my findings from Chapters 2 and 3 to create a picture of the near-bottom dispersion of pelagic organisms above vent and non-vent areas (Figure 4.1). In Chapter 3, I show that non-vent and smoker vent video and net tows capture similar numbers of zooplankton therefore, it is appropriate to use zooplankton densities calculated from Chapter 2 video data to compare with previous net tow studies in non-vent or typical deep sea areas. Calculations of zooplankton densities from video taken above diffuse vents (Chapter 2) are also used. However, it is important to note that these may be underestimated (Chapter 3). While I use these data to represent a static snapshot in time, the system I describe is dynamic. Tidal reversals, plume-induced currents, eddy circulation and topography all affect dispersion of pelagic organisms.

Figure 4.1 Illustration of vent influence on pelagic organisms near seafloor. Zooplankton are represented by pelagic adult copepods (large), pelagic copepodites (small), benthic adult copepods (stippled, large) and benthic copepodites (stippled, small). Zoarcids are small fish, macrourids are large. Shrimp and gelatinous zooplankton (jellyfish) are also represented. Numbers of copepods represent maximum measured zooplankton densities from video and net tow samples (smoker vent ~ 3-5 individuals/m^3, diffuse vent 20 mab 14 individuals/m^3, diffuse vent near-bottom ~7 individuals/m^3, non-vent within axial valley ranges from 3-17 individuals/m^3). How zooplankton densities in non-vent areas within the axial valley compare with densities beyond the plume influence ('true' non-vent areas) is unknown. Changes in theta (T) anomaly and light transmissivity are based on Chapter 2 data. Italics indicate that enhanced microbial concentration associated with vent effluent is speculated to occur based on previous studies (not measured in this study). Solid lines extending from smoker vent apex represent discrete, buoyant plume. Dotted lines extending from diffuse vent represent diffuse plume. A=smoker vent, B=diffuse vent, C and D=non-vent within axial valley and E=non-vent beyond plume influence.

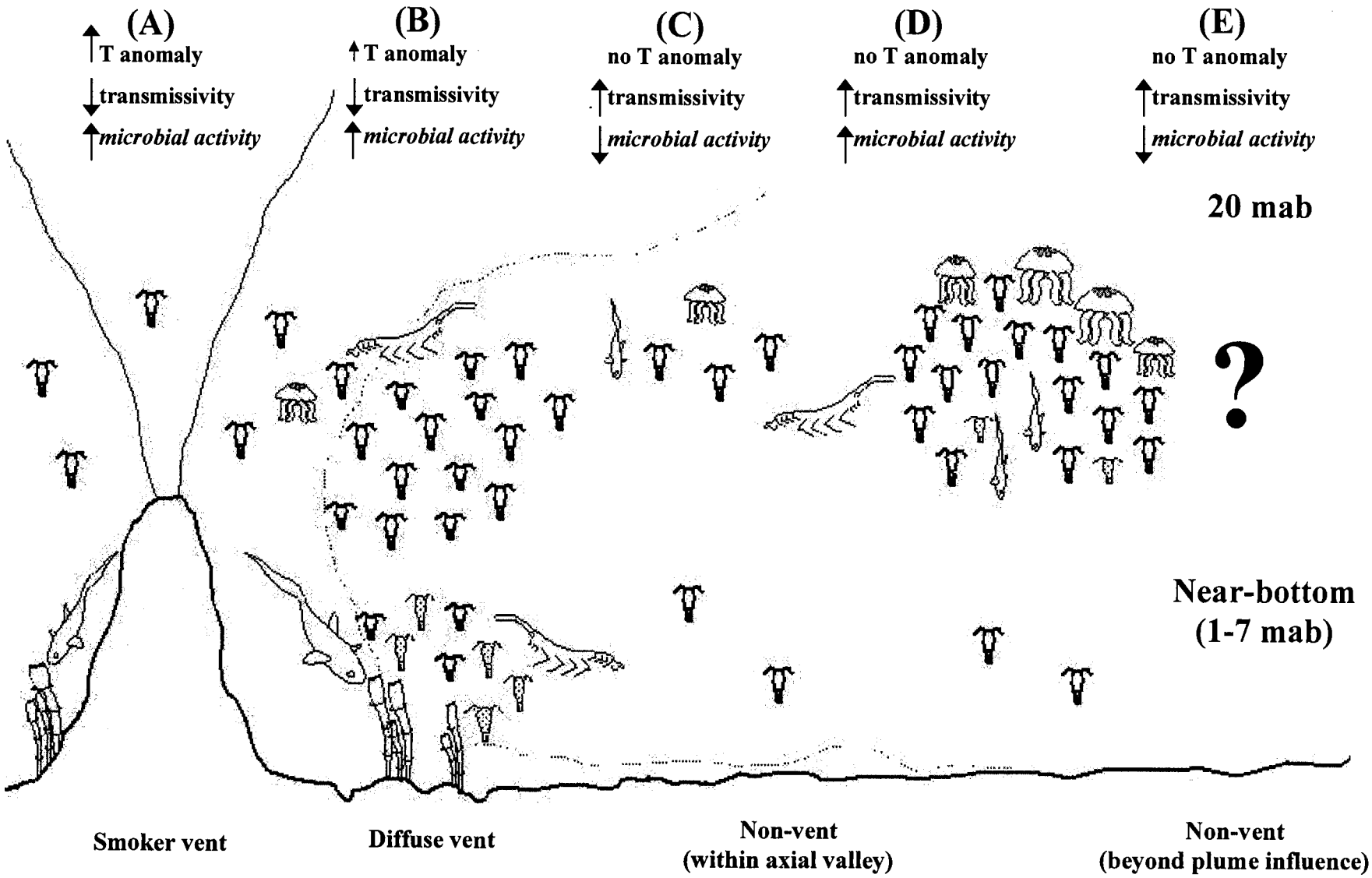
(A)
T anomaly
transmissivity
microbial activity
(B)
T anomaly
transmissivity
microbial activity
(C)
no T anomaly
transmissivity
microbial activity
(D)
no T anomaly
transmissivity
microbial activity
(E)
no T anomaly
transmissivity
microbial activity
20 mab
?
Near-bottom
(1-7 mab)
Smoker vent
Diffuse vent
Non-vent
(within axial valley)
Non-vent
(beyond plume influence)

A: Smoker vents

Abundance of all pelagic organisms is relatively low directly over areas of intense venting (Figure 4.1A). Zooplankton, both crustacean and gelatinous, appear to be most affected by venting. Zooplankton abundance is lowest along the central venting axes of the two high temperature vent fields, High Rise and MEF (Figure 2.30, Chapter 3 sample R685). These gaps correlate with strong physico-chemical effluent signature suggesting that zooplankton may be able to detect rapidly changing temperature anomalies, sulphide level or turbulence associated with the rising plume. Detection of these cues, or other unmeasured factors, may allow zooplankton to avoid areas of prolonged, intense venting. Despite intense venting, copepod densities over smoker vents are still relatively high in comparison to typical deep sea (Table 4.1).

Gelatinous zooplankton of all types (ctenophores, cnidarians, larvaceans, salps) occur in low abundance along the length of the central portion of the sample area. Near-bottom gelatinous zooplankton densities (1.1-1.8 individuals/m^3) are lower than those found associated with the neutrally buoyant plume over Endeavour Segment (0.7-12.8 individuals/m^3, Table 4.1). Low physiological tolerance of variable environmental conditions associated with effluent (e.g. increased turbulence, relatively steep thermal gradients, increased particulates) likely affect gelatinous zooplankton dispersion within the axial valley.

Nekton appear to concentrate at the edges of intense venting (Figure 2.29). Shrimp may be attracted to zooplankton and/or benthic resources (Figure 4.1A). Within the axial valley, shrimp densities are higher than previously measured densities at 10-25 mab in Kings Trough (4000 m depth) in the NE Atlantic (Table 4.1). While shrimp are less abundant over vent fields, vent effluent does not appear to be a strong factor influencing shrimp dispersion. Macrourids also appear to be attracted to vents, likely feeding on abundant vent benthos (Figure 4.1A). Macrourid densities above Endeavour Segment are almost five times higher than those measured from submersible observation of macrourids over abyssal plains in the Bay of Biscay, at a depth of 2100 m (Mahaut et al. 1990) (Table 4.1). Macrourids orient to food falls using plume odour that is dispersed by bottom currents (Priede and Merrett 1998). Similarly, effluent odour or

Table 4.1 Comparison of pelagic organism densities near the seafloor above vent and non-vent areas. Zooplankton densities (primarily copepods) from my study are based on video and net tows. Nekton densities are based on video (Chapter 2). *Macrourids are listed as number per 10,000 m^2 for purposes of comparison (calculated from Chapter 2 video densities of 5/100m^3). Only zooplankton and gelatinous zooplankton densities are separated into smoker and diffuse vent densities. Previous vent studies do not distinguish between diffuse vent and smoker vent samples. Last column distinguishes between vent, non-vent (deep sea within axial valley) and typical deep sea (beyond plume influence) studies. Non-vent area includes non-vent sections between vent fields. #Gelatinous zooplankton density range only includes samples from 1900-2200 m depth.

	My study		**Previous studies**	**Comments on previous studies**
	Vent	Non-vent		
Zooplankton (ind/m^3)	4-5 (smoker video)	9.6-17.3	1.1-1.9[a]	Pacific, deep sea
	0.7-3.5 (smoker net)		0.4[b]	Atlantic, deep sea
	8.5-10.3 (diffuse video)		0.8-6.7[c]	Pacific, vent
	8.5-14.6 (diffuse net)		0.5-2.2[c]	Pacific, non-vent
			2.7[d]	Pacific, vent
Gelatinous zooplankton (ind/m^3)	1-1.8 (smoker)	1.7-2.2	0.06-0.08[e]	Atlantic, neutrally buoyant plume
	0.9-1.1 (diffuse)		0.7-12.8[f]#	Pacific, neutrally buoyant plume
Shrimp (ind/100m^3)	10	20	0.1[g]	Atlantic, deep sea
Zoarcids (ind/100m^3)	5	9-10	?	-
Macrourids*	22/10,000m^2		4.5/10,000m^2[h]	Bay of Biscay, deep sea

[a] (Wishner 1980b); [b] (Christiansen et al. 1999); [c] (Berg and Van Dover 1987) (non-vent); [d] (Wiebe et al. 1988); [e] (Vinogradov et al. 2003); [f] (Burd and Thomson 2000); [g] (Domanski 1986); [h] (Mahaut et al. 1990)

odour from the benthos at vents likely play a role in attracting macrourids to the vent fields.

B: Diffuse vents

In comparison to smoker vents, zooplankton (copepods) are more abundant over diffuse vents (Figure 4.1B). Copepod densities at 20 mab can be as high as 14.6 individuals/m^3, up to an order of magnitude greater than that found in previous studies (Table 4.1). Zooplankton aggregations above diffuse vents may occur in response to elevated microbial activity and relatively weak physico-chemical effluent signature at 20 mab. *Oithona similis, Spinocalanus sp.* and calanoid copepodites, are abundant over diffuse vents and may be capable of feeding on microbes (Gowing and Wishner 1992, Fransz and Gonzalez 1995, Nielsen and Sabatini 1996, Nagata et al. 2000, Finlay and Roff 2003), including metal-encapsulated bacteria associated with effluent (Gowing and Wishner 1992).

Although based on few samples, near-bottom (1-7 m) zooplankton densities over diffuse vents appear to be lower (3.8-7.3 individuals/m^3) than zooplankton densities at 20 mab (8.5-14.6 individuals/m^3). Most adult pelagic copepods are virtually absent near the bottom whereas vent-specific dirivultid copepods and weak-swimming copepodites are abundant (Figure 4.1B). The high abundance of dirivultid species in near-bottom samples over diffuse vents indicates that dirivultids may be swept into the water column by rising effluent suggesting a mechanism for near-bottom transport of benthic organisms. Two phenomena may account for the lack of adult pelagic copepods in near-bottom water over diffuse vents. First, many pelagic copepods appear to avoid the seafloor as they are unable to feed or reproduce anywhere but in the water column (Fossa 1986, Angel 1990, Vereshchaka 1995, Mees and Jones 1997, Marcus and Boero 1998). Second, near-bottom sulphide levels or turbulence associated with diffuse venting may exceed copepod physiological tolerance. The abundance of early stage *Neocalanus plumchrus* copepodites suggests that conditions over diffuse vents may induce stage V *N. plumchrus* to moult and mate and lends weight to the plausibility of the latter hypothesis (see Section 3.5.3 Development Stage).

In comparison to gelatinous zooplankton densities associated with the Endeavour neutrally buoyant plume (Burd and Thomson 2000), near-bottom densities of gelatinous zooplankton over diffuse vents are relatively low (Table 4.1).

Nekton are relatively abundant near diffuse vents (Figure 4.1B). Shrimp and zoarcids likely feed on zooplankton abundant at 20 mab. Shrimp are also present near the seafloor and may feed on benthos (Chapter 3). Zoarcids however, appear to avoid the seafloor as none were seen in the near-bottom videos. As at smoker vents, macrourids are relatively abundant. Macrourids are likely feeding on benthos (Figure 4.1B).

C and D: Non-vent (within axial valley)

Although zooplankton abundance within the axial valley appears elevated above background levels, zooplankton are not evenly dispersed throughout non-vent areas (Figure 4.1C and D). At 20 mab, zooplankton abundance fluctuates despite relatively weak light transmission and thermal anomalies (Figure 2.38, Line 9). Near-bottom dispersion of zooplankton, as at 20 mab, may also be patchy. In the sole near-bottom non-vent sample (Chapter 3), copepod density is relatively low (1.6 individuals/m^3) although this may a function of small sample size. Alternatively, adult pelagic copepods may simply avoid the seafloor. Few adult dirivultids are present in 20 mab or near-bottom non-vent samples whereas dirivultid copepodites are relatively abundant. The presence of early dirivultid copepodid stages suggests transport between vent fields occurs during juvenile stages rather than as adults.

Occasionally, localized increases in zooplankton abundance appear over non-vent areas (Figure 4.1D). Chapter 2 data suggest this occurs within 100-200 m of a vent field (Figure 2.38, Line 8). High abundance is maintained over hundreds of metres and then suddenly drops to lower levels. Along line 8, zooplankton densities reach 17.3 individuals/m^3 in an area west of Clam Bed, exceeding densities found directly above diffuse vents (Table 4.1).

Aggregations of zooplankton in non-vent areas (e.g. Line 8) may be linked with vent effluent. Zooplankton tend to aggregate in response to physical or biological factors (Mackas and Boyd 1979, Amatzia et al. 1994, Burd and Thomson 1995, Folt and Burns 1999, Denny and Wethey 2001). In non-vent areas, temperature and light transmission

are relatively constant. It is possible that an unmeasured physical factor, indicative of vent effluent, causes zooplankton to aggregate. However, I speculate that zooplankton aggregate in response to a biological factor, the presence of enhanced microbial concentrations associated with vent effluent.

In this study, I use light transmission and temperature anomalies to indicate vent effluent signature. Despite constant light and temperature levels, due to mixing with ambient water, vent resources (e.g. metals, minerals and associated microbial populations) may still be present in the water layer. My results show vent effluent is carried primarily south and west from vent fields (Figure 2.10). The residence time of plume water is influenced by currents, topography, tides and the relative dilution of vent fluid with ambient water (Cowen and German 2003). Thomson et al. (2003) showed that while currents within the axial valley are predominantly northward flowing, current reversal is common in the autumn. In addition, cross-axis flow can also occur (Thomson et al. 2003) which may cause effluent to be carried west. Effluent from Clam Bed carried westward over line 8 likely coincides with the area in which zooplankton increase. Despite losing much of its physico-chemical signature (Figures 2.32c, 2.34c), effluent can retain metals and minerals over relatively long periods of time (Cowen et al. 1986, Cowen et al. 1990, Feely et al. 1990, Lilley et al. 1995, Cowen and German 2003). Residence time of the plume will strongly influence not only the distribution of chemical species, but also the structure of 'standing' microbial communities within the plume (Cowen and German 2003). Because resources necessary for chemosynthesis can be retained in the water column for at least a full tidal cycle (I. Garcia-Berdeal pers. comm.), it is possible that zooplankton are feeding on effluent-enhanced microbial populations away from the vent field where environmental conditions are more stable. Bradford-Grieve et al. (1993) find that zooplankton abundance increases hundreds of metres downstream of an upwelling site off the coast of New Zealand. A similar situation may be occurring over non-vent areas within the axial valley. Densities of zooplankton in aggregations in non-vent areas in this study exceed those found in previous typical deep sea studies (Table 4.1). Non-vent zooplankton aggregations are even more dense than aggregations found associated with vents on the East Pacific Rise ((Berg and Van Dover 1987), Table 4.1). Based on these comparisons, I speculate that chemosynthetic microbes associated with

vent effluent represent a significant food resource for near-bottom zooplankton within the axial valley.

Gelatinous zooplankton are most abundant where effluent signature is weakest (Figure 4.1D). Gelatinous zooplankton, especially ctenophores and salps, may be less physiologically tolerant of effluent. Vinogradov et al (2003) also remarked on the lack of these organisms near vent plumes in the Mid-Atlantic. Ctenophores may not be able to swim in and out of effluent easily and therefore, avoid it on the whole. Gelatinous zooplankton are often attracted to the edges of physical discontinuities (e.g. ocean fronts) in response to increases in zooplankton abundance (Graham et al. 2001). Vinogradov et al (2003) describe densities of 0.06-0.08 individuals/m^3 of gelatinous zooplankton above Rainbow vent field in the Mid-Atlantic at the upper boarder of neutrally buoyant plume at depths of 1800-2200 m (Table 4.1). In my study, densities of 1.3 individuals/m^3 and 2.2 individuals/m^3 are found over vent and non-vent areas respectively, suggesting that within the axial valley, gelatinous zooplankton are elevated above typical deep sea levels.

At depths of 2000 m, Vinogradov and Shushkina (2002) in the NW Pacific and Burd and Thomson (2000) over Endeavour Segment find similar species of gelatinous zooplankton. Whereas Kim and Mullineux (1998) speculate that a unique population of gelatinous holoplankton appeared to be tolerant of vent effluent, my results suggest that typical deep sea gelatinous zooplankton are able to capitalize on abundant zooplankton and tolerate conditions within the axial valley.

Based on video data from both chapters, zoarcids and shrimp are relatively more abundant in non-vent areas (Figure 4.1D). Likely, they are both feeding on zooplankton, which in turn, are likely feeding on resources associated with vent effluent. Macrourids are virtually absent from non-vent areas, suggesting that within the axial valley their main food resource is vent benthos.

E: Non-vent (beyond plume influence)

Do vents represent a significant food resource for near-bottom pelagic organisms? Because my study did not sample areas beyond plume influence, I can only speculate on how influential the vents are by comparing with previous deep sea and vent studies (Figure 4.1E). While zooplankton swarms are not encountered at vents on the Juan de

Fuca or Explorer Ridges, it appears that zooplankton, primarily copepod, abundance is at least of the same magnitude as that found above East Pacific Rise vents (Table 4.1). Within the axial valley, it appears that pelagic organism abundance is about an order of magnitude greater than typical deep sea levels at similar depths (Table 3.9; Table 4.1). Few benthopelagic studies exist in the northern Pacific; only Vinogradov (1970) appears to have any information on near-bottom zooplankton distribution. However, because 1) he does not separate out the different organism groups (e.g. zooplankton include copepods, amphipods, euphausiids, gelatinous zooplankton) and 2) his data are reported as biomass rather than as abundance, it is not possible to compare my results with his. Thus based on comparisons presented in Table 4.1, it appears that vents on the Juan de Fuca may represent a significant food resource for zooplankton however, it is not yet possible to completely resolve this debate.

Overall, the most important finding from this study is that diverse assemblages of zooplankton and nekton near the seafloor appear to be influenced by vent effluent. Different pelagic groups show different tolerances of venting although most groups tend to avoid areas of intense venting. This is particularly evident in the spatial patterns of weak swimming zooplankton (crustacean and gelatinous). I speculate that some pelagic organisms, zooplankton and macrourids, may be able to utilize vent resources on local scales, within the axial valley. If this is true, it suggests that near-bottom pelagic organisms may play a role in transferring vent production into the deep sea.

4.3 Future studies

It is apparent that vents influence pelagic organisms near the seafloor, but how significant is this influence? In order to address this question, studies of the dispersion off-axis near-bottom pelagic organisms need to be made. Sampling beyond plume influence is important to determine how significant vent resources are in the deep sea.

Based on my work, it appears that the minimum grain size for studying ecological heterogeneity and zooplankton dispersion above vents is 55 m. Is this true for other vent sites? Is this finding applicable to deep sea sites outside of the axial valley? As benthopelagic work is expensive and methods of continuous data collection become more widespread, it is necessary to identify optimal sampling scales.

Repeating the video portion of this study at (1) the same time of year (October) and (2) a different time of year (e.g. June-August) would be useful in determining if the above-mentioned patterns are seasonal. Replicate samples, using transect lines perpendicular to the length of the sample area, would also lend weight to these findings.

Are copepods feeding on microbes associated with vent effluent? Gowing and Wishner (1992) found metal-precipitating bacteria and their capsules in copepod guts using transmission electron microscope (TEM). Carbon and nitrogen isotope analysis may also be useful in identifying nutritional source as either photosynthetic and vent-derived resources.

This exploratory study uses data collection (video) and analysis (SADIE) techniques that provide the groundwork for future studies to address the hypothesis that vents represent a significant food resource for deep sea pelagic organisms.

4.4 References

Amatzia, G., Greene, C., Haury, L., Wiebe, P. H., Gal, G., Kaartvedt, S., Meir, E., Fey, C. and Dawson, J. 1994. Zooplankton patch dynamics: daily gap formation over abrupt topography. Deep-Sea Research I **41**: 941-951.

Angel, M. V. 1990. Life in the benthic boundary layer: connections to the mid-water and sea floor. Philosophical Transactions of the Royal Society of London A **331**: 15-28.

Berg, C. J. J. and Van Dover, C. L. 1987. Benthopelagic macrozooplankton communities at and near deep-sea hydrothermal vents in the eastern Pacific Ocean and the Gulf of California. Deep-Sea Research **34**: 379-401.

Bradford-Grieve, J. M., Murdoch, R. C. and Chapman, B. E. 1993. Composition of macrozooplankton assemblages associated with the formation and decay of pulses within an upwelling plume in greater Cook Strait, New Zealand. New Zealand Journal of Marine and Freshwater Research **27**: 1-22.

Burd, B. J. and Thomson, R. E. 1994. Hydrothermal venting at Endeavour Ridge: Effect on zooplankton biomass throughout the water column. Deep-Sea Research I **41**: 1407-1423.

Burd, B. J. and Thomson, R. E. 1995. Distribution of zooplankton associated with the Endeavour Ridge hydrothermal plume. Journal of Plankton Research **17**: 965-997.

Burd, B. J. and Thomson, R. E. 2000. Distribution and relative importance of jellyfish in a region of hydrothermal venting. Deep-Sea Research I **47**: 1703-1721.

Burd, B. J., Thomson, R. E. and Calvert, S. E. 2002. Isotopic composition of hydrothermal epiplume zooplankton: evidence of enhanced carbon recycling in the water column. Deep-Sea Research I **49**: 1877-1900.

Burd, B. J., Thomson, R. E. and Jamieson, G. S. 1992. Composition of a deep scattering layer overlying a mid-ocean ridge hydrothermal plume. Marine Biology **113**: 517-526.

Christiansen, B., Druke, B., Koppelmann, R. and Weikert, H. 1999. The near-bottom zooplankton at the abyssal BIOTRANS site, northeast Atlantic: composition, abundance and variability. Journal of Plankton Research **21**: 1847-1863.

Cowen, J. P., Bertram, M. A., Wakeham, S. G., Thomson, R. E., Lavelle, J. W., Baker, E. T. and Feely, R. A. 2001. Ascending and descending particle flux from hydrothermal plumes at Endeavour Segment, Juan de Fuca Ridge. Deep-Sea Research I **48**: 1093-1120.

Cowen, J. P. and German, C. 2003. Biogeochemical cycling in hydrothermal plumes. In: Halbach, P. E., Tunnicliffe, V. and Hein, J. R. (eds.), Energy and mass transfer in marine hydrothermal systems. Dahlem University Press, pp. 303-316.

Cowen, J. P., Massoth, G. J. and Baker, E. T. 1986. Bacterial scavenging of Mn and Fe in a mid- to far-field hydrothermal vent plum. Nature **322**: 169-171.

Cowen, J. P., Massoth, G. J. and Feely, R. A. 1990. Scavenging rates of dissolved manganese in a hydrothermal vent plume. Deep-Sea Research **37**: 1619-1637.

Denny, M. and Wethey, D. 2001. Physical processes that generate patterns in marine communities. In: Bertness, M. D., Gaines, S. D. and Hay, M. E. (eds.), Marine Community Ecology. Sinauer Associates Press, pp. 3-38.

Domanski, P. 1986. The near-bottom shrimp faunas (Decapoda: Natantia) at two abyssal sites in the Northeast Atlantic Ocean. Marine Biology **93**: 171-180.

Feely, R. A., Geiselmand, T. L., Baker, E. T. and Massoth, G. J. 1990. Distribution and composition of hydrothermal plumes particles from the ASHES vent field at Axial Volcano, Juan de Fuca Ridge. Journal of Geophysical Research **95**: 12,855-12,873.

Finlay, K. and Roff, J. 2003. Ontogenic changes in diet of coastal marine copepods. 3rd International Zooplankton Production Symposium.

Folt, C. L. and Burns, C. W. 1999. Biological drivers of zooplankton patchiness. Trends in Ecology and Evolution **14**: 300-305.

Fossa, J. H. 1986. Aquarium observations on vertical zonation and bottom relationships of some deep-living hyperbenthic mysids (Crustacea: Mysidacea). Ophelia **25**: 107-117.

Fransz, H. G. and Gonzalez, S. R. 1995. The production of Oithona similis (Copepoda: Cyclopoida) in the Southern Ocean. ICES Journal of Marine Science **52**: 549-555.

Gerbruk, A. V., Southward, E. C., Kennedy, H. and Southward, A. J. 2000. Food sources, behaviour and distribution of hydrothermal vent shrimps at the Mid-Atlantic Ridge. Journal of Marine Biological Association UK **80**: 485-499.

Gowing, M. M. and Wishner, K. F. 1992. Feeding ecology of benthopelagic zooplankton on an eastern tropical Pacific seamount. Marine Biology **112**: 451-467.

Graham, W. M., Pages, F. and Hamner, W. M. 2001. A physical context for gelatinous zooplankton aggregations: a review. Hydrobiologia **451**: 199-212.

Herring, P. J. and Dixon, D. R. 1998. Extensive deep-sea dispersal of postlarval shrimp from a hydrothermal vent. Deep-Sea Research I **45**: 2105-2118.

Kaartvedt, S., Van Dover, C. L., Mullineaux, L. S., Wiebe, P. H. and Bollens, S. M. 1994. Amphipods on a deep-sea hydrothermal treadmill. Deep-Sea Research I **41**: 179-195.

Kim, S. L. and Mullineaux, L. S. 1998. Distribution and near-bottom transport of larvae and other plankton at hydrothermal vents. Deep-Sea Research II **45**: 423-440.

Lilley, M. D., Feely, R. A. and Trefry, J. H. 1995. Chemical and biochemical transformations in hydrothermal plumes. In: Humphris, S. E., Zierenberg, R. A., Mullineaux, L. S. and Thomson, R. E. (eds.), Seafloor hydrothermal systems: Physical, chemical, biological and geological interactions. American Geophysical Union, pp. 369-291.

Mackas, D. L. and Boyd, C. M. 1979. Spectral analysis of zooplankton spatial heterogeneity. Science **204**: 62-64.

Mahaut, M.-L., Geistdoerfer, P. and Sibuet, M. 1990. Trophic strategies in carnivorous fishes: their significance in energy transfer in the deep-sea benthic ecosystem (Meriadzek Terrace - Bay of Biscay). Progress in Oceanography **24**: 223-237.

Marcus, N. and Boero, F. 1998. Minireview: The importance of benthic-pelagic coupling and the forgotten role of life cycles in coastal aquatic systems. Limnology and Oceanography **43**: 763-768.

Mees, J. and Jones, M. B. 1997. The hyperbenthos. Oceanography and Marine Biology: An Annual Review **35**: 221-255.

Mullineaux, L. S. and France, S. C. 1995. Dispersal mechanisms of deep-sea hydrothermal vent fauna. In: Humphris, S. E., Zierenberg, R. A., Mullineaux, L. S. and Thomson, R. E. (eds.), Seafloor hydrothermal systems: Physical, chemical, biological and geological interactions. American Geophysical Union, pp. 408-424.

Nagata, T., Fukuda, H., Fukuda, R. and Koike, I. 2000. Bacterioplankton distribution and production in deep Pacific waters: Large-scale geographic variations and possible coupling with sinking particle fluxes. Limnology and Oceanography **45**: 426-435.

Nielsen, T. G. and Sabatini, M. 1996. Role of cyclopoid copepods *Oithona* spp. in North Sea plankton communities. Marine Ecology Progress Series **139**: 79-93.

Polz, M. F., Robinson, J. J., Cavanaugh, C. M. and Van Dover, C. L. 1998. Trophic ecology of massive shrimp aggregations at a Mid-Atlantic Ridge hydrothermal vent site. Limnology and Oceanography **43**: 1631-1638.

Priede, I. G. and Merrett, N. R. 1998. The relationship between numbers of fish attracted to baited cameras and population density: Studies on demersal grenadiers *Coryphaenoides (Nematonurus) armatus* in the abyssal NE Atlantic Ocean. Fisheries Research **36**: 133-137.

Smith, K. L. J. 1985. Macrozooplankton of a deep sea hydrothermal vent: In situ rates of oxygen consumption. Limnology and Oceanography **30**: 102-110.

Thomson, R. E., Burd, B. J., Dolling, A. G., Gordon, R. L. and Jamieson, G. S. 1992. The deep scattering layer associated with the Endeavour Ridge hydrothermal plume. Deep-Sea Research **39**: 55-73.

Thomson, R. E., Mihaly, S. F., Rabinovich, A. B., McDuff, R. E., Veirs, S. R. and Stahr, F. R. 2003. Constrained circulation at Endeavour ridge facilitates colonization by vent larvae. Nature **424**: 545-549.

Van Dover, C. L. 2000. The ecology of deep-sea hydrothermal vents. Princeton University Press.

Van Dover, C. L., Kaartvedt, S., Bollens, S. M., Wiebe, P. H., Martin, J. W. and France, S. C. 1992. Deep-sea amphipod swarms. Nature **358**: 25-26.

Vereshchaka, A. L. 1995. Macroplankton in the near-bottom layer of continental slopes and seamounts. Deep-Sea Research I **42**: 1639-1668.

Vereshchaka, A. L. and Vinogradov, G. M. 1999. Visual observations of the vertical distribution of plankton throughout the water column above Broken Spur vent field, Mid-Atlantic Ridge. Deep-Sea Research I **46**: 1615-1632.

Vinogradov, G. M., Vereshchaka, A. L. and Aleinik, D. L. 2003. Zooplankton distribution over hydrothermal vent fields of the Mid-Atlantic Ridge. Oceanology **43**: 656-669.

Vinogradov, G. M., Vereshchaka, A. L., Musaeva, E. I. and Dyakonov, V. Y. 2003. Vertical zooplankton distribution over the Porcupine Abyssal Plain (Northeast Atlantic) in the summer of 2002. Oceanology **43**: 512-523.

Vinogradov, M. E. 1970. Vertical distribution of the oceanic zooplankton. Keter Press.

Vinogradov, M. E. and Shushkina, E. A. 2002. Vertical distribution of gelatinous macroplankton in the North Pacific observed by manned submersibles *Mir*-1 and *Mir*-2. Journal of Oceanography **58**: 295-303.

Wiebe, P. H., Copley, N., Van Dover, C. L., Tamse, A. and Manrique, F. 1988. Deep-water zooplankton of the Guaymas Basin hydrothermal vent field. Deep-Sea Research **35**: 985-1013.

Winn, C. D. and Karl, D. M. 1986. Microorganisms in deep-sea hydrothermal plumes. Nature **320**: 744-746.

Wishner, K. F. 1980b. Aspects of the community ecology of deep-sea, benthopelagic plankton, with special attention to Gymnopleid copepods. Marine Biology **60**: 179-187.